

A SIMULATION-BASED MULTI-CRITERIA MANAGEMENT SYSTEM  
FOR OPTIMAL WATER SUPPLY UNDER UNCERTAINTY

**Dissertation**

in partial fulfilment of the requirements for the degree of

Doctor rerum naturalium (Dr. rer. nat.)

submitted to the Faculty of Environmental Sciences

Technische Universität Dresden

by

**M.Eng. Pham Van Tinh**

Date of birth: 06.08.1974

Place of birth: Thai Binh - Vietnam

**Reviewers:**

Prof. Dr. habil. Niels Schütze – Technische Universität Dresden

Prof. Em. Dr. -Ing. habil. Gerd H. Schmitz - Technische Universität Dresden

Prof. Dr. Markus Disse - Technische Universität München

Examination location and date: Dresden, April 28th, 2015



***Customers:*** “We want great service at low price”

***Upper management:*** “Provide adequate capacity but remain within capital budget”

***Planning:*** “Meet demands even though there is a great deal of uncertainty in forecast”

***Engineering:*** “When in doubt, build it stout”

***Operation:*** “Give us flexibility and redundancy so we aren’t hanging on a single pipe or pump”

*(Walski et al., 2003)*



## Erklärung

Hiermit versichere ich, dass ich die vorliegende Arbeit ohne unzulässige Hilfe Dritter und ohne Benutzung anderer als der angegebenen Hilfsmittel angefertigt habe; die aus fremden Quellen direkt oder indirekt übernommenen Gedanken sind als diese kenntlich gemacht worden. Bei der Auswahl und Auswertung des Materials sowie bei der Herstellung des Manuskriptes habe ich Unterstützungsleistungen von folgenden Personen erhalten:

.....

Weitere Personen waren an der geistigen Herstellung der vorliegenden Arbeit nicht beteiligt. Insbesondere habe ich nicht die Hilfe eines oder mehrerer Promotionsberater(s) in Anspruch genommen. Dritte haben von mir weder unmittelbar noch mittelbar geldwerte Leistungen für Arbeiten erhalten, die im Zusammenhang mit dem Inhalt der vorgelegten Dissertation stehen.

Die Arbeit wurde bisher weder im Inland noch im Ausland in gleicher oder ähnlicher Form einer anderen Prüfungsbehörde zum Zwecke der Promotion vorgelegt.

Ich bestätige, dass ich die Promotionsordnung der Fakultät Umweltwissenschaften der TU Dresden anerkenne.

.....

Ort, Datum,

.....

Unterschrift (Vorname Name)



## Acknowledgments

During my studying time at the Chair of Hydrology, Technische Universität Dresden, Germany, I have received many helps. From my deepest heart, I would like to thank all those who have provided me the excellent working environment and scientific stimulations.

First and foremost, I would like to thank my supervisor, Prof. Dr.-Ing. habil. Gerd H. Schmitz, for giving me the opportunity to investigate a fascinating subject under a professional guidance in the field of optimal design and operation of pressured water distribution networks. Also, he has advised and driven me throughout the process that led to this dissertation.

Foremost amongst my colleagues, I would like to express my appreciation to Dr. Jens Grundmann. This study would not have been possible without his enthusiastic, perseverant, practical guidance as well as his proof-reading my work.

I also appreciate the guidance and discussion from my colleagues: Prof. Dr. habil. Niels Schütze, Dr. Alaxander Gerner, Dr. Ruben Müller, Stefan Werisch, Sebastian Kloth, Dr. Andy Phillip, and Ayisha Mohammed Humaid Al Khatri during my study.

I would also like to express my gratitude to other staff members at the Chair of Hydrology for their kind advice and facilitation of my work, particularly, the secretary of the chair, Ms. Anke Deuchert and the technical staff, Ms. Jutta Hofmann.

Also, I thank my friends at the Technische Universität Dresden who encouraged me more than past four years.

For infrastructural and financial support, I wish to thank the Ministry of Education and training of Vietnam, Vietnam Forestry University, DAAD, and the “Gesellschaft von Freunden und Förderern der TU Dresden e. V.” (GFF).

Last but by no means least I thank my parents, my beloved wife, and my two little sons for patiently waiting for me through the years of my studying far away from home and for providing the necessary motivation for finishing in a timely manner.





## ABSTRACT

For cost and reliability efficiency, optimal design and operation of pressurized water distribution networks is highly important. However, optimizing such networks is still a challenge since it requires an appropriate determination of: (1) dimension of pipe / pump / tank - decision variables (2) cost / network reliability - objective functions and (3) limits or restrictions within which the network must operate - a given set of constraints. The costs mentioned here consist in general of capital, construction, and operation costs. The reliability of a network mainly refers to the intrinsic capability of providing water with adequate volume and a certain pressure to consumers under normal and extreme conditions. These contradicting objective functions are functions of network configuration regarding component sizes and network layout. Because considerable uncertainties finally render the overall task to a highly complex problem, most recent approaches mainly focus only on finding a trade-off between minimizing cost and maximizing network reliability. To overcome these limitations, a novel model system that simultaneously considers network configuration, its operation and the relevant uncertainties is proposed in this study.

For solving this multi-objective design problem, a simulation-based optimization approach has been developed and applied. The approach couples a hydraulic model (Epanet) with the covariance matrix adaptation evolution strategy (CMA-ES) and can be operated in two different modes. These modes are (1) simulation-based Single-objective optimization and (2) simulation-based multi-objective optimization. Single-objective optimization yields the single best solution with respect to cost or network reliability, whereas multi-objective optimization produces a set of non-dominated solutions called Pareto optimal solutions which are trade-offs between cost and reliability.

In addition, to prevent a seriously under-designed network, demand uncertainties was also taken into account through a so called “robustness probability” of the network. This consideration may become useful for a more reliable water distribution network.

In order to verify the performance of the proposed approach, it was systematically tested on a number of different benchmark water distribution networks ranging from simple to complex. These benchmark networks are either gravity-fed or pumped networks which need to be optimally designed to supply urban or irrigation water demand under specific constraints. The results show that the new approach is able:

- to solve optimization problems of pressurized water distribution network design and operation regarding cost and network reliability;

- to directly determine the pumping discharge and head, thus allowing to select pumps more adequately;
- to simulate time series of tank water level;
- to eliminate redundant pipes and pumps to generate an optimal network layout;
- to respond well to complex networks other than only to simple networks;
- to perform with multiple demand loading;
- to produce reliable Pareto optimal solutions regarding multi-objective optimization.

In conclusion, the new technique can be successfully applied for optimization problems in pressurized water distribution network design and operation. The new approach has been demonstrated to be a powerful tool for optimal network design not only for irrigation but also for an urban water supply.

## TABLE OF CONTENTS

ABSTRACT .....	vii
NOMENCLATURE .....	xi
1 INTRODUCTION .....	1
2 PRESSURIZED WATER DISTRIBUTION NETWORK DESIGN AND OPERATION: AN OVERVIEW .....	5
2.1 Basics of pressurized water distribution network .....	5
2.2 Major components of PWDN in design and operation .....	7
2.3 PWDN design and operation problems.....	8
2.4 PWDN analysis methods .....	10
2.5 Engineering aspects of PWDN optimization .....	13
3 CURRENT RESEARCH EFFORTS IN OPTIMAL PRESSURIZED WATER DISTRIBUTION NETWORK DESIGN AND OPERATION .....	17
3.1 Introduction of PWDN optimization approach.....	17
3.2 PWDN optimization terminology .....	18
3.3 Distinct objective functions .....	22
3.4 Optimization techniques applied in PWDN design and operation problems.....	28
3.5 Simulation-based optimization techniques .....	29
3.6 Uncertainty in PWDN optimization.....	33
3.7 Conclusions and open consideration for further study.....	35
4 A NOVEL APPROACH FOR AN OPTIMAL DESIGN OF PRESURIZED WATER DISTRIBUTION NETWORK .....	37
4.1 Introduction.....	37
4.2 Outline of methodology for the proposed approach .....	38
4.3 Epanet toolkit .....	43
4.4 Covariance matrix adaptation evolution strategy algorithm (CMA-ES) .....	43
4.5 A proposed approach for simultaneously optimizing network components and layout	47
4.6 The identification of significant solutions from the Pareto optimal front .....	48
4.7 An approach for solving uncertain demand problem.....	50

5	VALIDATION OF THE PROPOSED PRESSURE WATER DISTRIBUTION NETWORK DESIGN STRATEGY .....	55
5.1	Sensitivity analysis .....	55
5.2	Simulation-based single-objective optimization module (CMA-ES-EP) .....	60
5.3	Simulation-based multi-objective optimization module (MO-CMA-ES-EP).....	75
5.4	Considering uncertainties in water demand .....	86
6	APPLICATION OF THE NEW APPROACH TO A REAL WORLD CASE STUDY ..	89
6.1	Study area .....	89
6.2	MO-CMA-ES-EP application: Simultaneous optimal design and operation of a PWDN .....	98
6.3	Pump scheduling optimization .....	107
6.4	Network robustness under demand uncertainty .....	108
6.5	Discussion .....	110
7	CONCLUSIONS AND OUTLOOK .....	111
	References .....	115
	List of Figures .....	129
	List of Tables .....	133
	APPENDIX .....	135

## NOMENCLATURE

### Abbreviations

ACCOL	Adaptive cluster covering with local search
ACOA	Ant colony optimization algorithm
BB	Backbone
BEP	Best efficiency point
BOP	Best operating point
CMA-ES	Covariance matrix adaptation evolution strategy
CMA-ES-EP	Simulation based single-CMA-ES optimization model
GANEO	Genetic algorithm and Epanet
GAs	Genetic algorithms
GEO	Genetic evolution optimization
HN	Hanoi water network
HS	Harmony search
H-W	Hazen-William
LP	Linear Programming
MAF	Ministry of Agriculture and Fishery of Oman
MC	Monte Carlo
MO-CMA-ES-EP	Simulation based multi-objective - CMA-ES optimization model
NWIP	National wells inventory project
NFEs	Number of function evaluations
PML	Predefined maximum layout
PWDN	Pressurized water distribution network
SA	Sub-area
SAO	Simulated annealing optimization
SCE	Shuffled complex evolution
TLN	Two-loop network
TS	Tabu search

## Symbols

$AD$	annual duration (365 days)
$\alpha_1$	coefficient regarding power unit
$\alpha_2$	coefficient regarding the unit of pump discharge and head
$\alpha_3$	coefficient regarding unit conversion factor
$\alpha_4$	constant regarding tank cost
$\alpha_p$	penalty factor
$APPV$	annual pump presents value coefficient
$C$	diameter uniformity
$CLR$	layout reliability level of current network
$C_{pen}$	penalty function
$C_{penL}$	Penalty function of required layout reliability
$C_{penP}$	Penalty function for head constraint
$C_{penT}$	Penalty function for tank constraint
$C_{penV}$	Penalty function for velocity constraint
$C_{penW}$	Penalty function for water quantity
$CPUMP$	unit power cost of pump construction (monetary unit/kW)
$CS$	cost objective function
$C_{W-H}$	William Hazen coefficient
$D$	pipe diameter
$\Delta t$	time step
$D^T$	tank diameter
$\varepsilon$	permitted difference of water level in tank after one operating cycle
$EC_w$	electrical conductivity of irrigation water (dS/m)
$EP$	energy price
$E_s$	surface evaporative losses
$ET$	evapotranspiration
$E_{to}$	reference crop evapotranspiration
$\gamma$	specific weight of water
$H$	nodal head

$h$	head loss
$H_p$	pump head
$\eta_p$	pump efficiency
$H_r$	reservoir head
$HT$	water level in tank
$HT^{beginning}$	beginning water level in tank
$HT^{ending}$	ending water level in tank after one operating cycle
$HT_{max}$	maximum water level in tank
$Humid$	humidity
$I_e$	Irrigation efficiency of the system
$K_c$	crop coefficient
$LF$	leaching fraction
$LP$	pipe length
$Le$	leaching efficiency
$max.ECe$	Maximum tolerable electrical conductivity of the soil saturation extract for a given crop (dS/m)
$Mi. \$$	million US dollars
$MSHI$	minimum surplus head index
$nn$	number of nodes in the network
$np$	number of pipes in the network
$npump$	number of pumps in the network
$NR$	network resilience
$nres$	number of reservoirs in the network
$NRL$	network reliability function
$ntank$	number of tanks on the network
$\overline{OLR}$	required layout reliability level of an optimal network
$P_{friction}$	power lost in the network to overcome friction
$PIC$	pipe cost
$P_{input}$	total available power into a network
$P$	pressure
$popsize$	population size

$PP$	power dissipated by pumps
$PU$	pump
$PUC$	pressure uniformity coefficient
$PUCC$	pump construction cost
$PUOC$	pump operation cost
$q$	nodal demand
$Qp$	pump discharge
$Qr$	discharge out of reservoir
$RI$	resilience index
$\sigma_x$	standard deviation
$T (^{\circ}C)$	temperature
$TCC$	tank construction cost
$TSHI$	total surplus head index
$UWTC$	unit water level cost of tank (\$/m)
$UWTC(D^T)$	unit cost of tank with diameter $D^T$
$v$	flow velocity
$V$	annually capable of supplying water
$WR_{crop}$	water requirement for crop
$x_{ini}$	Initial decision variable
$X_j$	weighted surplus power at node j
$X_{max}$	maximum surplus power



## 1 INTRODUCTION

During the last decades, the gulf between decreasing freshwater availability and rising water requirements is increasing worldwide. Major reasons are, among others, population growth and the socio-economic development (OECD, 2010). These contradictory trends may possibly be balanced by an efficient water management. An optimally designed pressurized water distribution network is an important component in this regard. Pressurized water distribution networks (PWDN) are responsible for delivering water from sources to individual consumers in a required quantity and at sufficient pressure. They are widely used in water supply for domestic, industrial, and agricultural purposes.

In practice, a PWDN not only overcomes obstacles of traditional networks (i.e., open networks) but also provides considerable advantages in water distribution and allocation. PWDN reduces transmission losses caused by leakage and evaporation in open channels. In addition to the easier operation, maintenance, and management, PWDN can overcome the topographic difficulties. Using water meters within the PWDN, it is easier to establish water fees based on volumes of allocated water. This way, uncontrolled water exploitation can be avoided (Phocaides, 2000, Lamaddalena et al., 2005). Moreover, advances in manufacturing process and constructing techniques have considerably reduced the pipe investment compared to alternative techniques (Mays, 2004).

However, how acceptable a PWDN configuration can be for ensuring its main purpose under constraints of both cost and technical issues is still a problem. If any of the network components is under-dimensioned, it may cause the network to underperform, i.e., several demand nodes cannot be supplied with sufficient water quantity and pressure or, even, the network can fail. Moreover, inefficient networks cannot provide extra capacity for future growth. In contrast, an uneconomic network configuration is explicitly unavoidable. Both cases of under- and over-dimensioned design of any component can cause serious consequences and greater effort should be made to balance the risk against cost saving and technical issues in a PWDN (Nyende-Byakika, 2011).

Network layout optimization is a particularly crucial issue that has not received considerable attention. Most studies have been conducted with a given network configuration that can be either branched or looped. A branched PWDN is not preferred due to its lacking reliability. Failure or scheduled maintenance of any of the pipes would lead to a part of the network being cut off from the source nodes. In contrast, a looped network can overcome the drawback of a branched network (Swamee and Sharma, 2008). According to Afshar and Jabbari (2008), neglecting layout geometry optimization would not lead to the optimum network configuration.

Another problem is how uncertain factors (such as uncertainty of water demands, water sources, pipe roughness, status of devices, etc.) affect the hydraulic system. Due to the significance of uncertainties involved in the decision making process, the need for considering uncertainties in PWDN design and operation problem is obvious (Kapelan et al., 2005). Among the most uncertain conditions is the uncertain demand, as it directly impacts nodal pressure heads as well as other hydraulic parameters (Babayan et al., 2005; Sun et al., 2011). Consequently, developing a methodology which takes demand uncertainty into account when predicting the behavior of a PWDN is of great interest.

Thus, it is more reliable and economical to consider network components and network layout simultaneously under demand uncertainty.

In order to achieve a highly appropriate, efficient, satisfactory, and economical PWDN, it has to be designed in an optimal manner. The term PWDN optimization refers to a process of finding the most advantageous solution for a PWDN configuration, such as pipe diameters, pump and tank characteristics, as well as network layout. The optimally designed PWDN is able to transfer the required quantities of water from sources to consumers while satisfying some given constraints.

The primarily typically optimal PWDN design and operation problem is to find separately either the minimum solution for the total cost objective function or to maximize the network reliability. Both are functions of network configuration regarding component sizes and network layout. The total cost referred to here may consist of initial capital, construction, and operational costs, while network reliability expresses the capability of the network to overcome any failure and to guarantee the delivery of water to users under uncertainties. Recently, in terms of optimal PWDNs design, network reliability and total cost have been taken into consideration simultaneously. Therefore, multi-objective optimization approaches are the appropriate methods for these purposes. The concept of multi-objective optimal design of PWDNs may involve finding so-called Pareto optimal solutions, which are trade-offs between contradicting objectives.

Although many mathematical optimization algorithms have been developed and applied to the optimal PWDN design problems for last decades, there are still several obstacles for achieving the expected results. Some examples are: Only near optimum solutions are obtained; large number of function evaluations is required; or the process of finding suitable parameter set for the model is complicated. Hence, optimal approaches in the PWDN design sector need to be further researched, developed, and applied.

Very recently, together with the strong development of hydraulic modeling approaches and calculating techniques, simulation-based optimization methods, which are coupling of a hydraulic simulation model with an optimization algorithm, have received much attention in solving optimization problems in PWDNs design and operation. A simulation-based optimization model can be single objective- (Abebe and Solomatine, 1998; Reza and Martinez, 2006; Afshar and Jabbari, 2008) or multiple-objective functions (Todini, 2000;

Prasad and Park, 2004; Raad et al., 2009). The biggest advantage of the coupled hydraulic model is that conservation laws of mass and energy are automatically solved and checked; hence, the number of function evaluations of the optimization process can be considerably reduced (Walski et al., 2003).

However, an integral approach which simultaneously considers network configuration, its operation and the relevant uncertainties has not been developed yet.

Therefore, this study proposes a simulation-based multi-criteria approach which simultaneously considers an optimal design and operation of PWDN component sizes and its layout under uncertainty. The new model builds upon coupling a hydraulic model (Epanet) with the covariance matrix adaptation evolution strategy (CMA-ES). The main objective of the approach is to obtain the most suitable network configuration, i.e., trade-offs between total cost and network reliability for real world case studies under multiple demand loading, demand uncertainty, as well as additional hydraulic constraints.

The response to demand uncertainty is taken into account in order to consider network behavior through a so called “robustness probability” of the network. With the assumption that uncertain nodal demands follow normal distribution, the Latin hypercube sampling technique is used to evaluate the wide range of uncertain demand input variables. The corresponding hydraulic outputs are then evaluated by using a hydraulic model. The robustness probability of the network is finally computed as the ratio of the number of times that required constraints are met simultaneously in the whole network compared with the total number of samples.

In order to verify its performance, the proposed approach was systematically tested on a number of different benchmark water distribution networks ranging from simple to complex. These benchmark networks are either gravity-fed or pumped networks which need to be optimally designed to supply urban or irrigation water demand under specific constraints.

The exemplary application of the proposed approach is finally performed in a study area in the Batinah region (Sultanate of Oman). A pressurized water distribution network is designed including several pumps, tanks and a main pipe system responsible for distributing water from several kinds of sources to cultivate an area of around 3,750 ha which requires more than 54  $\text{Mi.m}^3/\text{year}$ .

The results showed that the new approach is able to simultaneously solve the common design and operation problems of a full water distribution network including network layout and size of pipes, pumps, and tanks under demand uncertainty.

The present work is divided into seven parts. The first part is the introduction. The second part provides basic background about hydraulics of pipe networks and PWDN design principles. State of the art approaches for solving optimization problems of a PWDN design are discussed in part three. This part also comes up with research gaps and outlines the proposed new approach for optimally designing a PWDN. The novel approach is presented

in detail in part four. To verify the capability of the new method, part five presents the comparison of optimization results for several benchmark networks. In part six the new method is applied to a real world case study to parts of the Batinah plain (Sultanate of Oman). Finally, the last part contains conclusions and an outlook.

## 2 PRESSURIZED WATER DISTRIBUTION NETWORK DESIGN AND OPERATION: AN OVERVIEW

### 2.1 Basics of pressurized water distribution network

According to Phocaides (2000); Mays (2000); Larock et al. (2000); and Trifunović (2006) open channel systems and pressurized water distribution networks are two major types of water distribution networks used for conveying water from sources to consumers. The selection depends on, among other factor, topography, head availability, economic considerations, construction conditions, and water quality.

In practice, the choice of an open channel network must involve the topography which will permit gravity flow from sources to consumers with low required pressures. This type of network has to cope with big losses due to evaporation and seepage if it is not unlined. The lifespan of open networks is not as long as expected and high costs for maintenance and repair are often required during their operation. In addition, the potential of pollution threat must be considered when transporting water for domestic purpose.

In contrast, a PWDN does not only overcome obstacles of traditional networks (i.e., open networks), but also provides considerable advantages in water distribution and allocation (Phocaides, 2000). By using a PWDN, water supply to consumers can be achieved with both sufficient discharge and pressure requirements. Due to the high efficiency of PWDN, water loss through conveying process caused by leakage and evaporation can be negligible. Consequently, with the same volume of withdrawn water more users may be supplied. In addition to their easier operation, maintenance, and management, PWDNs can overcome topographic difficulties. Moreover, they make it easier to establish water fees based on volume of consumed water by using water meter that aims to avoid uncontrolled water exploitation (Lamaddalena et al., 2005). Advances in manufacturing processes and constructing techniques have considerably reduced the capital investment compared to open canals (Mays, 2000).

Due to numerous advantages, PWDNs have become remarkably competitive as an infrastructure for delivering water from sources to consumers with an appropriate pressure for various loading conditions (May, 2000).

However, there are also critical problems with regard to both design and operation of a PWDN. Designing and operating a PWDN is a multidisciplinary task solving both technical and economical issues (Nyende-Byakika, 2011). For each PWDN configuration, solving technical problems commonly means the consideration of hydraulic conditions, i.e., balancing flows, head losses, velocities, and nodal pressures (or nodal heads). The economic issues

mentioned here may involve capital, construction, and operation costs. A successfully designed PWDN requires a balance between these two issues, yet this aspect has not received much attention. Therefore, an optimal approach for designing and operating a PWDN plays a significant role.

A typical PWDN generally consists of four major, interconnected components which represent the zones in which the components operate (Mays, 2000), namely, (i) Sources of water: reservoirs, rivers, wells, wastewater treatment plants, and so on; (ii) Interconnected pipes that carry water between sources and water users; (iii) Pumps used to feed water into the network; and (iv) Tanks.

PWDN can also include some kind of valves. Pressure reducing valves (PRV) are used to limit the pressure at a point in the network. Pressure sustaining valves (PSV) are placed to maintain a predefined pressure at a specific point. Flow control valves (FCV) are installed to limit the flow to a specified amount. Shutoff valves and check valves are used to completely open or close pipes which they are placed.

Pipes in a PWDN are connected by nodes which are associated with an elevation. Nodes refer to connected points at the end of pipes and can be either demand nodes or non-demand nodes. Demand nodes represent flow out of the network required by consumers. Reservoirs and tanks are referred to as fixed-grade nodes.

All these components are interconnected by either branched (Figure 2.1) or looped layout (Figure 2.2). Looped PWDNs are preferred from the reliability point of view. In looped structures, there may be several different pipes which transfer water from sources to a particular demand node. Therefore, they can still supply water to consumers if one or more pipes are closed for maintenance or because of failure.

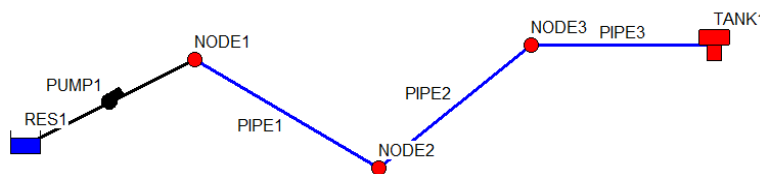


*Figure 2.1: A simple branched PWDN including a reservoir, a pump, a tank, 3 nodes, and 3 pipes*

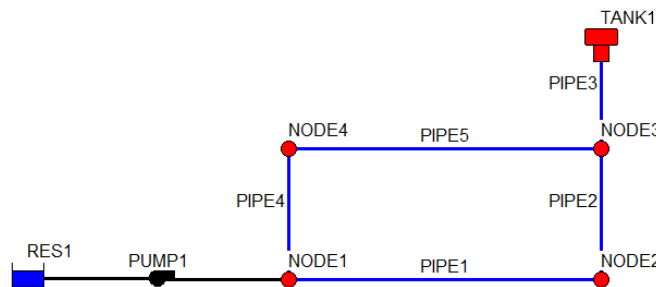


*Figure 2.2: A simple looped PWDN*

Flow conditions in a PWDN are analyzed by using the continuity equation and equation of energy (Appendix A). According to Bhawe (1991) and Swamee and Sharma (2008), these governing laws for flow in a PWDN were formulated with respect to steady flow in which the flow properties are independent of time. However, during the operation of a PWDN, water demand commonly changes from time to time depending on the behavior of consumers. Consequently, the network is not supposed to operate under steady conditions. These changes in demand will lead to unsteady flow. Due to the complex analysis with respect to unsteady flow, a more restrictive concept is usually used: “*A flow is considered to be steady if the temporal mean velocity does not change over brief periods*” (Larock et al., 2000). Also, with respect to the performance of a large PWDN, the changes in demands are normally slow and not enough to cause sudden effects on flow. Furthermore, the elastic effects of pipes can be ignored and water demands in a PWDN change discretely, not sequentially. Flow conditions in such a situation can be considered to consist of a series of steady-state flows.

## **2.2 Major components of PWDN in design and operation**

Pipes, pumps, and tanks in a PWDN are considered as major components, in which each one is closely related with the others (Mays, 2000; Larock et al., 2000).

Pipes are the primary components and also the largest capital investment in a PWDN. Pipes are commonly manufactured in different diameter sizes, according to the global standard, as well as from different materials such as steel, polyvinyl chloride (PVC), cast or ductile, asbestos cement, reinforced or pre-stressed concrete, polyethylene, and fiberglass.

The interdependency of characteristics like pipe length and diameter, flow, head loss, and velocity in each individual pipe can be represented by one out of the three head loss equations, i.e., Darcy-Weisbach, Hazen-William, and Chezy-Manning. This relationship generates a so-called system curve in which head increase will lead to discharge increase, and vice versa (red curve line in Figure 2.3).

Pumps in PWDNs are considered to be the heart of the system. They are responsible for supplying energy to flow in network. The relationship between pump discharge ( $Q_p$ ) and pump head ( $H_p$ ) can be expressed by a pump curve, in which the amount of pump discharge increases with decreasing total pump head and vice versa. As regards pumped PWDNs, total pump head consists of static head and friction head. The static head is the difference in height that the pump will be required to provide. Friction head is power used to overcome losses due to friction and local obstruction.

Another pump characteristic is pump efficiency, which is a function of pump discharge and head. To make a PWDN with pumps as efficient as possible, a pump curve must be designed to match the system curve, so that the pump operates at or close to the best efficiency point (Figure 2.3).

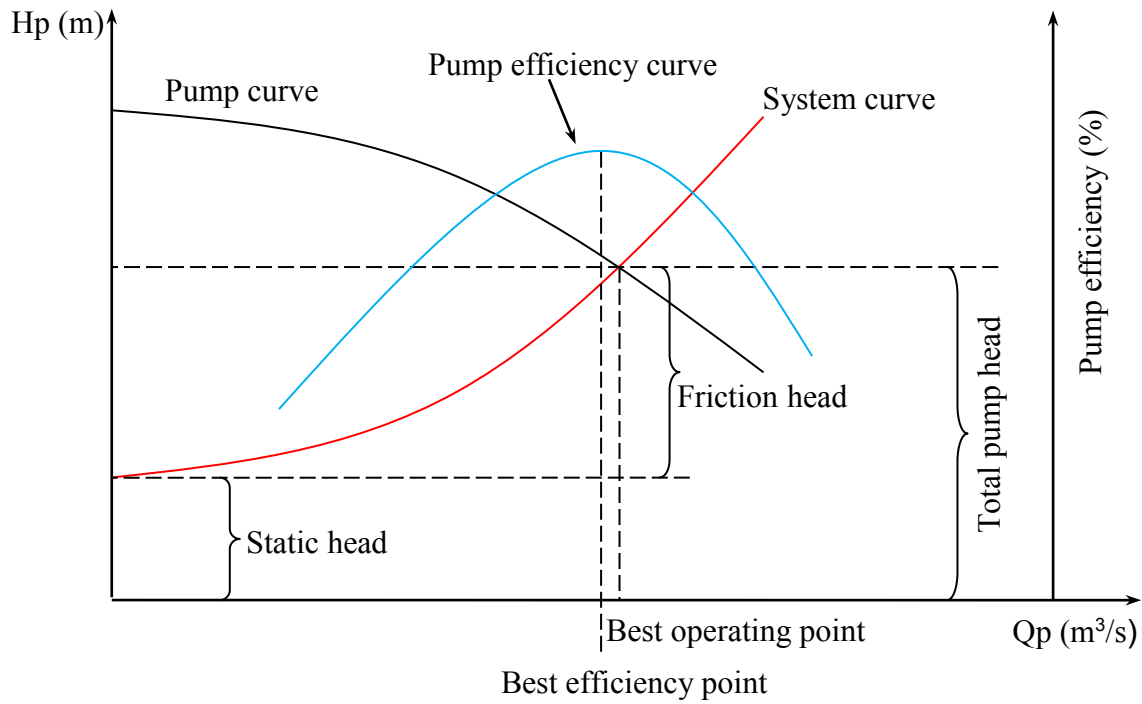


Figure 2.3: A typical pump curve along with system curve (Mays, 2000)

Tanks are commonly used in pumped PWDNs due to their low investment but high benefits (Vamvakeridou-Lyroudia et al. 2007). One of the largest tanks' benefits is that they can store a specific water volume pumped in the low (peak off) demand period and can return water to the network at the peak demand period. Therefore, they can reduce the peak pumping discharge at the peak period. Because the energy cost is commonly highest in the peak consumption time, this leads to reduced operational costs. Also, they can provide an energy head.

Other advantages are the ability to reduce pipe sizes, to improve operational flexibility and efficiency, and to prevent hydraulic transient. In general, large tanks with considerable volume can meet all the above functions while small tanks are often used for maintaining head regulating purpose.

Apart from that, pumps are not necessary to instantaneously respond to the corresponding changes in demands if tanks are included in the network. Hence, highly efficient but less expensive constant pumps become a suitable choice (Vamvakeridou-Lyroudia et al., 2007)

However, it is very complicated designing and operating a PWDN in an optimal manner when there is a considerable number of tanks connected to the network. Numerous issues need to be considered when designing tanks, such as their locations shape, volume, initial water volume, maximum and minimum level, etc.

## 2.3 PWDN design and operation problems

The major objective of PWDN design and operation is to ensure that there is sufficient pressure at the node of water supply to provide an adequate water allocation to consumers in



the most reliable and economic way under several uncertain conditions such as water use demand, uncertain measurements, estimated parameters, etc.

Many authors agree with the point of view that the question whether consumer demand is satisfied or not mostly depends upon the amount of water fed into the network (Rossman, 2000; Nyende-Byakika et al., 2010). By using an example of the PWDN which was constructed in Kampala City (Uganda), Nyende-Byakika et al. (2011) demonstrated that there are still a lot of complaints from consumers due to insufficient supply as well as due to heads lower than required in several local nodes, though daily inflow into the network is likely to be higher than the sum of daily demand. By emphasizing the urgent necessity for an adequately designed PWDN, they conclude that *“the culprit to system underperformance is not necessarily production but the distribution network”*. This means that many questions need to be answered. How big should each network component be to supply water under required amount and pressure? How reliable must a network configuration be to avoid shortage or failure? How much is a network cost to be an economic solution? An adequately designed PWDN is fundamentally based on the understanding of the non-linear network behavior under different conditions.

In order to comprehensively understand the behavior of a network, the impact of network configuration and different sources of uncertainty have to be considered and managed. For instance, a constant discharge of 18,726 m<sup>3</sup>/h is supplied to a node at elevation of 0.0m from a reservoir at elevation of 97.23 m through a pipe (100 m of length) whose diameter can be changed from 800 mm to 2000 mm. A negative nodal pressure at (-12.85 m) was yielded with diameter 800 mm due to very high unit head-loss (81.54 m/km) and velocity of 10.35 m/s.

In general, the bigger the diameter, the higher the pressure but the lower the velocity and the head-loss (Figure 2.4). The aim of PWDN design is to raise nodal pressure in order to supply a sufficient demand and volume to consumers. However, this is likely to be a costly solution.

Together with the impact of network configuration, hydraulic parameters are also directly impacted by varying demands. Figure 2.5 expresses the impact of various flows on hydraulic conditions in a network with constant pipe diameter. It can be proved that the bigger the flow in pipe, the lower the pressure but the higher the velocity and the head-loss.

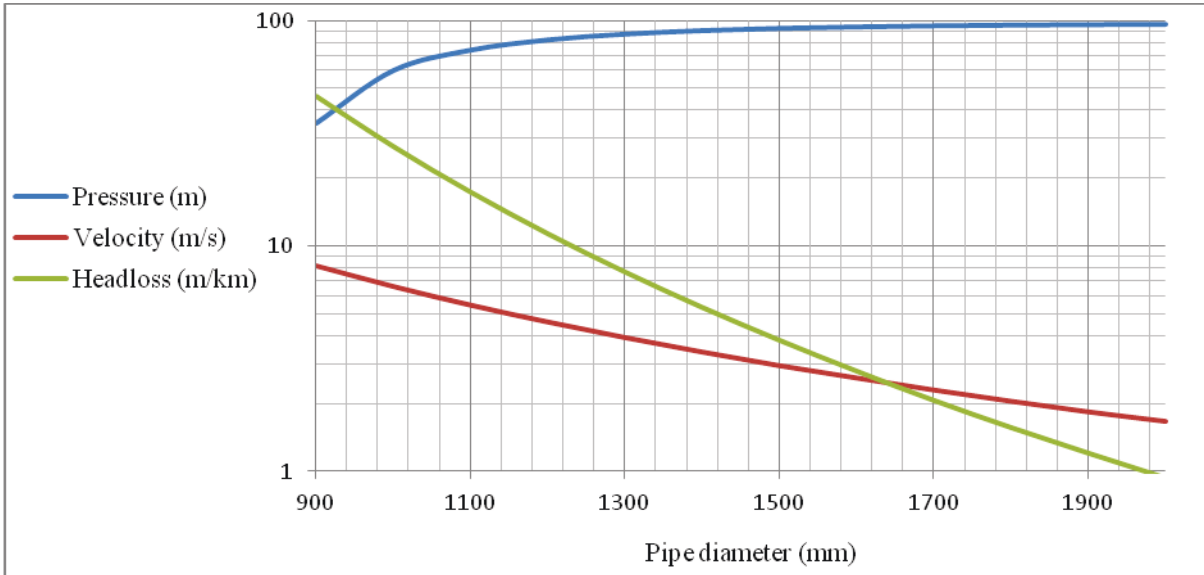


Figure 2.4: An outline of non-linear impact of various pipe diameter on nodal pressure (m), flow velocity (m/s), and unit head-loss (m/km)

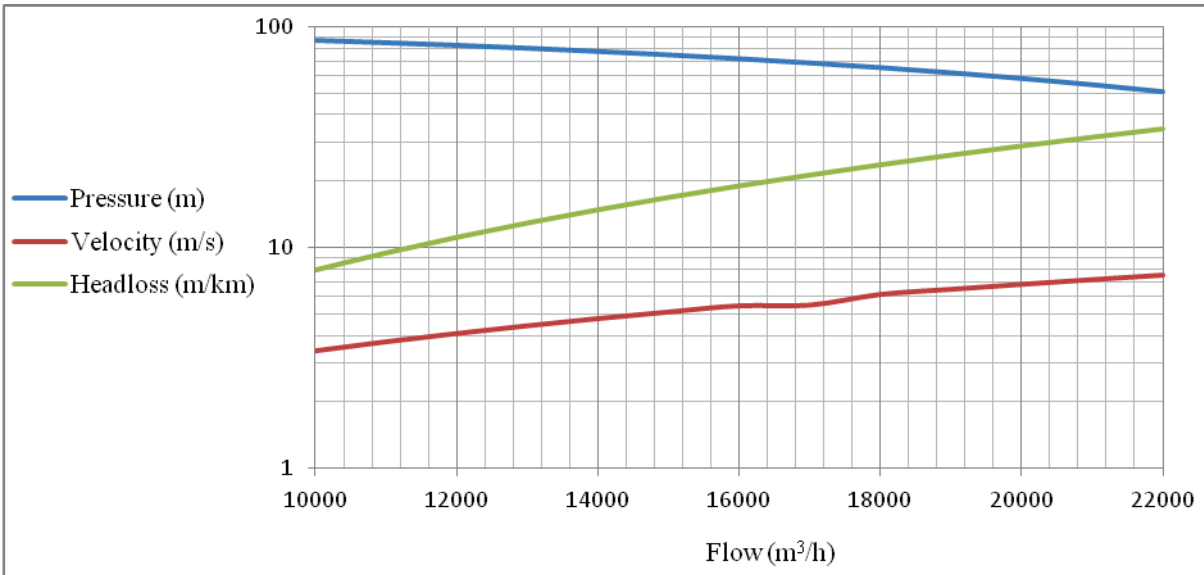


Figure 2.5: Non-linear impact of various flows on nodal pressure (m), flow velocity (m/s), and head-loss (m/km) in a constant pipe diameter of 1016 mm.

## 2.4 PWDN analysis methods

### Mathematical modeling approaches

Regarding a very simple network, hydraulic parameters can be solved using laws of conservations of mass and energy. However, a real PWDN does not consist of only a single pipe or node; therefore, it cannot be calculated by a single set of continuity and energy equations. On account of non-linear relationship of the conservation equations, it is impossible to solve a complex network analytically. For a really complex PWDN, which can

encompass hundreds main pipes and nodes, the number of these equations can reach thousands. In fact, the more loops a PWDN has, the more sophisticated is the calculation.

For solving these non-linear equations, there are four popular systematic approaches written in one out of three forms: node, loop (flow equations), and pipe equations. These approaches require iterative solution schemes (Bhave, 1991; Swamee and Sharma, 2008).

(1) Hardy Cross method: This is an application of Newton' method in order to improve computational efficiency for complex network. The conservations of mass and energy are expressed in term of flows (flows are principally unknown and are assumed to satisfy the conservation of mass at each node). At each step of the process, a correction  $\Delta Q$  is determined for each loop. The corrections are developed so that they maintain conservation of mass. Based on these corrections, flows are continuously updated until the correction value is less than a defined tolerance.

(2) Newton-Rapson method: In this method, the node equations are the conservation of mass relationships written in term of the unknown nodal heads. At each iteration, this method is applied to the set of nodal heads for determining unknown corrections  $\Delta Q$ .

(3) Linear theory method: This method solves also the loop equations, in which pipe flows are unknown parameters using the linearized energy conservation. Flows can be obtained by solving this set of linear equations

(4) Gradient method: This method was written in the form of pipe equations. Unlike the previous forms, the pipe equations solve flows and nodal heads simultaneously. In which, conservation of mass at a node is linear but the component flow equations are non-linear. For solving this, an iterative scheme is required. The component flow equations are linearized using the previous evaluations.

More detailed description and comparison of these methods can be found in Bhave (1991) as well as in Swamee and Sharma (2008).

Computer programs which utilize these approaches are known as mathematical hydraulic models or hydraulic simulators. Several well-known hydraulic models have been developed and frequently applied (Mays, 2000), such as Epanet (US EPA, Rossman, 2000), InfoWater (Innovyze company), HydroNet (Tahoe design software), Kypipe (University of Kentucky), WatDis (Lewis publishers), etc. These sophisticated models can provide many advantages:

- They can simulate the flow dynamic behavior, track the water flow in each pipe, pressure (or head) at each node, tank water level variation, and so on, during simulation process.
- They can provide very sophisticated and intuitive graphic as well as the full library of hydraulic network components including pumps, tanks, and valves characteristics with information management systems. These utilities make it much easier for

engineers to construct, calibrate, manipulate, visualize, modify, and communicate what is happening in the network.

- They are able to link to other software such as CAD (computer aid design), GIS (geographic information system), spreadsheets, etc.
- They are capable of solving other kind of network analyses such as optimal pipe sizing, optimal operating.

Despite of their usefulness for conceptualizing, these simulators are computationally time consuming and require modeler's experiences as well, especially with regards to complex PWDNs including multi-input sources, pumps, and tanks.

### *Epanet*

Amongst the hydraulic models, Epanet (Rossman, 2000) is evaluated by many researchers as the one mostly used due to its stunning capabilities (Abebe and Solomatine, 1998; Todini, 2000; Liong and Antiquazzaman, 2004; Geem, 2006; Reza and Martínez, 2006; Afshar, 2008, Vasan and Simonovic, 2010; Baños et al., 2011).

In principle, Epanet is based on the Gradient Method introduced by Todini and Pilati (1988) and applies one out of the three friction head loss formulas, i.e., Darcy-Weisbach, Hazen-William, and Chezy-Manning, to pipes as well as minor head loss to bends, fittings, etc. for determining the hydraulic properties occurring in the network during operation. By using Epanet, it is clearly recognized that conservation equations of mass and energy are always satisfied (Vasan and Simonovic, 2010). Epanet provides a fully equipped and extended period simulation which consists of a series of steady-state flows caused by any change in water demand, water level in reservoir and tank, and so on. Therefore, Epanet can immediately demonstrate the hydraulic properties at any node and pipe at a specific period of time. Epanet can also express the results of analyses under various convenient types such as table and graph. Particularly, contents of the standard Epanet input data file (\*.inp file - see Figure 2.6), which describes the network being simulated, can be analyzed, interpreted, and stored in a sharable memory area and can be assessed by a specific tool. This file can either be created external Epanet or by Epanet itself. The capability of the Epanet simulator can be outlined as in Figure 2.7.

Network components	System operation	Water Quality	Options and reporting	Network Map/Tags
[TITLE]	[CURVES]	[QUALITY]	[OPTIONS]	[COORDINATES]
[JUNCTIONS]	[PATTERNS]	[REACTIONS]	[TIMES]	[VERTICES]
[RESERVOIRS]	[ENERGY]	[SOURCES]	[REPORT]	[LABELS]
[TANKS]	[STATUS]	[MIXING]		[BACKDROP]
[PIPES]	[CONTROLS]			[TAGS]
[PUMPS]	[RULES]			
[VALVES]	[DEMANDS]			
[EMITTERS]				

Figure 2.6: Contents of the standard Epanet input file (Rossman, 2000)

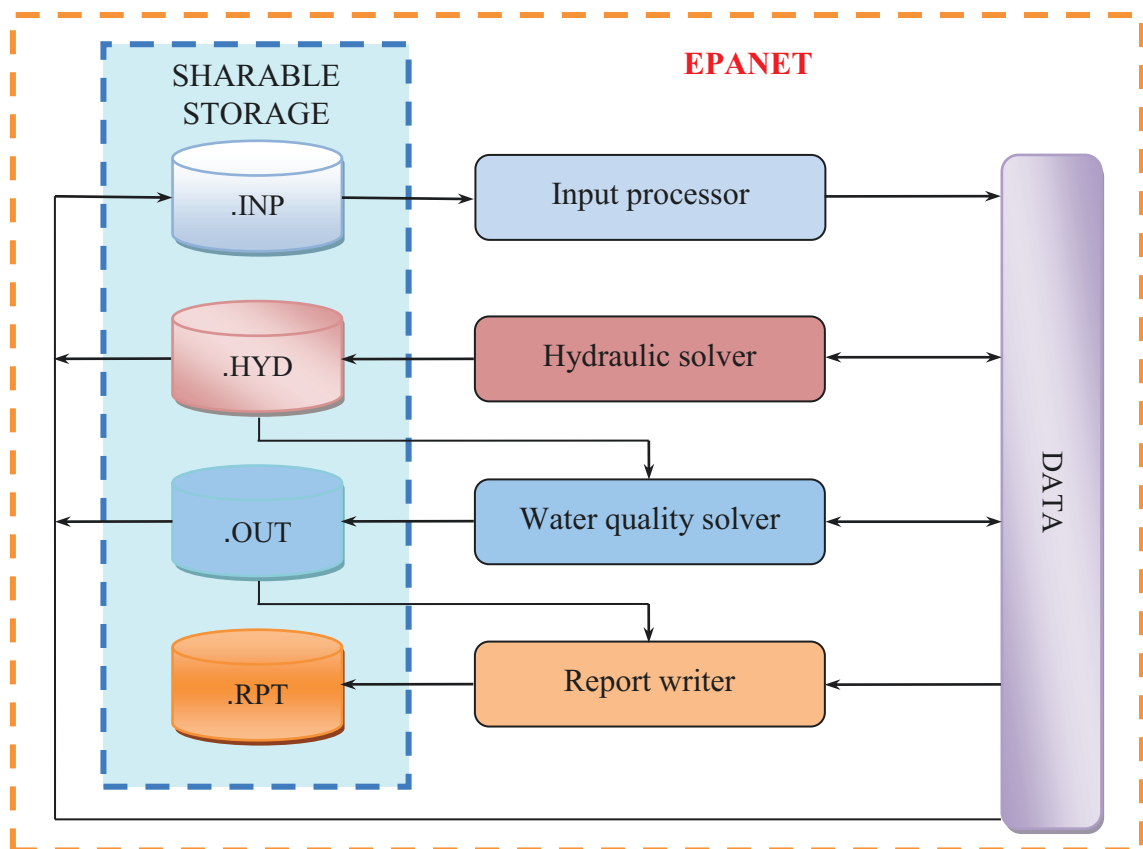


Figure 2.7: Outline of the Epanet capability (derived from Rossman, 2000)

## 2.5 Engineering aspects of PWDN optimization

From the engineering point of view, the objective of PWDN optimization is to decide what features are important and to retain them in defining the PWDN design and operation. For

large PWDN the following aspects need to be considered during the design and operational process.

### *Network layout*

It is commonly accepted fact that optimal designed PWDNs were commonly obtained by addressing a “given layout” for the network to be optimally designed. Studies seemed to neglect the relationship between component sizes and network layout due to the complexity of layout optimization. In fact, with respect to a large PWDN some appropriate solutions with different network layouts usually occur during the optimization process. Moreover, pipe size optimization without considering the network layout may not lead to an optimal network configuration (Afshar and Jabbari, 2008).

### *Multiple demand loadings*

Another vital aspect of defining a PWDN is to determine which demands should be specified. In practice, water demands vary during a day or from day to day. A single demand pattern was considered for optimal design of PWDNs

To simulate the behavior of a PWDN to variation of water demands with time, the concept of extended period simulation is used (Larock et al., 2000). Extended period simulation relies on demand changes in which new parameters are formed based on the updating over a time increment of the past parameters. The following characteristics commonly vary with demand changing that need to be determined with each step of time:

- Piezometric heads (or pressures) at each node;
- Flow rate, head-loss and velocity in each pipe;
- Water surface level in tank;
- Pump’s characteristics

### *Data uncertainty*

Since a PWDN is commonly designed and planned with a predicted future data, it may have to meet uncertain conditions during its operating lifespan. A number of major technical uncertain conditions in its performance can be considered in two types. The first is hydraulic uncertainties, which refer to uncertainties such as demand prediction and cost estimation. The other one is mechanic uncertainties, which refer to uncertainties of network configuration regarding components and network layout (Farmani et al., 2006).

Out of these hydraulic uncertainties, together with analyses in Section 2.3, water demand uncertainty is supposed to directly impact every parameter in a PWDN; in other words, impact directly hydraulic conditions within the system (Babayan et al., 2005; Kapelan et al., 2005; Sun et al., 2011).

### *Multi-input water source*

PWDN can take its charge from a single source or from multi-source provided that the chosen source of supply is large enough to satisfy various water demand conditions, and is capable of meeting the maximum demand during operating scheduling. In general, a multi-source PWDN is planned since mostly it is impossible to extract water from single source due to an overall high water demand. According to Swamee and Sharma (2008), multi-input water network can reduce the pipe sizes of the system because of distributed flows. However, this adds extreme difficulties to the optimal design of a PWDN. The flow directions in some pipes are not unique and can change because of the spatial or temporal variation in water demands as well as due to the input source supplying flows the network.

Obviously, the non-linear relationships amongst network components are very sophisticated and difficult to understand even for quite small networks. Adding more engineering aspects as mentioned above makes the optimal PWDN design and operation procedure become a big challenge. However, it would be worth-while to consider these aspects together in a PWDN optimization process. Theoretically, this challenge can be solved using a modeling approach, but it is time consuming and laborious.





### 3 CURRENT RESEARCH EFFORTS IN OPTIMAL PRESSURIZED WATER DISTRIBUTION NETWORK DESIGN AND OPERATION

#### 3.1 Introduction of PWDN optimization approach

PWDN optimization is simply another type of modeling approach (Walski et al., 2003) and is one of the most well-researched areas in the hydraulics profession (Djebedjian et al., 2005). In order to overcome the time consuming issue of the modeling approach, the optimization approach in PWDN provides an efficient way of automatically adjusting a broad range of network components which will be changed to get the “best” or an “optimal” configuration. From a technical point of view, network configuration relates to cost and network benefit. The bigger the network components, the larger are capital cost and network benefits and vice versa.

To apply an optimization approach in accordance with the objective of PWDN design and operation, the problem can be generally stated as follows (Mays, 2000):

Objective function(s): Minimize total cost and/or Maximize network benefit

Subject to:

- Conservation laws of mass and energy
- Water demand, nodal head requirements, constraints related to design/operational parameters and network layout as well.

Figure 3.1 shows a typical PWDN optimization problem

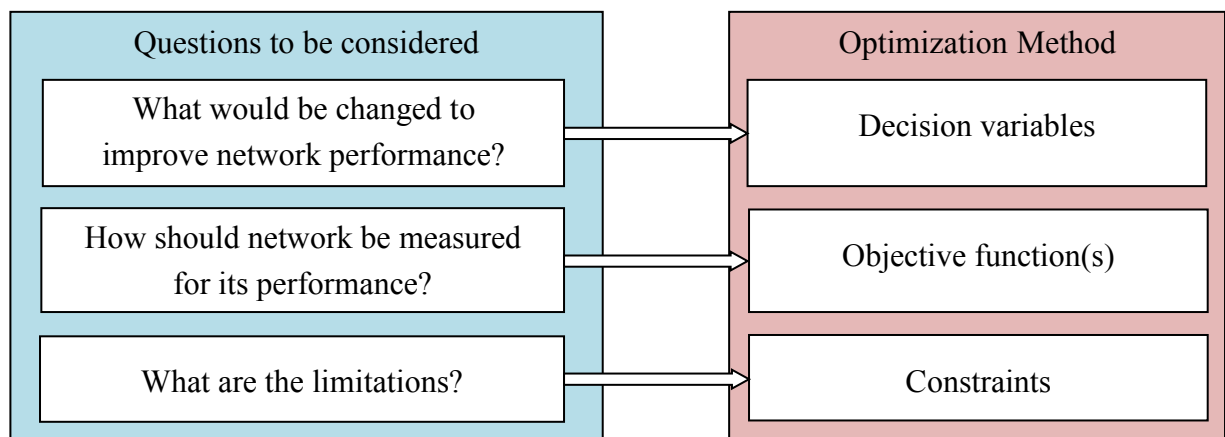


Figure 3.1: A typical optimization formulation procedure (Walski et al., 2003)

### 3.2 PWDN optimization terminology

As to PWDN design and operation optimization problem, the procedure mentioned above is a challenge that requires an appropriate determination of: (1) decision variables (2) objective functions, and (3) a given set of constraints.

#### 3.2.1 Decision variables

The quantifiable decision variables are the numbers of unknown parameters which can be changed to improve the performance of a PWDN. With respect to specific PWDN design pipe, pump, and tank's characteristics can be considered as decision variables in a process of optimization. Any limitation to each kind of decision variables must be clearly stated in the beginning of the optimization process (Walski et al., 2003). For example, a set of available discrete pipe diameters needs to be given for the optimal design of pipes. Based on objective function, the optimal design procedure will select alternative pipe diameters taken only out of this set.

#### 3.2.2 Objective function in PWDN design optimization

A mathematical equation that formulates the relationship among terms of decision variables and seeks to optimize (that is, minimize or maximize) is called an objective function. Depending on the number of objective functions, PWDN design optimization can be either a single or a multi-objective optimization method.

##### *Single-objective optimization in PWDN design*

The aim of using single objective PWDN optimization is to find either the “least cost” or “most benefit” solution.

Cost is likely to be the primary, most frequent emphasis in PWDN design. It would commonly be divided into two main groups of cost: (i) initial capital cost used for purchase and construction of pipes, pumps, tanks, etc.; and (ii) operation costs for energy consumption to operate the system over time (Mays, 2000). As expressed in Figure 3.2, initial capital cost increases as pipe diameter increases, while operational cost decreases. These two contradicting trends cause the total cost at first to decrease to minimum value and then to increase with increasing pipe size. Pipe diameter corresponding to this minimum cost value would be selected (Larock et al., 2000). Generally, the total cost ( $CS$ ) objective for optimizing PWDN is the function of nodal head ( $H$ ) and the size of various design/operation decision variables ( $D$ ) (Eq. 3.1).

$$\min(CS) = \min(f_C(H, D)) \quad (3.1)$$

It is clear that the least-cost PWDN design produces the optimum solution that consists of possible smallest sizes of components under specific constraints. However, a frequently

asked question arising from this is how reliable the behavior of the least-cost designed PWDN will be in case any failure or uncertainty occurs. For instance, suppose that a PWDN is designed properly with water being delivered at each node satisfying the nodal demand in terms of design flows and required piezometric pressures (or heads). As analyzed in Section 2.2, whenever demand increases the water flow will increase; consequently, the original hydraulic condition will be transformed into a new one with higher internal head losses and velocity. This problem can be solved by considering more objective functions together with cost optimization. A network benefit called “network reliability” (NRL) has received much attention recently (Todini, 2000; Prasad and Park, 2004; Araque and Saldarriaga, 2005; Cheung et al., 2005, Araque and Saldarriaga, 2006; Raad, et al., 2009). Network reliability of a PWDN mainly refers to the intrinsic capability of providing water to consumers with adequate volume and required pressure under normal and extreme conditions (Farmani et al., 2006). In this regard, the optimization procedure often finds the maximum network reliability which is also a function of nodal head ( $H$ ) and size of decision variables (Eq. 3.2).

$$\max(NRL) = \max(f_{NR}(H, D)) \quad (3.2)$$

From the reliability point of view, a PWDN with largest selected pipe diameters will have smallest head losses within the network and the capability of water supply will likely be maximal. However, this selection will lead to the most expensive investment. In order to obtain a trade-offs solution between cost and reliability, a multi-objective optimization approach will be employed.

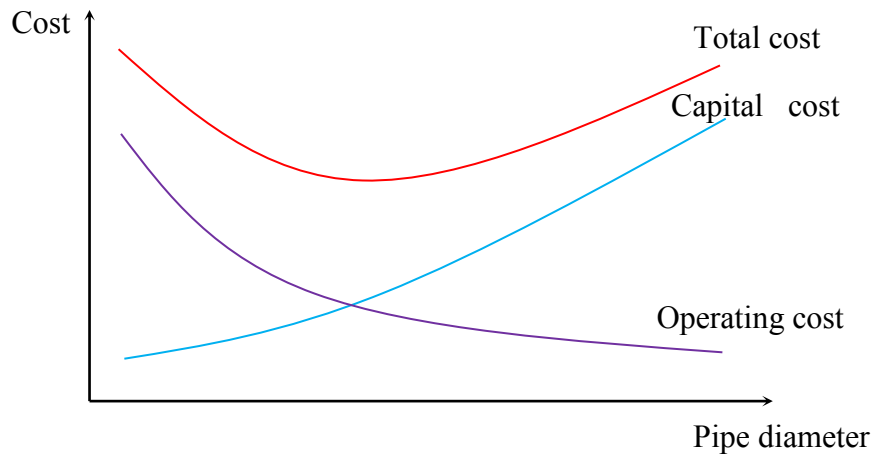


Figure 3.2: Total cost of a PWDN as an objective function of pipe diameter (Lock et al., 2000)

#### *Multi-objective optimization in PWDN design*

Basically, the principle of multi-objective optimization is different from that of single-objective optimization. In multi-objective design optimization of a PWDN, two contradicting single-objective functions mentioned above (Eq.3.1 and 3.2) can be simultaneously integrated in one model in which one objective function computes total cost while the other

one computes network reliability. In this case, the interaction among different objective functions in the optimization process will produce a set of trade-off solutions between two contradicting objectives, known as Pareto optimal solution (or Pareto optimal front) (Figure 3.3). No solution on the Pareto optimal front is dominated by any other solution with respect to all objectives. Pareto optimal front provides alternative solutions offering a wide range of costs and network reliability, fulfilling the role of a decision support tool for designers.

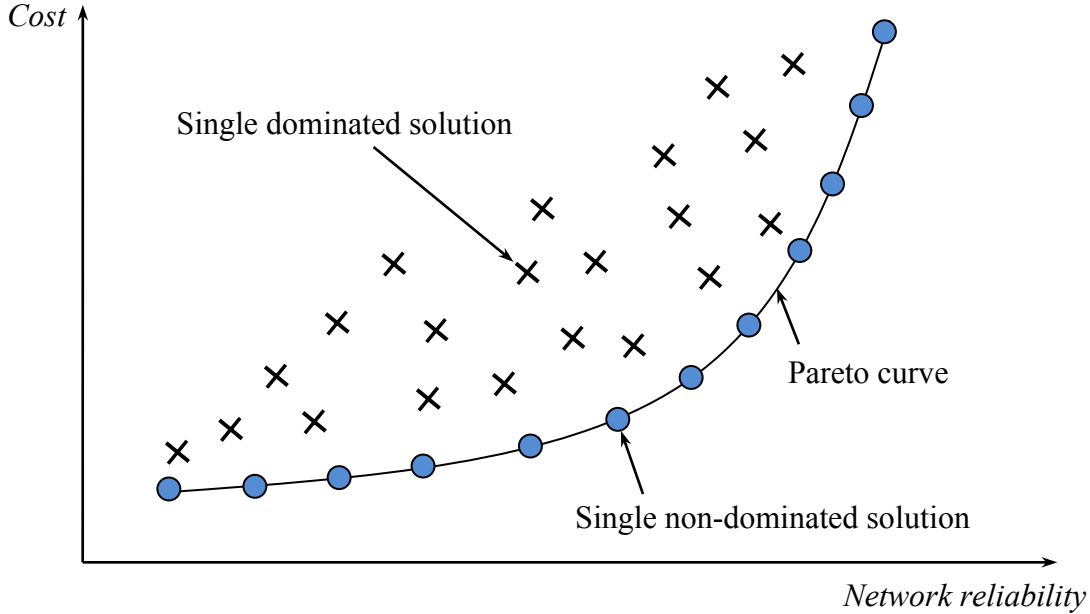


Figure 3.3: Pareto solutions of two contradicting objective functions (Walski et al., 2003)

### 3.2.3 Constraints

When finding the best or optimal solution for a PWDN design and operation, it is notable to consider the limiting conditions in which the system will be designed and operated in an economic and technical manner. These limiting conditions are called constraints and they serve to define the decision variable space that is the set of all possible solutions to the problem (Walski et al., 2003). In general, those constraints can be defined as follows:

#### (i) Laws of conservation of mass and energy

These constraints have general mathematical forms of (Eq.2.1 and Eq.2.2 in Appendix A) which include a set of nonlinear equations associated with flow and head loss relating to the selected design variables, nodal heads, and nodal demands. These equations need to be satisfied at each node or in each pipe or loop.

#### (ii) Decision variables constraints

$$D_i^{min} \leq D_i \leq D_i^{max} \quad (3.3)$$

$D^{min}$ ,  $D^{max}$  are permitted minimum and maximum decision variables, respectively, that specify physical limitations from which components may be selected. Decision variables can be pipe, pump, and tank characteristics.

*(iii) Nodal head bounds*

$$H_i^{min} \leq H_j < H_i^{max} \quad (3.4)$$

$H^{min}$ ,  $H^{max}$  are permitted minimum and maximum nodal pressure heads at node, respectively. These limits are often prescribed for each node. The lower bound is likely related to required outlet equipment, whereas the upper bound may be for maintaining structural integrity or for maximum working pressure of pipe material.

*(iv) Constraints related to other design parameters*

$$W_i^{min} \leq W(H(D)) \leq W_i^{max} \quad (3.5)$$

A general set of constraints (i.e. in the form of Eq.3.5) may be used to express limitations regarding hydraulics and design variables. Common limitations refer to flow velocities in each pipe, pumps and tanks operational conditions, water quantity and so on.

*(v) Constraints related to layout optimization*

Todini (2000) demonstrated that the approach of optimum cost optimization inevitably leads to a branched network layout unless specific constraints are added. In order to avoid this, an additional constraint (Eq. 3.6), proposed by Afshar and Jabbari (2008), can be used when simultaneously optimizing both network components and layout. Firstly, a maximum layout including all possible candidate links will be generated. Theoretically, this layout encompasses many pipes. However, considerable pipes can be reduced due to physical conditions such as road, basic infrastructures, topography conditions, etc. to get a simpler network layout, which is referred to as “predefined maximum layout”. In the process of optimizing the predefined maximum layout to achieve the optimal network, it is necessary to add a proper layout reliability constraint that is used here as:

$$CLR \geq \overline{OLR} \quad (3.6)$$

where  $CLR$  is the layout reliability of current network. It is defined as the minimum number of independent pipes connecting to a node out of all nodes of a current network.  $\overline{OLR}$  is the required layout reliability level of an optimal network. It is a given minimum number of independent pipes connecting to a node out of all nodes to generate the optimal network layout.

In fact, a node of a PWDN may have only one or several pipes connecting to it. It is clear that a designed network layout would likely be either branched or looped as  $\overline{OLR} = 1$ , otherwise, it would surely be a looped layout as  $\overline{OLR} \geq 2$ .

### 3.3 Distinct objective functions

#### 3.3.1 Cost objective function

Cost objective often relates to capital and operational costs. Capital cost is for buying and constructing pipes, pumps, and tanks, whereas operational cost is for pumping energy, maintenance, etc.

##### (i) Pipe cost (PIC)

Investment for pipes in a PWDN, which is the most expensive and depends on network configuration, can be evaluated as in Eq. 3.7:

$$PIC = \sum_{i=1}^{np} f_l(D_i, L_i) \quad (3.7)$$

With  $f_l$  is an appropriate cost function of pipe diameter ( $D_i$ ) and length ( $L_i$ ).  $np$  is the number of pipes in the network.

It is clear that when a PWDN is optimized using a given network layout, the cost depends only on the pipe diameters. However, when network components and layout of a PWDN are simultaneously optimized, the cost likely depends on all these elements.

##### (ii) Pump cost

Pumps must be designed with optimal construction and operational cost. The lifetime operating cost can be about hundred times of its constructional cost, because “*pumping is a very energy-intensive process*” (López-Ibáñez et al., 2008). Tarquin and Dawdy (1989) demonstrated that the saving rate is estimated at only 5% reduction of the total power consumed for water supply; that makes the United State, e.g., save approximately \$48,000,000 a year.

Generally, pump construction and operational cost relate directly to pumping discharge and head. Therefore, in this study, pumping discharge and head are considered as decision variables for optimal pump design, while pump efficiency is considered as constant.

\* Pump construction cost ( $PUCC$ ), which is the direct cost incurred in constructing facilities, such as the cost for materials, labor, and equipment, depends mainly on maximum pump power (maximum pump discharge –  $Qp_{max}$  and head –  $Hp_{max}$ ) and can generally be calculated according to Eq. 3.8:

$$PUCC = \alpha_1 \cdot f_2(Hp_{max}, Qp_{max}) \quad (3.8)$$

Where  $f_2$  is an appropriate cost function of the maximum pump head ( $Hp_{max}$ ) and maximum pump discharge ( $Qp_{max}$ ) and  $\alpha_1$  is coefficient regarding power unit.

\* Pump operational cost ( $PUOC$ )

$PUOC$  depends upon the amount of power dissipated by pumps ( $PP$ ) and energy price ( $EP$ ).

The power dissipated by each pump depends mainly upon discharge through the pump, head supplied by the pump, and efficiency of the pump at time duration  $i^{th}$ . The pump discharge has to meet the total demand of the network while the head affects intensively the pipe diameters of the network. If pipes are too small, the operational cost increases due to the increasing head losses and vice versa. Power dissipated of a pump ( $P_p$ ) can be calculated by a general equation as follows:

$$PP_i = \alpha_2 \cdot f_3(Q_{p,i}, H_{p,i}, \eta_{p,i}) \quad (3.9)$$

Where  $f_3$  is an appropriate cost function of the average flow rate of pump ( $Q_p$ ), the head supplied by the pump ( $H_p$ ), and the efficiency of pump ( $\eta_{p,i}$ ) at time duration  $i$  and  $\alpha_2$  is the coefficient regarding the unit of pump discharge and head. The energy cost is often given by electricity tariff which may vary according to daily time period. The price is commonly high at peak hours and low at off peak hours.

If the operational period is divided into a number of time intervals,  $NT$ , the total pump operation cost for  $n$  pumps,  $npump$ , can be evaluated as Eq. 3.10:

$$PUOC = \alpha_3 \cdot \left( \sum_{j=1}^{npump} \left( \sum_{i=1}^{NT} EP_i \times PP_{j,i} \cdot \Delta t_i \right) \right) \quad (3.10)$$

in which  $\alpha_3$  is coefficient regarding unit conversion factor and  $\Delta t_i$ : time step. For the purpose of simplification, time step can be chosen equally on the time series of hourly demand; consequently, the total cost of energy can be reduced as:

$$PUOC = \alpha_3 \cdot \sum_{j=1}^{npump} \left( \sum_{i=1}^{NT} EC_i \times PP_{j,i} \right) \quad (3.11)$$

The pump construction and operational cost directly regard pump discharge and head. It is comprehensible that if these parameters are directly computed, that will help designers more easily to choose appropriate pumps.

### (iii) Tank cost

Tank objective function is commonly based on tank construction cost (TCC). TCC depends on the maximum capacity of a tank, in other words, tank diameter,  $D^T$ , and the maximum water level in tank,  $HT^{max}$  and can be calculated as Eq. 3.12:

$$TCC = \alpha_4 \cdot \sum_{t=1}^{ntank} f_4(UWTC(D_t^T), (HT_t^{max})) \quad (3.12)$$

Where  $f_4$  is an appropriate cost function of unit cost of tank with diameter  $D^T$  ( $UWTC(D^T)$ ) and maximum water level in tank,  $HT^{max}$ ;  $\alpha_4$  is a constant expressed in monetary unit per square meters and  $ntank$  is the number of tanks.

Finally, a general formulation of cost objective function ( $CS$ ) with respect to a full PWDN can be expressed as Eq. 3.13:

$$CS = [ (PIC + PUCC + PUOC + TCC) ] \quad (3.13)$$

### 3.3.2 Network reliability measure

Due to the importance of network reliability when designing a PWDN, many reliability measures have been proposed. Here, five measures that are more frequently used in practice nowadays would be mentioned (Todini, 2000; Prasad and Park, 2004; Cheung et al., 2005, Araque and Saldarriaga, 2006; Farmani et al., 2006).

#### (i) Minimum surplus head index (MSHI)

The surplus head at node  $j$  ( $MSHI_j$ ) is the deviation between actual head ( $H$ ) at which the demand ( $Q_j$ ) is provided and the minimum required head ( $H^{req}$ ) at that node. This surplus head expresses the necessary dissipated energy. Accordingly, the  $MSHI$  is defined as in Eq. 3.14:

$$MSHI_j = \min(H_j - H_j^{req}) \quad j=1, \dots, nn \quad (3.14)$$

$nn$ : number of nodes in the network

The minimum available surplus head value is at the most depressed node, which is commonly at highest elevation and furthest away from the water sources. Hence, it can be considered as one criterion to estimate the optimization procedure. The network reliability is improved when maximizing this value.

#### (ii) Total surplus head index (TSHI)

Total surplus head is the summation of surplus head at each node. Mathematical formulation of this index can, therefore, be expressed as in Eq. 3.15:

$$TSHI = \sum_{j=1}^{nn} MSHI_j \quad (3.15)$$

#### (iii) Resilience index (RI)

Regardless of the optimization approach used for PWDN design, “least cost” design optimization inevitably leads to a branched network layout with no redundancy unless specific constraints are imposed. In this situation, in order to reduce the risk if any failure arise, adding more pipes to create new looped network so that flow can reach the nodes from alternative links is the common way designers have to use. In the looped network, Todini



(2000) assumes that it is necessary to provide at each node more power than required to compensate the power lost internally in case of failures. Derived from that idea, the resilience index ( $RI$ ) of a PWDN, based on the concept of the needed power input into a network, must be equal to the power lost internally to overcome the friction and the power delivered at demand nodes:

$$P_{input} = P_{friction} + P_{deliver} \quad (3.16)$$

In which  $P_{input}$  is the total available power into a network. In gravity network supplied by reservoirs, the total input power can be calculated:

$$P_{input} = \gamma \sum_{r=1}^{nres} Q_r \cdot H_r \quad (3.17)$$

If the network is also supplied by pumps, the total input power can be modified as:

$$P_{input} = \gamma \sum_{r=1}^{nres} Q_r \cdot H_r + \sum_{p=1}^{npump} PP_p \quad (3.18)$$

$Q_r, H_r$ : discharge and head corresponding to reservoir  $r$

$nres$ : number of reservoirs;  $npump$ : number of pumps in the network

$PP_p$ : power supplied by pump  $p$

$P_{deliver}$ : power that is delivered in terms of demand  $q_j$  and head  $H_j$  at each node:

$$P_{deliver} = \gamma \sum_{j=1}^{nn} q_j \cdot H_j \quad (3.19)$$

and  $P_{friction}$  is the amount of power lost in the network to overcome friction to satisfy the total demand.  $\gamma$  is the specific weight of water.

Then, the resilience index of a network can be defined as:

$$RI = 1 - \frac{P_{friction}}{P_{friction}^{max}} \quad (3.20)$$

$P_{friction}^{max} = P_{input} - \gamma \sum_{j=1}^{nn} q_j H_j^{req}$  is the maximum power that would be dissipated internally in

order to satisfy the design demand ( $q_j$ ) and design head ( $H_j^*$ ) at node  $j$ . After substituting, the final resilience index is as follows:

$$RI = \frac{\sum_{j=1}^{nn} q_j (H_j - H_j^{req})}{\left[ \sum_{r=1}^{nres} Q_r \cdot H_r + \sum_{p=1}^{npump} PP_p / \gamma \right] - \sum_{j=1}^{nn} q_j H_j^{req}} \quad (3.21)$$

(iv) *Network resilience (NR)*

Maximization of surplus head or power at nodes alone may not reflect the nature of network reliability since it does not express the effect of redundancy. For instant, a branched network with sufficient surplus head may adapt to increased demands, but a pipe failure will cause serious consequences at downstream nodes.

Consequently, a reliability network, called network resilience (*NR*), was proposed (Prasad and Park, 2004); it combines the effects of both surplus power and reliable loops. The surplus power at any node  $j$  is given by:

$$P_j = \gamma \cdot q_j (H_j - H_j^{req}) \quad (3.22)$$

Reliable loops can be ensured if the pipes connected to a node are not widely varying in diameter. The general form of diameter uniformity is given by:

$$C_j = \frac{\sum_{i=1}^{np_j} (D_{i,j})}{np_j \times \max(D_{i,j})} \quad (3.23)$$

$np_j$  is the number of pipes connected to node  $j$

$D_{i,j}$ : diameter of pipes connected to node  $j$

The combined effect of both surplus power and nodal uniformity of node  $j$ , called weighted surplus power, is expressed as:

$$X_j = C_j \times P_j \quad (3.24)$$

This equation may be normalized by dividing with maximum surplus power to get network resilience as:

$$NR = \frac{X}{X_{max}} = \frac{\sum_{j=1}^n C_j \cdot q_j (H_j - H_j^{req})}{\left[ \sum_{r=1}^{nres} Q_r \cdot H_r + \sum_{p=1}^{npump} PP_p / \gamma \right] - \sum_{j=i}^{nn} q_j \cdot H_j^{req}} \quad (3.25)$$

According to theory, in case of no violation it is  $0 \leq NR \leq 1$ . In real world application, the value of  $NR$  cannot, however, reach 1 due to two main reasons: (1) the inequality between supplied heads and actual nodal heads because of network friction; and (2) the diversity of pipe diameters in a network.

(v) *Pressure uniformity coefficient (PUC)*

In a PWDN, the level of energy dissipated internally causes a pressure distribution which somehow affects the delivery of an optimal network. From the hydraulic point of view, the

more uniform the pressure degree the more reliability of a PWDN, because the conservation of energy is maximized.

Derived from that idea, Araque and Saldarriaga (2006) suggest that when maximizing the resilience index, which expresses the relation between the internally dissipated power, the current pipe configuration, and the optimal power dissipated, pressure uniformity is achieved. The index employed to analyze the degree of the pressure uniformity in the network is called pressure uniformity coefficient (PUC), which can be expressed as:

$$PUC = \frac{\sum_{j=1}^{nn} P_j}{nn \times \max\{P_j\}} \quad (3.26)$$

$P_j$  : pressure at node  $j$ .

A general formulation of the network reliability function can be expressed as follows:

$$NRL = [Network\ reliability\ measure] \quad (3.27)$$

### 3.3.3 Objective functions and penalty function method for constraint handling

In the context of an optimization problem, the constraints mentioned in 3.2.3 must be taken into account. Therefore, the final objective functions related to cost and network reliability of a PWDN can be expressed in additive form as follows (Yeniay, 2005):

$$\min(CS) = \min \begin{cases} (PIC + PUCC + PUOC + TCC) & \text{if no violation occurs} \\ [(PIC + PUCC + PUOC + TCC) + C_{pen}] & \text{otherwise} \end{cases} \quad (3.28)$$

and

$$\max(NRL) = \max \begin{cases} [Network\ reliability\ measure] & \text{if no violation occurs} \\ [Network\ reliability\ measure + C_{pen}] & \text{otherwise} \end{cases} \quad (3.29)$$

Where  $C_{pen}$  presents a penalty function if there is any violation in (Eq. 3.3 – 3.6).

By using its additive form, the penalty function  $C_{pen}$  can be demonstrated as follows:

$$C_{pen} = \begin{cases} 0 & \text{if no violation occurs} \\ C_{penP} + C_{penV} + C_{penW} + C_{penT} + C_{penL} & \text{otherwise} \end{cases} \quad (3.30)$$

$C_{penP}$ ,  $C_{penV}$ ,  $C_{penW}$ ,  $C_{penT}$ , and  $C_{penL}$  are positive penalty functions if there is any dissatisfaction of required bounds of pressure, velocity, water quantity, tank storage, or level of required layout reliability, respectively. These terms can be evaluated separately as:

$$C_{penP} = \alpha_p \cdot f(\text{nodal head constraints}) \quad (3.31)$$

$$C_{penV} = \alpha_p \cdot f(\text{velocity constraints}) \quad (3.32)$$

$$C_{penW} = \alpha_p \cdot f(\text{water quantity constraints}) \quad (3.33)$$

$$C_{penT} = \alpha_p \cdot f(\text{tank constraints}) \quad (3.34)$$

$$C_{penP} = \alpha_p \cdot f(\text{required layout reliability constraints}) \quad (3.35)$$

$\alpha_p$  is a penalty factor with large positive value when a constraint is violated, and zero value otherwise.  $\alpha_p$  can be experimentally determined (Raad et al., 2009).

### 3.4 Optimization techniques applied in PWDN design and operation problems

Optimization techniques refer to mathematical algorithms employed to automatically find a wide range of alternative solutions to generate new, improved solutions. These techniques range from simply analytical mathematical algorithms for solving unconstrained problems to sophisticated search methods that mimic various natural processes in their approaches for solving set of constrained problems (Walski et al, 2003). A considerable number of mathematical techniques have been successfully developed and applied for optimizing design problem of a PWDN in the last decades. These optimization techniques can be categorized into two major groups (Djebedjian et al., 2005): Deterministic optimization and stochastic optimization techniques (to be classified as evolution algorithms - EAs).

#### 3.4.1 Deterministic optimization techniques

Several possible techniques, which have been developed and applied at the beginning of optimization of PWDN design and operation, can be considered, e.g., dynamic programming (Liang et al., 1974), linear programming (Alperovits and Shamir, 1977), and non-linear programming (Lansey and Mays, 1989; Fujiwara and Khang, 1990).

Studies show that although these techniques have already contributed significantly to PWDN optimization, they have not received much attention so far due to their considerable obstacles. The techniques commonly require numerous simplifying assumptions and are suitable for basic PWDNs with a limited number of pipes. They often fail (or reach just local optimum) in offering solutions with respect to problems with a large number of decision variables and non-linear objective functions (Elbeltagi et al., 2005). Also, they are time consuming even for small design problems (Walski et al, 2003). Therefore, it is difficult to completely solve complex problems of PWDN design optimization with these techniques.

#### 3.4.2 Stochastic optimization techniques

To overcome the restrictions of deterministic approaches, more recent works have focused on stochastic optimization techniques (or meta-heuristic optimizations) which are classified as evolutionary optimization algorithms. By using stochastic optimization techniques, a set of solutions is dealt with simultaneously during the search for the global optimum. The

search strategy is mainly based on the objective functions and given constraints (Simpson et al., 1994).

Generally, when searching for an optimal solution with a stochastic optimization, the objective function is evaluated for a set of solutions of decision variables (for example, pipe diameters in a PWDN pipe-size optimization problem). Based only on the objective function of the previous solutions, new and better-oriented values of decision variables would be generated (Mays, 2000).

Many kinds of stochastic techniques have received much attention in PWDN optimization, such as genetic algorithms – GAs (Simpson et al., 1994; Savic and Walters, 1997; Abebe and Solomatine, 1998; Gupta et al., 1999; Kulkarni and Patil, 2011), simulated annealing optimization – SAO (Cunha & Sousa, 1999), ant colony optimization algorithm – ACOA (Maier et al., 2003; Afshar et al., 2006; Ostfield, 2008), harmony search optimization – HS (Geem, 2006), differential evolution – DE (Adeyemo and Otieno, 2010), shuffled complex evolution – SCE (Liong and Atiquzzaman, 2004), particle swarm algorithm – PSO (Suribabu and Neelakantan, 2006), and tabu search algorithm - TS (Cunha and Ribeiro, 2004). Studies show that these algorithms are able to produce overwhelming results compared to those obtained from deterministic optimization techniques. Other advantages of these methods include their robustness, flexibility, general application, and capability of solving large combinatorial problems. However, each optimization algorithm possesses its own set of controlled parameters that affects its performance in terms of solution quality and processing time (Elbeltagi et al., 2005). Also, they require high computational intensity (Djebedjian et al., 2005).

### **3.5 Simulation-based optimization techniques**

More recently, a novel method, namely simulation-based optimization, which couples an optimization technique with a computer simulation model, has been widely developed and applied in many real-world engineering design problems in general, as well as in PWDN optimization problems in particular. This approach has showed promising results and, thus, it has been encouraging further development (Mays, 2000).

In this couple, optimization techniques bring a measure of automatically, efficiently finding the best, or optimal, solution to a PWDN problem, for example, the least-cost design or the best possible performance. Of the two groups of optimization techniques mentioned above, stochastic algorithms are popular due to their outperforming capacity of producing optimal solutions under given pre-conditions. In addition, the significant advantage of these techniques is that they can be directly linked with any simulation model “*without requiring further model simplification or the calculation of derivatives*” (Schütze et al., 2012).

A computer simulation model requires developing a program which mimics the behavior of a hydraulic system as it evolves over time and which records the overall system

performance. The simulation allows the designers to easily reproduce the future behavior of water distribution network and to apply any optimization method. With the continuing developments in computer technology, simulation-based optimization is receiving increasing attention as a decision-making tool (Hachicha et al., 2010).

The simulation-based optimization method solving only one objective function is considered as simulation-based single objective optimization. Otherwise, it is called simulation-based multi-objective optimization.

The simulation-based Single-objective optimization methods used over the years produce the “best” solution corresponding to minimization or maximization of objective. Nevertheless, it cannot easily provide a set of trade-offs solutions between contradicting objectives (Walski et al., 2003).

The simulation-based multi-objective optimization is considered a more informed approach in real engineering designs. It generally identifies a broad range of alternative solutions empowering the decision maker. However, selecting the most appropriate solution among a very large set of Pareto solutions is still a challenge (Chaudhari et al., 2010; Grundmann et al., 2013).

The basic framework of the simulation-based optimization for PWDN design can be characterized as in Figure 3.4 below:

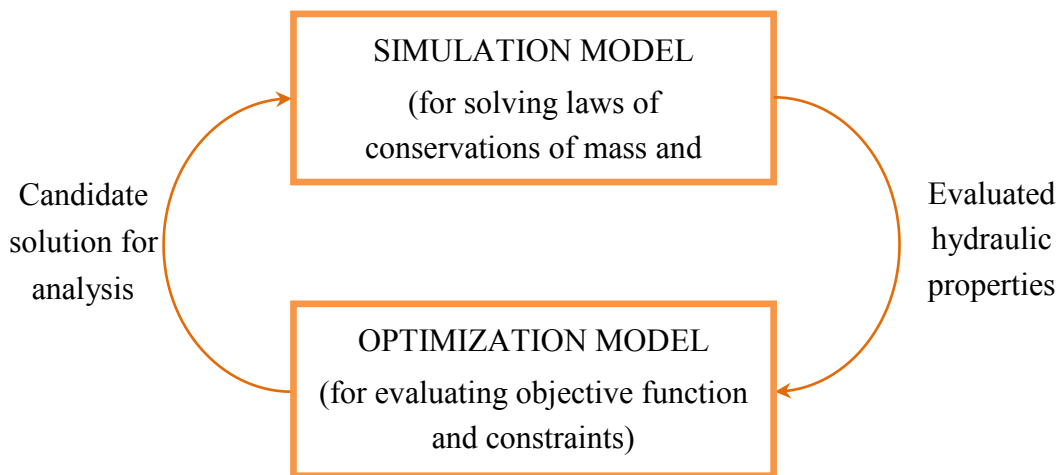


Figure 3.4: A basic simulation-based optimization method based on Mays (2000)

### 3.5.1 Simulation-based Single-objective optimization in PWDN design and operation

This type of approach is a useful tool for providing decision makers with insights into the nature of the problem of PWDN optimization. Single objective commonly relates to either minimization of cost or maximization of network benefit. Obviously, the cost is likely to be a prior function when solving PWDN optimization problems and has been addressed by many researchers in a number of different ways in past decades (Mays, 2000).

For solving problem of pipe size optimization, Abebe and Solomatine (1998) applied the combination of a global optimization tool (GLOBE) and Epanet (Rossman, 1993) on two benchmark networks, i.e., two-loop network (TLN) and Hanoi network (HN). Four random search algorithms used in GLOBE included: Controlled random search (CRS2), CRS4, genetic algorithm (GA), and adaptive cluster covering with local search (ACCOL). The proposed approach revealed the capacity of handling a typical loading condition of each optimization algorithm and its effectiveness. However, with respect to large networks this technique produced just near optimal as well as required a considerable number of function evaluations.

Sánchez et al. (1999) developed a couple of GAs and a hydraulic model, called CNetwork, for optimally designing a branched irrigation PWDN. With this approach, the best performance can be found if several experiments used to adjust the parameters of the algorithm are employed.

The Shuffled complex evolution (SCE) algorithm coupling with Epanet was applied by Liong et al. (2004) to identify the least cost of the TLN and HN. A better performance, in terms of optimal cost design and computational time compared to the previous, was achieved with respect to TLN. As to a larger network such as Hanoi network, the method produced near optimal results.

Another computer model, called Genetic algorithm pipe network optimization model, GENOME, was introduced by Reca and Martinez (2006) to optimally design a looped irrigation PWDN. The performance of this algorithm was analyzed by applying it to two benchmark networks (TLN and HN) and then to a real world irrigation water distribution network. It can be concluded that the model performed well with small networks. However, the performance of the method should be improved when solving large-scale networks for practical application.

From the results obtained by applying PSO coupling with Epanet on two benchmark water networks (i.e., Hanoi and New York), Montalvo et al. (2008) demonstrated that this coupling can be considered as an excellent algorithm by its flexibility and adaptability in accommodating either type of continuous or discrete variables, and since it requires a relatively small number of function evaluations when performing its approximation. However, the obtained results were not really amongst the best results compared to the published results using GA, ACOA to the same networks.

Vasan and Simonovic (2010) applied DENET, which coupled the differential evolution algorithm (DE) with Epanet simulator. The model was tested with two benchmark PWDNs, TLN and HN, for optimization of network cost., Even though DENET can be a potential selection for PWDN design with its simplicity and robustness, it produced only a near optimal solution when comparing to previous solutions applied on two these networks.

A quite new method, namely HS interfacing with Epanet, was applied in the PWDN design optimization by Geem et al. (2001). By applying to five studied PWDNs, the obtained cost were either the same or less than those of some compared stochastic algorithms described above, such as GA, SAO, under similar or less favorable conditions. However, this model also requires a very large number of function evaluations.

To the complex networks including pumps and tank, the target is commonly to minimize the total cost including initial capital, construction, and operation costs. The optimal principle relies basically on number of hours in which a pump is turned on or off (Ostfeld and Tubaltzev, 2008). In their application, the modified ACOA coupling with Epanet was extended the PWDN proposed by Maier et al. (2003) for PWDN optimal design and operation. Besides pipe diameters, pump power was considered as a decision variable; therefore, it can be directly determined. However, the significant pump properties, namely, pump discharge and head, were not computed, causing the difficulty in selecting an appropriate pump.

For simulation of floating in the tank system for water network design optimization, a coupling of GAs and Epanet was used in Vamvakieridou-Lyroudia et al. (2007). Tank volume and minimum water level were considered as decision variables while other tank properties were derived. The result obtained from application on the Anytown network showed that it was quite promising compared to the previous study on the same problem (Walters et al., 1999).

The studies above show that obviously the simulation-based single optimization approach produced only single optimal or near optimal solution. There is still a number of other factors which should be taken into account in the search space optimization, such as reliability, safety, water quality, and so on (Goulter, 1986). Therefore, this method may not be convenient for PWDN optimization because decision makers are normally interested in identifying the whole compromising solutions between the objectives. Consequently, an alternative approach is to consider the PWDN optimization in the multi-objective (Formiga et al., 2003).

### ***3.5.2 Simulation-based multi-objective optimization in PWDN design and operation***

In contrast to the single objective optimization, the multi-objective optimization with contradicting objectives reflects the “overall picture” rather than just a solution. The multi-objective optimization method allows the designers to examine the trade-offs between several contradicting objectives by finding a set of Pareto optimal solutions which commonly provides a wide range of optional solutions and more information about these solutions to decision makers (Walski et al., 2003). Among the network benefits, network reliability has received much attention since it expresses capability of providing water to consumers of the designed PWDN.



Todini (2000) suggests that a PWDN should be designed in a way that can reduce risk from sudden failure occurring in the process of water delivery. Therefore, beside the cost, the resilience index objective function was taken into account for solving PWDN optimal design problems. Based on these contradicting objective functions, multi-objective optimization approach produces the optimal Pareto front that provides more possibilities for designers to select the most suitable solution which would be consistent both with the budget and the resilience index.

The optimal Pareto set, which allows satisfactory solutions to be found as a trade-offs between cost and network resilience, was also achieved by Prasad and Park (2004) by using GA coupling with Epanet.

Farmani et al. (2006) applied non-dominated sorting genetic algorithm (NSGA II) coupling with Epanet for solving the problem that was posed as a multi-objective optimization problem with total cost and the number of demand nodes with head deficiency as optimization criteria. The design decision variables were the inclusion of new pipes, sizing of new tanks, and operation of a PWDN including pump and tank.

Raad et al. (2009, 2011) combined a multi-algorithm, genetically adaptive multi-objective called AMALGAM, which was introduced by Vrugt and Robinson (2007), and Epanet for solving multi-objective PWDN design problems including the minimization of cost and maximization of network resilience. The optimal Pareto fronts achieved from several trials on well-known benchmark water networks showed that this technique would be quite a suitable tool for more complex loop networks.

Chandramouli et al. (2011) developed a new parameter for assessing the overall network reliability and then incorporated this parameter into a two objective optimization models for design of a PWDN using a combination of GA and the Epanet. Tested with two loops network, the method have shown that the number of function evaluations, cost reliability ratio and cost per unit reliability, and unit length are all smaller than those of previous researchers; also the network reliability parameter is larger than that of other methods when compared with previous researchers.

Baños et al. (2011) used the Strength Pareto Evolutionary Algorithm 2 (SPEA 2) and coupled it with Epanet to solve multi-objective optimization problems including cost function and three different resilience indexes: Resilience index, network resilience, and a modified resilience index in order to determine whether the solutions become infeasible under a large number of over demand scenarios.

### **3.6 Uncertainty in PWDN optimization**

The aim of PWDN design is to serve consumers over a long period of time. During the operation, many technical design parameters would be impossible to characterize with any accuracy, such as required pressure heads, future required demands, network capacity,

network configuration, etc. (Lansey et al., 1989; Kapelan et al., 2005; Babayan et al., 2005). These studies have definitely demonstrated that neglecting uncertainties in the design process may lead to serious under-designed PWDNs.

The most notable source amongst uncertainties in PWDN design is water demand at nodes, since it directly impacts the uncertainty in nodal pressure head as well as other hydraulic parameters (Babayan et al., 2005; Kapelan et al., 2005; Chung et al., 2009; Seifollahi-Aghmiuni et al., 2011; Sun et al., 2011; Shibu and Reddy, 2012).

There are several techniques solving uncertainty in PWDN design (Babayan et al., 2005; Kapelan et al., 2005; Ezzeldin et al., 2008).

Xu and Goulter (1999) proposed the so-called first order reliability method FORM algorithm that evaluated the network reliability under the uncertainty in nodal demands and pipe capacity. The FORM required repetitive computation of the first order derivatives and matrix inversion; this is computationally very demanding and may lead to a considerable number of numerical problems.

This was the main reason why Babayan et al. (2005) developed a new approach where the standard GA is linked with Epanet to an integration-based uncertainty quantification method. In this study, the uncertain demand was assumed to follow the normal probability density function (PDF) with a predefined standard deviation of 10% from mean value. The network reliability was then determined using full Mont Carlo simulation (MC) with large number of samples. The results compared to available deterministic solutions demonstrated the importance of applying the uncertainty concept in PWDN optimization. However, the level of robustness of the designed network was not estimated directly and explicitly.

Kapelan et al. (2005) assumes that a lot of information is required to define probability density functions of input parameters by using MC and, therefore, a lot of time is consumed. Hence, the Latin hypercube sampling technique (LHST) was used in the multi-objective optimization framework to identify the optimal robust Pareto fronts of minimizing the cost and maximizing the robustness. A small number of samples was enough for each objective evaluation leading to significant computational savings when compared to the full sampling approach.

Sun et al. (2011) proposed a fast approach to improve computational efficient when addressing the multi-objective PWDN design optimization including cost and robustness under uncertain nodal demands. Compared to traditional methods (MC and LHST) the fast approach saves a large amount of computational time but it produces somewhat more expensive designs, particularly in the part of the Pareto front where the solutions have a robustness greater than 80%.

Moreover, in real PWDNs, nodal demands are highly correlated due to abnormal conditions, e.g., hot, dry weather that affects the network as a whole. For solving this situation, nodal demands were assumed to be Gaussian distributed and temporally correlated at a coefficient

of 0.5 between any two nodes. The technique used to solve correlated demands is that of Iman and Conover (Kapelan et al., 2005).

### **3.7 Conclusions and open consideration for further study**

Over the last decades, a considerable number of studies have been conducted to solve optimization problems of PWDN design and operation. A very wide range of mathematical optimization algorithms, from simple analysis to sophisticated optimization algorithms, has been developed and applied in order to obtain an optimal PWDN in terms of cost and network benefit. Based on the results achieved, some conclusions can be drawn as follows:

(i) As regards deterministic optimization methods: they have led to quite some success in the initial period of PWDN design optimization; however, these methods are not preferred recently due to their capacity limitations.

(ii) Even though stochastic optimization methods can be efficiently used, there are still several obstacles:

- They do not surely guarantee optimal solutions with respect to more complex networks (i.e., Hanoi, New York, etc.). A large number of function evaluations are still required.
- Optimal solutions achieved by stochastic optimization methods depend commonly on the parameters which control the optimization procedure. Consequently, different solutions would be achieved when changing any of these parameters.
- Although GAs have received much attention, they still poorly perform compared to several latter optimizations such as DE, ACOA, and HS. On the other hand, their ability to reach successful solutions decreases as the number of decision variables increases. Moreover, when dealing with complicated problems, GAs do not have a clear strategy. By using simple encoding and reproduction mechanisms, GAs turn out to solve some extremely difficult problems.
- The performance of, e.g., PSO and SCE is unstable as applied to different optimization problems and with a large number of decision variables.
- Some techniques need to be applied when executing ACOA to avoid the premature convergence. This leads to increasing processing time.

(iii) Most of the applications have been executed with gravity networks due to the very complexity of the PWDN optimization problem when pumps and tanks are included.

(iv) In the majority of PWDN optimizations, a given layout has been commonly assumed. While there are still benefits in this argument, there may exist alternative layouts which provide improved performance. In reality, there is a tight interaction between component sizes and network layout (see Afshar and Jabbari, 2008).

(v) The simulation-based optimization method has been developed and applied more and more recently due to its promising results. Together with the very strong development of mathematical algorithms and computer technology, this method will promise the optimal design process of PWDNs to be simpler and more flexible.

(vi) Amongst the recent mathematical algorithms, covariance matrix adaptation evolution strategy (CMA-ES) is estimated as the more powerful one for real-valued optimization with many successful applications (Hansen and Ostermeier, 2001). It is evaluated to be able to solve faster the problem of non-linear, non-convex, non-separated ill-condition in continuous domain. Particularly, its advantages were expressed with various search dimensions (Igel et al., 2007) that would be consistent with PWDN optimization problems.

Consequently, in this study a new simulation-based stochastic optimization approach will be developed for simultaneously solving all design and operation optimization problems of a full PWDN including network layout and sizes of pipe, pump, and tank under uncertainty.

## 4 A NOVEL APPROACH FOR AN OPTIMAL DESIGN OF PRESURIZED WATER DISTRIBUTION NETWORK

### 4.1 Introduction

Studies have shown that urban and irrigation PWDN can be optimally designed using the same approaches. These approaches base on the principles of optimizing cost and/or network benefit objective(s) to achieve an optimal network configuration which satisfies both economic and technical criteria (Hassanli and Dandy, 1996; Sánchez et al., 1999; Theocharis et al., 2005; Reca and Martínez, 2006; Alandí et al., 2007; Farmani et al., 2007; Kulkarni and Patil, 2011).

Based on the general structure of simulation-based optimization outlined in Figure 3.4, a novel simulation-based optimization approach, (MO)-CMA-ES-EP, has been developed and verified (Figure 4.1). This new approach couples a hydraulic model (Epanet) with the covariance matrix adaptation evolution strategy (CMA-ES) and can be operated in two different modes. These modes can be (1) simulation-based Single-objective optimization and (2) simulation-based multi-objective optimization. The Single-objective optimization mode yields the best solution which corresponds to the minimum or maximum value of the objective function. By contrast, the multi-objective optimization mode produces a set of trade-offs solutions between network cost and reliability (Pareto optimal solutions). Obviously, these two objectives are in conflict and compete with each other. The more expensive the cost, the higher the network reliability and vice-versa

The general principle of the new technique can be described as follows: An objective function(s) associated with a range of decision variables, constraints and other parameters will be mathematically interpreted in the interface module. The set of initial decision variables, which are arbitrarily assigned using optimization model, is firstly denormalized and transferred to the Epanet. Epanet solves the hydraulic processes based on the laws of conservation of mass and energy and then produces the hydraulic parameter values such as discharge, flow velocities, head losses in pipes, nodal heads (or pressures) and so on. These values are then transferred back to the optimization mode and to be checked in terms of given constraints and then, at the end of an iteration, objective function(s) can be estimated. The forth and back transference of these decision variables and parameters between these two modes is done through the interface module programmed in Matlab language. Whenever there is a violation of any given constraint (for instance, minimum required nodal pressures, limits of velocity, design parameters, constraint related to optimal layout, etc...), the penalty function will be added to the objective function value. By comparing to the previous objective value, the decision variables are automatically adjusted afterwards to move to a

better solution. The process continues until any defined stop criterion is met. Finally, the optimal decision variables for designing PWDN will be selected which satisfy all given constraints. In order to give the designers as much understanding as possible if uncertainty needs to be taken into account, the Latin hypercube sampling technique is applied to the optimal solution for estimating the network robustness.

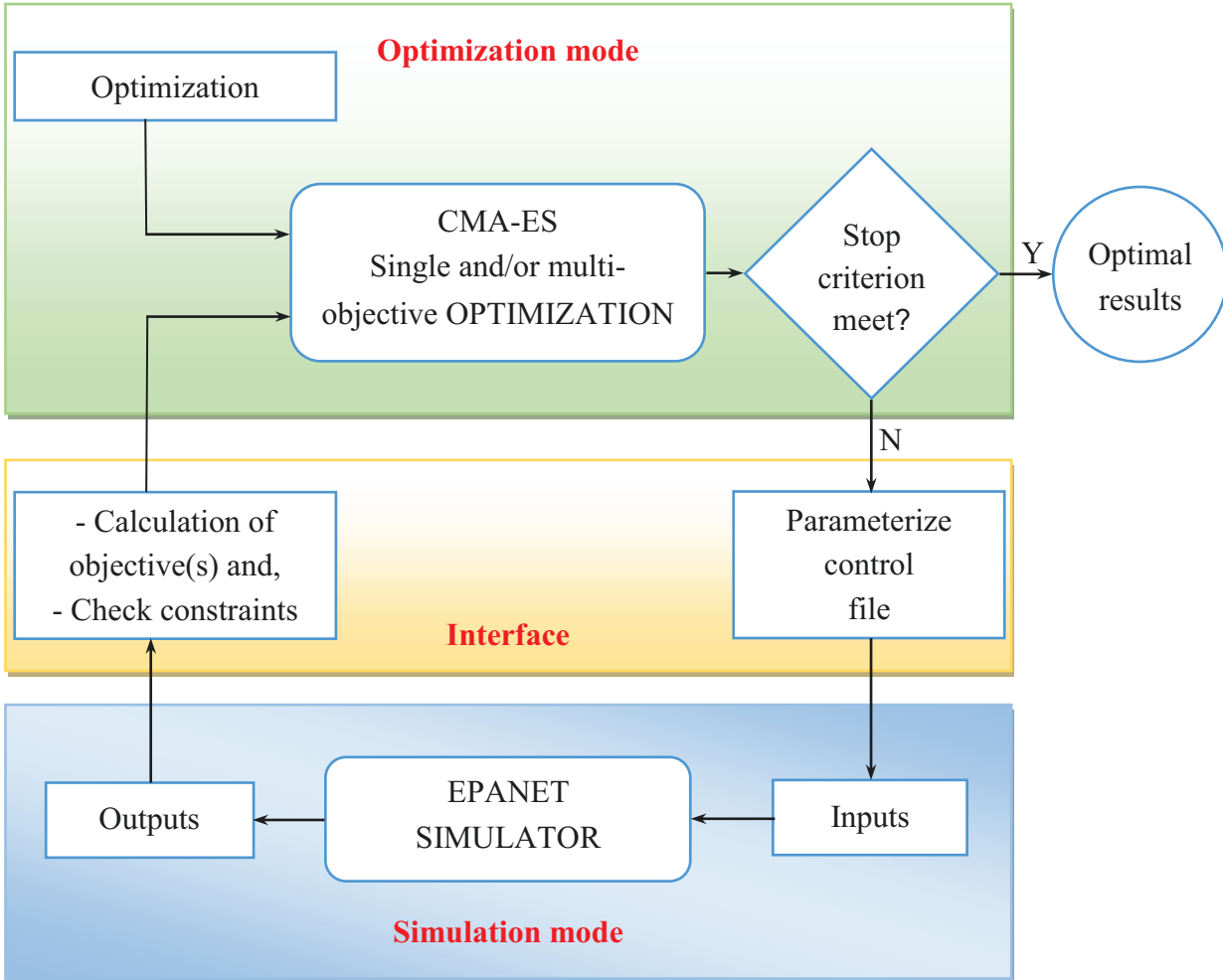


Figure 4.1: The outline of the simulation-based CMA-ES optimization approach

## 4.2 Outline of methodology for the proposed approach

The new proposed approach includes two modes: The simulation-based Single-objective optimization (CMA-ES-EP) and the simulation-based multi-objective optimization (MO-CMA-ES-EP).

### 4.2.1 The simulation-based Single-objective optimization approach

This mode is used to minimize the network cost or to maximize the network benefit. The principle of the simulation-based Single-objective optimization is schematically described in Figure 4.2 and can be interpreted as in the following procedure:

\* *Pre-processing:*

- (1) Define optimization problems including decision variables (for instant, pipe diameters, pump and tank characteristics), objective function (cost or network reliability), and given constraints (limits of nodal pressures, flow velocities, tank constraints, etc...).
- (2) Set up an Epanet performance for the PWDN to be analyzed using an arbitrary set of decision variables on which the objective function depends directly and other given hydraulic properties. A set of big values for the decision variables would be preferred in order to ensure that the network can perform normally. Epanet solves the hydraulic equation system of conservation of mass and energy and consequently provides flows, pressures, velocities, and other characteristics as outputs.
- (3) Create the analyzed result under the specific form of standard Epanet input file (\*.inp) that is consistent with the structure required in Epanet.
- (4) Create initial settings for model such as normalized initial decision variables, standard deviations, model parameters, model criteria, and other given data.
- (5) Set up an appropriate interface

*\* Interface*

- (6) Formulate the objective function (i.e. cost minimization or network reliability maximization), constraints and other given parameters in interface module.
- (7) The CMA-ES optimization mode starts with a set of initially normalized compatible decision variables which receive the values within interval [0 1]. This set is then denormalized and transferred to Epanet.
- (8) The toolkit loads the Epanet input file to obtain a description of the network to be analyzed and must close itself down once all analyses are completed. At this time, all parameters that define the design and operation of the PWDN being analyzed are retrieved and set by using other specific toolkit function such as the function for node, pipe, pattern, option, etc.
- (9) The description of the PWDN characteristics including flow rates, head losses, velocities in pipes, piezometric nodal head (also nodal pressure) at nodes and so on is then transferred back to the interface module.
- (10) Check the user-predefined constraints.
- (11) Calculate the objective function for current iteration with the assigned decision variables regarding current network configuration.
- (12) If there is any violation of the constraints occurring in any iteration, penalty functions will be added to the objective function.

(13) Based on the comparison of two objective function values i.e. the previous objective function value and the current one, optimization mode evaluates a new set of initial decision variables which would be adjusted to move to better values for the next iteration.

(14) Steps (6) - (12) above are repeated until a criterion is met. Several criteria used in CMA-ES are given in Hansen (2011) and will be discussed later.

*\* Post-processing*

(15) Minimum solution corresponding to an optimal layout is produced when the model stops. The Latin hypercube sampling technique is applied to this solution to evaluate the network robustness in case demand uncertainty is taken into account.

Several major Matlab codes for this procedure are presented in detail in Appendix B. With respect to a maximization problem, the sign of the objective function needs to be changed and then the same procedure as described above can be applied.

Because the simulation-based Single-objective optimization produces only one minimum compatible objective value, other possible considerations would be neglected leading to the fact that this solution may not be the best. For example, with least cost design of a PWDN, this simulation based Single-objective optimization may not consider network reliability, network risk and so on. Therefore, the multi-objective optimization which overcomes the limitations of the single optimization would be an appropriate choice for solving the optimization problem of PWDN design and operation.

#### ***4.2.2 The simulation-based multi - objective optimization approach***

The principle of the simulation-based multi-objective optimization is described in the flow chart in Figure 4.3.

Steps (1) – (14) described in sub-section 4.2.1 above for the Single-objective optimization approach are fully applicable to this multi-objective optimization approach. The difference is that, in step (6), two objective functions, namely, cost and network reliability, are simultaneously set up in the optimization model.

Apart from steps 1 – 14 as above, additional steps of the procedure for multi-objective optimization which belong to post-processing are as follows:

(15) A Pareto optimal front is generated which includes all compromise solutions evaluated from search space when the model stops. According to the theory of multi-objective optimization, there is no best solution but the trade-offs solutions between total cost and network reliability are achievable.

(16) Based on the significance of objective functions, several representative solutions are proposed.

(17) Adding a criterion of network robustness evaluation would likely be necessary in order to support designers in choosing the most suitable solution.



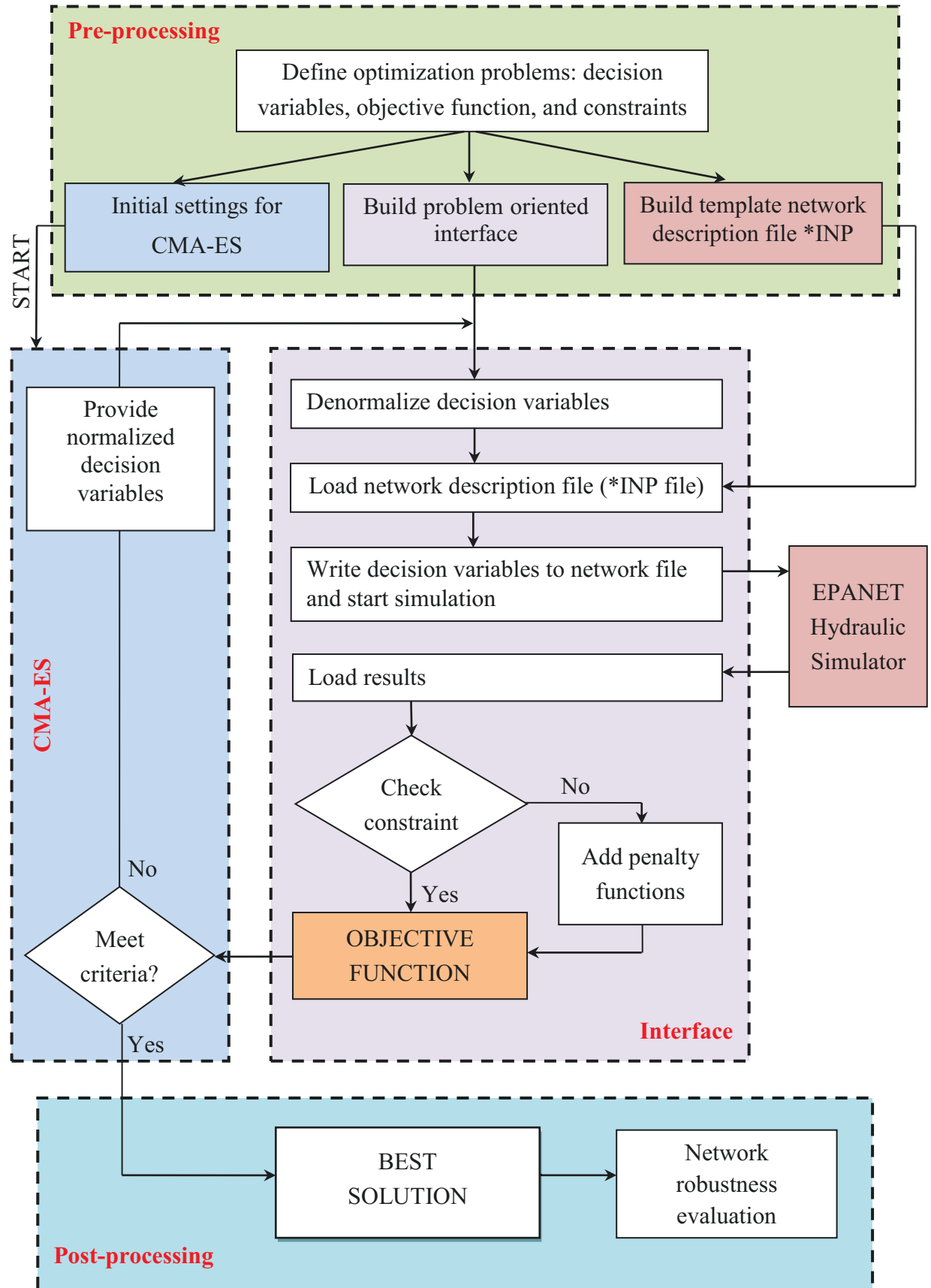


Figure 4.2: The basic flowchart of simulation-based single optimization CMA-ES-EP

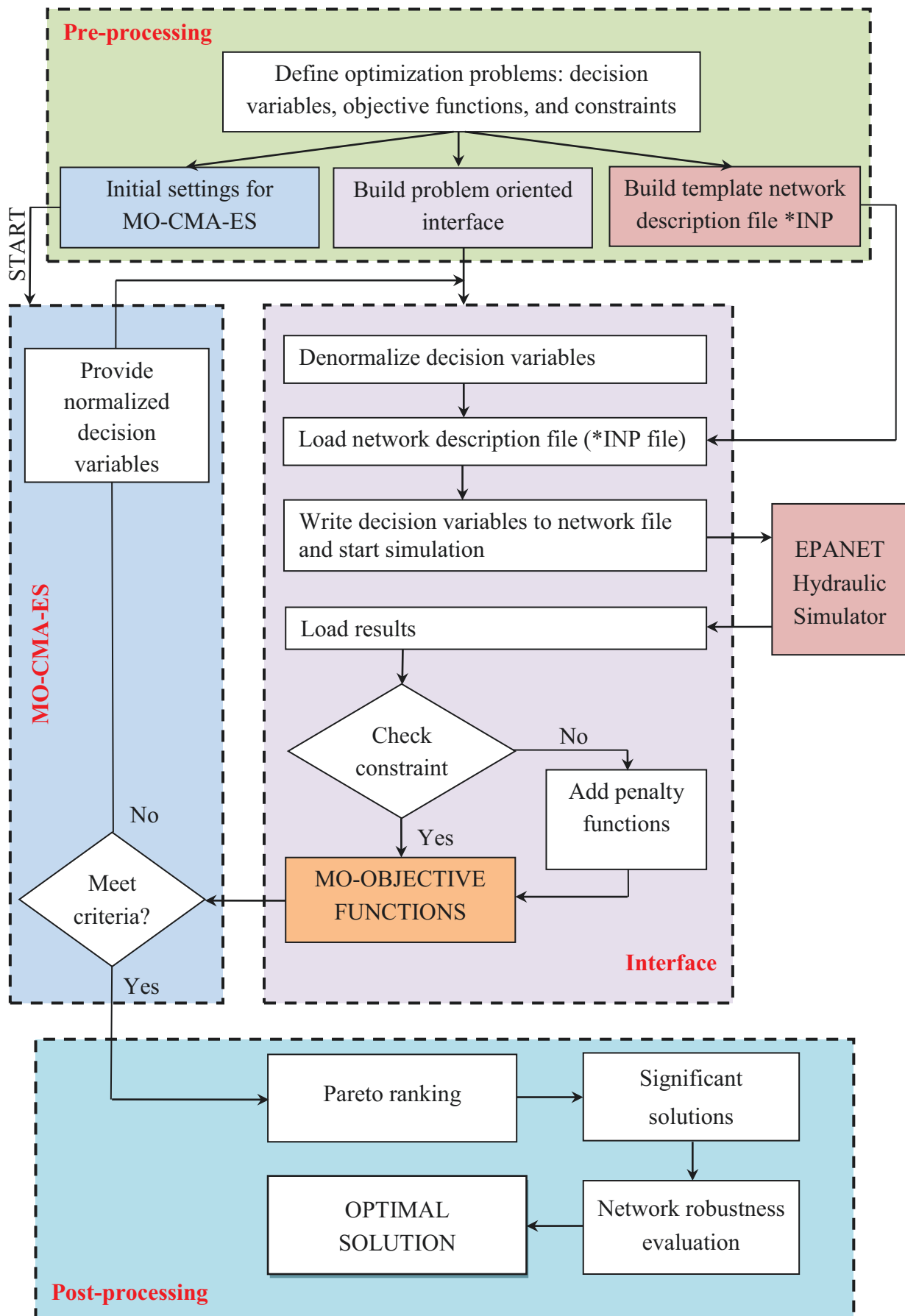


Figure 4.3: The basic flowchart of simulation-based multi-objective optimization (MO-CMA-ES-EP)

### 4.3 Epanet toolkit

The Epanet toolkit is a dynamic link library (DLL) of functions which permits designers to connect Epanet with a programming language that can call these functions<sup>1</sup>, for example C++, Visual Basic, Matlab, etc... These functions can retrieve and set all characteristics of a water network described in a suitable format file (\*.inp file, see Figure. 2.6) and write results in an output file as well. The toolkit is useful for optimization or automated calibration application that requires network analysis.

Retrieval functions are included in the Epanet toolkit which all begin with ENget (for example ENgetlinkvalue, Engetnodevalue, etc...) while the functions employed for setting parameters begin with ENset (for example ENsetlinkvalue, ENsetnodevalue, etc...). Most of these functions employ an index number to refer to a specific network component.

For carrying out a network analysis from developed programming, at first, the toolkit must open the Epanet input file (\*.inp file) to get a description of the analyzed network before any of its other functions can be called. A component would be determined by a series of existing functions through its index number. In the end of analysis, it must close itself down to free all allocated memory. The interactive procedures between DLL storage and the Matlab programming language were developed by (Jonkergouw, 2007) and then upgraded by Eliades (2009)<sup>2</sup>.

### 4.4 Covariance matrix adaptation evolution strategy algorithm (CMA-ES)

#### 4.4.1 Covariance matrix adaptation evolution strategy algorithm (CMA-ES)

CMA-ES was introduced by Hansen and Ostermeier (2001) based on the normally distributed mutative steps to survey search space while adjusting its mutation distribution to produce likely successful steps in the future from the current search. This algorithm is considered as a robust search method for real parameter optimization of non-linear, non-convex, non-separated as well as ill-conditioned problems in continuous domain. CMA-ES can be reliably implemented with small population sizes that help reduce the number of function evaluations. Also, CMA-ES can overcome some other typical problems which are commonly associated with evolution algorithms such as premature convergence and degeneration process as well.

Theoretically, CMA-ES utilizes two basic design principles, namely, invariance and unbiased of the variation of object and strategy parameters. Invariance characteristics cause compatibility classes of objective functions and therefore allow for generalization of empirical results. The algorithm includes four major procedures and can be described briefly

---

<sup>1</sup> [http://epanet.info/wpcontent/uploads/2012/10/tool-kit\\_help.pdf](http://epanet.info/wpcontent/uploads/2012/10/tool-kit_help.pdf)

<sup>2</sup> <http://www.mathworks.de/matlabcentral/fileexchange/25100-epanet-matlab-toolkit>

in Figure 4.4. Further details can be found in Hansen et al. (2001, 2003, and 2011) and Igel et al. (2007, 2008).

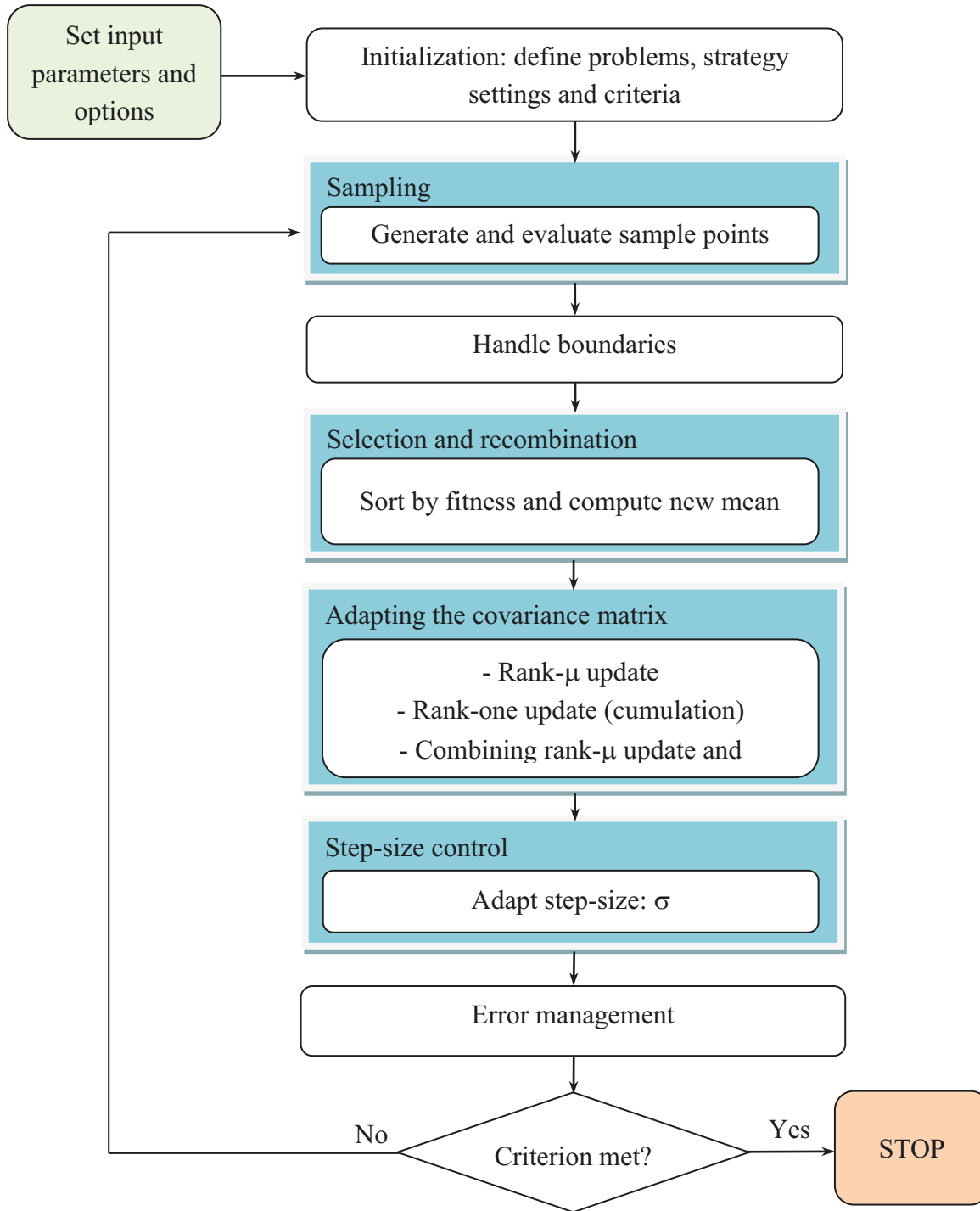


Figure 4.4: General CMA-ES procedure flow chart

#### 4.4.2 Multi-objective covariance matrix adaptation evolution strategy algorithm (MO-CMA-ES)

Several successful multi-objective optimization algorithms have been developed such as non-dominated sorting genetic algorithm, NSGA (Srinivas and Deb, 1995), elitist non-

dominated sorting genetic algorithm, NSGA II (Deb, 2000), non-dominated sorting differential evolution approach, NSDE (Iorio and Li, 2005), and AMALGAM (Vrugt and Robinson, 2007). The major working principles of these approaches are to force the solutions toward the Pareto optimal front which includes trade-offs solutions between objectives and to maintain the diversity among solutions in the Pareto front.

The MO-CMA-ES was developed by Igel et al. (2007). This approach is a combination between the strategy parameter adaptation and multi-objective selection mechanism which is based on non-dominated sorting approach (Deb et al., 2000). MO-CMA-ES is superior compared to NSGA and NSDE. Several specific MO-CMA-ES model parameters are shown in Table 4.1 (Müller, 2012).

*Table 4.1: Notable parameters need to be defined for CMA-ES model*

$N_0$	Parameters	Notes
1	Dimension	number of decision variables
2	Population size	sample size, number of offspring
3	Parent number	number of selected search points in the population
4	Iteration	number of iterations to stop model
5	InitSeed	the initially random number of generators
6	Measure	criteria used for sorting indicators hyper-volume measure crowded distance
7	Lower_Bnd	set of the lower boundaries for the decision variables
8	Upper_Bnd	set of the upper boundaries for the decision variables
9	InitStepS	sets the initial step size for algorithm
10	Penalty_T	defines the used penalty function for infeasible parameter set

By using the concept of Pareto efficiency, accordingly, any two solutions  $x_1$  and  $x_2$  may have one of two possibilities: one dominating the other, or neither dominating the other. A solution, for instant  $x_1$ , is considered to dominate the other solution,  $x_2$ , if both the following conditions are satisfied (Prasad and Park, 2004):

- (i) The solution  $x_1$  is no worse than  $x_2$  in all objectives, and
- (ii) The solution  $x_1$  is thoroughly better than  $x_2$  in at least one objective.

If there is any condition violated,  $x_1$  is considered to be dominated solution, otherwise  $x_1$  is a non-dominated solution (Figure 3.3).

In addition, MO-CMA-ES uses contributing hyper-volume as the second sorting criterion (Igel et al., 2007). This is necessary to rank the solutions with the same level of non-dominance if there are more non-dominated solutions in the population than solutions to be selected. Consequently, a wide range of solutions will be provided.

#### 4.4.3 Box constraint handling method associated with CMA-ES

The box constraint handling is associated with the algorithm in order to guarantee that each evaluated solution must lie within feasible space ( $X_f$ ). The feasible search space is a hypercube defined by the lower and upper boundary values for each decision variable. The algorithm influences individually the computation of the solutions and requires the steps as follows (Hansen et al., 2008):

(i) An infeasible solution  $x$ , from the infeasible search space ( $X$ ) can be mapped to the nearest feasible point ( $feasible(x)$ ) in feasible search space ( $X_f$ ) in the following way in the handling box constraint:

$$feasible(x) = (\min(\max(x_1, x_1^l), x_1^u), \dots, \min(\max(x_n, x_n^l), x_n^u)) \text{ with } x \in R^n \quad (4.1)$$

Hence, the feasible solution is evaluated itself and the infeasible is evaluated on the boundary of the feasible space. The new feasible solution is then used for the evaluation on objective function and for computing a penalty function.

(ii) A penalty function is added objective function penalizing infeasible solutions. In this study, to save computational time, the Squared Euclidean death penalty of the infeasible candidates computed directly by (Eq.4.2) is used in the MO-CMA-ES (Müller, 2012):

$$f_m^{penalty} = \alpha \sum_{i=1}^n (x_i - feasible(x)_i)^2 + \beta \quad (4.2)$$

where the penalty factor  $\alpha$  and the offset  $\beta$  will be experientially chosen.

#### 4.4.4 Stopping criteria

In order to terminate CMA-ES optimizing process, several stopping criteria have to be predefined. Herein are five useful stopping criteria which should be considered as problem dependent. More details about stop criteria can be seen in Hansen (2011).

(i) MaxFunEvals: A criterion describing the maximum evaluations of optimization procedure. The optimizing process is stopped when a given maximum number of function evaluations is reached (recommended  $MaxFunEvals = 10^3 * N^2$ , where  $N$  is number of decision variables).

(ii) StopFitness: the model stops if objective function value is smaller than given StopFitness value (recommended  $StopFitness = 10^{-10}$ )

(iii) TolXUp: stop if  $(\sigma \cdot \max(\text{diag}(D)))$  increased by more than  $10^{15}$ , where  $D$  is the diagonal matrix whose elements are square roots of eigenvalues of the covariance matrix ( $C$ ) and correspond to the respective columns of the orthogonal matrix ( $B$ ).

(iv) TolFun: this stops optimizing process if the range of the best fitness values of the last  $(10 + \lceil 30.N/\lambda \rceil)$  generations and all function values of the recent generation is smaller than a given TolFun value of  $(10^{-15})$  with  $\lambda$  is the population size.

(v) TolX: the model stops if  $\sigma$  of the normal distribution is smaller than all coordinates and  $\sigma \cdot p_c$  is smaller than TolX in all components (recommended  $\text{TolX} = \sigma \cdot 10^{-15}$ ).  $p_c$  is the evolution path.

#### 4.5 A proposed approach for simultaneously optimizing network components and layout

Afshar and Jabbari (2008) clearly demonstrated that “*simultaneous layout and size optimization is unavoidable in a search towards optimal or near optimal design of pipe networks*”. Neglecting the simultaneous layout and pipe size optimization of PWDNs may not lead to an optimal solution. Hence, this problem must be solved in the new proposed model.

By using Epanet, every link (refer to both pipe and pump) is assigned to either “open” or “closed” status during the simulation of a PWDN. Water is allowed to go through only the open links. In this study, a procedure that uses “closed” status is developed to automatically assign to any link which violates any predefined criterion such as limits of pipe diameters, limits of velocity (with respect to pipes), and limits of tank water level (with respect to pumps).

In order to achieve an optimal pipe layout from a predefined maximum layout (discussed in subsection 3.2.3), the constraint related to optimal layout proposed by Afshar and Jabbari (i.e. Eq. 3.6) is employed with the following modification. An additional diameter that is smaller than the smallest value given in the set of commercial pipe diameters (but not zero as per the Epanet principle) is added to this set. At every iteration of the optimization process, redundant pipes that violate any predefined constraint will be firstly assigned with this diameter and then with the “closed” status.

As for pumps, the simple control associated with Epanet that specifies the status of pumps as function of tank water level is used to control the pump performance (Rossman, 2000). Some of these pumps are controlled to be “closed” if the water level in tanks exceeds a predefined upper value. When water level in tank drops below a predefined lower level, these “closed” pumps are controlled to be “open” again to supply water for network. The number of “open” pumps depends on the tank water level.

The resulting network is in fact the same the predefined maximum layout in which the redundant links are set to “closed” status that does not allow water to go through. Finally, these “closed” links will be excluded from the network to provide a much simpler network layout without any influence to the hydraulic condition in the network.

#### 4.6 The identification of significant solutions from the Pareto optimal front

Theoretically, a multi-objective optimization technique produces the Pareto optimal front that includes a considerable number of non-dominated solutions between the analyzed objectives (Todini, 2000; Prasad and Park, 2004; Araque and Saldarriaga, 2005; Farmani et al., 2006; Raad et al., 2009, etc ...). Selecting an appropriate compromise solution from such a large set is difficult for any decision maker (Chaudhari et al., 2010). Therefore, this large set needs to be reduced to a few representative solutions (Reddy and Kumar, 2007). In order to achieve this reduction, two different following approaches are applied. These approaches are helpful for decision makers that do not have any preferential criterion regarding the relative importance of contradicting objectives in a multi-objective optimization problem.

##### 4.6.1 A clustering approach for an informed selection of centroid solutions

Clustering algorithms organize data by abstracting underlying structure either as a grouping of individuals or as a hierarchy of groups. Objects in the same groups (called a cluster) are more similar to each other than to those in other clusters. In fact, there are many proposed definitions regarding clustering algorithms (Jain and Dubes, 1988), in which, k-means clustering approach divides data into  $k$  mutually exclusive clusters, and returns the index of the cluster to which it has assigned to each observation. The k-means finds a partition in which objects within each cluster are as close to each other as possible and as far from the objects in other clusters as possible. Each cluster is defined by its member objects and by its centroid or center. The centroid solution for each cluster is the efficient representative point to which the sum of distances from all objects in that cluster is minimized. The procedure is based on the following steps<sup>1</sup>:

- (i) Based on the Pareto optimal solutions achieved by the MO-CMA-ES, k-means technique partitions all these solutions into  $k$  clusters. This iterative partitioning minimizes the sum, over all clusters, of the within-cluster sums of point to cluster - centroid distance.
- (ii) Optimal number of clusters,  $k$ , is determined using the silhouette value. The silhouette value for each point is a measure of how similar that point is to points in its own cluster, when compared to points in other clusters and ranges from -1 to +1. The silhouette value for point  $i^{th}$ ,  $S_i$ , is computed as:

$$S_i = \frac{(b_i - a_i)}{\max(a_i, b_i)} \quad (4.3)$$

---

<sup>1</sup> <http://www.mathworks.de/de/help/stats/kmeans.html>



Where  $a_i$  is the average distance from the  $i^{th}$  point to the other points in the same cluster,  $b_i$  is the minimum average distance from the  $i^{th}$  point to points in a different cluster, minimized over clusters. The clustering solution is considered appropriate when most points have a high silhouette value. On the other hand, the clustering solution may have either too many or too few clusters when many points have a low or negative silhouette value.

If the number of clusters in the data are unknown, it is instructive to experiment with a range of several values for  $k$ . Based on the highest average silhouette value, the optimal number of clusters,  $k$ , can be determined. Also, a suggestion proposed by Miller (1956) that number of clusters in the range of  $7 \pm 2$  may be taken into consideration in order to provide decision makers more options of significant solutions from Pareto optimal front.

(iii) Each centroid solution of a cluster is computed as the mean of the points in that cluster and is a representative solution for that cluster.

#### 4.6.2 An approach for selecting the best compromise solution

This solution is determined by the shortest distance towards a hypothetical Utopia point -  $U(x_U, y_U)$ , the point in which all objectives are perfectly satisfied (Figure 4.5 - a). Firstly, all distance from the single non-dominated solution lying on the Pareto front to the Utopia point are calculated using the Euclidean equation ( $d_{euc}^i$ , Eq. 4.4) and then the shortest distance ( $d_{euc}^{min}$ ) is determined as follows:

$$d_{euc}^i = \sqrt{(x_i - x_U)^2 + (y_i - y_U)^2} \quad (4.4)$$

with  $d_{euc}^i$  being Euclidean distance from single non-dominated solution  $i^{th}$  with coordinate  $(x_i, y_i)$  to the  $U(x_U, y_U)$  (Werisch, S. et al., 2013). From Eq. 4.4, it is clear that these distances depend mainly upon the position of hypothetical Utopia point. Two different ways can be used to define this position: (1) a reference point, in which both objectives are perfectly satisfied and (2) an intersection of the two elongation axes of two extreme solutions and this is a favorable approach. In addition, in order to obtain the most suitable compromise solution, normalized method is executed in case if there is big difference between the two axes. In this case, the corresponding  $U(1, 0)$  is an appropriate Utopia point (Figure 4.5 - b).

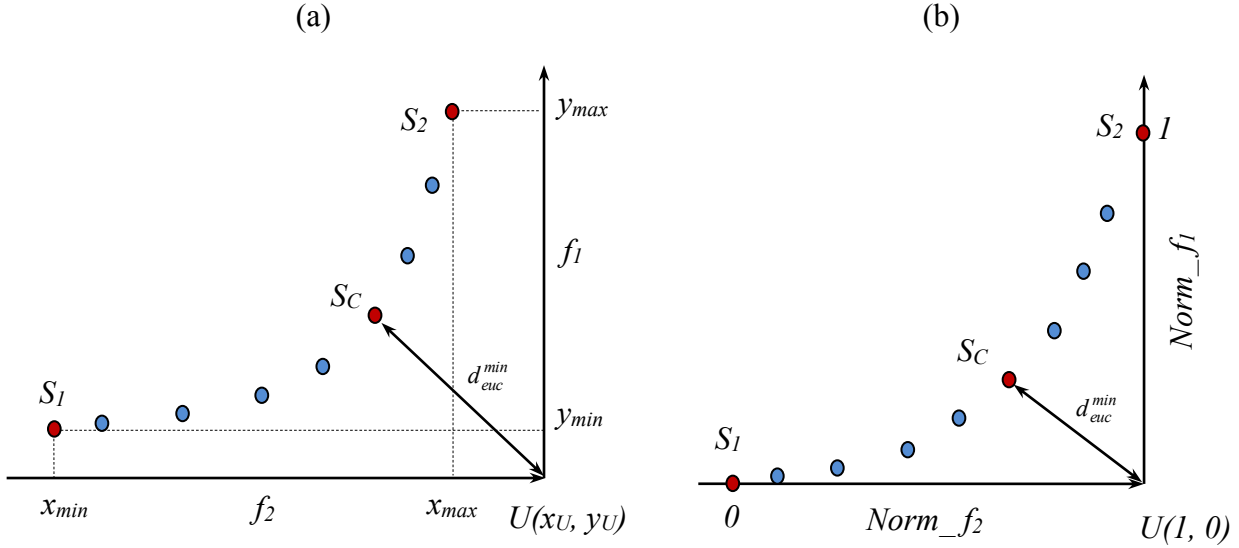


Figure 4.5: Illustration for the measure of determining the best compromise solution from the Pareto optimal front

Normalized solution  $S_{norm}(x_i, y_i)$  can be calculated as:

$$S_{norm}(x_i, y_i) = \frac{S(x_i, y_i) - S(x_{min}, y_{min})}{S(x_{max}, y_{max}) - S(x_{min}, y_{min})} \quad (4.5)$$

Where  $S(x_i, y_i)$  is the solution  $i^{th}$  from the Pareto optimal solutions.  $S(x_{min}, y_{min})$ ,  $S(x_{max}, y_{max})$  are the minimum and maximum solutions, respectively, corresponding to cost minimization and network reliability maximization.

Based on several most significant solutions that are identified by these two approaches with respect to the Pareto data, a superior trade-off between the objectives can be more easily chosen for solving a multi-objective optimization problem of PWDN design and operation.

#### 4.7 An approach for solving uncertain demand problem

Since PWDNs are commonly designed and planned with a predicted future data, they may have to meet uncertain conditions along their performing lifetime. Within an optimal PWDN design procedure, studying uncertain conditions which impact network reliability has received considerable attention in the research community (Babayan et al. 2004, 2005; Bhawe and Gupta, 2004; Kapelan et al., 2005; Ostfeld, 2005; Baños et al., 2011).

As mentioned in section 2.5, water demand uncertainty will be considered in this study. Water demand uncertainty arises mainly due to the different behaviors of water users and the change of network configuration when it is expanded to new consumers. In this study, a network robustness probability is defined to evaluate the network robustness under demand uncertainty.

Sampling technique is the approach to generate series of random uncertain input variables (nodal demands). This procedure can be obtained by many ways depending mainly upon the distribution of a sample set. Since demand changes may follow the normal distribution (Babayan et al., 2005; Kapelan et al., 2005), Monte Carlo (MC) simulation has been used frequently. However, this technique is time consuming since it requires a very large number of samples (hundred thousands) to produce an acceptable result. In contrast, the Latin hypercube sampling technique (LHST) needs only small number of samples. A dominant advantage of the LHST, compared to MC, is a better random sample stratification, i.e. nodal demands, which leads to a more accurate evaluation of the nodal pressures.

In practice, nodal demands in a PWDN can also be not independent because they may temporally depend on the scale of some factors which affect the network as a whole. For instance, hot and dry weather can result in a significant extra consumption for all nodes. Hence, LHST with a procedure proposed by Iman and Conover (1982) will be employed to produce a rank correlation matrix of uncertain correlated demand variables in this study. The procedure to produce correlation matrix of nodal demands can be briefly described as follows and more details can be found in Iman and Conover (1982).

Suppose that  $R$  ( $N_s \times N_v$ ) as the matrix of independent random samples is generated based on mean and standard deviation.  $N_s$  is the number of samples and  $N_v$  is the number of uncertain nodal demand input variables.

Let  $C$  ( $N_v \times N_v$ ) be the desired correlation matrix with the desired correlation coefficient. Because correlation matrix  $C$  is positive definite and symmetric, it may be written as  $C = PP'$  where  $P$  is the lower triangular matrix obtained by using Cholesky factorization.

Matrix  $R^*$  with the desired correlation coefficient is achieved as  $R^* = RP'$ . The rank correlation matrix  $M$  of  $R^*$  should be close to  $C$ .

The samples in  $R$  are finally rearranged column-wise to have the same rank ordering as the corresponding column of  $R^*$ . Thus, the input values have the same sample rank correlation matrix that  $R^*$  has. Each row of input values matrix now represents a single correlated demand loading condition.

By using this procedure, a set of random uncertain input nodal demands are generated based on a set of expected values (or mean values -  $\mu$ ) and standard deviations ( $\sigma$ ). Expected values are assumed equaling to the deterministic demands at nodes. While standard deviations are hypothesized equaling to 10% and 30% of the corresponding expected values (Kapelán et al, 2005).

The uncertain output variables (nodal heads or pressures) corresponding to these uncertain input variables are then calculated using the Epanet model. Subsequently, the robustness probability is computed as the ratio (percentage) of the number of times that a particular criterion is satisfied at all nodes (i.e. nodal pressures are not smaller than corresponding minimum required pressures) to total number of samples (Eq. 4.6):

$$P_R = \frac{N_C}{N_S} \quad (4.6)$$

where  $P_R$  is robustness probability of network,  $N_C$  is number of times that the minimum required heads are met simultaneously at all nodes

Procedure solving the PWDN optimal design under demand uncertainty is expressed in Figure. 4.6 and can be interpreted as follows:

(i) From the Pareto front, several significant solutions are proposed

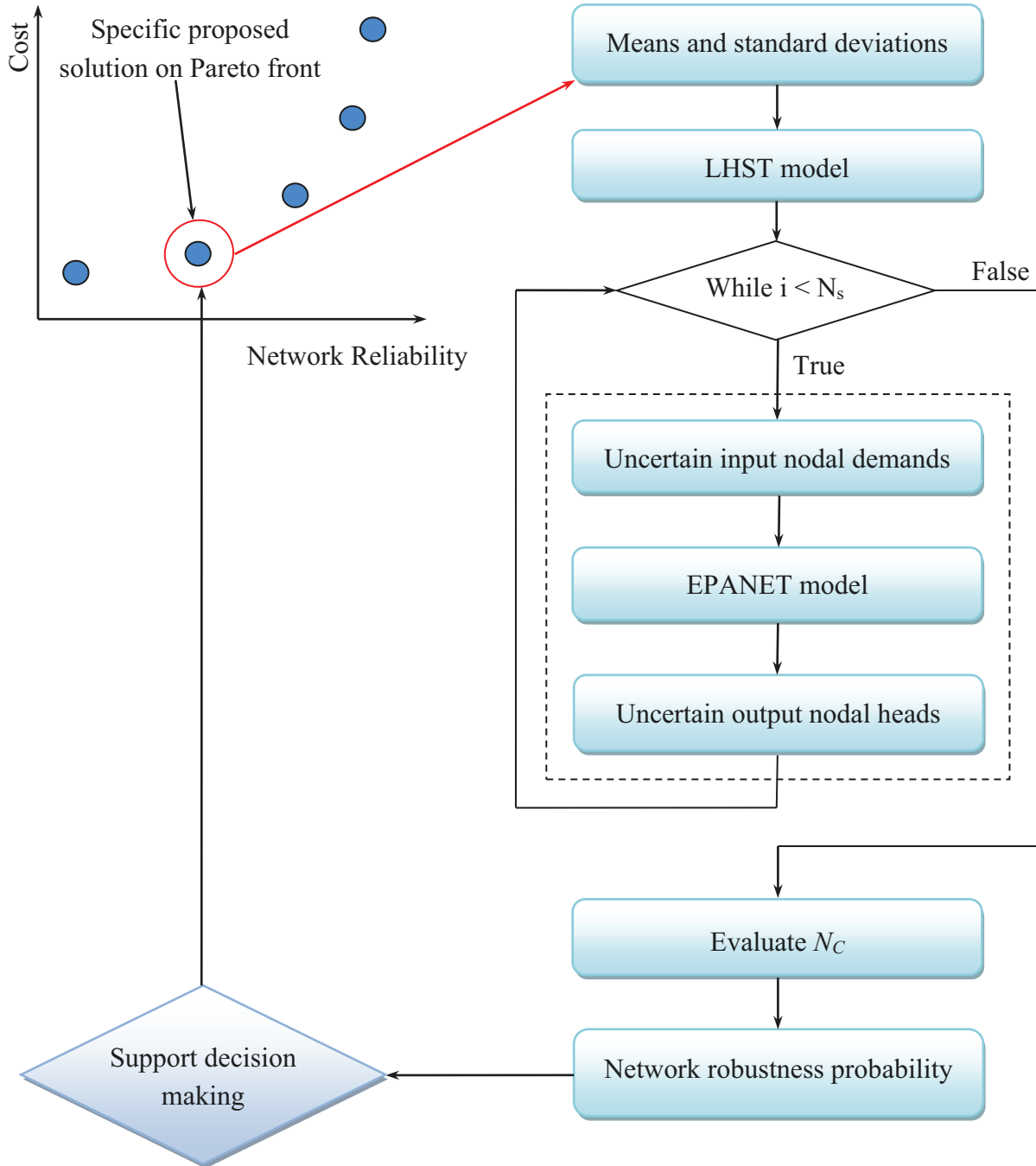


Figure 4.6: Procedure for evaluating robustness probability of PWDN optimal design under demand uncertainty

- (ii) Nodal demands are the only uncertain variables, which are assumed following a normal distribution with means equal to the deterministic demands at demand nodes and an assumed standard deviation.
- (iii) The LHST is in turn executed with the proposed solution to generate a matrix including  $N_s$  rows and  $N_v$  columns of random uncertain input nodal demands. Based on either uncertain uncorrelated demands or uncertain correlated demands, a different LHST procedure is used.
- (iv) Corresponding to each row of input nodal demand matrix, a set of corresponding nodal heads is evaluated using Epanet model. Finally, a matrix of random nodal heads is evaluated including  $N_s$  rows and  $N_v$  columns.
- (v) Calculate network robustness probability equivalent to the network configuration using Eq. 4.6. Associate the robustness probability with cost and network reliability the results will support designers to select an appropriate solution under demand uncertainty.



## 5 VALIDATION OF THE PROPOSED PRESSURE WATER DISTRIBUTION NETWORK DESIGN STRATEGY

The aim of this section is to test and verify two modes of the new proposed approach, namely CMA-ES-EP and MO-CMA-ES-EP by using several published benchmark networks in order to evaluate its capability for solving PWDN optimization problems. For comparison purposes, all given data and conditions of the published benchmark networks were kept unchanged for the verification of the new approach in this study.

### 5.1 Sensitivity analysis

An optimal result obtained regardless of any stochastic optimization techniques is influenced by a set of parameters that control the optimization procedure. Therefore, the foremost necessary task is to find an appropriate parameter set through sensitivity analysis.

Sensitivity analysis aims at exploring the optimal solution corresponding to each modification made in the parameter set or constraints; or in other words, this procedure explores the behavior of the model based on the effect on other parameters due to a change in a single parameter or constraint (Bhave, 1991). The sensitivity analysis of the CMA-ES model was performed with different combinations of each parameter. There are several significant specific parameters which can influence the model result as mentioned in subsection 4.4.2 in which some parameters are constant or default values while others can be changed. Sensitivity analysis of these changeable parameters is based on either their proposed variable intervals or mean values. Five sensitivity analyses were carried out with cost minimization for two-loop network (TLN – referred to as *Benchmark network No.1*) as described below.

#### *The basic performance and population sizes*

The TLN is a simple benchmark network introduced by Alperovits and Shamir (1977). It consists of 8 pipes, 6 junction nodes and is supplied by the single elevated reservoir No.1 (Figure 5.1). The Hazen – William friction factor  $C_{H-W} = 130$  is used for all pipes and the minimum pressures required for all nodes are 30 m. More basic data applied in TLN can be found in Appendix C.1. The most difficult problem of this network optimization is that higher demands are required at further nodes 5, 6, and 7 from Reservoir No.1.

Decision variables are the diameters of the eight pipes. Each pipe diameter has to be chosen from a commercially available set of pipes consisting of 14 different values. Hence, there is a total of  $14^8$  possible solution combinations for this network. The objective function is the initial capital cost for pipes, which is expressed in terms of decision variables (Alperovits and

Shamir, 1977) as:

$$PIC = \sum_{i=1}^{np} (C(D_i) \times L_i) \quad (5.1)$$

Besides the minimum required pressures, a maximum velocity of 2.0 m/s in pipes (Todini, 2000) was proposed as another constraint in this study. The penalty functions of the nodal head and velocity constraints can be written as (Afshar and Jabbari, 2008):

$$C_{penP} = \alpha_p \left( \sum_{j=1}^{nnode} \left( \frac{H_j - H_j^{min}}{H_j^{min}} \right)^2 \right) \quad (5.2)$$

$$C_{penV} = \alpha_p \left( \sum_{i=1}^{np} \left( \frac{v_i - v_i^{max}}{v_i^{max}} \right)^2 \right) \quad (5.3)$$

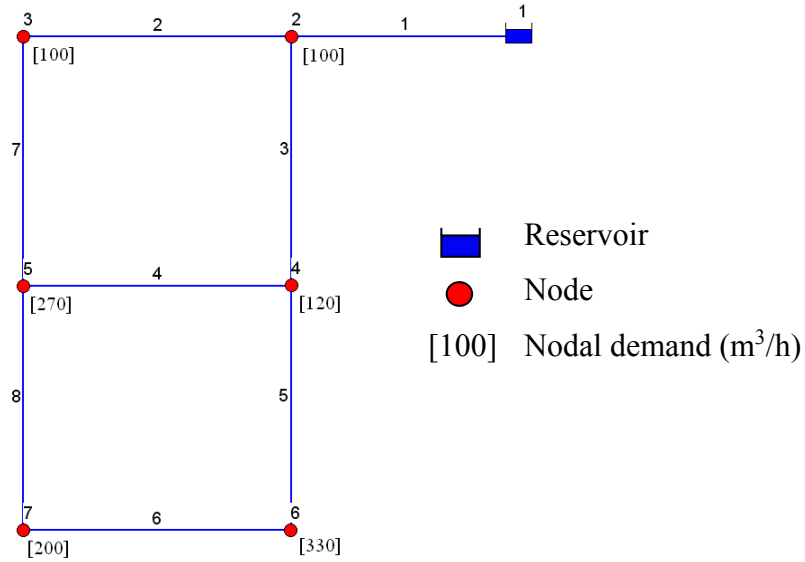


Figure 5.1: Layout and nodal demands of the two-loop benchmark network.

Theoretically, the competitive performance of CMA-ES relates closely to the population size which can be freely chosen. A small population size is acceptable, yet it may not lead to a global optimal solution as in the other stochastic optimization techniques. In contrast, a large population size helps to avoid local optima, but it may lead to a time-consuming performance. Consequently, in sensitivity analysis 1, it is necessary to find a reasonable population size to avoid local optima as well as time consumption.

To track the convergence of decision variables, three forms of population sizes were used. They were abbreviated as “popsize” and were expressed in Matlab language under the following forms:

$$popsize = floor(2 * \log(N)) \quad (5.4.a)$$

$$popsize = floor(20 * \log(N)) \quad (5.4.b)$$

$$popsize = floor(40 * \log(N)) \quad (5.4.c)$$



where  $N$  is the number of decision variables that will be tested in the model (Table 5.1). The parent number, the number of selected search points in the population number, was determined under the form:

$$\text{Parent number} = (\text{floor}(\text{popsize}/2)) \quad (5.5)$$

With these forms, the population size and parent number are dependent upon the number of decision variables. Choosing by experimentation, initially normalized decision variables ( $x_{ini}$ ) and standard deviations ( $\sigma_x$ ) corresponding to all input decision variables were chosen to be equal to 0.7 and 0.4, respectively.

With the first population size, the cost of \$448,000 with 425 numbers of function evaluations (NFEs) was obtained (Appendix C.1.3.a). A better solution of \$442,000 with around 2,200 NFEs was produced with the second population size (Appendix C.1.3.b). These results do not dominate previous researchers' results (see Table 5.2).

By using the third population size form, the least cost of \$419,000 was obtained with 3,670 NFEs (see Appendix C.1.3. c). The results showed that the larger the population size, the smaller the objective value, but the bigger the NFEs.

*Table 5.1: Optimization results obtained by CMA-ES-EP for TLN network with  $N = 8$*

Trials	popsize 1	popsize 2	popsize 3
Population size	4	41	83
Parent number	2	20	41
NFEs	425	2,200	3,670
Cost (\$)	448,000	442,000	419,000

By tracking the convergence process, which is indicated in Figure 5.2, normalized decision variables for pipes may be assigned to exceed the interval [0 1] at around the first 300 NFEs. However, at the subsequent iterations, a box constraint handling method adjusts this infeasible decision variable to a feasible one in accordance with the CMA-ES theory.

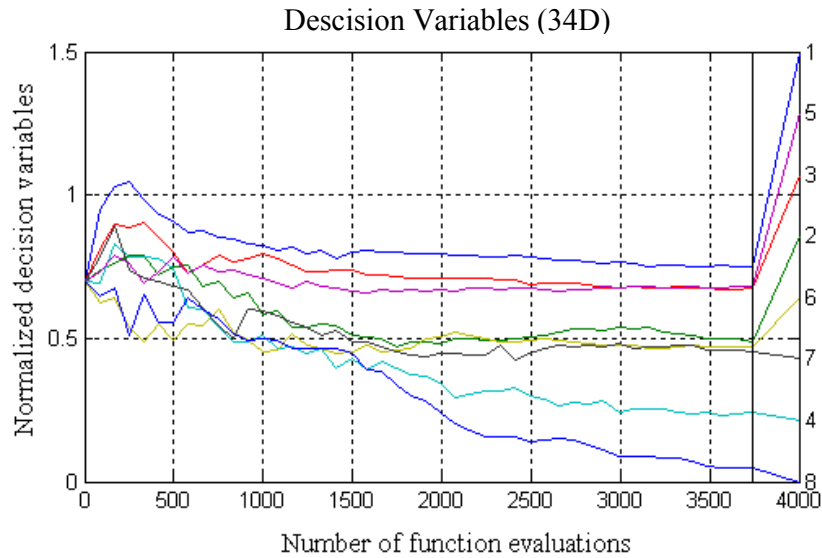


Figure 5.2: Convergence of norm-decision variables of TLN optimization with popsize 3.

Table 5.2: Comparison of optimization results for the two-loop network

Method	(1)	(2)	(3)	(4)	(5)	(6)	(7)	(8)
	LPG	CRS2	GA	ACCOL	GEO	GANE0	ACOA	CMA-ES-EP
Cost (\$)	497,525	422,000	424,000	447,000	419,000	419,000	419,000	419,000
NFEs	-----	10,009	3,381	1,810	7,467	100,000	3,000	3,670

Compared with previous studies as reflected in Table 5.2, the optimal cost produced by CMA-ES-EP in Column 8 was lower than the results produced by LPG (Column 1) and CRS2, GA, and ACCOL (Columns 2, 3, and 4) and was exactly equal to the optimum results obtained from GEO, GANE0, and ACOC (Columns 5, 6, and 7). CMA-ES-EP produced the optimal result with acceptable NFEs of 3,670 compared to the other approaches. Particularly, CMA-ES-EP led to a considerable cost reduction compared to the method that couples GA with Epanet performed by Dijk et al., 2008 (Column 6). In addition, compared to the total possible solution combinations ( $14^8 = 1.48 \times 10^9$ ), the NFEs proved the effectiveness of the new proposed approach. Pressures at nodes and velocities in pipes corresponding to the optimal solution satisfied the given limitations and are depicted in Figure 5.3.

(1) Alperovits and Shamir (1977) used Linear Programming Gradient method – LPG which may split pipeline into segments with different lengths and diameters

(2, 3, 4) Abebe and Solomatine (1998) used three methods: Controlled Random Search 2 – CRS2, Genetic algorithm – GA, and Adaptive Cluster covering with local search – ACCOL;

(5) Wu (2001) used Genetic Evolution Optimization – GEO

(6) Dijk et al. (2008) used GA and Epanet – GANE0

(7) Afshar (2009) used Ant colony optimization algorithm – ACOA

NFEs: Number of function evaluations

CMA-ES-EP performance with  $popsiz = \text{floor}(40 * \log(N))$ ,  $x_{ini} = 0.7$ , and  $\sigma_x = 0.4$  produced the optimal result. Therefore, it was referred to as the basic performance used for comparing the results of further sensitivity analyses with respect to TLN.

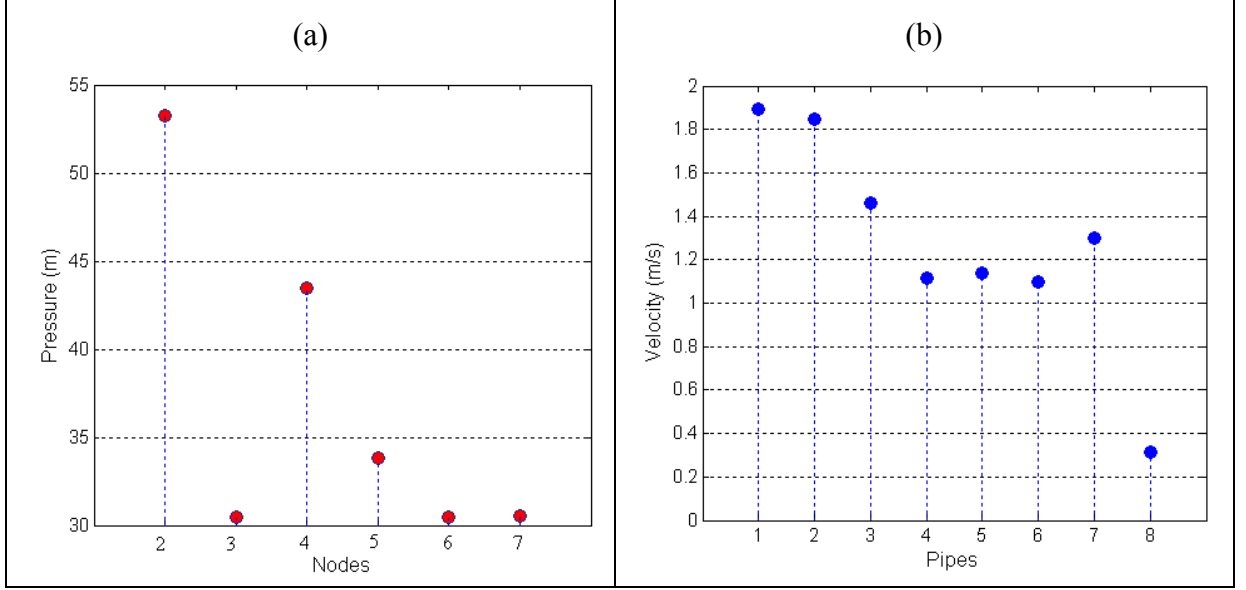


Figure 5.3: Nodal pressures (a) and velocities in pipes (b) produced by optimal solution

#### Initial decision variables ( $x_{ini}$ )

In sensitivity analysis 2, all normalized initial decision variables were set equal to 0.1 while the values at the basic performance were 0.7. In this case, the cost rose to \$428,000 (an increase of 2.1%) with more than 4,000 iterations. Cost also increased to \$427,000 at around 3,850 NFEs when all normalized initial decision variables were set equal to 0.9 (Appendix C.1.4). Thus, values of normalized initial decision variables that are either too low or too high would be not appropriate.

#### Standard deviations ( $\sigma_x$ )

In sensitivity analysis 3, standard deviations corresponding to all input decision variables were set equal to 0.1, compared with the basic performance whose values were 0.4. In this case, the optimal cost was achieved (Appendix C.1.5.a).

Similarly, standard deviations set equal to 0.9 also cannot produce the optimal cost as the basic performance (Appendix C.1.5.b).

#### The lowest nodal pressure

In sensitivity analysis 4, the minimum required pressure at node 6 was set at 35 m instead of 30 m in basic performance. The pressure yielded by the basic performance at this node was lowest due to the highest elevation and biggest demand. As a result, the cost increased to \$487,000 for a pressure of 35.6 m at this node.

*Velocity in the smallest pipe*

In sensitivity analysis 5, the smallest velocity in pipe 8 (corresponding to the smallest diameter yielded by the basic performance) was set equal to 1.5 m/s, while other parameters were intact. The cost in this case increased to \$699,000 corresponding to the velocity of 1.61 m/s in pipe 8 (whose diameter was 203.2 mm) and the smallest pressure of 30.60 m occurring at node 7. The smallest velocity of 0.30 m/s was in pipe 4 with diameter of 76.2 mm.

Based on these sensitivity analyses, it can be concluded that the cost and network configuration vary according to every unsuitable adjustment regarding model parameters as well as user-predefined constraints. Consequently, a proposed set of parameters should be chosen accordingly as shown in Table 5.3.

*Table 5.3: Selected parameters for the model*

No	Parameters	Variable interval	Selecting value/bound
1	Population size ( <i>popsiz</i> e)	$2 \leq \text{popsiz}$ e	floor( $40 \cdot \log(N)$ )
2	Initial decision variables ( $x_{ini}$ )	$0 \leq x_{ini} \leq 1$	Should be larger or equal to mean value
3	Standard deviations ( $\sigma_x$ )	$0 \leq \sigma_x \leq 1$	Should be smaller or equal to mean value

## 5.2 Simulation-based single-objective optimization module (CMA-ES-EP)

To verify the capacity of the CMA-ES-EP, this mode was tested on optimization problems regarding PWDN design and operation as well.

### 5.2.1 Minimizing pipe diameters with given layout and single demand loading

The objective of this section is to determine a set of pipe diameters with minimum capital cost while satisfying all the given constraints. The Hanoi network, a more complex network, is used to test this function of the new model.

#### *Benchmark network No. 2: The Hanoi water network*

The Hanoi water network is a more complex benchmark network consisting of 34 pipes, 32 nodes, and 3 loops which is supplied by a single fixed head source (Reservoir No.1) at an elevation of 100 m (Figure 5.4). It was introduced by Fujiwara and Khang (1990) and then was studied by many other researchers such as Savic and Walters (1997), Abebe and Solomatine (1998), Cunha and Sousa (1999), Liong et al. (2004), Geem (2006), Montalvo et al. (2008), Bănos et al. (2010), and Suribabu (2010).

Decision variables are the diameters of 34 pipes which have to be chosen from a specified set

of 6 different values [304.8, 406.4, 508, 609.6, 762, and 1016]. Thus, there is a total of  $6^{34}$  ( $2.87 \times 10^{26}$ ) possible combinations of pipe diameters for this network. More detailed information of the network can be found in Appendix C.2.1, 5.2.2, and in Fujiwara and Khang (1990). The cost objective function is expressed as in Eq. 5.6 below with the penalty function of the nodal head and the velocity constraints given as in Eq. 5.2 and Eq. 5.3.

$$PIC = \sum_{i=1}^{np} (1.1 \times (D_i)^{1.5} \times L_i) \quad (5.6)$$

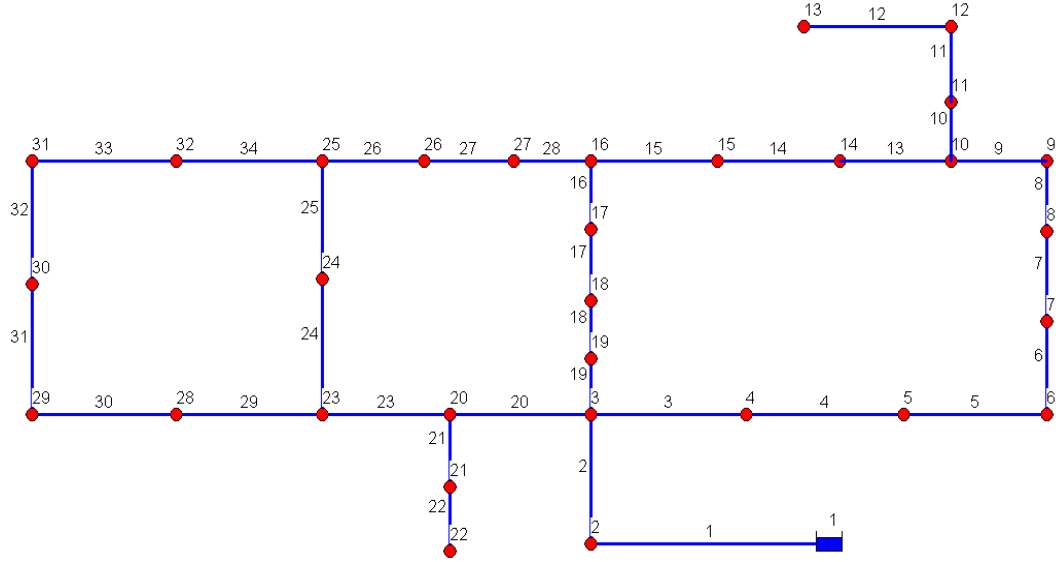


Figure 5.4: Hanoi water network layout representing nodes and pipes.

Three forms of population size (Eq.5.4), parent number (Eq. 5.5) and other parameters proposed in section 5.1 were also applied to this benchmark network.

Table 5.4: Population size and optimization results for testing model with the HN network

Trials	popsize 1	popsize 2	popsize 3
Population size	6	69	138
Parent number	3	34	69
NFEs	7,500	10,800	12,800
Cost (Mi. \$)	6.35	6.18	6.046

Through the visible convergence process, in the optimization process, many normalized decision variables exceed the interval [0 1] at around the first 5,000 iterations. Afterwards, the box constraint handling method adjusted these infeasible decision variables to feasible ones at subsequent iterations as shown in Figure 5.5.

As can be seen in Column 9, Table 5.5, CMA-ES-EP using the popsize 3 produced a more economic solution but a relatively low number of function evaluations (12,800). This has become the best result obtained to date. The smallest surplus head yielded by this optimal solution is 0.17 m at node 13. More detail about the optimal diameter set and corresponding

nodal pressures and velocities in pipes can be found in Appendix C.2.1- Appendix C.2.3.

From Table 5.5, two solutions obtained by Savic and Walters (Column 3) appeared to be reasonable, yet according to Liong and Atiquzzama (2004) the resulting pressure heads were violated at two nodes (13 and 30) and six nodes (13, 16, 17, 27, 29, and 30) corresponding to GA (Column 3) and SA (Column 6), respectively. The higher cost solutions by Abebe and Solomatine (Column 4 and 5) using GA and ACCOL by Liong and Atiquzzama (Column 7) were certainly not optimal compared to other solutions. Although the HS approach produced an appropriate cost (Column 8), it required very large NFEs.

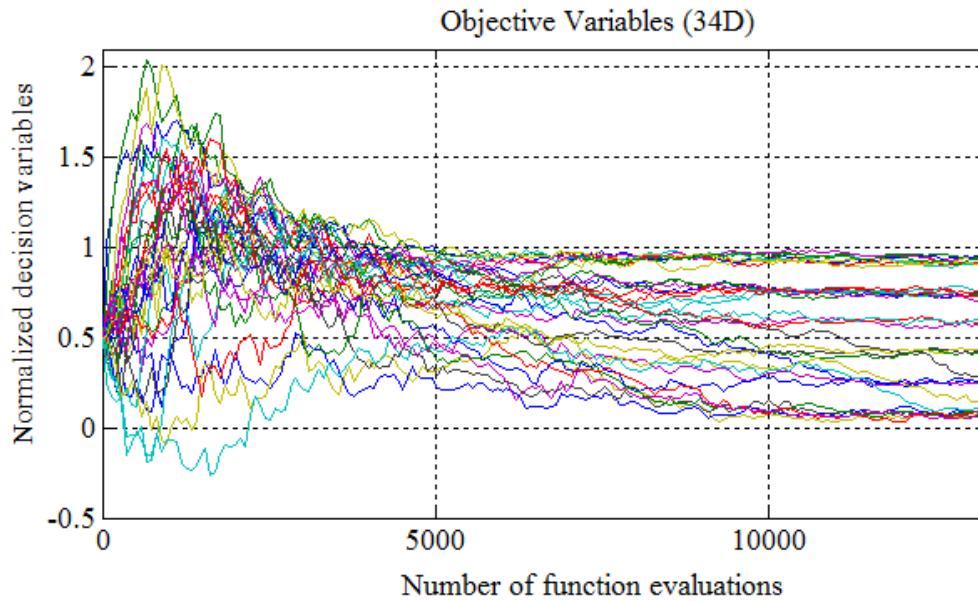


Figure 5.5: The convergence of decision variables of Hanoi with popsize 3

Table 5.5: Comparison of optimization results for the Hanoi network.

Methods	Fujiwara & Khang (1990)	Savic & Walters (1997)	Abebe & Solomatine (1998)		Cunha & Sousa (1999)	Liong et al. (2004)	Geem (2006)	Current Study
	LP	GA	GA	ACCOL	SA	SCE	HS	CMA-ES
1	2	3	4	5	6	7	8	9
Cost (Mi. \$)	6.320	6.073	7.00	7.80	6.056	6.22	6.056	6.046
NFEs	\	\	16,910	3,055	53,000	25,402	200,000	12,800
Minimum surplus head (m)	1.05	1.16	0.13	0.55	1.15	0.05	1.15	0.17

Based on these two application results, the basic set of CMA-ES-EP with the *popsize* 3, the

set of initial norm-decision variables  $x_{ini} = 0.7$ , and the standard deviation  $\sigma_x = 0.4$  is also used for performance of other benchmark networks.

### 5.2.2 Minimizing pipe sizes with multi-demand loadings

The aim of this section is to determine the corresponding reaction of the model to the change of demand with time. To facilitate the observation process, this feature of the model is tested on the Benchmark network No.1. Two assumptions made to this test were that basic deterministic nodal demands were kept the same as in Alperovits and Shamir (1977) and they change hourly during a 24-hour operation scheduling under the demanded multiplier expressed in Figure 5.6 a. Decision variables, cost objective, and constraints are taken as the same as those for TLN.

The lowest cost of \$419,000, which is the same as in single demand (presented in Section 5.1.1), was achieved by CMA-ES-EP corresponding to the largest demand period.

Figure 5.6.b presents a time series of nodal pressures corresponding to multiple demand loadings. Nodal pressures are minimum during the highest demand period, so-called peak period (from 12:00 to 18:00). The other periods are off-peak.

The fact is that every PWDN has to be performed under demands varying with time; therefore, it is necessary to simulate the very complicated hydraulic conditions inside the system with such a capable model.

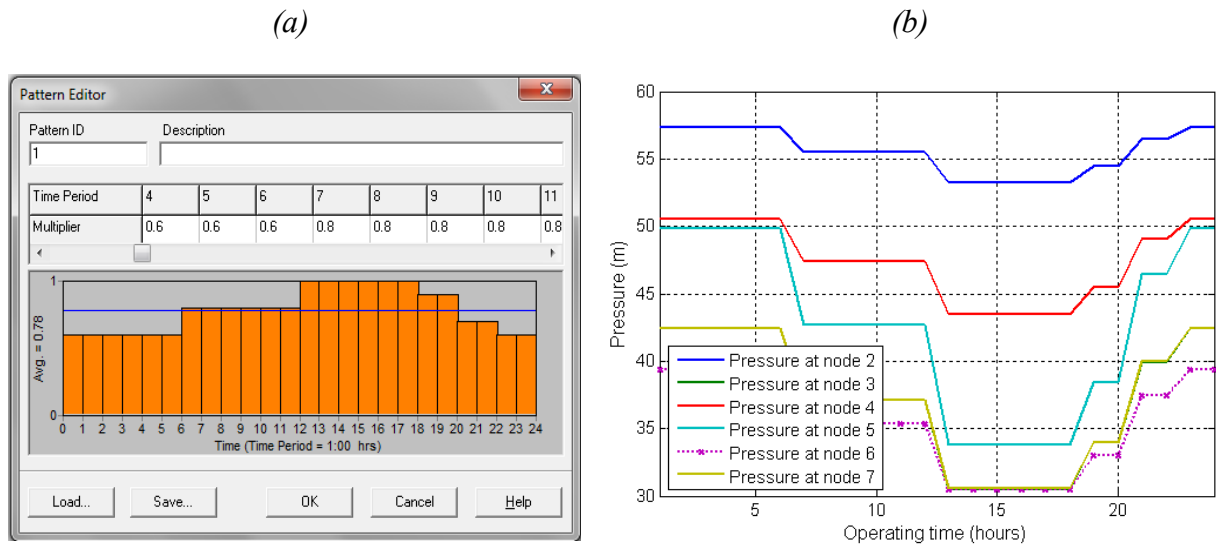


Figure 5.6: (a) Pattern of demand multipliers for an operation scheduling and (b) time series of nodal pressures corresponding to multi-demand loadings of TLN.

### 5.2.3 Maximizing network reliability

As discussed in Section 3.3.2, five formulations including minimum surplus head index (MSHI), total surplus head index (TSHI), resilience index (RI), network resilience (NR), and pressure uniformity coefficient (PUC) have been proposed to evaluate the reliability of a

network. Benchmark network No.1 was used to analyze and determine the most appropriate network reliability measure. Decision variables were pipe diameters. The penalty function for the nodal heads was added if there was any violation of the minimum required pressure.

As a result, five maximum solutions of network reliability definitions applied for two-loop network corresponding to 5 network reliability measures were evaluated and predicted in Appendix C.1.7. From these results, it can be concluded that:

When in turn and independently maximizing MSHI, TSHI, and PUC, the optimal procedure of CMA-ES-EP cannot produce the maximum network configuration (at the maximum cost of Mi.\$4.4 because there was still at least one pipe which does not meet the biggest diameter. Thus, they cannot reflect exactly the behavior of the network as its configuration is close to the maximum one. An important observation was that both maximum MSHI and TSHI can appear in solutions without maximum network configuration. With respect to PUC, the same maximum value was produced by different network configuration.

Maximizing RI can produce the maximum network configuration, but the maximum value of RI (0.9038) also appeared when maximizing TSHI and PUC, whose configuration is not a maximum network. Regarding the economic point of view, the solution obtained by maximization of RI was clearly worse than the solution obtained by maximization of TSHI. Therefore, RI was not likely to be the best measure for evaluating network reliability.

With regard to NR maximization, the maximum value of 0.9038 was produced only once together with the maximum network configuration at the cost of Mi.\$4.4. Moreover, distinctly different NR values were observed among different network configurations.

In fact, both RI and NR were closely competitive and have frequently been used for solving network reliability problem. As analyzed above, maximizing NR can cover all possible network configurations. Another advantage of the use of network resilience instead of the resilience index is that it produces more robust designs and clearly meets reliable loops of equal pipe sizes by penalizing sudden changes in pipe diameter (Raad et al., 2009). In addition, NR can provide increases of both capacity and redundancy, which are prioritizations of PWDN design (Prasad and Park, 2004; Banos et al., 2011). For this reason, its formulation (Eq. 3.25) would be proposed to measure the network reliability towards a PWDN design optimization.

#### ***5.2.4 Simultaneous design of component sizes and layout of a PWDN***

Whether to use a branched or a looped network is a question that arises whenever optimal design of a PWDN is required. Besides pipe diameter optimization, the network layout optimization problem also plays an important role regarding cost and network reliability. For testing the capacity of the CMA-ES-EP approach in a simultaneous and optimal design of network layout and pipe diameters, two aforementioned levels of the required layout



reliability, namely,  $\overline{OLR} = 1$  and  $\overline{OLR} = 2$  (in Section 4.5), were used in turn.

The objective function is the cost of pipes as written in Eq. 5.1. Decision variables are diameter of pipes. Penalty functions given in Eq. 5.2 and Eq. 5.3 are used if there is any violation of minimum required nodal pressures and maximum velocity in pipes. In addition, the penalty function related to optimal layout reliability ( $C_{penL}$ ) can be empirically determined as follows:

$$C_{penL} = nn.CS_{max} \quad \text{if} \quad CLR < \overline{OLR} \quad (5.7)$$

$CS_{max}$  is the most expensive cost of network and  $nn$  is the number of nodes of the current network violating the required layout reliability level.

With the use of the procedure proposed in Section 4.5, redundant pipes will be assigned by the additional diameter value with the corresponding zero cost. The number of working pipes (open status) will, therefore, change from one iteration to the next. In the optimal solution, redundant pipes are removed from the predefined maximum network.

The benchmark networks used for testing the model include the network introduced by Geem et al. (2000) and a more complicated network introduced by Morgan and Goulter (1985). These networks were then studied by Afshar and Jabbari (2008). By using the required layout reliability, their approach was closer to the global optimum as regard simultaneous layout and pipe sizes.

#### *Benchmark network No.3: Geem et al. 's network*

The network proposed by Geem et al. (2000) (Figure 5.7.a) consists of one reservoir (node 9) at an altitude of 50 m, 8 demand nodes (from node 1 to node 8) at an altitude of 0 m, and 12 interconnected pipes. The length of all pipes is 100 m with the same Hazen – William coefficient assumed equaling to 130 m. The minimum required pressure is 30 m for all the demand nodes. Other network's characteristics can be found in Appendix C.3 and Geem et al. (2000).

CMS-ES-EP achieved a remarkably low cost of \$38,600 with the absence of pipes 1, 3, 5, and 9 (Figure 5.7.d). This cost was, in turn, 2.1% and 3.1% cheaper than that of Afshar and Jabbari method (\$39,400) and Geem et al. study (\$39,800), respectively. The lowest pressure of 30.07 m is performed at node 2 (i.e. minimum surplus head = 0.07 m).

All three results above show that optimum or near optimum cost solutions were achieved only if the network had the simplest layout (branched layout). In each solution, the absence of four pipes occurred and there were three nodes connecting to source node by only one pipe. It is clear that these optimized networks satisfy the required layout reliability level 1 ( $\overline{OLR} = 1$ ).

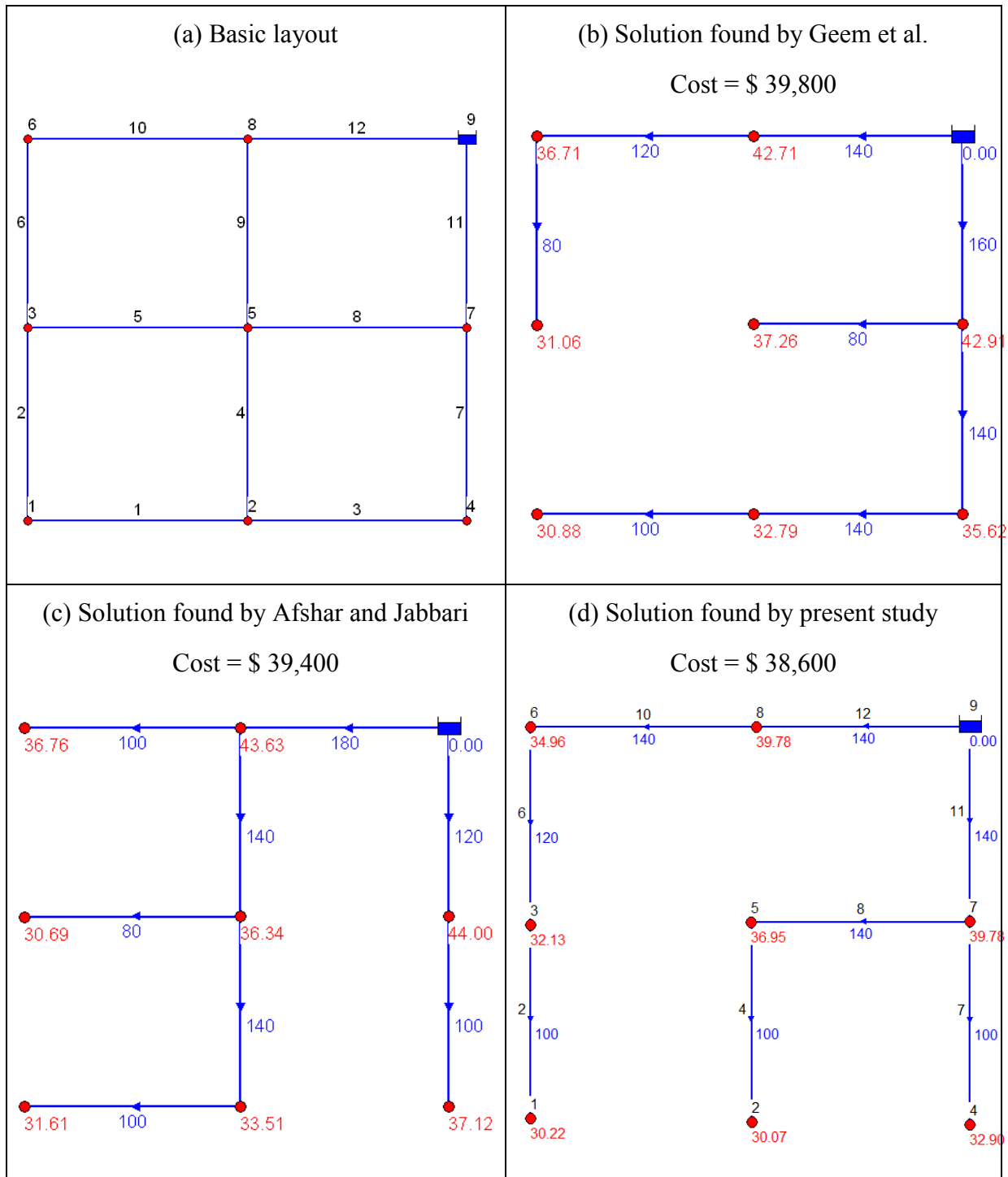


Figure 5.7: (a) Basic layout for Benchmark network No.3 and three optimal layouts representing pipe diameters and nodal pressures obtained by (b) Geem et al., (c) Afshar and Jabbari, and (d) current study.

#### Benchmark network No.4: Part of the Winnipeg network

Another more complex example network as shown in Figure 5.8.a is a part of the Winnipeg network. This network, consisting of 2 sources (node 5 and 16), 18 junction nodes, and maximum 37 possible pipelines, is used to test the performance of the new technique CMA-ES-EP. All possible pipelines generate the predefined maximum network layout. The other

available data are presented in Appendix C.4 and Afshar and Jabbari (2008).

The objective is to economically design this network with both required layout reliability levels 1 and 2 beside the constraint of minimum required pressure. Practically, once the required layout reliability level is not considered as additional constraints, a complex multi-source PWDN is separated into sub-networks. Generally, the number of sub-networks depends on the number of source nodes connecting to the network. As presented in Figure 5.8.b, the two-source PWDN was divided into two separated sub-networks. Consequently, the required layout reliability not only improves the network reliability but also ensures the network to be analyzed is not separated into sub-networks.

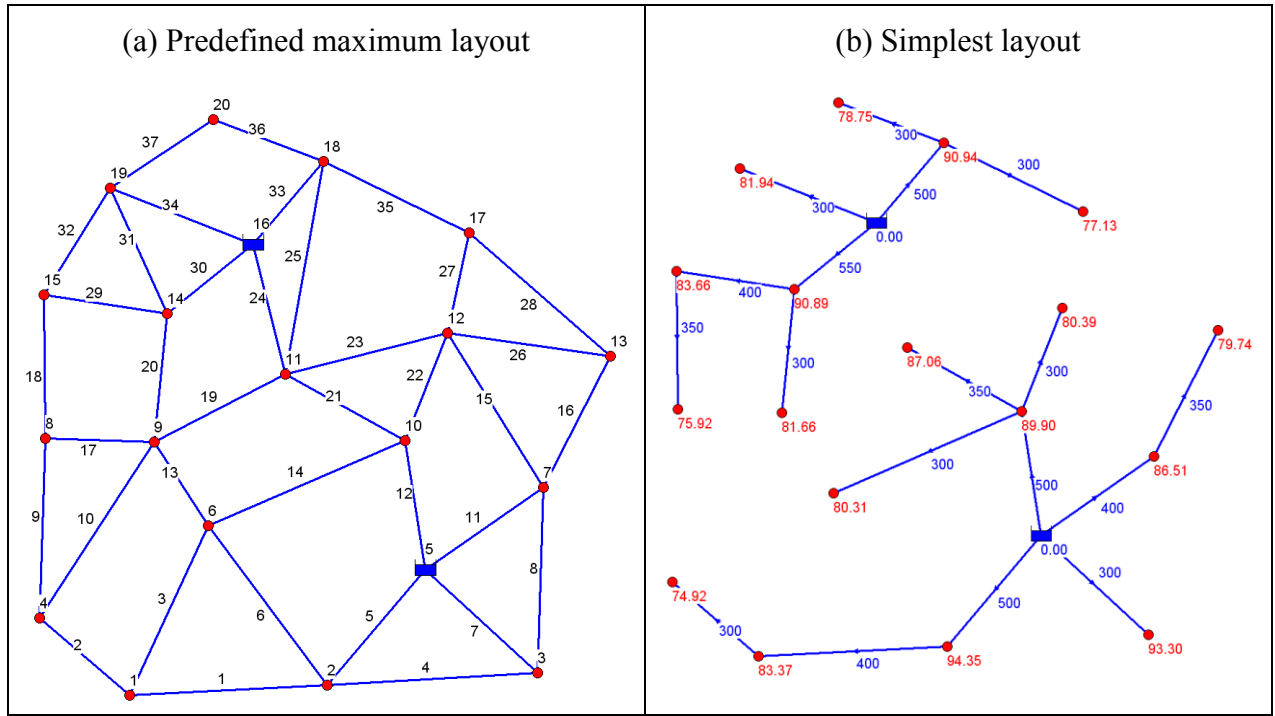


Figure 5.8: (a) Pipes and nodes of the predefined maximum layout and (b) the simplest layout achieved by CMA-ES-EP without any additional required layout reliability.

Required layout reliability level 1 ( $\overline{OLR} = 1$ )

As shown in Figure 5.9.a and b, the two lowest cost solutions representing the smallest pipe diameters and the lowest set of nodal pressures associated with the branched network layouts were obtained by GA with the cost of \$1,783,086 (Afshar and Jabbari, 2008) and by CMA-ES-EP model with the cost of \$1,716,324. Although these solutions had the same number of pipes (19 pipes), they were different in configuration.

A lower cost was achieved by CMA-ES-EP. It can also be demonstrated that the PWDN fed by multi-sources is not divided into sub-networks during optimization process if the required layout reliability is added.

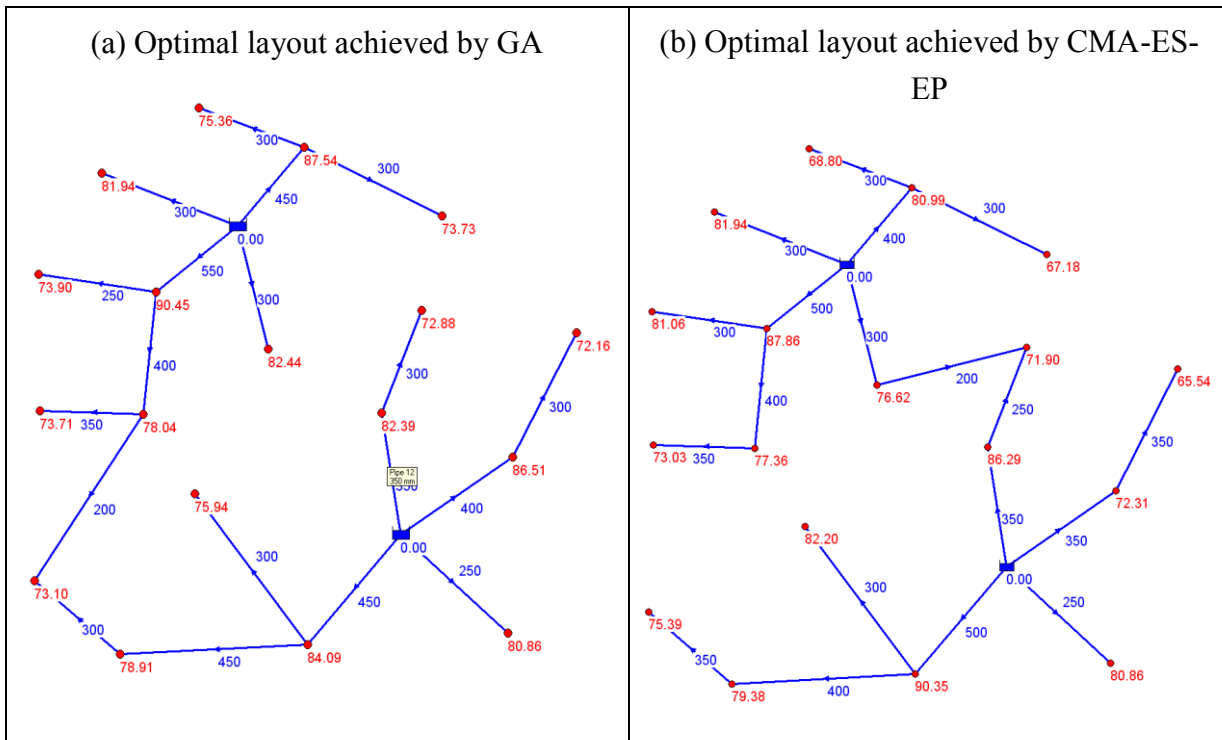


Figure 5.9: Different optimal layout solutions representing pipe diameters and nodal pressures obtained with required reliability level 1 by using (a) GA and (b) CMA-ES-EP.

Required layout reliability level 2 ( $\overline{OLR} = 2$ )

By using linear programming method (LP), a 28-pipe network layout was determined with the cost of \$1,950,698 by Morgan and Goulter (Figure 5.10.a). However, this solution associated - with the negative pressures at several nodes (in which, the minimum negative pressure of - 29.51 m at node 13) - was an explicit evidence for the infeasible solution.

Another more economical solution of \$2,056,739 with 25-pipe layout was obtained by Afshar and Jabbari (2008) by using the GA approach (Figure 5.10.b). The satisfaction of pressures at all nodes with the minimum surplus head of 0.21 m supports that this approach can produce appreciated solutions.

However – as shown in Figure 5.10.c the CMA-ES-EP approach attains even a more economical solution (\$1,985,252) with a 26-pipe network. All nodal pressures satisfied the given constraints with the smallest surplus head at only 0.16 m. All the results are indicated in Table 5.6.

These three results show that the network layout obtained with the required layout reliability level 2 is clearly to be looped regardless of either an optimal or nearly optimal solution.

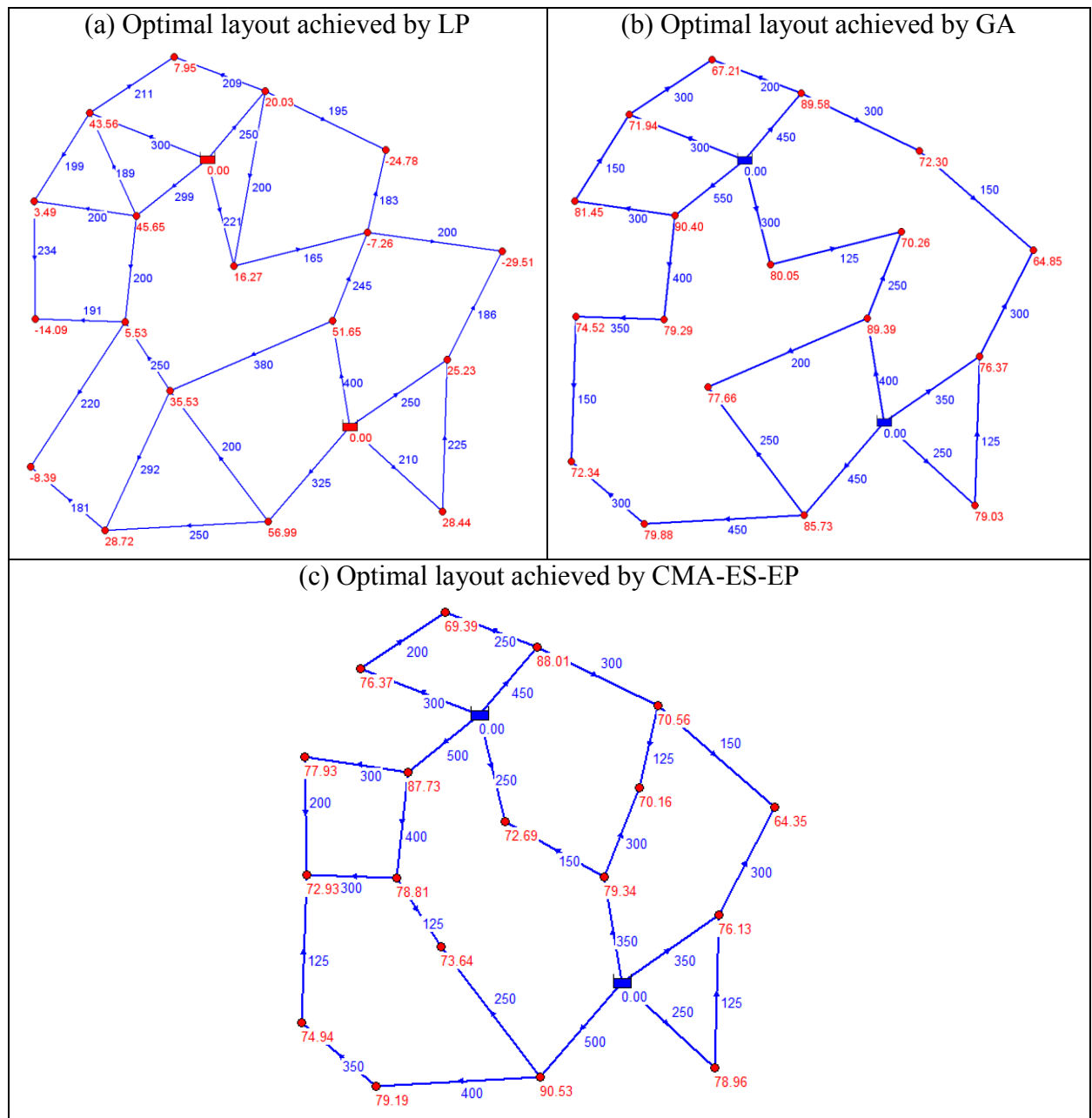


Figure 5.10: Different layout solutions representing pipe diameters and nodal pressures achieved with required layout reliability level 2 by different methods.

Table 5.6: Solutions obtained with different approaches for Benchmark network No.4

Method	LP - Morgan and Goulter (1985)	GA – Afshar and Jabbari (2008)		CMA-ES-EP	
		Level 1	Level 2	Level 1	Level 2
Cost (\$)	1,950,698	1,783,086	2,056,379	1,716,324	1,985,252
Minimum surplus head(m)	- 29.51 (for continuous diameters)	0.90	0.21	0.18	0.16

From the results above, it is clear that the new proposed technique is capable of optimally

designing simultaneously a PWDN configuration including layout and sizes. The evaluation of the layout is based on a maximum predefined network under specific constrained conditions and a required layout reliability level. Without specific additional conditions, the network may tend to be separated into sub-networks during optimization.

### 5.2.5 Integral consideration of design and operation

In practice, a PWDN often consists of all main components such as pipes, pumps, and tanks. Hence, the hydraulic condition in such a network is considered as a series of quasi-steady states (Larock et al., 2000). The objective in this case is not only for the cheapest investment but also for a low operating cost which makes it very complicated for the integral optimization of a PWDN. In this section, an approach will be proposed for optimizing a PWDN consisting of pumps and tanks.

Besides pipe diameters, pump discharges and pump heads are also considered as decision variables. In this application, these parameters were determined by using the single point pump curve method which is included in the Epanet model for each pump (Rossman, 2000). Notably, when these two most important parameters of pumps are considered as decision variables, the pumps can be directly computed. This innovative point will assist designers to more easily choose appropriate pumps.

The objective in this case is to minimize the total cost (Eq. 3.13). The pipe cost is estimated as in Eq. 5.1, while others, including the pump construction (Eq. 3.8), the operation cost (Eq. 3.11), and the tank construction cost (Eq. 3.12), respectively, can be evaluated as follows (Ostfeld and Tubaltzev, 2008):

$$PUCC = \frac{CPUMP}{270 \times \eta_p} \sum_{p=1}^{npump} \max[(Hp_{1,p} \times Qp_{1,p}), \dots, (Hp_{t,p} \times Qp_{t,p}), \dots, (Hp_{NT,p} \times Qp_{NT,p})] \quad (5.8)$$

$$PUOC = AD \times APPV \times \frac{\Phi}{\eta} \times \sum_{p=1}^{npump} \left( \sum_{i=1}^{NT} EC_i \times PP_{p,i} \right) \quad (5.9)$$

$$\text{and} \quad TCC = \sum_{t=1}^{ntank} (UWTC(D_t^T) \times \max(HT_t)) \quad (5.10)$$

Where:  $CPUMP$ : unit power cost of pump construction (monetary unit/kW)

$AD$ : annual duration (365 days)

$APPV$ : annual pump presents value coefficient, and depends on two factors: annual interest rate and total pump lifetime (year). In this test,  $APPV$  is assumed equaling to 10.04.

$UWTC$ : unit water level cost of tank (\$/m) depends on tank diameter.

$\Phi$ : unit conversion factor

$\eta_p$ : pump efficiency, assumed to be constant

Besides the constraint of minimum nodal pressures (Eq. 5.2), constraints of available water quantity (Eq. 5.11) and tanks operation (5.13), respectively, are taken into account in terms of penalty functions:

$$C_{penW} = \alpha_p \sum_{r=1}^{nres} \left( \frac{Q_r - V_r}{V_r} \right)^2 \quad r = 1, \dots, \text{number of water sources} \quad (5.11)$$

$$\text{if} \quad Q_r > V_r \quad (5.12)$$

$$\text{and} \quad C_{penT} = \alpha_p \sum_{t=1}^{ntank} \left( \frac{HT_t^{beginning} - HT_t^{ending}}{HT_t^{ending}} \right)^2 \quad t = 1, \dots, ntank \quad (5.13)$$

$$\text{if} \quad |HT_t^{beginning} - HT_t^{ending}| > \varepsilon \quad (5.14)$$

where  $Q_r$  is annual pumping water volume from source  $r^{th}$ .  $V_r$  is annually capable of supplying water from source  $r^{th}$ .  $HT^{beginning}$  and  $HT^{ending}$  are water levels in tank at the beginning and in the ending of an operating cycle, respectively.  $\varepsilon$  is permitted difference of water level in tank after one operating cycle.

Apart from these considerations, a simple rule which is associated with the Epanet model was employed to control the status of pumps based on water level in tanks.

The proposed method in this thesis was tested on two published benchmark networks studied by Ostfeld and Tubaltzev, 2008.

#### *Benchmark network No.5 (Example 1 - Ostfeld and Tubaltzev, 2008)*

This benchmark network was assumed and studied by Ostfeld and Tubaltzev (2008) consisting of 11 pipes, 6 demand nodes (from 1 to 6), 2 junction nodes (7 and 8), 1 equalizing tank (10), 2 pumps (14 and 15) that supply water for the network from two constant head reservoirs (11 and 12) and one elevated reservoir 9 (Figure 5.11). Reservoir 9 takes charge of balancing the water supply due to the limit of water in the other reservoirs. The length of all pipes is 1,000 m, except for the length of pipe 11 which is 1,100 m and that of pipe 10 which is 100 m. Tank diameter and initial water level in tank are assumed to be 36 m and 2.0 m, respectively. Water quantity supplied in each reservoir is assumed to be limited to 20,000 m<sup>3</sup>/day. Permitted difference of water level in tank after one operating cycle,  $\varepsilon$ , is assumed to be 10E-2 m. The optimization process is performed for a typical day, divided into four loading conditions, and starting at 00:00. More detailed data is given in Appendix C.5.1 to C.5.3.

With this network, decision variables are 15 parameters including 11 pipe diameters which are selected from the set of 14 different values, discharges and heads of two pumps which are evaluated from interval of [1 10000] m<sup>3</sup>/h and [1 1000] m, respectively. Pumps are set off if the tank water level reaches the user-predefined maximum level.

Tables 5.7 and 5.8 show the comparison between the results obtained by using the CMA-ES-

EP approach and ACOA (Ostfeld and Tubaltzev, 2008). A considerable reduction of 21.8% in pump construction cost was achieved due to a smaller pump power (see Table 5.8) while pipe construction and tank construction costs were almost the same.

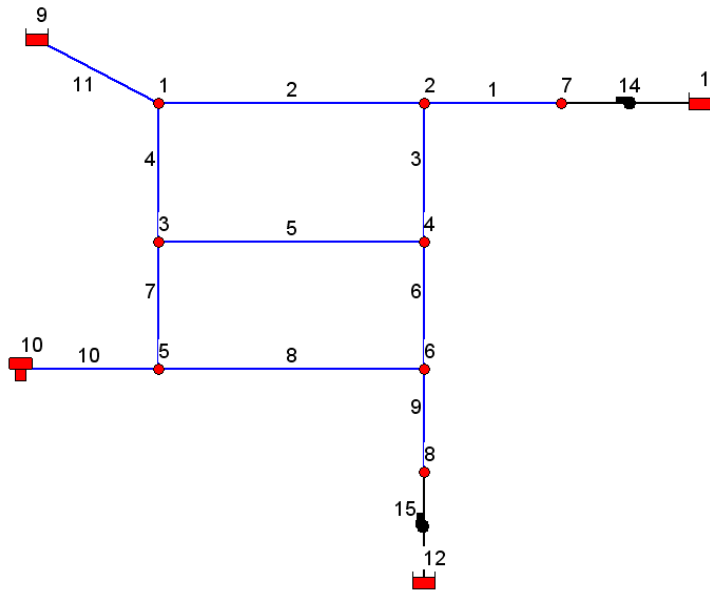


Figure 5.11: Layout representing pipes, pumps, nodes, tank, and reservoirs for Benchmark network No.5.

Tank water level at the end of an operating scheduling which returned almost the same as the beginning value is shown in Figure 5.12. The water level deviation of only 0.007 m (0.0037% of volume) between the beginning and the end of one operating cycle was satisfactory.

Table 5.7: Comparison of optimal cost solutions obtained by ACOA and CMA-ES-EP

Component costs	Reference study (ACOA)	Current study (CMA-ES-EP)
Pipe cost, PIC (\$)	395,300	413200
Pump operational cost, PUOC (\$)	1,397,651	1,312,300
Pump construction cost, PUCC (\$)	1,862,395	1,101,700
Tank construction cost, TCC (\$)	230,101	211,440
Total cost, CS (\$)	3,885,447	3,038,600



Table 5.8: Comparison of optimal pump powers

Pumps	ACOA	CMA-ES-EP			
	Max power (kW)	H <sub>P</sub> (m)	Q <sub>P</sub> (m <sup>3</sup> /h)	Average Power (kW)	Max Power (kW)
Pump 1	103.70	204	563	111.64	121.19
Pump 2	330.50	213	530	125.83	131.92
Total	434.20	-	-	237.47	253.11

In addition, from the engineering point of view, an operating scheduling for a PWDN encompassing all main components such as pipes, pumps, and tanks is appreciated only if the quantity of supplied water for a tank is largest during the off-peak period of time. A part of the total supplied water for the network is used for required demands, while the rest is stored in tanks and run back to the network during the peak period. Through water level in tanks, evaluation can be conducted to see whether an operating scheduling is suitable or not.

Therefore, when compared to tank water level in an operating scheduling obtained by ACOA (Figure 5.12.a), it was obvious that the result from CMA-ES-EP was the better one because under the four given loading conditions, the largest inflow to tank was occurring during the peak-off period regarding the lowest electric cost, from 00:00 to 06:00 and the largest outflow from tank was taking place during the peak period regarding the highest electric cost, from 12:00 to 18:00 (Figure 5.12.b).

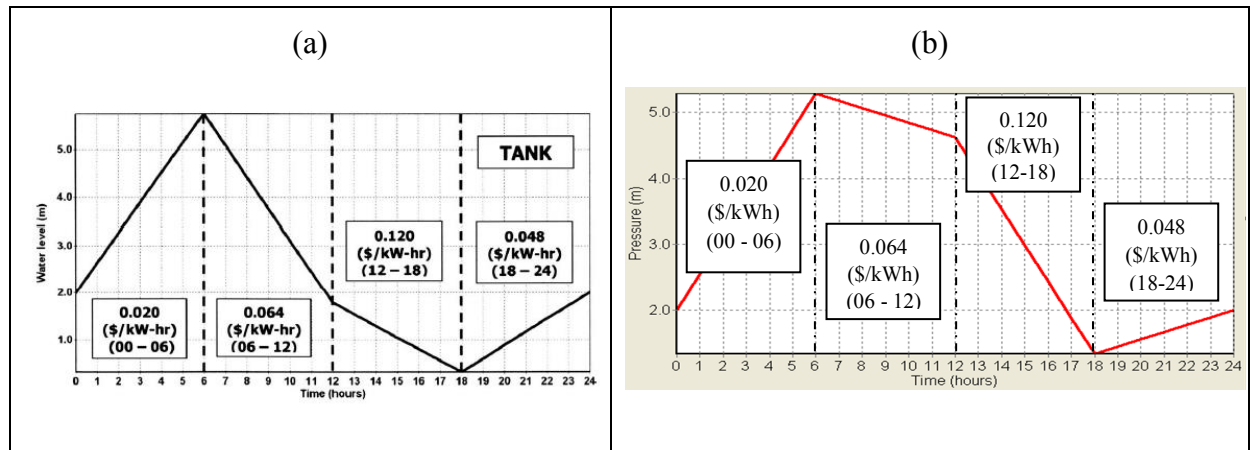


Figure 5.12: Time series of water level in tank (Tank 10) obtained by (a) Ostfeld and Tubaltzev using ACOA and (b) current study using the CMA-ES-EP approach

Moreover, as expected, this method resulted in the two most important features of a pump's characteristics, discharge and head, making it easier to choose pumps that are consistent with a PWDN (Table 5.8).

Nodal pressures at any time satisfied the minimum required condition, in which the smallest value was in node 6 at 6:00pm when there was no outflow from tank 10 (Appendix C.5.5).

*Benchmark network No.6 (Example 2 - Ostfeld and Tubaltzev, 2008)*

A more complex benchmark network consisting of 34 pipes, 16 demand nodes, and 1 tank is supplied by 2 pumps (Figure 5. 13). The length of pipes 1, 2, 3, 30, and 32 is 3000 m, of pipe 34 is 100 m, and of the rest is 1000 m. The initial water level in the tank is 10 m with an assumed tank diameter of 36 m. The distribution of the demand and energy tariffs for the four loading conditions, the unit cost of the candidate pipe diameters, and other assumptions are as in Benchmark network No.5. More detailed basic data can be seen in Appendix C.6.1.

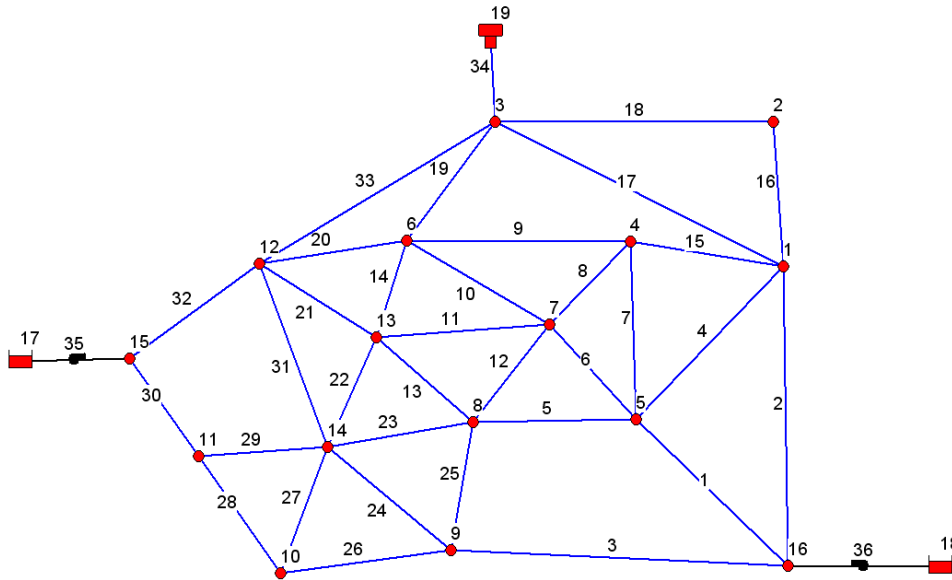


Figure 5.13: Network layout representing pipes, pumps, nodes, tank, and reservoirs for Benchmark network No.6 (Ostfeld and Tubaltzev, 2008)

The best solution was produced by CMA-ES-EP. The nodal pressures at 18:00, where the demand is maximum and the tank water level is lowest, satisfied the required minimum pressure (Appendix C.6.2).

A comparison between costs obtained by the CMA-ES-EP and ACOA method (used by Ostfeld and Tubaltzev, 2008) was conducted (Appendix C.6.3). Except for tank construction cost, which was a little more expensive than the reference cost, the others were somewhat more economical solutions. A much cheaper solution came from pump construction cost due to considerably less power being used (Appendix C.6.4).

Through the results produced by the CMA-ES-EP method for two case studies and the comparison with the solutions obtained by the ACOA method (Ostfeld and Tubaltzev, 2008), it is clear that:

- By using the same conditions as ACOA's for optimizing pipe and pump sizes, the CMA-ES-EP model produced more economical solutions, in which a set of smaller diameters expressed the cheaper pipe investment. Moreover, both pump construction costs were much lower due to the smaller pump powers achieved by CMA-ES-EP.
- In the CMA-ES-EP model, pump discharge and head were considered as decision variables.

This created a more convenient support for selecting a pump than the solution produced by the ACOA method, in which pump power was considered as decision variable, because pumps are now manufactured series with given operating parameters. Out of all available operating parameters, discharge and head are the most notable.

- Tank water level at the end of the operating cycle reached the beginning value with an acceptable tolerance showing that CMA-ES-EP was good not only for optimizing pipe and pump sizes but also for operating a PWDN including tanks.
- It is obvious that the solutions produced by ACOA in Benchmark network No.5 and No.6 were less suitable since outflow from tank was largest during the “between” period (from 6:00 – 12:00), whereas the solution produced by the CMA-ES-EP method seemed to be a more appreciated operating solution because the largest outflow from tank occurred during the peak period of time (from 12:00 – 18:00).

### **5.3 Simulation-based multi-objective optimization module (MO-CMA-ES-EP)**

The least cost approach using optimization algorithms has received considerable attention for the optimal design of PWDNs. However, this method clearly yields the minimum pipe diameter solution that mainly leads to the failure in the operating period. Consequently, it is not likely to be an appropriate method in the area of PWDN design.

As mentioned in Part 3, more recently the prevailing method of optimizing PWDN design and operation is based on the multi-objective optimization. In this section, MO-CMA-ES-EP is applied on several aforementioned benchmark networks. In general, the objectives of MO-CMA-ES-EP are to minimize the total cost and, as analyzed in Section 5.1.3, to maximize network resilience. The goal is to find the Pareto optimal front that includes a series of trade-offs solutions between these objectives (Figure 3.3). It is difficult to say which solution of this series is better than the others without any further consideration. A low cost solution or a low network reliability of designing PWDNs means that the networks will operate with low surplus head, high head loss and high risk, and vice versa.

In practice, higher level decision-making among the trade-off solutions is commonly required to select one of them for implementation (Savic, 2002). However, if there is no important criterion among these contradicting objectives, the approach proposed in Section 4.6 is applied to choose the optimal solution among few representative solutions consisting of the centroid and the best compromise solutions.

The capability of the MO-CMA-ES-EP method was compared to AMALGAM model (a multi-algorithm, genetically, adaptive multi-objective) applied on the same PWDN examples. The AMALGAM method was introduced by Vrugt and Robinson (2007) and successfully applied for optimal PWDN design by Raad et al., (2009). More details of the AMALGAM can be found in Vrugt and Robinson (2007).

### 5.3.1 Simultaneously optimizing network cost and reliability

A multi-objective optimization problem in PWDN design including cost and network reliability developed in the MO-CMA-ES-EP model was tested on Benchmark networks No.1 and No.2 under conditions mentioned in section 5.1. Both  $\alpha_p$  and  $\beta$  coefficients were chosen equaling to 10E+6 (Müller, 2012).

#### *Benchmark network No.1: The two-loop network*

Figure 5.15 expresses the corresponding relationship for all solutions produced by the MO-CMA-ES-EP optimization procedure between the total capital cost for pipes and the network resilience. The blue x-marks represent all dominated solutions while the colorful circles represent the Pareto optimal solutions. This appropriate Pareto optimal front can be densely created within only around 2,000 iterations. The minimum cost solution was in strong agreement with results obtained from the Single-objective optimization CMA-ES-EP as well as the previous results (Todini, 2000; Prasad and Park, 2004). Each solution on the Pareto front was a trade-offs between cost and network resilience and was not dominated by any other.

In order to apply k-means technique to this Pareto data to reduce this large set of compromising solutions, the optimal number of clusters must be determined. A range of the number of clusters from 2 to 10 was conducted in order to evaluate corresponding average silhouette values. As presented in Figure 5.14, the optimal number of clusters of three allowed the highest average silhouette value. Hence, there were three corresponding centroid solutions representing these three clusters (Figure 5.15).

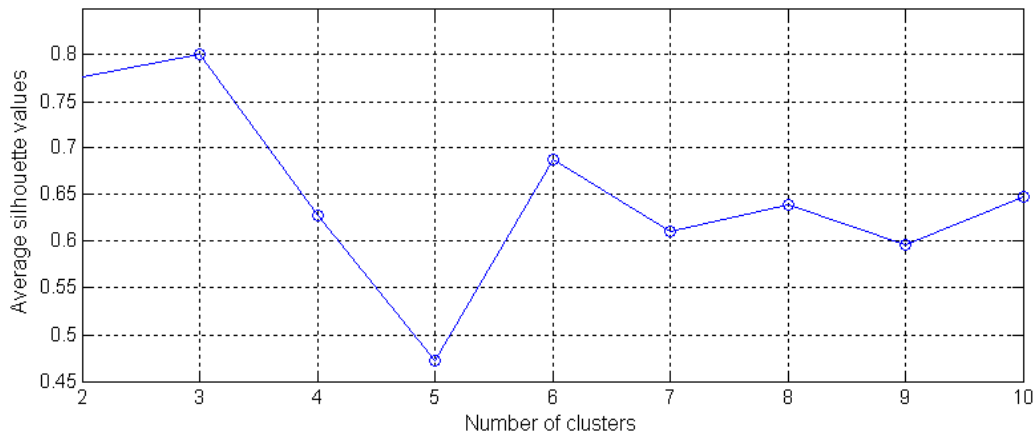


Figure 5.14: Average silhouette values corresponding to the number of clusters with respect to TLN Pareto data

Also, the Pareto optimal front showed that its shape may be separated into two stages at the best compromise solution (red circle), which was determined using the method mentioned in Section 4.6.2 and was closest to the Utopia point.

The first stage of the Pareto front encompassed the range of points from the minimum cost

solution to the best compromise solution. In this stage, a moderately higher cost coordinated with a considerable increase of network resilience.

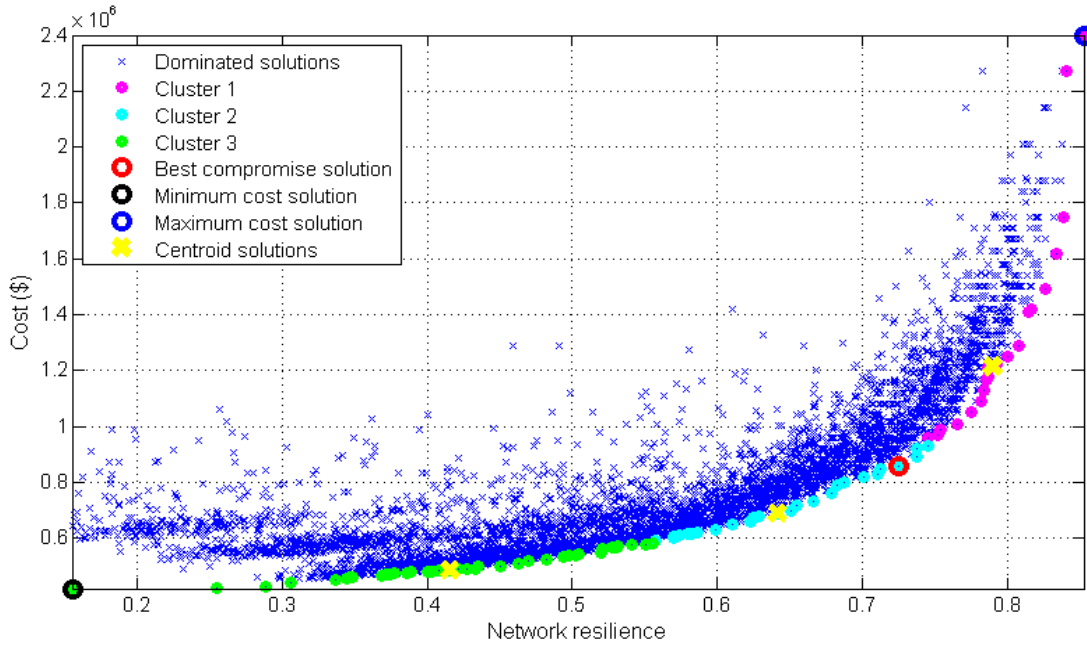


Figure 5.15: Three corresponding centroid solutions (yellow cross) and the best compromise solution (red circle) on the TLN optimal front

The comparison of the three first proposed solutions at the first stage (i.e. the minimum cost, centroid cluster 3, and centroid cluster 2 – Table 5.9 and Appendix C.1.8) showed that network resilience increased to almost triple and quadruple with an increase of cost from the smallest value of \$419,000 to \$487,000 and to \$690,000, respectively. In other words, when cost increased only 16.2% and 64.7%, network resilience increased 170.6% and 318.0%, respectively.

In contrast, along the remaining of the Pareto optimal front, a small increase in the network resilience index produced a bigger increase in cost value, particularly at points near the end of the Pareto front.

Table 5.9: Several representative solutions produced by MO-CMA-ES-EP

Solution	Minimum cost solution	Centroid of cluster 3	Centroid of cluster 2	Best compromise solution	Centroid of cluster 1
Cost (\$)	419,000	487,000	690,000	860,000	1,210,000
NR	0.1535	0.4153	0.6418	0.7251	0.7874

Depending on the specific objective, the optimal solution will be chosen at an appropriate stage. With regard to PWDN, cost is a common priority (Mays, 2000), so an appropriate solution should be chosen at the first stage of Pareto optimal front. Otherwise, it is explicitly uneconomic.

In order to verify the feasibility of this approach, a comparison of results performed by

AMALGAM and MO-CMA-ES-EP for two-loop network was conducted. Both methods successfully produced the same minimum cost solution at a cost of \$419,000 and NR of 0.1535. The trends of two Pareto optimal fronts were in strong agreement (Fig 5.16).

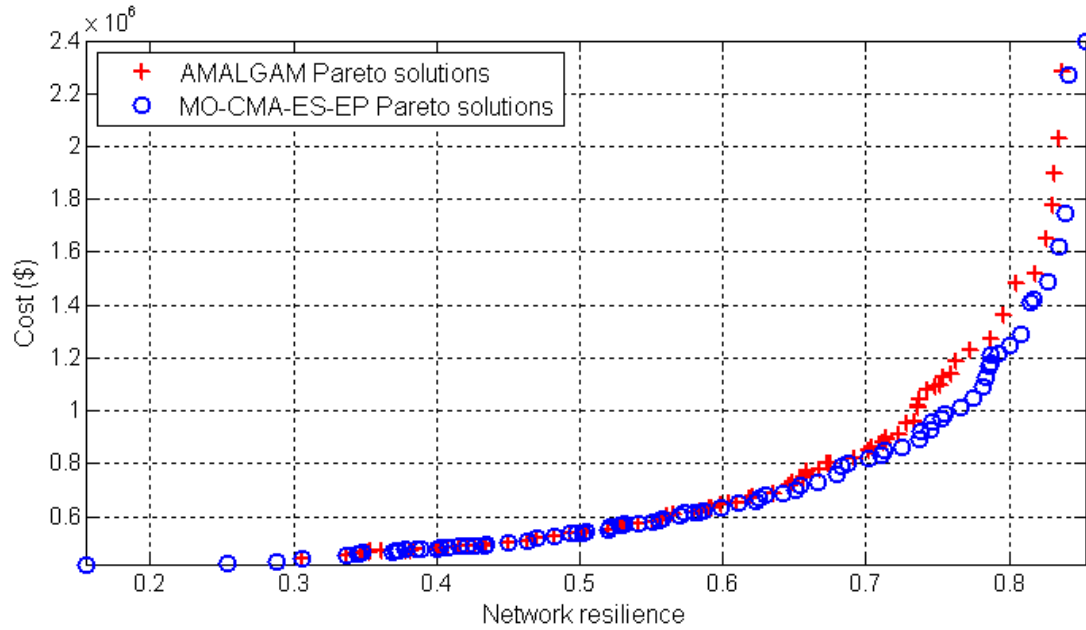


Figure 5.16: Comparison of the Pareto solutions obtained by AMALGAM (red crosses) and MO-CMA-ES-EP (blue circles) with respect to the two-loop network optimal design

#### Benchmark network No.2: Hanoi network

Colored circles in Figure 5.18 show the Pareto solutions achieved by the MO-CMA-ES-EP model. A good approximation was assured, i.e. the minimum cost solution can also be identified by using the single objective CMA-ES-EP and the tendency of Pareto optimal solutions was in agreement with the previous study (Prasad and Park, 2004).

In order to provide more selections for the decision makers, the number of clusters of  $(7 \pm 2)$ , which was consistent with the suggestion of Miller (1956), was taken into consideration in this Pareto data. As can be seen in Figure 5.17, the highest average silhouette value corresponds to 5 clusters.

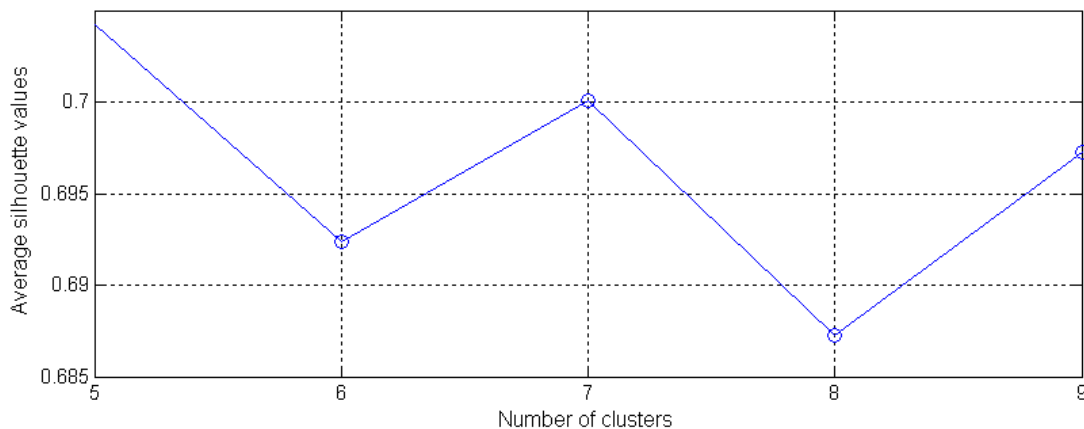


Figure 17: Average silhouette values corresponding to five clusters from Hanoi Pareto data

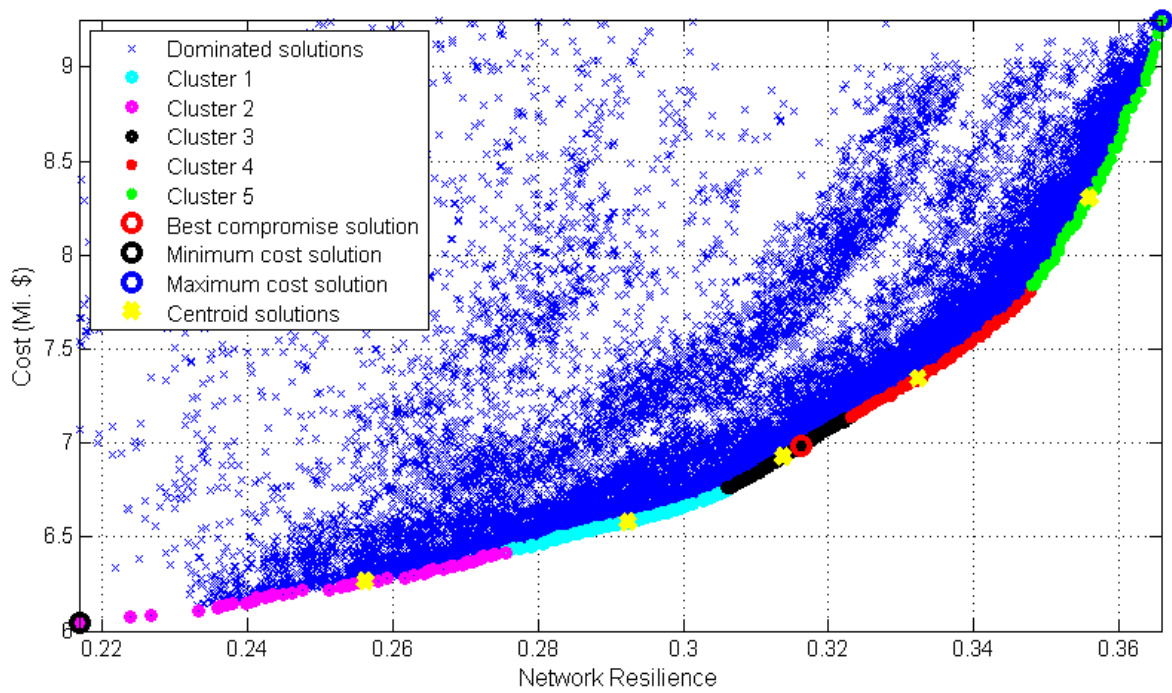


Figure 5.18: Five corresponding centroid solutions (yellow cross) and the best compromise solution (red circle) on the Hanoi Pareto optimal front

As a result, five representative solutions presenting a non-dominated relationship of cost and network resilience for Hanoi Pareto solutions were determined. The best compromise solution (red circle) that was quite close to the centroid solution of cluster 3 was selected as a representative solution for this cluster. Corresponding cost and NR of these representative solutions are depicted in Table 5.10, while pipe diameters of these solutions can be seen in Appendix C.2.4.

Table 5.10: Representative solutions produced by MO-CMA-ES-EP

Solution	Centroid of cluster 2	Centroid of cluster 1	Best compromise	Centroid of cluster 4	Centroid of cluster 5
Cost (\$)	6.4504	6.6039	6.9822	7.3438	8.2901
NR	0.279	0.295	0.3163	0.3324	0.3558

Figure 5.19 presents a comparison of the trends of Pareto optimal front obtained by AMALGAM and MO-CMA-ES-EP. In the second stage from the best compromise to maximum cost solution, two Pareto fronts were in strong agreement. It was notable that, in the first stage, the MO-CMA-ES-EP model approved a lower cost and smaller NR values. Consequently, of the two minimum cost solutions produced by AMALGAM and MO-CMA-ES-EP, the second one was likely to be more comprehensive (Table 5.11).



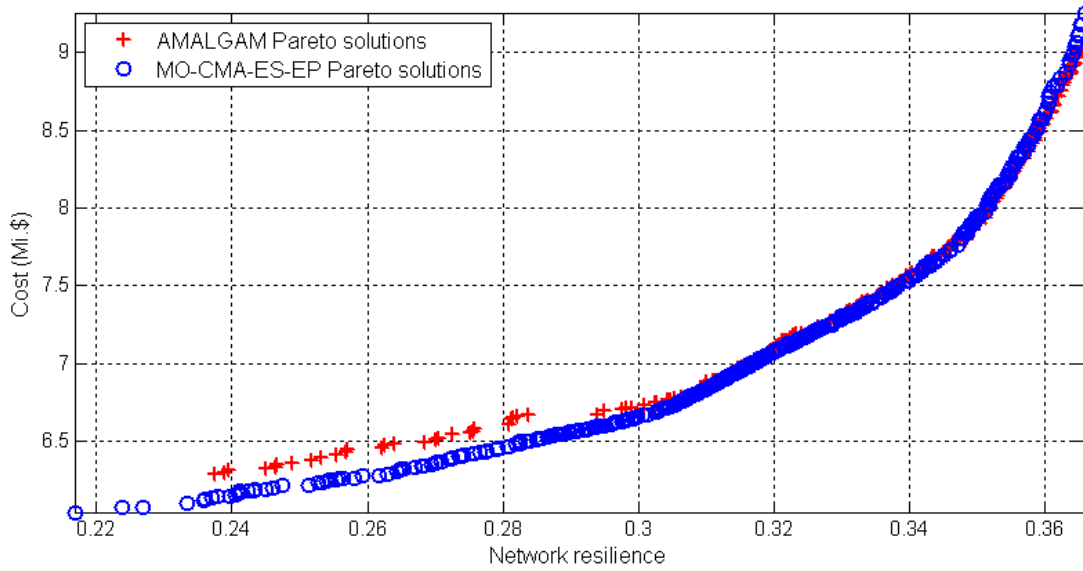


Figure 5.19: Comparison of the Pareto solutions obtained by AMALGAM (red crosses) and MO-CMA-ES-EP (blue circles) with respect to the Hanoi network optimal design

Table 5.11: Comparison of the minimum cost solutions obtained by AMALGAM and MO-CMA-ES-EP

Method	AMALGAM	MO-CMA-ES-EP
Cost (Mi.\$)	6.2885	6.046
NR	0.2374	0.2168

Explicitly, the Pareto optimal front approached by MO-CMA-ES-EP results in trade-offs between cost and network reliability, and effectively provides more choices for designers. In both applications, MO-CMA-ES-EP reproduced the same result as CMA-ES-EP. By applying the techniques selecting the significant solutions, the number of choices is reduced considerably from this very large set of non-dominated solutions.

### 5.3.2 Multi-objective optimal design of a PWDN including network layout

The quite complex predefined network layout of Benchmark network No.4 (i.e. part of the Winnipeg network) was again chosen for applying proposed technique with two required layout reliability levels,  $\overline{OLR} = 1$  and  $\overline{OLR} = 2$ . Decision variables were alternative pipe diameters. Two objective functions were minimization of initial cost and maximization of network resilience under constraints of required nodal pressure, limit of velocity, and the additional constraint related to the required layout reliability level (Eq. 3.6).

#### Required layout reliability level 1 ( $\overline{OLR} = 1$ )

There were 806 Pareto optimal solutions generated with the required layout reliability level 1 produced by MO-CMA-ES-EP (colored circles in Fig 5.20).



Unlike the case of optimal PWDN design with a given layout the Pareto optimal front was a gentle change. In this case, both pipe diameters and network layout changed from solution to solution leading to an unsmooth Pareto optimal front.

As presented in Figure 5.20, five significant solutions (yellow cross) were determined to be representative for 5 clusters. The best compromise solution (red circle) was determined within cluster 1; hence, it was chosen to be the representative solution for this cluster.

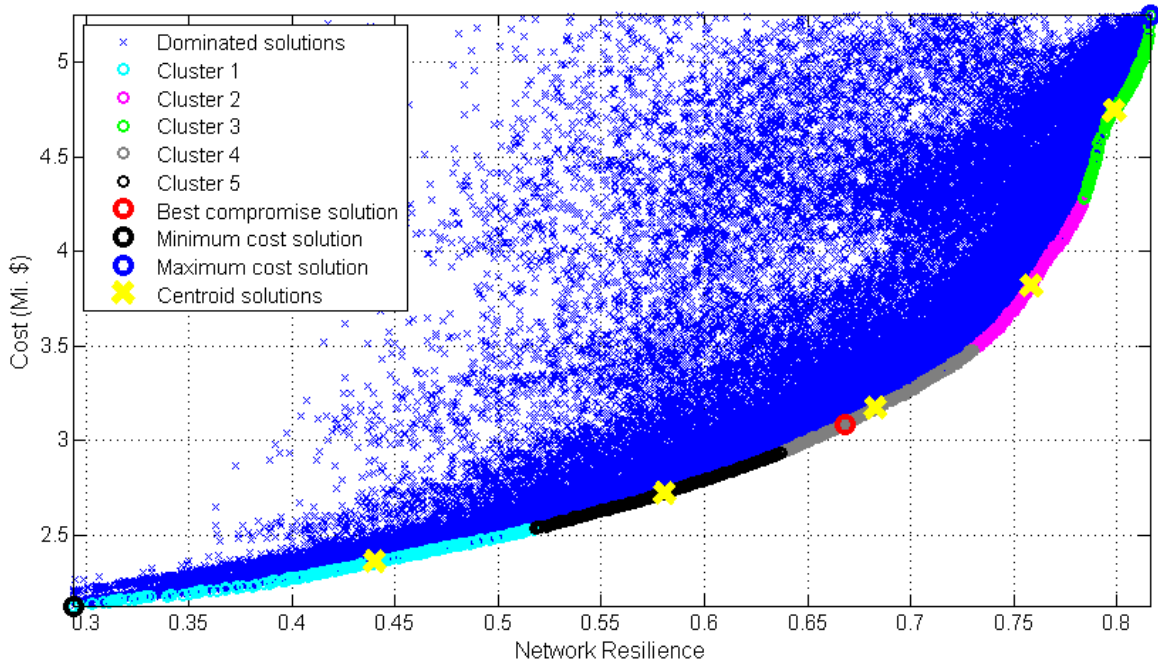


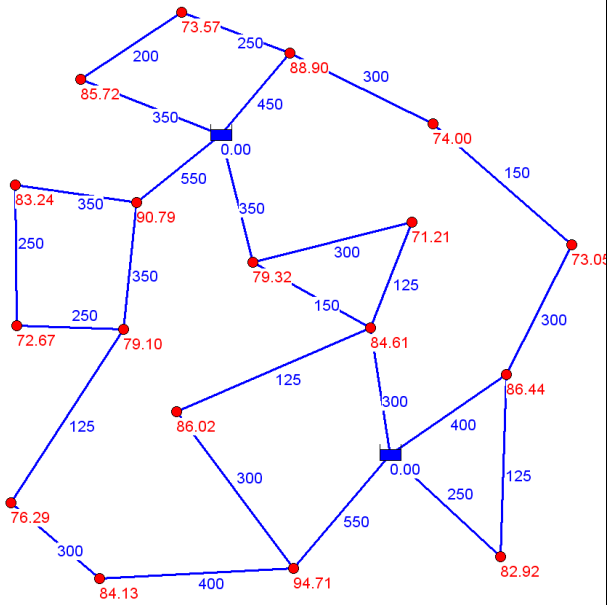
*Figure 5.20: Five corresponding centroid solutions (yellow cross) and the best compromise solution (red circle) derived from the Pareto solutions of Benchmark network No.4 optimization with the required layout reliability level 1*

The first Pareto stage including solutions from the minimum cost to the best compromise solution seemed to be a smooth range indicating the small changes of network configuration. In contrast, the unsmooth remaining range of the Pareto front indicated the big differences in diameters and network layout.

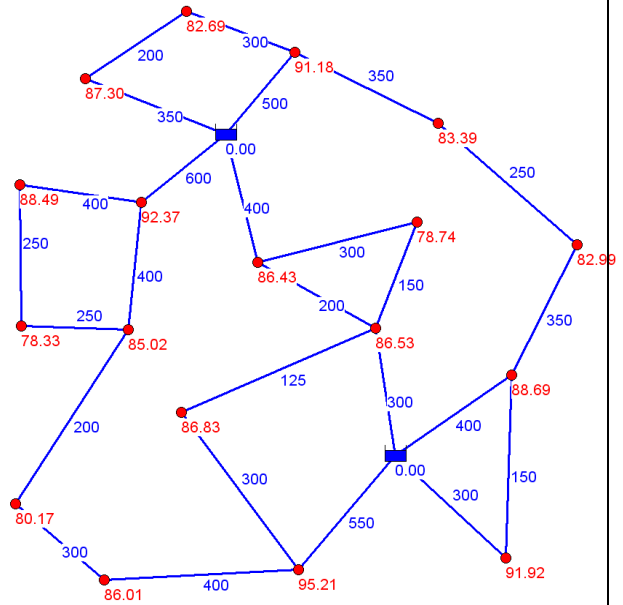
Figure 5.21 shows the solutions specifying pipe diameters and nodal pressures of six different configurations including the minimum cost, centroid solutions, and the best compromise solutions. Corresponding cost, network resilience, and minimum surplus head can be seen in Appendix C.4.3.

The minimum surplus head strongly increased with a small change in cost but a large difference in network reliability with respect to the solutions in the first Pareto stage. In contrast to the second one, this value increased inconsiderably with a large climb in cost but a small rise in network reliability, and even it seemed to be reduced towards the maximum cost solution.

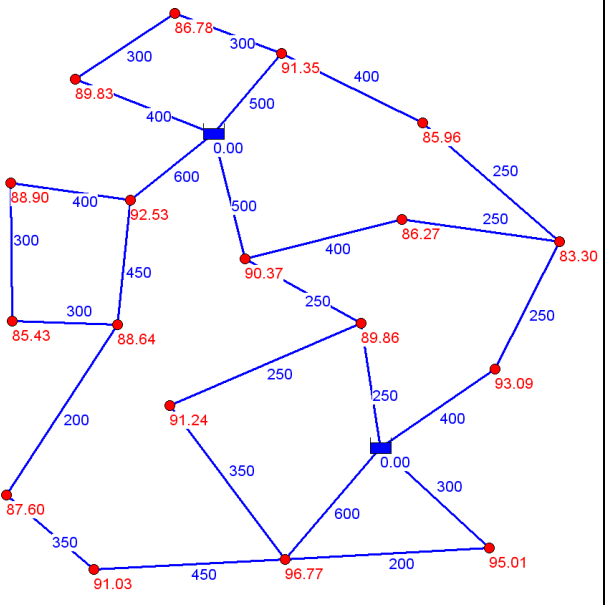
(a) Minimum cost solution



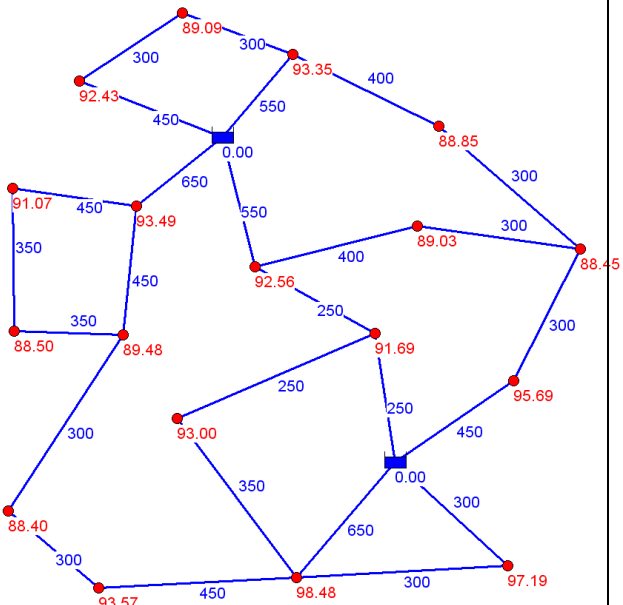
(b) Centroid solution of cluster 1



(c) Centroid solution of cluster 5



(d) The best compromise solution



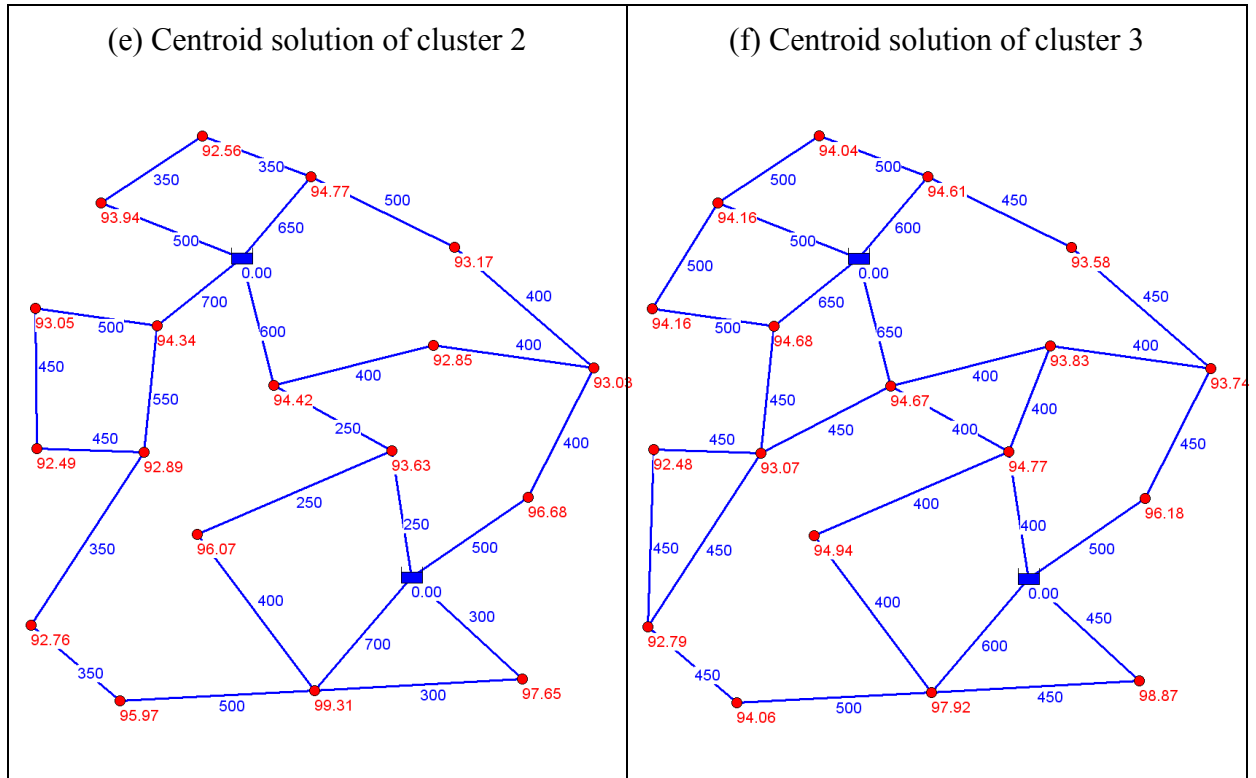


Figure 5.21: Different configurations specifying pipe diameters and nodal pressures of the Benchmark No.4 optimization under the required layout reliability level 1

Required layout reliability level 2 ( $\overline{OLR} = 2$ )

With the required reliability level 2, all of the 856 Pareto optimal solutions (colored circles in Figure 5.22) produced by the MO-CMA-ES-EP approach were certainly looped network layouts. These solutions were different from either pipe diameters or layout or both.

Based on average silhouette values and the proposal of Miller (1956), the optimal number of 6 clusters was chosen. From the Pareto optimal front, there were 6 centroid representative solutions for these 6 clusters (yellow cross). The best compromise solution (red circle) was determined at the cost of Mi.\$3.2557 and the network reliability of 0.7066. Since the best compromise solution was close to the centroid solution of cluster 1, it was the representative for this cluster. The Pareto optimal front also tended to be divided into two parts by this solution.

At the first smooth stage, a small cost increase corresponded to higher network reliability. The change of network configuration was mainly due to pipe diameters while the layout was almost intact (Figure 5.23. a, b, and c).

The considerable changes in network configuration at the second unsmooth stage with both pipe diameters and network layout can be seen in Figure 5.23. d, e, and f.

As reflected in Appendix C.4.4, the minimum surplus head hiked with respect to three first solutions but rose slightly with respect to the others.

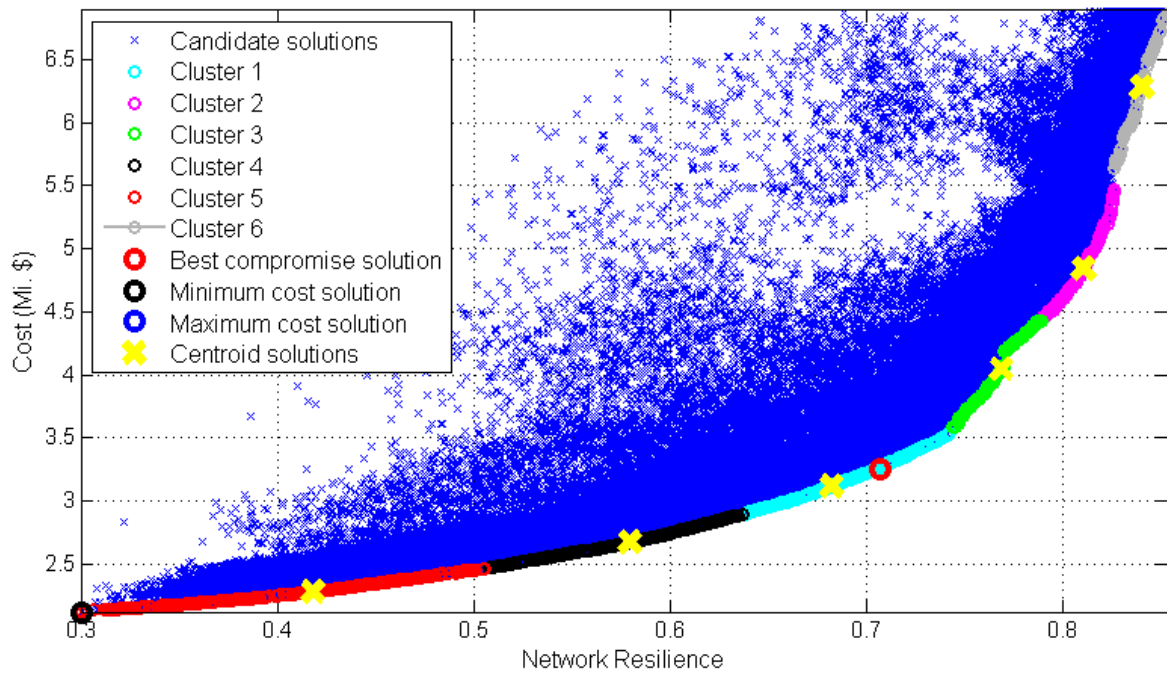
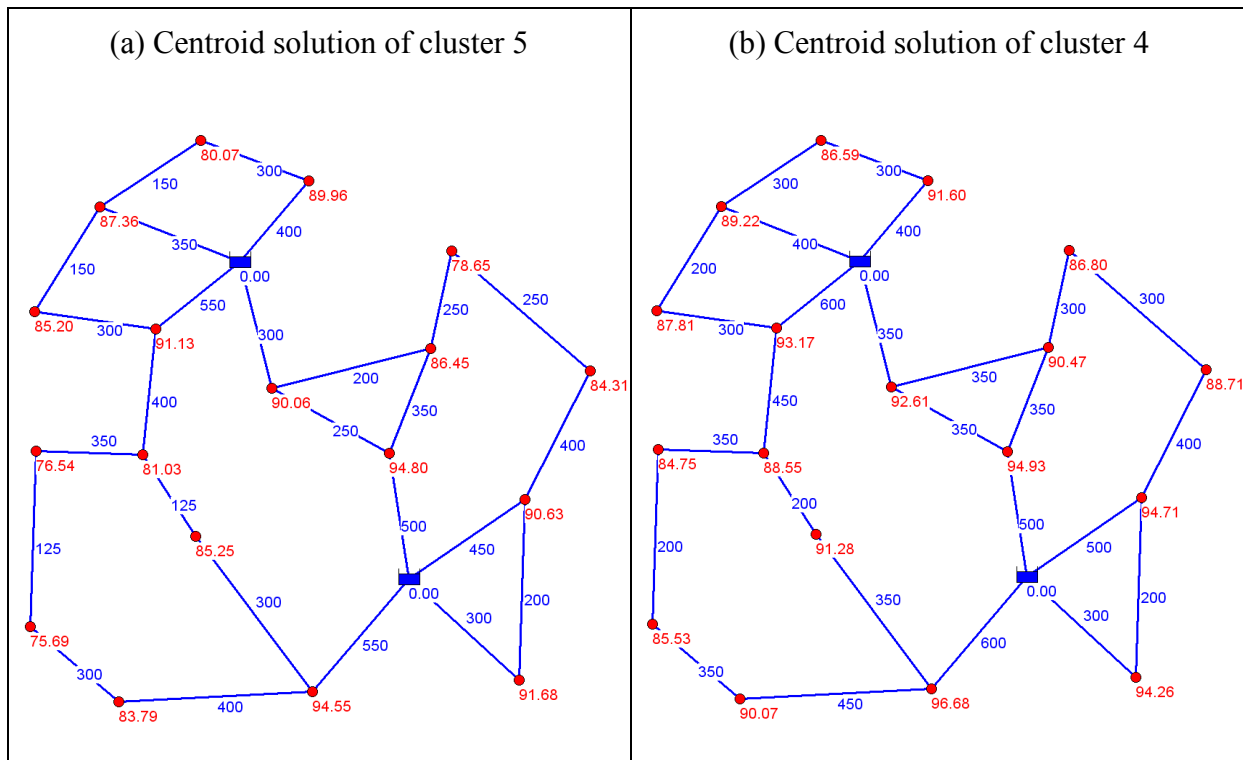


Figure 5.22: Six corresponding centroid solutions (yellow cross) and the best compromise solution (red circle) derived from the Pareto solutions



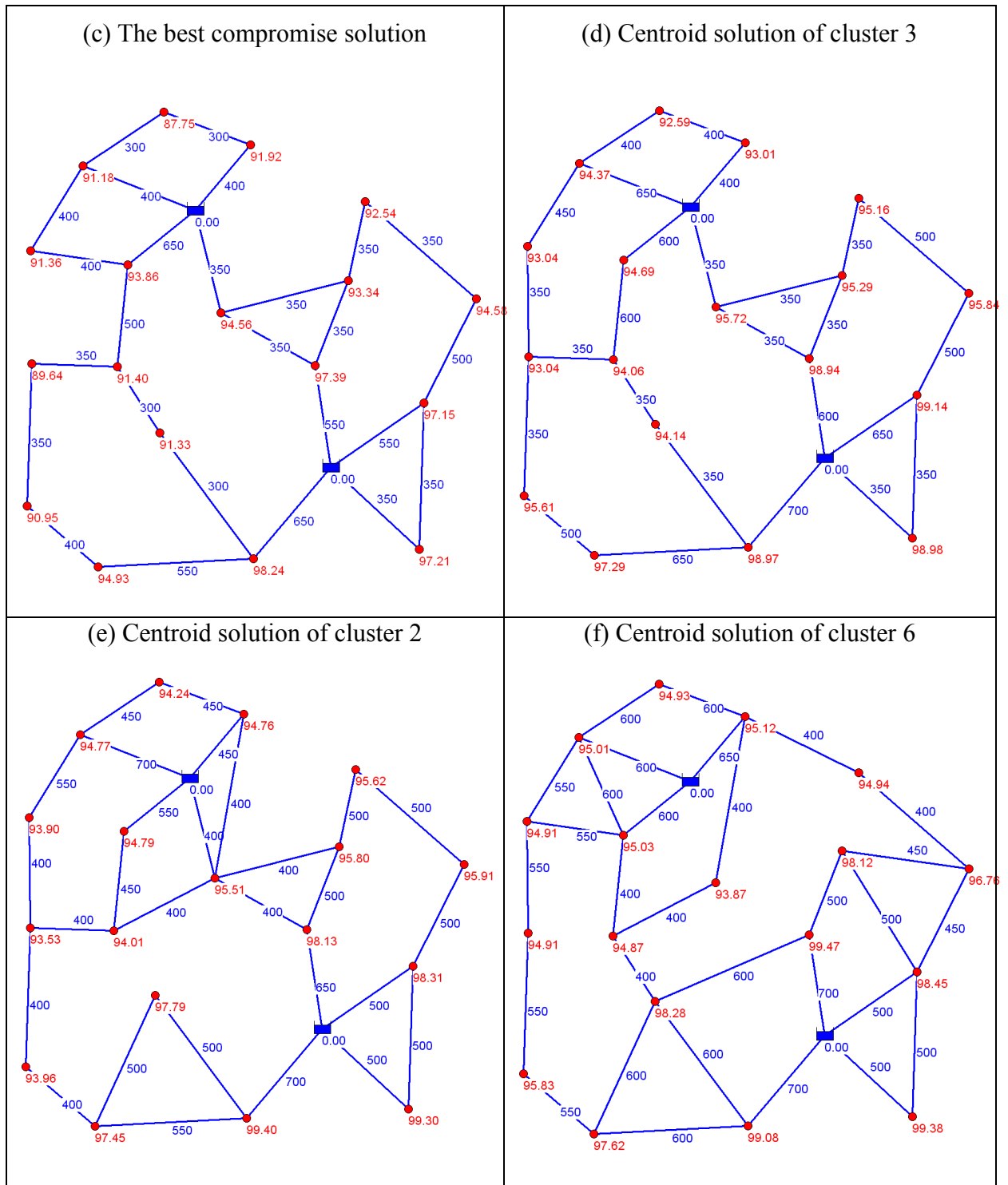


Figure 5.23: Different configurations representing pipe diameters and nodal pressures of the Benchmark No.4 under the required layout reliability level 2.

The results obtained using MO-CMA-ES-EP with the two required layout reliability levels (i.e. level 1 and 2) expressed that the change of network configuration with required reliability level 2 was more severe than that with required reliability level 1, particularly in the second stage with large diameters. Obviously, many more solutions of network layouts and their pipe diameters were obtained which will allow designers to select the most suitable network under given economic and technical criteria.

## 5.4 Considering uncertainties in water demand

Demand uncertainties can be either uncorrelated or correlated as discussed in Section 4.7. Uncorrelated demand occurs whenever an uncertain demand taking place at a node does not impact the others; otherwise it is the case of correlated demand. The capability of the proposed approach in this thesis was evaluated based on its application on TLN and HN networks.

### 5.4.1 Uncertain uncorrelated demands

#### 5.4.1.1 Determining an appropriate sample size using TLN

Expected nodal demands are shown in Figure 5.1 and standard deviation was considered under two cases:  $\sigma = 0.1\mu$  and  $\sigma = 0.3\mu$ . Applying procedure as in section 4.7 to five proposed network configurations based on the Pareto optimal front (Table 5.9), the robustness probabilities for two-loop network were achieved. To obtain theses, three different sample sizes of (a) 1,000; (b) 10,000; and (c) 100,000 samples were used in order to verify the stunning performance of LHST. Corresponding results are demonstrated in Table 5.12. The robustness probability value decreases when the demand uncertainty increases, or in other words, robustness probability rose with the higher cost and network reliability as well.

*Table 5.12: Robustness probability under uncertain uncorrelated demands corresponding to five different cost solutions and different samples (a: 1,000 samples; b: 10,000 samples, and c: 100,000 samples)*

Solutions	Cost (\$)	Network reliability	Robustness probability with demand uncertainty (%)					
			Case 1: $\sigma = 0.1\mu$			Case 2: $\sigma = 0.3\mu$		
			a	b	c	a	b	c
Solution 1	419,000	0.1535	39.1	39.15	39.08	30.6	31.55	31.62
Solution 2	487,000	0.4153	88.7	88.68	88.51	60.3	60.20	60.25
Solution 3	690,000	0.6417	100	100	100	99.00	99.01	98.98
Solution 4	860,000	0.7251	100	100	100	100	100	100
Solution 5	1,210,000	0.7874	100	100	100	100	100	100
Average running time: (a) 2.10; (b) 23.4; and (c) 910.0 seconds, respectively (computer: AMD Dual Core 2.0 GHz)								

Table 5.12 shows that there were only small differences among the results produced by three different numbers of samples. Consequently, the number of samples of 1,000 can be large enough to reflect the precise results. Also, it can reduce a considerable computational time. Therefore, this value would be used for calculating robustness probability of networks.

#### 5.4.1.2 Exemplary application on TLN and HN network

By applying the same procedure on five proposed solutions for Hanoi network, the robustness probability with 1,000 samples can be achieved as presented in Appendix C.2.5.

Comparing results produced in two cases for TLN and HN network (Figure 5.24), the equivalent robustness probability was higher in case of smaller standard deviation (Case 1). In other words, for the same robustness probability, Case 1 with lower demand fluctuation was more cost-effective than Case 2 with higher demand fluctuation.

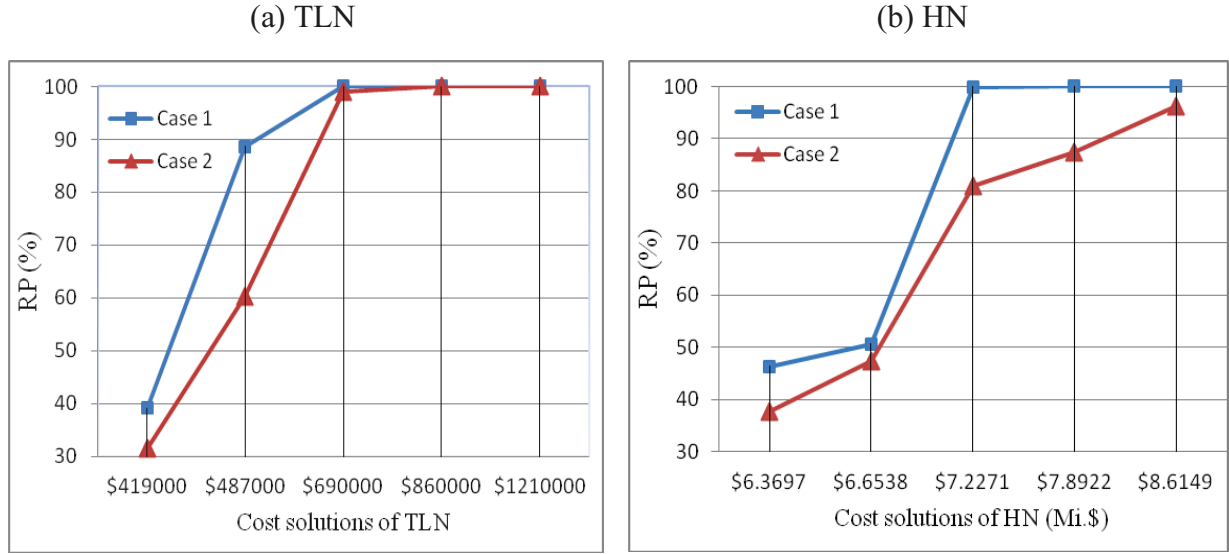


Figure 5.24: Robustness probabilities corresponding to two assumptions of standard deviations (Case 1 and Case 2) for five representative solutions of (a) TLN and (b) HN network

#### 5.4.2 Uncertain correlated demands (Case 3)

This situation occurs due to the change of the amount of water requirement at the same time, on the whole system, for example, the effect of hot, dry weather to irrigation demand. All nodal demands were assumed to follow normal distribution and their standard deviations were assumed to equal 10%. The correlation coefficient between demand nodes was assumed to equal 0.5 (Tolson et al., 2004; Kapelan et al., 2005) to investigate its impact. In this circumstance, the correlation matrix  $C$  (mentioned in Section 4.7) was created with the desired correlation coefficient, i.e. the correlation matrix of 1.0 on the main diagonal and 0.5 elsewhere.

The corresponding robustness probabilities to five proposed solutions for TLN and HN network were also estimated using the Latin hypercube sampling technique (Appendix C.1.9 and C.2.6). Errors corresponding to each TLN solution between the rank correlation matrix and the desired correlation matrix were evaluated and can be considered to be reasonable (Appendix C.1.10).

Comparing the results derived from 2 cases having the same standard deviation, i.e. Case 1 and Case 3 (Figure 5. 25), showed that:

For the lower cost interval, in general, the robustness probabilities achieved in Case 3 are higher than the corresponding solutions obtained in Case 1.

In contrast, for the higher cost interval, the robustness probabilities in Case 3 tend to be lower than in Case 1, or in other words, they are more costly than the corresponding solutions in Case 1.

From this comparison, it can be said that a consequence of the correlation between nodal demands was acknowledged. Accordingly, the impact of uncertain demand is more serious in case of lower cost (or lower reliability) and vice versa.

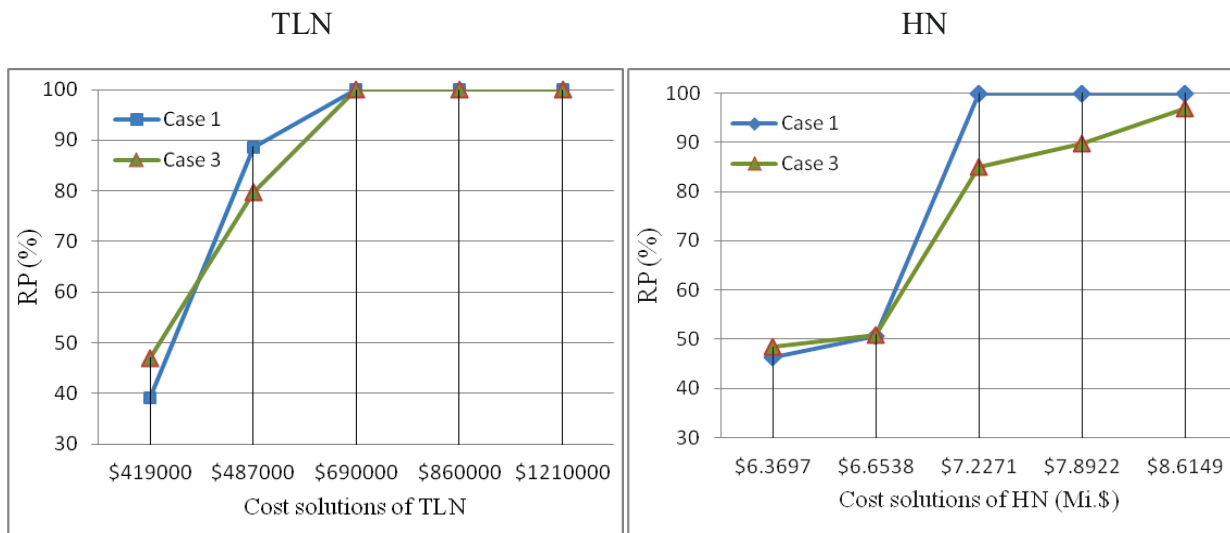


Figure 5.25: The comparison of robustness probabilities under uncertain uncorrelated and correlated demands (Case 1 and Case 3) for five representative solutions of (a) TLN and (b) HN network

As a result of two applications above, the multi-objective optimization with respect to PWDN design problem is assured to provide more alternatives for a network configuration. The selected network configuration based on either cost or network reliability may not be advanced. To guarantee the configuration under demand uncertainty, it is necessary to consider a robustness probability. Therefore, a demand uncertainty consideration may become useful for a more reliable PWDN design.



## 6 APPLICATION OF THE NEW APPROACH TO A REAL WORLD CASE STUDY

The real world case for the application of the optimal design and operation is a part of a new irrigation PWDN in the Southern Batinah region. It is the aim of this section to find an appropriate design for this PWDN based on multi-objective optimization between two contradicting functions, namely, minimization of total cost and maximization of network reliability.

### 6.1 Study area

The study area is located in the Al Batinah coastal plain, roughly 60 km to the North-West of Muscat, capital of the Sultanate of Oman (Figure 6.1). Al Batinah is the most concentrated farming area of the Oman, accounting for more than 50% of the land area under cultivation (FAO, 2008). However, this area is also one of the most water stressed regions of the world due to little rainfall and high evaporation. Therefore, crop productivity depends significantly on irrigation. More than 80% of the abstracted, limited water is used for irrigated agriculture through wells and falaj systems (Ministry of agriculture and fishery – MAF, 1994). Most of the farms located near the coastline have been irrigated by often uncontrolled pumping of water from the coastal aquifers (Schmitz et al., 2010; Grundmann et al., 2012, 2013).

Unfortunately, an over-abstraction of water in the past decades, due to inefficient irrigation methods, severely affected water in the aquifers. Aquifer recharge is generally smaller than withdrawal, leading to declining groundwater. Due to the decrease in the groundwater table, saltwater intrusion has appeared deep inland. This has caused a continual decrease in the cultivation area lying near coastline due to soil degradation (National well inventory project - NWIP, 2005).

Consequently, to preserve quality and quantity of groundwater as well as of soil in the cultivation area, solutions are presently being sought by which irrigation water use can be reduced. The two most notable solutions, which can be applied to the study, are to adjust the cropping pattern and increase irrigation efficiency through modern irrigation technology. To adjust the cropping pattern, the crops requiring more water, such as perennials and trees crops, would have to be cut down while increasing vegetable and field crops. In order to reduce irrigation losses, a modern irrigation system is a powerful tool (Schmitz et al., 2010). In such a system, losses such as in the falaj system do not occur. In addition, costs needed in the modern irrigation for operation, maintenance, and so on are from 1/10 to 1/4 less than those required for the traditional system (Phocaides, 2000).

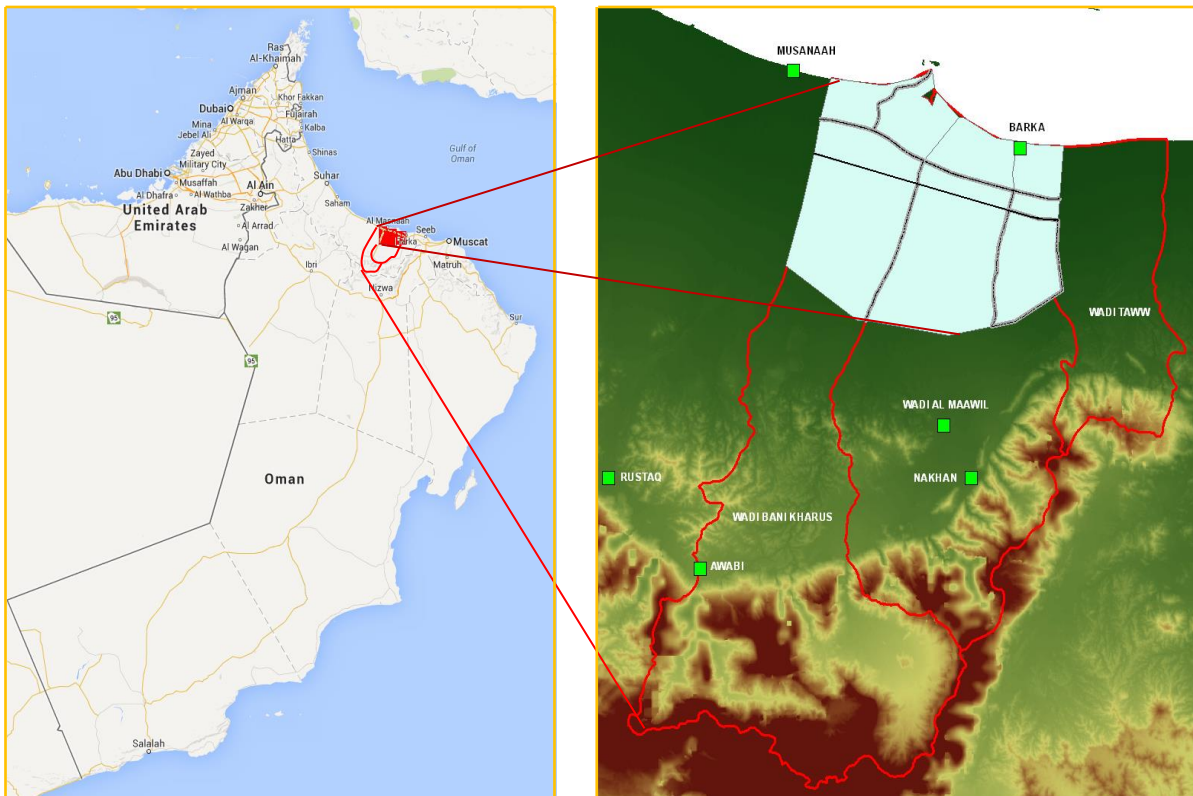


Figure 6.1: Study area

### 6.1.1 Climate conditions in the study area

The main average climate data for the southern Batinah region is based on three weather stations in south Batinah: The station at Seeb airport, the Rumais agricultural research station, and station at Muladdah. The data is given in Table 6.1.

The climate in the Batinah region is divided into two distinct seasons: summer and winter. The hot summer lasts from June to September and is characterized by generally high daytime temperature of around  $40^{\circ}\text{C}$  and  $25^{\circ}\text{C}$  at nighttime. The mild winter season covers the period from October to May with daytime temperature of  $25^{\circ}\text{C}$  to  $30^{\circ}\text{C}$ . The average temperature is  $27.3^{\circ}\text{C}$ .

Rainfall is very irregular from year to year and any month can be totally dry. The mean annual rainfall is low but highly variable, exceeding 350 mm in the mountainous area, but falling below 100 mm in the plain. More than 90% of the annual rainfall has been observed during the wintertime.

Evapotranspiration in the area is in great distribution from year to year as well as from month to month. The average evapotranspiration is 1789 mm/year; however, the maximum value can reach 3000 mm/year and the minimum can drop to 1660 mm/year. Evapotranspiration reaches a high value in the period from May to July and a low value in the period from December to February.

The observed average relative humidity is approximately 66% and varies greatly. The higher monthly average humidity is 70% to 80% in August and from December to February. The lower value is around 50% from April to July.

*Table 6.1: Estimated average monthly temperature (T), rainfall, evapotranspiration (ET), and humidity (Humid) for South Batinah region (Volume 1 –MAF, 1994)*

Time	Jan	Feb	Mar	Apr	May	June	July	Aug	Sept	Oct	Nov	Dec	Year
T (°C)	20.4	20.8	24.0	29.0	31.5	34.1	34.3	30.9	30.3	27.3	23.7	20.8	27.3
Rainfall (mm)	10.4	23.0	13.9	11.8	4.4	0.8	0.2	0.6	0	0.8	5.5	10.0	81.4
ET (mm)	86.8	92.4	127.1	168	217	207	220.1	173.6	162	148.8	102	83.7	1789
Humid (%)	72	72	68	55	53	56	63	76	72	65	69	73	66

### ***6.1.2 Land use and water requirements for agricultural irrigation***

Annually, the Batinah plain provides almost 60% of the total agricultural production and has witnessed vigorous development in recent years with the main crops being dates, fruit trees, alfalfa, vegetables, Rhodes grass, and other forage crops. The data considered here refer to land use and water requirement for irrigation in 1994 and 2004 with respect to whole Willayat of Barka and Musanaah. Land use and irrigation water requirements estimated for the proposed scenario with respect to the study area were referred to afterwards.

#### *Land use and water requirements for agricultural irrigation in 1994*

Figure 6.2 shows the cropping pattern for whole Willayat of Barka and Musanaah, in which fruit trees were the largest crop and occupied 63% of the total cropped area. The following crops were fodder and vegetables. Field crops were negligible.

Over 80% (MAF – Volume 3) of the irrigated area was under traditional surface systems, including flooding, boarder, basin, and furrow irrigation methods. With these methods, water pumped from wells was discharged in reservoirs or directly to existing concrete or earth channels and then distributed to the farms.

With traditional surface irrigation systems, the irrigation efficiency was quite low and evaluated to be less than 50%. The total water requirement for crops irrigation can be estimated at 172 Mi. m<sup>3</sup>.

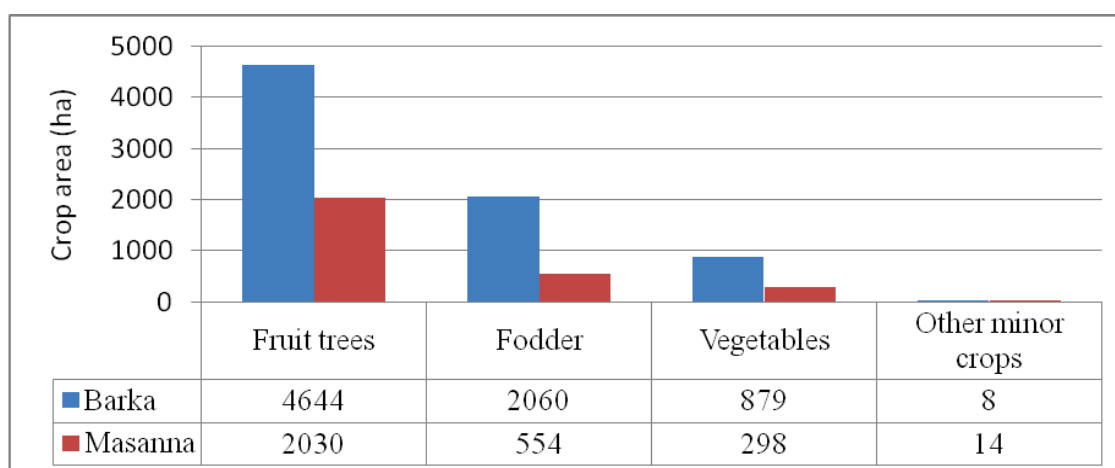


Figure 6.2: Cropping pattern in the study area in 1994 (Volume 1 - MAF, 1994)

#### Land use and water requirements for agricultural irrigation in 2004

By comparing the pattern crops, the major crop of fruit trees have been reduced from 6674 ha in 1994 to 3625 ha in 2004 (a reduction of 42%) of the cultivated area. On the contrary, the second important crop, forage, has increased from 2614 ha in 1994 (25%) to 3637 ha in 2004 (43%). There was a small shifting of field crops when they occupied 1.5% of the total cropped area (Figure 6.3). The total cropped area reduced during period 1994 – 2004 was 1991 ha.

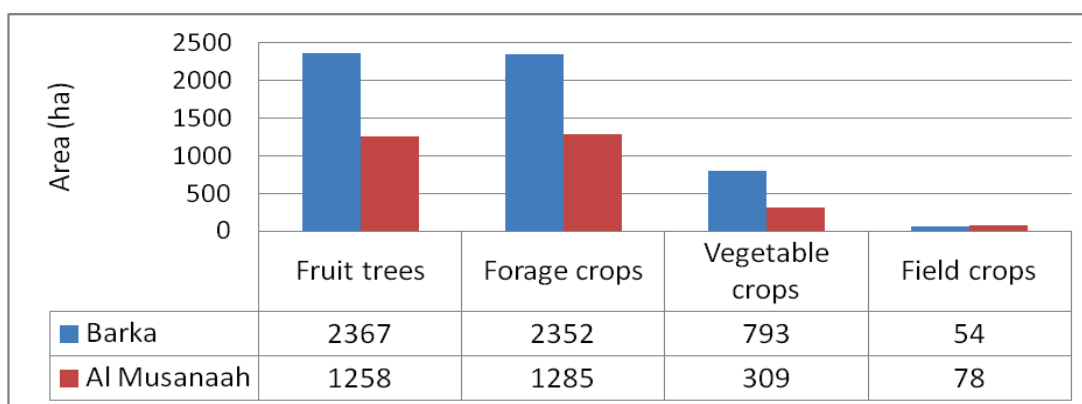


Figure 6.3: Global cropping pattern in the Batinah area in 2004 (Agriculture Census, 2004)

In addition, modern irrigation systems such as drip, bubbler, spray, and sprinkler methods were applied in several areas in this time in order to improve irrigation efficiency. Drip was used for vegetables and trees, bubble was used for perennial forage crops and tree crops, and sprinkler irrigation systems were used for perennial forage crops and field crops. However, these modern irrigation systems were owned by the individual with uncontrolled irrigation water volume.

Figure 6.4 expresses the proportion between the applied irrigation method for each type of crop in the study area in 2004 (Agricultural census 2004). It reveals that, until 2004, modern irrigation methods were not widely used in the study area in particular, and in the whole

Batinah plain region in general. As expressed in Figure 6.4, around 60% of the crop area is still irrigated by a flood irrigation system, which is considered to be the lowest of all techniques and estimated at below 50% efficiency compared to more than 80% efficiency achieved by modern irrigation. By reducing crop area and applying partially modern irrigation methods, the estimated total amount of water abstracted for irrigation in 2004 was 124 Mi.m<sup>3</sup> (NWIP, 2005), a reduction of 48 Mi.m<sup>3</sup>.

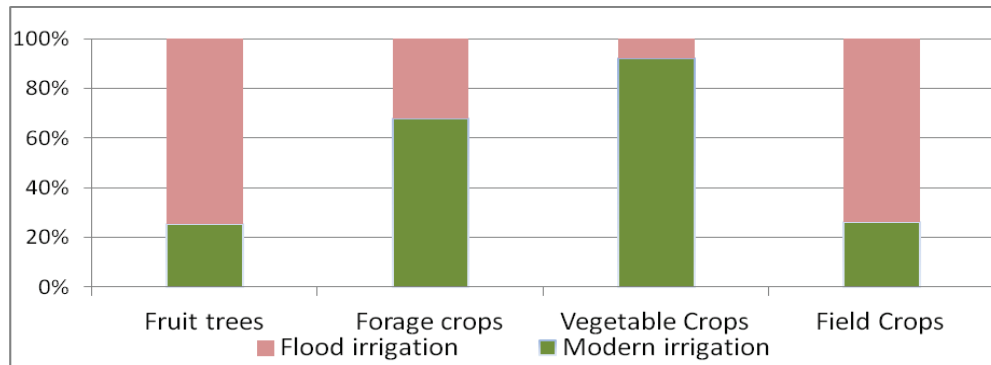


Figure 6.4: The irrigation method applied in the study area (Agriculture Census, 2004)

#### *Land use and irrigation water requirements for study area*

Aiming to conserve quality and quantity of ground water and due to salt intrusion to the inland, the cropping pattern needed to be changed to fit the new conditions. Reducing water consumption in the study area can be performed by two alternative solutions: by adjusting the cropping pattern in the area, and by reducing irrigation losses through the use of modern irrigation technology.

Adjusting the cropping pattern remains the most efficient and sustainable way to reduce water consumption. From the estimation in Volume 1 – 3 (MAF), perennial crops, including several main fruit trees and grasses that consumed more water than the seasonal crops, such as cereals and vegetables, consequently had to be reduced.

In order to preserve groundwater resources, a scenario of crop area reduction can be projected. Based on the scenario proposed by MAF (Volume 1), a scenario of cropping pattern was estimated as in Figure 6.5 and 6.7. The study area was separated into 10 sub-areas with considerable changing cropping patterns in order to significantly reduce irrigation water requirements.

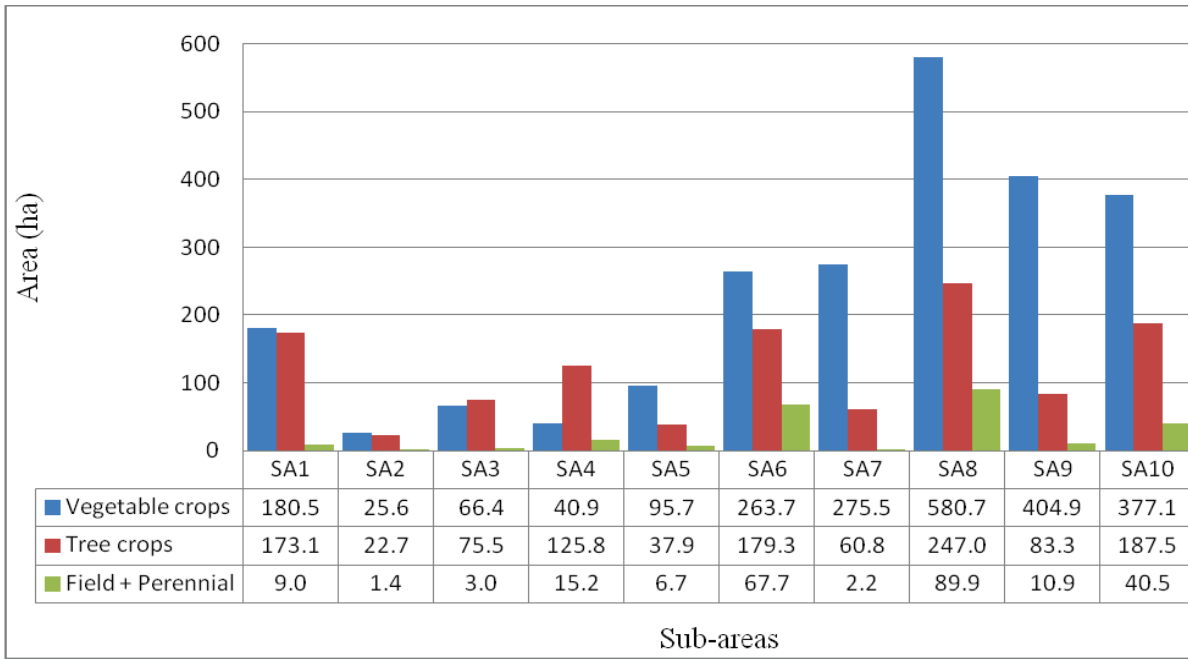


Figure 6.5: Proposed scenario cropping pattern in the study area (SA: Sub-area)

The water demand for agricultural irrigation in the future was estimated on the basis of this proposed cropping pattern scenario and can be evaluated as follows.

The water requirement ( $WR_{crop}$ ) is calculated by (FAO's proposal – MAF, 1994):

$$WR_{crop} = K_c * ETo \quad (6.1)$$

$K_c$ : Crop coefficient

$ETo$ : Reference crop evapotranspiration

The gross irrigation water requirement,  $I_r$ , is calculated by:

$$I_r = \frac{WR_{crop}}{Ie \left( 1 - \left( \frac{LF}{Le} \right) \cdot (1 - Es) \right)} \quad (6.2)$$

in which:  $Ie$  is irrigation efficiency of the system (i.e., depends mainly on irrigation method),

$LF$ : Leaching fraction

$$LF = \frac{ECw}{(2 \times \max.ECe)} \quad (6.3)$$

$ECw$ : Electrical conductivity of irrigation water (dS/m)

$\max.ECe$ : Maximum tolerable electrical conductivity of the soil saturation extract for a given crop (dS/m)

$Le$ : Leaching efficiency, which is a function of soil type

$Es$ : Surface evaporative losses which vary significantly between irrigation methods

All these parameters can be found in Volume 1 and Volume 3 – MAF (1994). Based on the data provided by MAF, the scenario of the proposed cropping pattern (Figure 6.5), and an assumption of 100% area irrigated by the modern system, the estimated water demand for the proposed crop is expressed in Table 6.2.

*Table 6.2: Water requirements for the proposed scenario (Mi.m<sup>3</sup>)*

Crops	Area (ha)	Main irrigation method	$I_r$ (m <sup>3</sup> /ha)	Scenario water required (Mi.m <sup>3</sup> )
Vegetable crops	2,310.95	Drip	9,256	22.66
Tree crops	1,192.83	Bubbler	24,209	27.63
Field + Perennial crops	246.42	Sprinkler	18,723 & 31,604	4.56

The monthly irrigation water demand was estimated as in Table 6.3, based on the analysis of MAF (Volume 3) and NWIP about monthly climate condition, cropping pattern, crop growing period, and irrigation frequency. The distribution of irrigation water demand is shown in Figure 6.6.

The irrigation schedule should be based on time period in years, plant type and the stage of plant growth, type of soil, etc. A greater amount of irrigation water is required from April to June due to very little rainfall, relatively low humidity, and high temperature, all of which cause considerable amount of evapotranspiration in this time of the year. Irrigation water requirement from September to February is mainly used for seasonal crops (i.e. vegetables and fields crops). Large irrigation water demands are in turn in SA8, SA10 and SA6, while SA2 and SA5 require small volume. Most cropping areas are below the altitude of 20 m above sea level.

An irrigation scheduling for the study area is proposed based on the proposal of MAF (Volume 3 – 1994) and WMPP (Water Metering Pilot Project, 1994-2000) in which irrigation frequency is suggested to be 2 days with an operating 24-hour cycle. The best time of irrigation scheduling is divided into two periods, in the early morning and late afternoon, in order to avoid the highest evapotranspiration at sunshine time. Therefore, irrigation water demand is estimated as in Figure 6. 6. The largest irrigation water demand, 7512 m<sup>3</sup>/h, is in May and the smallest, 4829 m<sup>3</sup>/h is in December. The distribution of irrigation water demand in the study area is depicted as in Figure 6. 7.

### **6.1.3 Irrigation water sources**

#### *Current sources*

Generally speaking, since rainfall is very scarce and irregular, there is almost no permanent surface water flow in the study area. Ground water is the major source for agricultural

irrigation in the Batinah plain. Ground water is derived from the alluvial deposits, which are recharged annually by storm run-off down the wadis and, over longer periods, by continuous underground flows from the Hajar Mountains (MAF, 1994).

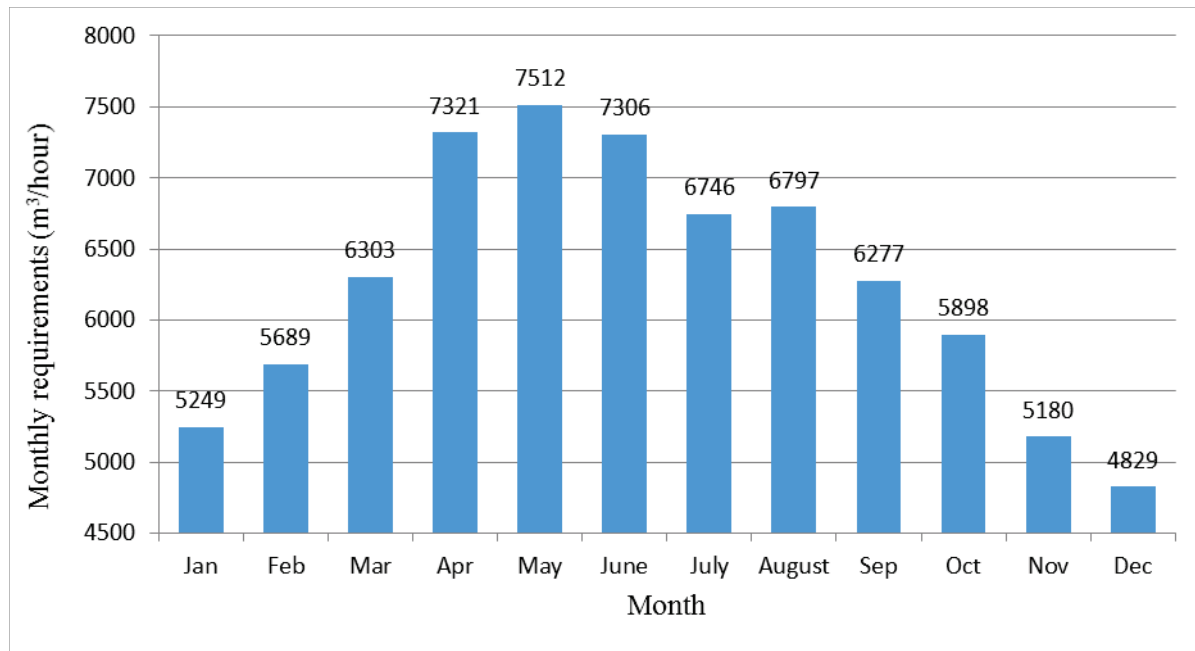


Figure 6.6: Demand diagram in the study area

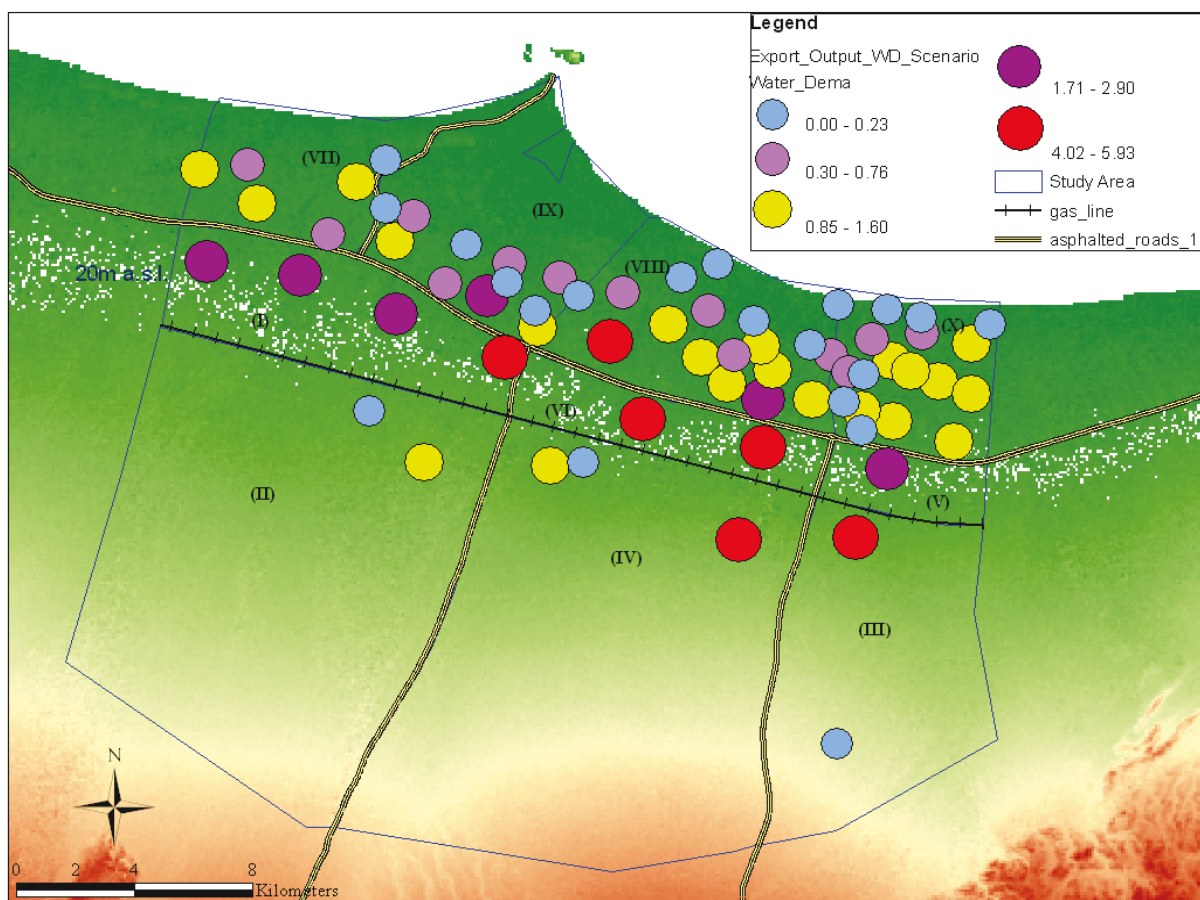


Figure 6.7: Distribution of irrigation water demand in the study area



Recently, most of the irrigation water has been over-pumped, uncontrolled, from private wells along the coastal area leading to sea water intrusion into the inland. Thus, the problem of salinity in the area bordered by the main highway and the sea has been becoming more and more serious (NWIP, 2005).

According to Ai-Shaqsi (2004) and Sana et al. (2013), ground water in the valley and highland zones, which are located between the mountain range and the Batinah plain, is stable because these regions receive natural replenishment from rainfall and have not experienced the increase in abstraction like the plain areas. Therefore, a so-called well-field is proposed to be located in the mountain-front area (Grundmann, 2011). The details of these wells are given in Appendix D.2, for which the water table data was provided by the Ministry of Regional Municipality and Water Resources of Oman.

#### *Possible future sources*

Several future prospects for expanding the use of other water sources can be projected as follows (Grundmann, 2011).

##### (i) Treated wastewater

At present, a number of treated wastewater plants have been built in big cities such as Muscat, A'Seeb, etc., in order to meet the needs of the increasing population. The production can be projected to increase several times in years to come<sup>1</sup>. Besides providing water for households, these treated wastewater plants can compensate the irrigation water shortage.

##### (ii) Desalination plants

The Barka II Power and Desalination Plant, which is a combination of an electric power plant and sea water desalination plant<sup>2</sup> with a capacity of 120,000 m<sup>3</sup>/day, makes an important contribution to water supplies for not only drinking purposes but possibly also for irrigation in this area.

##### (iii) Transfer from neighboring catchments

Another source of irrigation is transfer of water from futile, cultivated adjacent areas to the productive southern Batinah fields.

Compared to ground water sources, these sources will be costly due to very high costs of producing and conveying. In this application of the new approach on the real world case study, i.e., the southern Batinah region, only the current irrigation water sources were considered as the main supply sources.

---

<sup>1</sup> <http://www.arabwatercouncil.org/administrator/Modules/CMS/Oman-Country-Report.pdf>.

<sup>2</sup> <http://www.stomo.com.om/aboutus.html>

## 6.2 MO-CMA-ES-EP application: Simultaneous optimal design and operation of a PWDN

The aim of this section is to apply the proposed approach on the real world case study in order to find the appropriate network configuration and operating schedules based on the trade-offs between total cost and network resilience. At first, network configuration and operation must be optimized for meeting the maximum irrigation water requirement in May. Afterwards, pump operation schedules were optimized for the other months of the year using the determined optimal configuration.

Based on sub-area demand, there are 22 demand nodes which represent a large demand node or several small demand nodes in a specific sub-area (Swamee and Sharma, 2008), and are set to appropriately distribute the evaluated irrigation supply. Their properties can be seen in Appendix D.1 – 6.2.

Two scenarios were considered here as user-predefined network layouts for applying the proposed approach: A given backbone network (BBN) and a predefined maximum layout (PML). These networks are assumed to be supplied only by current water sources (Figure 6.8 and 6.11).

### 6.2.1 Optimization problems

#### 6.2.1.1 Decision variables

- Pipe diameters (D): These design variables were arbitrarily selected from a set of commercial, reinforced concrete lined pipes. Reinforced concrete pipe has high load capacity, less susceptible to damage during construction, maintenance, and operation (Mays, 2000). In addition, its cost is normally lower than compatible cost for other pipe materials such as steel, plastic, etc. Nowadays, reinforced concrete pipe is commonly used in large PWDNs. Pipe diameters with their corresponding costs are expressed in Table 6.3<sup>1</sup>.

Table 6.3: Pipe cost data

D (mm)	600	750	900	1050	1350	1650	1800	1950	2250	2550
Cost (\$/m)	139.5	281.9	392.3	492.9	756.7	1108.3	1339.3	1553.2	2025.6	2670.2

- Pump discharge and pump head: Every single pump discharge-head combination was estimated on the basis of a given continuous interval, with pump discharge interval

<sup>1</sup> <http://www.concastpipe.com/pricing/cc-2014-price-list.pdf>

having  $[1\ 10000]$  m<sup>3</sup>/h and pump head interval being  $[1\ 1000]$  m. The number of pumps was assumed to be as many as possible; then, through an optimization procedure, unavailable pumps were assigned with the “closed” status and, finally, were eliminated from the network.

- Initial water level in tank: According to Vamvakieridou-Lyroudia et al., 2007, some tank properties are parameters rather than decision variables, such as tank shape, overflow level, and emergency volume. These parameters are usually set beforehand. Some properties such as maximum, minimum water level and volume can be derived from others. In this application, diameter and shape were assumed to be given; through optimizing the initial water level in the tank the other tank parameters were determined.

#### 6.2.1.2 Objective functions

Regarding the multi-objective of optimal design and operation of a PWDN, the first objective is to minimize total costs in terms of initial investment and operational cost (Eq. 5.1, 5.10, 5.11, and 5.12). In this study, unit power cost of pump construction is  $CPUMP = 4,000$  (\$/kW); unit water level cost of tank is  $UWTC = 45,000$  (\$/m of tank height).

The second objective is to maximize the network resilience, which is a function of nodal demand and head. As illustrated in Figure 2.5, an increasing nodal demand leads to a decreasing nodal head. Consequently, the network resilience that reflects the network behavior corresponding to the most stressed water demand period needs to be evaluated.

These two objective functions are subject to the constraints presented in the following section.

#### 6.2.1.3 Constraints

Owing to physical limitations and the requirements of the network’s operation, the following constraints were included:

*Minimum required nodal pressures:* Depending mainly on modern irrigation methods, the minimum required pressure of 45 m has to be maintained at all demand nodes (MAF – 1994).

*Flow velocity constraints:* According to Walski et al. (2003), maximum velocity depends on three factors including discharge, diameter, and pipe material. Generally, a maximum value of 8 ft/s (or 2.4 m/s) was proposed to be used for velocity constraint. Therefore, this value was also applied in this study.

*Water quantity limits:* Maximum water pumped annually from well-field cannot exceed the annual recharge into this area, which is estimated at 68 Mi.m<sup>3</sup>/year (Gerner, A., 2013).

*Tank constraint:* Tank water level at the end of an operational schedule must return to the initial level with a user-predefined tolerance,  $\varepsilon$  (m). According to Vamvakeridou-Lyroudia et al. (2007), a tolerance of 10% can be adopted in order to account for inaccuracies.

*A constraint related to the required optimal layout* (e.g.  $\overline{OLR} = 1$ ) was used in case of optimal design and operation of the predefined maximum layout.

Once a constraint is violated, a corresponding penalty function, as mentioned in Section 5, was added to the objective function(s).

#### 6.2.1.4 Electricity tariff

As in many electricity supply PWDNs, the model incorporates a cheap and a more expensive electricity price at off-peak and peak period, respectively. According to the irrigation scheduling proposed by MAF (1994), high demand was set to occur twice a day, from 5:00 to 10:00 and from 17:00 to 22:00. The rest periods were considered off-peak. The optimization period was divided into intervals of one hour in this study.

Based on the electricity price applied in agriculture and fisheries in Oman<sup>1</sup> and the assumed multipliers for hourly demand, electricity tariffs were estimated as shown in Table 6.4.

Table 6.4: Demanded multiplier and energy tariff (\$/kWh)

Time of day	1	2	3	4	5	6	7	8
Multiplier	0.6	0.6	0.6	0.6	1.6	1.6	1.6	1.6
Energy tariff	0.0312	0.0312	0.0312	0.0312	0.0832	0.0832	0.0832	0.0832
Time of day	9	10	11	12	13	14	15	16
Multiplier	1.6	1.6	0.2	0.2	0.2	0.2	0.2	0.2
Energy tariff	0.0832	0.0832	0.0104	0.0104	0.0104	0.0104	0.0104	0.0104
Time of day	17	18	19	20	21	22	23	24
Multiplier	1.6	1.6	1.6	1.6	1.6	1.6	0.6	0.6
Energy tariff	0.0832	0.0832	0.0832	0.0832	0.0832	0.0832	0.0312	0.0312

#### 6.2.1.5 Other assumptions

Several other parameters were assumed as following:

<sup>1</sup> <http://www.dynamic-ews.com/Tariffs/Electricity%20Tariffs/Oman.pdf>

Pump efficiency:  $\eta_{pump} = 0.75$  for all pumps

Roughness coefficient with respect to reinforced concrete pipe:  $C_{W-H} = 130$  for all pipes (Rossman, 2000).

The pipes that connect pumps and tanks were not taken into account in this application because they are commonly fixed in their diameter and length.

### **6.2.2 Results**

#### *6.2.2.1 Backbone network*

Backbone is referred to as a main pipeline network. With the real physical conditions in the study area, the biggest obstacles were the main asphalt road system and considerable geographical deviation.

Because of these obstacles, the backbone network, consisting of 32 pipelines connecting 2 tanks (44-45), 22 demand nodes (1-22), 9 junction nodes (23-31) and 12 pumps (PU1 – PU12) which pump water from 12 wells (32 – 43) to the tanks, was proposed as shown in Fig 6.8 and 6.11.

Two tanks were placed at the highest locations, compared to all nodes, in order to collect pumped ground water from the wells and to conveniently distribute water to nodes. Tanks were assumed to be cylindrical with a diameter of 40 m and maximum height of 25 m.

Two main pipelines (1 and 2) were placed along the Abyat road and Barka-Nakhl road to convey water from the tanks to the cultivated area. Another main pipeline system (pipe 6 - 11), which also connects pipe 1 and pipe 2, was placed along road No.1. The backbone network crossed road No.1 at seven points (junction node 25 - 31) to supply irrigation water to the coastal sub-areas. Pipe and pump numbers can be seen in Figure 6.11. More detailed data of nodes, tanks, and reservoirs are given in Appendix D.1 and Appendix D.2.

In this application there were 58 decision variables consisting of alternative diameters of 32 pipes, pump curve representing discharge and head of 12 pumps, and initial water level in 2 tanks.

In this case there was no change in the number of pipes; however, the number of pumps could be changed during the optimization process. By using the simple control in Epanet, which specifies the status of pumps as function of tank water level, pump status could be determined to be either open or closed.

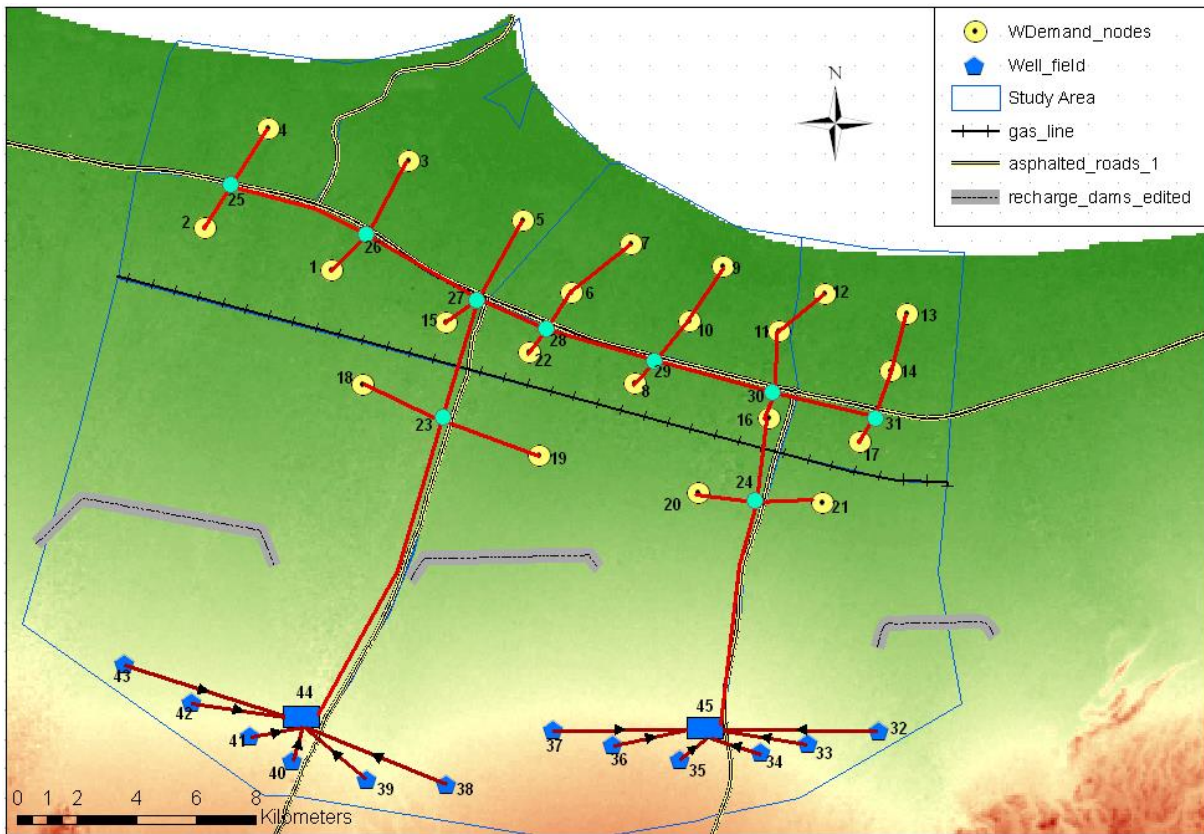


Figure 6.8: The backbone network layout representing node, tank, and well locations

The obtained Pareto optimal front included many diverse trade-offs non-dominated solutions (colored circles in Figure 6.9). The minimum surplus head of only 0.005 that was produced by the minimum cost solution at 10:00 at node 4, the furthest node from the sources, revealed that this solution seemed to be optimal.

By applying the approach determining the significant solutions from this Pareto data, eight representative solutions were determined, namely, the minimum cost, maximum cost, best compromise (red circle), and five representative solutions (yellow cross) for five clusters. As the best compromise solution (at the total cost of Mi.\$ 107.1546 and NR of 0.8756) almost coincided with the centroid solution of cluster 3, it was chosen to be representative for this cluster.

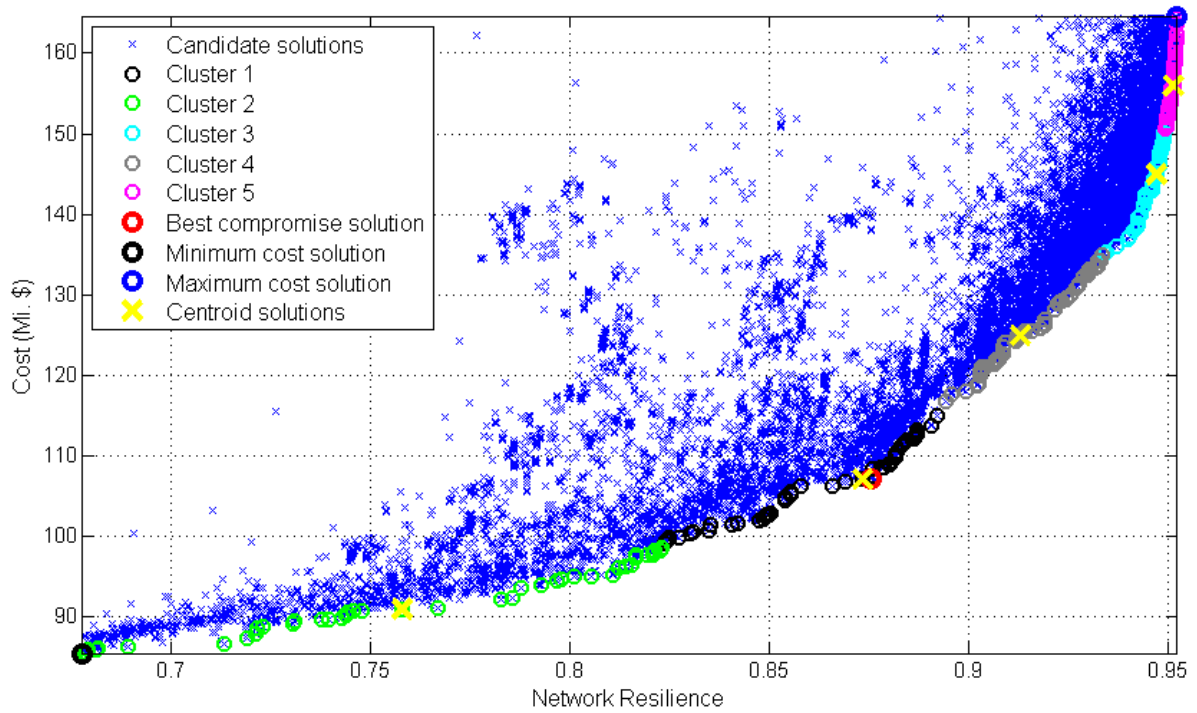


Figure 6.9: The significant solutions on the Pareto front achieved from backbone design and operation optimization

As can be seen in Appendix D.3, seven corresponding optimized results of these representative solutions were expressed and the objective network reliability increased as pipe cost increased. Pump operational and construction cost decreased due to a reduction in the number of pumps used; this was due to a reduction of dissipated power in the network. Set of pipe diameters and nodal pressures of the minimum cost solution and the best compromise solution were depicted in Appendix D.4.

The minimum surplus head increased rapidly from the minimum cost solution to the centroid solution of cluster 1; it then seemed to decline as the number of working pumps was reduced. Due to total head loss decreases as pipe diameter increase the total dissipated pump power tended to decrease.

The appropriate differences of water level in tanks (all were less than 2% for 7 representative solutions), together with the appropriate deviations between the total maximum power and total average power dissipated within one operating cycle demonstrated that the operation process was optimized.

The optimizing results were also proven through an illustration of time series of pumped water and demand. Figure 6.10 demonstrates a more visible, hourly pumped volume and demand over an operating cycle corresponding to the best compromise solution. The exact amount of water has to be pumped in each time interval in order to achieve the trade-offs solution under water quantity and tank constraints.

There was a considerable oscillation in the tank water levels (see Figure 6.15.a) even though the volume water pumped during peak periods was not much different from that during off-peak periods. This was due to a large amount of pumped water that was stored in tanks during the off-peak period and then discharged during the peak periods. An extra reason was that all pumps worked regularly regardless of off-peak or peak periods.

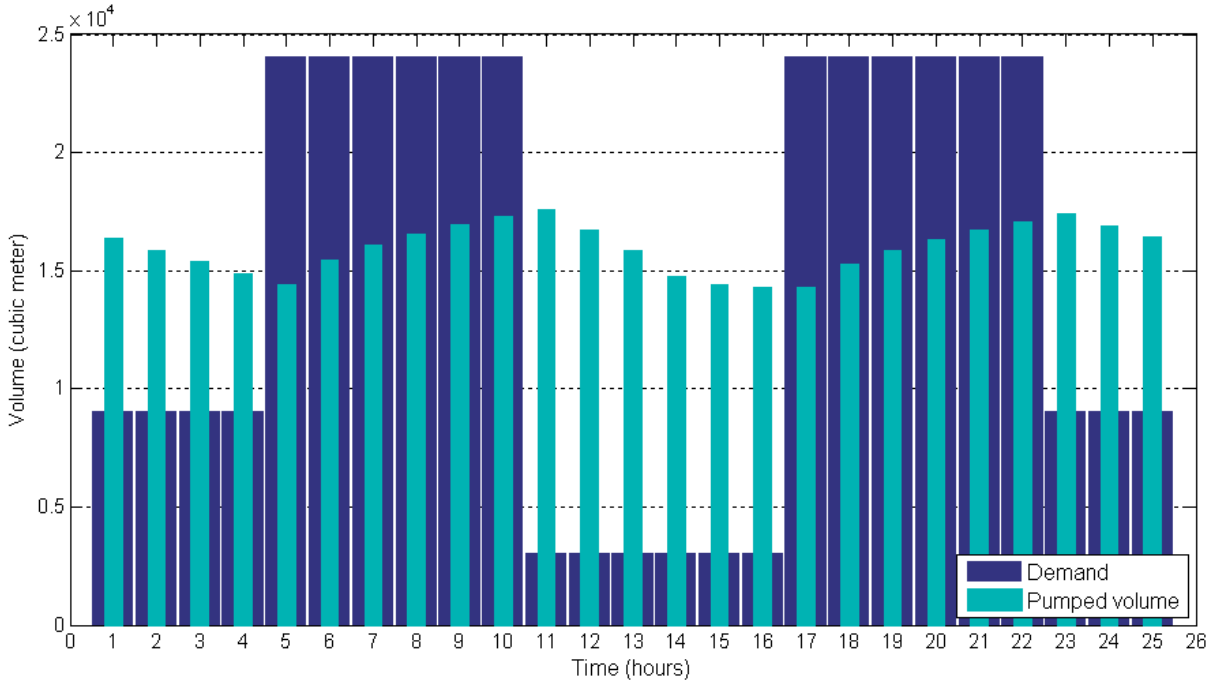


Figure 6.10: Hourly pumped volume and demand corresponding to the best compromise solution with respect to the backbone network

#### 6.2.2.2 Predefined maximum layout

The aim of this section is to simultaneously and optimally design and operate a PWDN including a network layout. The optimal layout will be derived from a predefined maximum layout based on the optimization principles described in Section 4.5. The PML in this case, outlined in Figure 6.11, consisted of a total of 54 pipelines linking 2 tanks, 22 demand nodes, and 9 junction nodes as in the backbone case. More details can be seen in Appendix D.1 and D.2.

According to Cisty (2012), a branched network can be accepted for irrigation since most crops can suffer the condition of lacking water for a couple of days during repairing or maintaining periods. Consequently, in this application, only the required layout reliability level 1 ( $\overline{OLR} = 1$ ) was used during the optimization process to determine optimal network configuration.

The Pareto optimal solutions obtained using the MO-CMA-ES-EP (colored circles in Figure 6.12) included many trade-offs solutions. The unsmooth Pareto optimal front demonstrates that these trade-offs solutions strongly varied from one solution to another.



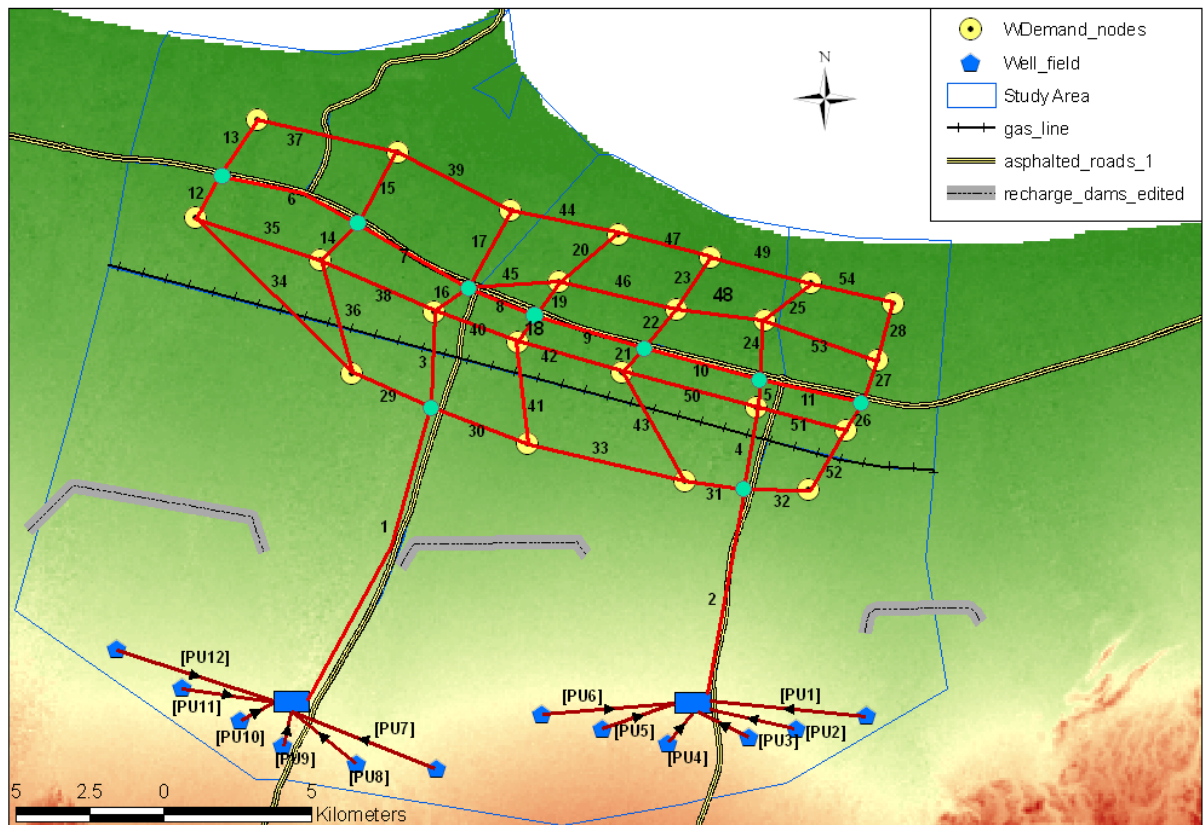


Figure 6.11: The PML representing pipes and pumps

The procedure determining the optimal number of clusters to this Pareto data was applied. As a result, five clusters corresponding to the largest silhouette value of 5 were partitioned. It can be easily seen in Figure 6.12 that each cluster groups a set of solutions in such a way that, in the same cluster, they were more similar to each other than to those in other clusters. Also, the best compromise solution was determined at the total cost of Mi.\$134.2948 and NR of 0.7287. The more detailed characteristics of representative solutions including the minimum cost, maximum cost, the first four representative centroid solutions, and the best compromise solutions are illustrated in Appendix D.9. The centroid solution of cluster 1 was not taken into consideration here because the maximum cost solution was selected as representative for this cluster.

As shown in Appendix D.9, the network layout varied among distinct solutions due to different working pipes and pumps. Several pipes and pumps, corresponding to each solution, were assigned to be “closed” during the optimization process.

The operation process was likely to be optimized through the acceptable tolerances of water level in tanks after one operating cycle (all were smaller than 3%). Compared to the backbone case, there was a bigger difference between total maximum power and total average power in this case. This was due to more pumps being turned on/off during their operation in order to satisfy operational constraints.

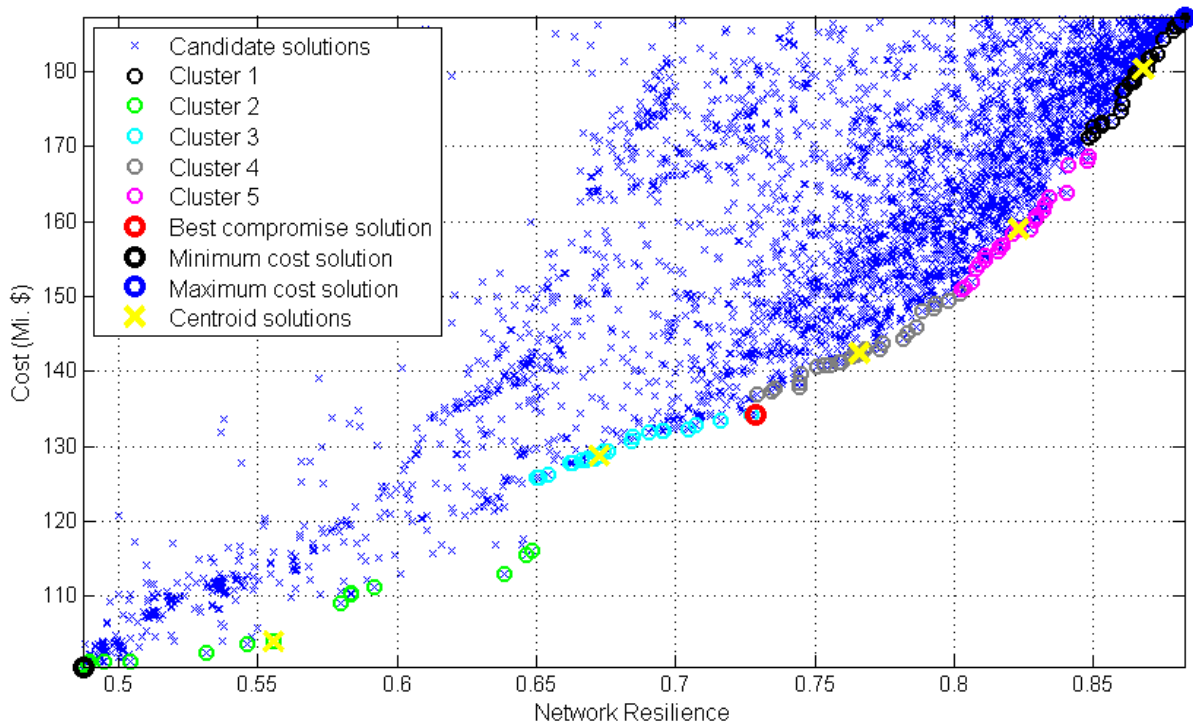


Figure 6.12: The significant solutions on the Pareto front obtained from the predefined maximum layout network design and operation optimization

A visible comparison between the hourly pumped volume and demand over a 24-hour operating cycle, corresponding to the best compromise solution, is shown in Figure 6.13. There was a delay of pumped volume at the beginning of peak periods in this case, which was the consequence of closing several pumps in several time intervals during, or right after, off-peak periods when the tanks had been fulfilled.

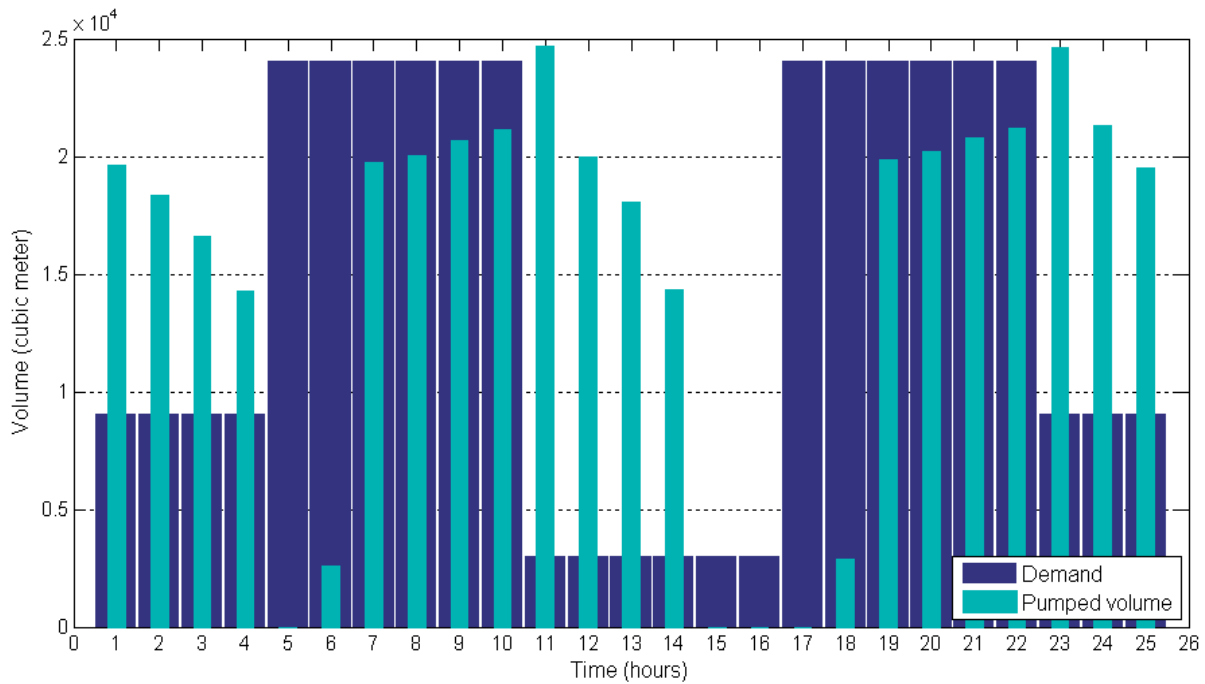


Figure 6.13: Hourly pumped volume and demand corresponding to the best compromise solution with respect to the predefined maximum layout

Set of pipe diameters and minimum nodal pressures at 22:00 were produced by two configurations, i.e., the minimum cost solution and the best compromise solution. The corresponding eliminated pipes and pumps are presented in Appendix D.10.

With the appropriate Pareto solutions obtained from two applications of MO-CMA-ES-EP on the backbone and the predefined maximum layout it can be said that the new approach executed successfully with decision variable of initial water level in tank besides other ones, such as pipe diameters, discharge, and head of pump.

This approach was also capable of eliminating redundant pipes and pumps during its optimization performance. Even though the number of eliminated pipes was not as high as expected in this case study, this proved the capability of the proposed approach.

Regaining water level in tanks resulted after each operational scheduling with an appropriate tolerance, revealing that the network components and the operational process were likely to be optimized. In addition, tracking the time series of tank water level shows that both tanks were filled at the end of the off-peak periods and discharged during peak periods (Figure 6.14).

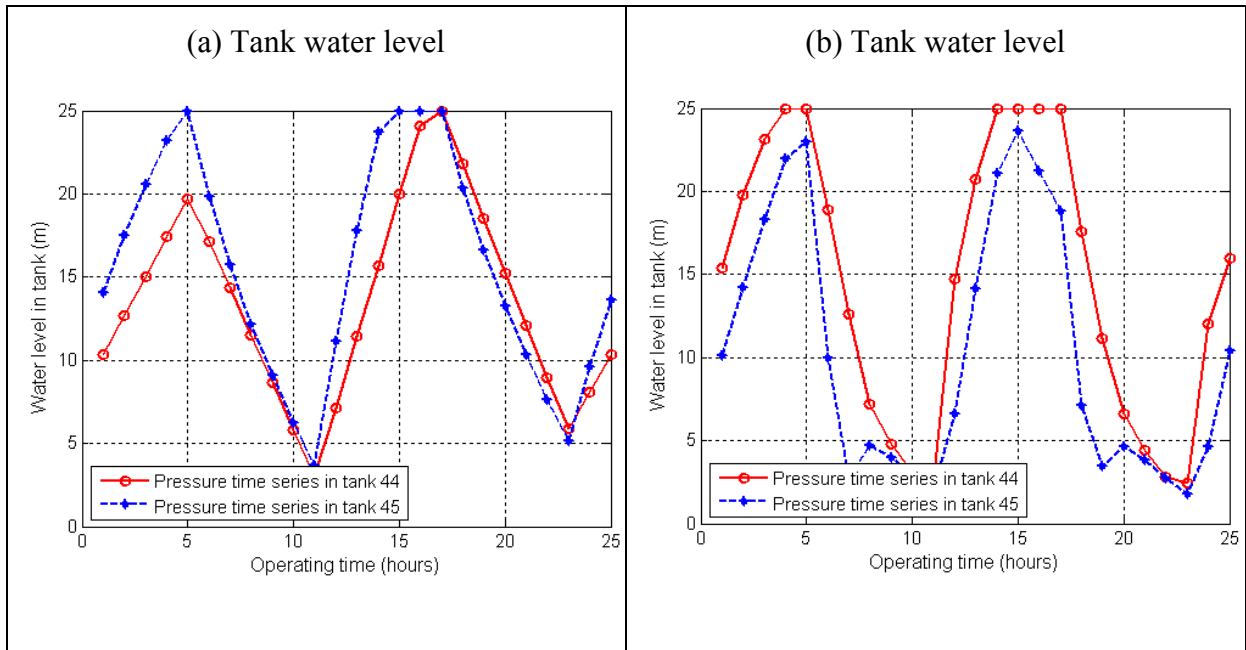


Figure 14: Water level in tanks during a 24-hour operating cycle corresponding to the best compromise solution with respect to (a) the backbone network and (b) the predefined maximum network

### 6.3 Pump scheduling optimization

Finding optimal operation schedules for pumps is an important and difficult task because it may be affected by multiple loadings in water demand, the complexity of the PWDN problem, and complex electricity tariff structure. This problem is equivalent to the

minimization of pump operational cost without making any change to the basic PWDN components.

The most commonly used approach for solving this optimization problem is to find a combination of ON/OFF pumps (López-Ibáñez et al., 2008) with the smallest pump operational costs while satisfying the following constraints, which are incorporated into the current algorithm as penalties:

- (i) Minimum required nodal pressures
- (ii) Capacity of tanks
- (iii) Regaining water level in tanks after one operating cycle

In this application, two network configurations were used as the basic PWDNs. These configurations correspond, respectively, to the two best compromise solutions obtained from optimal design and operation of the backbone and the predefined maximum layout network for monthly maximum demand in May (see Appendix D.4, D.5, D.10, and D.11). Based on monthly irrigation water demands (Figure 6.6), pump operational costs had to be optimized for the months from January to December by using the single CMA-ES-EP.

In practice, it is difficult to keep a pump operating consistently with the BEP (as discussed in Section 2.2) because the network usually performs with unstable demands. However, one of the ways to reduce overall operating costs is to keep a pump within a reasonable range of its BEP (*ITP and HI, 2006*). In order to retain the appropriate pump efficiency, the interval here was predefined to be  $(BOP_{opt} \pm 30\%)$ , in which  $BOP_{opt}$  is the optimal head on the pump curve. Otherwise, the pump must be shut off.

Average monthly discharges of the optimal set of pumps corresponding to the backbone network were evaluated, as shown in Appendix D.6. Similarly, monthly average pump discharges for the predefined maximum layout were optimized (Appendix D.12).

These results show that using various types of pumps allows the network to operate closer to the optimal operation. During operation, several pumps were working continuously, while others had to be turned on and off in accordance with the constraints. Appendix D.7 and D.13 present pump schedules corresponding to the typical demands (maximum in May and minimum in December) for the backbone network and predefined maximum layout.

#### **6.4 Network robustness under demand uncertainty**

As analyzed in Section 5.4, the result achieved by using a small number of LHST samples was in very good agreement with that achieved from a very large sampling approach; hence, the sample of 1,000 was used to evaluate network robustness probability in this application. The same procedure was applied under the specific required pressure of modern irrigation devices for all nodes of 45 m at the end of peak period, at which maximum nodal demands

and minimum nodal pressures occur. Demand uncertainty was considered in two cases: Uncertain uncorrelated demands and uncertain correlated demands.

Figure 6.15 a and b express the robustness probabilities corresponding to all solutions on the two Pareto optimal fronts, which were achieved by optimizing the backbone and predefined maximum layout network (Figure 6.9 and 6.12), were evaluated with  $\sigma = 10\%$ , under uncertain uncorrelated and correlated demands, respectively.

It is clear that as network cost increased the robustness probability of the optimized backbone solutions increased in case demand uncertainty was taken into account. Robustness probability of a network as defined in Section 4.7 is mostly affected by minimum surplus head; hence it rose quickly with solutions at the beginning of Pareto front since the minimum surplus head increased strongly. This was the case for both uncertain uncorrelated and correlated demands (Appendix D.8).

However, this was not likely to be assured with respect to the optimized predefined maximum network solutions. Due to the strong change in network configuration as well as the on/off status of working pumps among the PML Pareto solutions, the minimum surplus heads produced by these solutions did not increase conspicuously as cost increased (Appendix D.9). Moreover, a lower tank head supplied by a smaller total average pump power was used to overcome a bigger total head loss in PML solutions (Appendix D.14) compared to the backbone solutions. Consequently, it was difficult for robustness probability to reach maximum value with respect to the initial PML Pareto solutions. Accordingly, there were some quite low robustness probabilities produced by quite high-cost solutions. Particularly, unreliable robustness probability was more clearly in case of uncertain correlated demands because of the effect of the correlation among nodal demands.

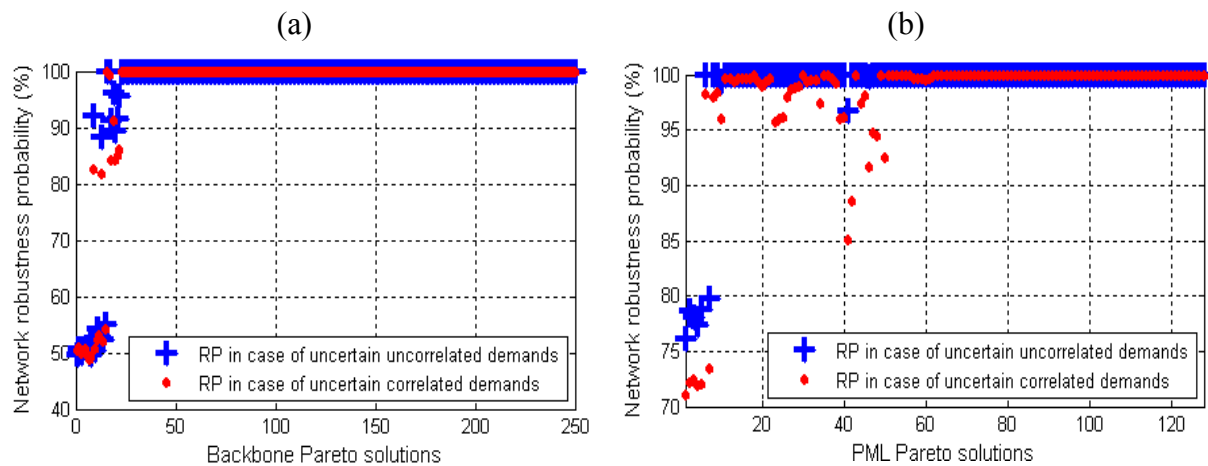


Figure 6.15: Robustness probability corresponding to uncertain uncorrelated and correlated demands of (a) backbone Pareto solutions and (b) PML Pareto solutions

## 6.5 Discussion

The proposed approach was systematically tested on a number of different benchmark PWDNs ranging from simple to complex with the common optimization problems of PWDN design and operation. It was successfully executed with various kinds of decision variables, such as pipe diameters, pump discharge and head, and initial water level in tank. The CMA-ES-EP produced the best solution with respect to objective function, whereas MO-CMA-ES-EP produced the Pareto optimal solutions which are trade-offs between contradictory objectives. Compared to the previous studies, the achieved results were the same or better (with respect to the complex networks). The minimum cost solution obtained by MO-CMA-ES-EP can also be supported by CMA-ES-EP.

The new approach was successfully developed and applied to the real world case study. Two scenarios considered as user-predefined network layouts for applying the proposed approach: a given backbone network (BB) and a predefined maximum layout (PML). The new approach capacity was demonstrated through the true Pareto front and the regaining water level in tanks. Generally, total cost for the PML was much higher than that for the backbone network. The reason is that the number of eliminated pipes through optimization was not as high as expected. However, the operational cost (PUOC) of the PML was much lower than that of the BB (for instance, PUOC to the best compromise solution of Mi.\$ 6.74/year compared to Mi.\$ 9.19/year). Thus, considering long term operation, the solution obtained from PML optimization may be more economical. But it should be carefully considered when demand uncertainty is taken into account, especially with respect to PML. Neglecting this consideration may lead to a serious under-designed problem. Furthermore, it should be noted that optimization of PWDN design and operation problems requires experiences to achieve a practicable solution.

## 7 CONCLUSIONS AND OUTLOOK

### Conclusions

This study focused on simulation-based single and multiple objective optimizations for optimally designing and operating a PWDN towards the objectives of minimizing total cost and maximizing network resilience under specified constraints. The new proposed model couples Epanet with the covariance matrix adaptation evolution strategy (CMA-ES) and can be operated in two different modes, namely, (1) simulation-based Single-objective optimization (CMA-ES-EP) and (2) simulation-based multi-objective optimization (MO-CMA-ES-EP).

By using a wide range of decision variables, including pipe diameters, pump discharges, pump heads, and initial water level in tank, PWDN design and operation optimization problems of the benchmark as well as the real world networks were completely solved. The optimization procedure was subject to several constraints such as set of available pipe diameters, bounds of required nodal pressure, velocity, and other design parameters, as well as an additional constraint related to layout optimization. Furthermore, in order to evaluate the robustness of an optimally designed PWDN, demand uncertainty was taken into account. It can be concluded that the new approach was useful to obtain comprehensive and generalized results. Various verifications and application to the real world case of the proposed approach conducted in this study have shown that the new technique is a powerful tool for optimally designing and operating a PWDN for a multi-purpose water supply system.

The new approach successfully solved the pipe size optimization of the PWDN design problem. It is the most popular problem in PWDN design optimization and received considerable attention from researchers. Compared with previous results, the same result with a relative number of function evaluations was produced (with respect to small networks such Benchmark network No.1). For large networks, for example, Benchmark network No.2, a more economical solution has been obtained.

The new approach successfully simulated hydraulic processes in the system responding to multi-demand loadings. This is necessary due to the fact that demand is a varying quantity according to time variation during operation. Hydraulic conditions in this case were usually assumed to be a series of quasi-steady state in which the temporal mean velocity was a constant over a predetermined time step. The optimal solution was determined corresponding to the peak demand period.

The new approach was successfully applied to simultaneously optimize network components and layout. By using the constraint related to required layout reliability level of the optimal network and the simple control associated with this model, a much simpler network was achieved from a user-predefined maximum layout. The required layout reliability level is a given minimum number of independently available pipes connecting to a node out of all nodes to generate the optimal layout. During the optimization process, redundant links (including pipes and pumps) were assigned to the “closed” status and were eliminated from the network afterwards. The proposed approach achieved more economical solutions when applying the new approach to Benchmark networks No.3 and No.4 as compared to the previous study by Geem et al. (2000) and Afshar and Jabbari (2008).

Integral consideration of design and operation of a PWDN including pumps and tanks is a very complex and difficult task because of contradictory objectives, i.e., investment and operational cost, as well as many accompanying constraints of pumps and tanks. Applied to Benchmark networks No.5 and No.6, the novel approach produced appropriate operating schedules in which the largest quantity of water was supplied for tanks during off-peak periods and was discharged out of tanks during the peak periods. Using pump discharges and heads as decision variables will help the selection of pumps to become more adequate.

Together with the cost, the concept of network reliability is taken into consideration in the context of simulation-based multi-objective optimization (MO-CMA-ES-EP) in order to provide more options in improving the network capability. Among five proposed network reliability measures, network resilience, which incorporates the effect of surplus head and pipe diameter uniformity, was used due to its overwhelming nature. The Pareto optimal front yielded by MO-CMA-ES-EP was in strong agreement with previous studies. Theoretically, the Pareto optimal front contains a considerable number of non-dominated solutions between the analyzed objectives. This large set of Pareto solutions needs to be reduced to a few representative solutions for designers to reasonably consider in case they do not have any preferential criterion regarding the relative importance of contradicting objectives. Two techniques were employed for determining the significant solutions from a large set of Pareto solutions, namely, (1) the k-means clustering technique for determining centroid solution to be a representative for each cluster, and (2) the technique for determining the best compromise solution. As a result, several significant solutions would be proposed to decision makers.

Uncertain conditions were taken into consideration in order to predict the behavior of the designed network. Among the uncertainties, uncertain nodal demand is the most important one because it directly affects other hydraulic parameters. Normally, demands can be considered as uncertain uncorrelated. However, in some extreme cases, such as hot and dry weather, demands can be increased at all nodes and are then considered uncertain correlated. Both cases were taken into account. The common way to solve uncertainty is to implement the Monte Carlo technique with hundreds of thousands of samples. Rather than doing that, with only thousand samples the Latin hypercube sampling technique was capable of



producing a good range of random output variables corresponding to uncertain input variables. The minimum required nodal pressures were referred to as criteria to evaluate network robustness probability. The result will support more options for designers to select the most appropriate network configuration and it is clear that neglecting demand uncertainty may lead to a seriously under-designed network.

The new approach was successfully applied to a part of the new irrigation PWDN in the Southern Batinah region. Two scenarios were considered as user-predefined network layouts for applying the new methods, namely, (i) a backbone and (ii) a predefined maximum layout network. In both cases, the maximum demand in May was used for the optimization procedure. The Pareto optimal fronts corresponding to these two cases were produced. The minimum surplus heads yielded by the minimum cost solutions (0.005 m and 1.54 m with respect to backbone and predefined maximum layout, respectively) showed that these Pareto solutions were reasonable. In addition, the regaining initial tank water level proved that the operating schedules were satisfied. Based on the determined network configuration for each scenario, operating schedules were then optimized for the remaining months of the year.

Regarding the design and operation optimization of predefined maximum layout of case study, even though the number of eliminated links (both pipes and pumps) was not as high as expected, this result proved the new approach's capacity.

From both economical and engineering points of view, the optimal solution should be in the first Pareto stage that consists of solutions from the minimum to the best compromise, because a moderate cost increase coordinates with a considerable increase of network resilience. In contrast, the minimum surplus head increases inconsiderably with a large cost increase in the remaining stage of the Pareto.

## **Outlook**

Optimal design and operation of a PWDN, even with respect to a simple network, is still a sophisticated multi-task. Although this study coped with major optimization problems of PWDN design and operation, there are several challenges for future work.

Expanding the new approach: Together with a new optimal design, PWDN optimal rehabilitation is a necessary, complex, and long term task. The MO-CMA-ES-EP may be extended to incorporate rehabilitation over time.

The network robustness probability can be used as another objective function by using LHST, because it does not require as many samples as MC. Hence, performance time can be considerably reduced.

One notable challenge of PWDN design optimization is that it is highly time-consuming; the computing time rises exponentially according to the dimension of decision variables. It is expected that significant speed enhancement may be achieved by using multi-threads with multi-parallel processors.

Further investigating the practice application should avoid many assumptions which make the optimization results become impracticable, and further survey and acquisition data for real world application are strongly required. On this basis, more parameters can be referred to as decision variables, such as tank diameter, tank location, and so on.

Generally, there remain a few issues which require further discussion and clarification; however, the proposed approach using the coupling of (MO-)CMA-ES and Epanet has proven to be a very powerful tool for simultaneously and optimally designing and operating a full PWDN with layout included.

## REFERENCES

- Abbasi, H., Afshar, A., and Jalali, M. R., 2010. *Ant-colony-based simulation-optimization modeling for the design of a forced water pipeline system considering the effects of dynamic pressures*. Journal of Hydroinformatics, pp. 212 – 224.
- Abebe, A.J. and Solomatine, D., 1998. *Application of global optimization to the design of pipe networks*. Proceeding 3rd International Conference on Hydroinformatics, Copenhagen.
- Adachi, J. and Gupta, A., 2005. *Simulation-based parametric optimization for long-term asset allocation using behavioral utilities*. Applied Mathematical Modelling, Vol. 29, pp. 309–320.
- Adeyemo, J. and Otieno, F., 2010. *Differential evolution algorithm for solving multi-objective crop planning model*. Agricultural Water Management, Vol. 97, pp. 848–856.
- Afshar, A., 2009. *Application of a compact genetic algorithm to pipe network optimization problems*. Transaction A: Civil Engineering. Vol. 16, No. 3, pp. 264-271.
- Afshar, A., Abbasi, H. and Jalali, M. R., 2006. *Optimum design of water conveyance systems by ant colony optimization algorithms*. International Journal of Civil Engineering. Vol.4, No.1, pp. 1-13.
- Afshar, M.H., 2007. *Evaluation of selection algorithms for simultaneous layout and pipe size optimization of water distribution networks*. Scientia Iranica, Vol. 14, No. 1, pp 23-32.
- Afshar, M. H. and Rajabpour, R., 2007. *Optimal design and operation of irrigation pumping systems using particle swarm optimization algorithm*. International Journal of Civil Engineerng. Vol. 5, No. 4.
- Afshar, M.H. and Jabbari, E., 2008. *Simultaneous layout and pipe size optimization of pipe networks using genetic algorithm*. The Arabian Journal for Science and Engineering, Volume 33, Number 2B, pp. 391-409.
- Al-Shaqsi, S. S., 2004. *The socio-economic and cultural aspects in the implementation of water demand management: A case study in the sultanate of Oman*. University of Nottingham.
- Aklog, D. and Hosoi, Y., 2003. *Reliability-based optimal design of water distribution networks*. Water Science and Technology: Water Supply, Vol. 3, No 1–2, pp. 11–18.
- Alandi, P., Pérez, C., Álvarez, O., Hidalgo, J.M., and Martín-Benito, 2007. *Optimization of irrigation water distribution network, layout included*. Agricultural Water

- Management. Vol. 88, pp. 110-118.
- Alperovit, E. and Shamir, U., 1997. *Design of optimal water distribution systems*. Water Resource Research, Vol. 13, pp. 885 – 900.
- Araque, D. and Saldarriaga, J., 2006. *Water distribution network operation optimization by maximizing the pressure uniformity at service nodes*. Proceedings of 8th Annual International Symposium on Water Distribution Systems Analysis.
- Arkeman, Y., Wahanani, N. A., and Kustiyo, A., 2012. *Clustering K-Means Optimization with Multi-Objective Genetic Algorithm*. International Journal of Electrical and Computer Sciences IJECS-IJENS Vol. 12, No. 05.
- Arnold, D. and Hansen, N., 2012. *A (1+1)-CMA-ES for Constrained Optimisation*. GECCO.
- Auger, A. and Hansen, N., 2005. *A Restart CMA Evolution Strategy With Increasing Population Size*. Proceedings of the IEEE Congress on Evolutionary Computation.
- Babayan, A., Kapelan, Z., Savic, D., Walters, G., 2005. *Least-cost design of water distribution networks under demand uncertainty*. Journal of Water Resources Planning and Management, Vol. 131, No. 5, pp. 375–382.
- Babayan, A. V., Savic, D. A. and Walters, G. A., 2004. *Multi-objective optimization of water distribution system design under uncertain demand and pipe roughness*. Journal of Water Resources Planning and Management.
- Baños, R., Gil, G., Reca, J. and Montoya, F.G., 2010. *A memetic algorithm applied to the design of water distribution networks*. Applied Soft Computing, Vol. 10, pp. 261–266.
- Baños, R., Reca, J., Martínez, J., Gil, C. and Márquez, A., 2011. *Resilience indexes for water distribution network design: A performance analysis under demand uncertainty*. Springer Science Business Media B.V.
- Baños, R., Gil, C., Reca, J., and Ortega, J., 2008. *A Pareto-based memetic algorithm for optimization of looped water distribution systems*. Engineering Optimization, pp.1–20.
- Bhave, P. and Gupta, R., 2004. *Optimal design of water distribution networks for fuzzy demands*. Civil Engineering and Environmental Systems, Vol. 21. No. 4, pp. 229-245.
- Boman, B. and Shukla, S., 2001. *Materials and installation of delivery pipes for irrigation systems*. Agricultural and biological engineering department, Institute of Food and Agricultural sciences, University of Florida.
- Brown, P.D, Cochrane, T.A., and Krom, T.D., 2010. *Optimal on-farm irrigation scheduling with a seasonal water limit using simulated annealing*. ScienceDirect, pp. 892–900.
- Buchholz, P., 2009. *Optimization of stochastic discrete event simulation models*. Dagstuhl Seminar Proceedings.
- Censor, Y. (1977). *Pareto optimality in multi-objective problems*. Applied mathematics and optimization, Vol. 4, pp. 41 – 59.

- Chandramouli, S. and Malleswararao, P., 2011. *Reliability based optimal design of a water distribution network for municipal water supply*. International Journal of Engineering and Technology, Vol. 3, pp. 13-19.
- Chaudhari, P.M., Dharashar, and Thakare, V. M., 2010. *Computing the most significant solution from Pareto front obtained in multi-objective evolutionary*. International Journal of Advanced Computer Science and Applications, Vol. 1, No. 4.
- Cheung, P.B, Reis, F. R., Formiga, T. M., Chaudhry, H., and Ticona, W. C., 2003. *Multi-objective evolutionary algorithms applied to the rehabilitation of a water distribution system: A comparative study*. Evolutionary multi-criterion optimization Lecture Notes in Computer Science, Vol. 2632, pp. 662-676.
- Chung, G., Lansey, K., and Bayraksan, G., 2009. *Reliable water supply system design under uncertainty*. Environmental Modeling and Software, Vol. 24, pp. 449–462.
- Cisty, M., 2012. *Optimal design or rehabilitation of an irrigation project's pipe network<sup>1</sup>*.
- Cunha, M.C. and Ribeiro, L., 2004. *Tabu search algorithms for water network optimization*. European Journal of Operational Research, Vol. 157, pp. 746–758.
- Cunha, M.C and Sousa, J., 1999. *Water distribution network design optimization: simulated annealing approach*. Journal of Water Resources Planning and Management, Vol. 125, No. 4, pp. 215–221.
- Daccache, A., Lamaddalena, N., and Fratino, U., 2009. *On-demand pressurized water distribution system impacts on sprinkler network design and performance*. Springer Verlag.
- Dandy, G. C., Simpson, A. R. and Murphy, L., 1996. *An improved genetic algorithm for pipe network optimization*. Water resource research, Vol. 32, No. 2, pp. 449 - 458.
- Davidson, J.W. and Goulter, I.C., 1995. *Evolution program for design of rectilinear branched networks*. Journal of Computing in Civil Engineering, ASCE, Vol.9, No.2, pp.112-121.
- Davies, D. and Bouldin, D. W., 1979. *A cluster separation measure*. IEEE transaction on pattern analysis and machine intelligence, Vol. PAMI-1, No. 2.
- Deb, K. and Gupta, H., 2005. *Searching for robust Pareto-optimal solutions in multi-objective optimization*. Springer-Verlag Berlin Heidelberg.
- Dercas, N. and Valiantzas, J., 2011. *Two explicit optimum design methods for a simple irrigation delivery system: comparative supplication*. Irrigation and Drainage.
- Dijk, M. V., Vuuren, S., and Zyl, J., 2008. *Optimizing water distribution systems using a weighted penalty in a genetic algorithm*. Water SA, Vol. 34, pp. 537 – 548.

---

<sup>1</sup> www.intechopen.com.

- Djebedjian, B., Yaseen, A., and Rayan, M.A., 2005. *A new adaptive penalty method for constrained genetic algorithm and its application to water distribution systems*. Ninth International Water Technology Conference, Sharm El-Sheikh, Egypt.
- Djebedjian, Mohamed, M. S., Mondy, A., and Rayan, M. A., 2005. *Network optimization for steady flow and water hammer using genetic algorithms*. Ninth International Water Technology Conference, Sharm El-Sheikh, Egypt.
- Djebedjian, B., Yaseen, A., and Rayan, M.A., 2006. *Optimization of large water distribution network design using genetic algorithms*. Tenth International Water Technology Conference, IWTC10, pp. 447-477.
- Dong, X., Liu, S., Tao, T., Li, S., and Xin, K., 2012. *A comparative study of differential evolution and genetic algorithms for optimizing the design of water distribution systems*. Journal of Zhejiang University-SCIENCE A, Vol. 13, pp. 674-686.
- Dorigo, M. and Coloni, A., 1996. *The ant system: Optimization by a colony of cooperating agents*. IEEE Transactions on Systems, Man, and Cybernetics–Part B, Vol.26, No.1, pp.1-13.
- Eiger, G., Shirmir, U., and Bental, A., 1994. *Optimal design of water distribution networks*. Water resource research, Vol. 30, No. 09, pp. 2636 – 2646.
- Ekinci, Ö and Konak, H., 2008. *An optimization strategy for water distribution networks*. Water Resour Manage, Vol. 23, pp. 169–185.
- Elbeltagi, E., Hegazyb, T., and Griersonb, D., 2005. *Comparison among five evolutionary-based optimization algorithms*. Advanced Engineering Informatics, Vol.19, pp. 43–53.
- Ezzeldin, R., Abdel-Gawad, H., and Rayan, A., 2008. *Reliability - based optimal design for water distribution networks of El-Mostabal city, Egypt (case study)*. Twelfth International Water Technology Conference, IWTC Alexandria, Egypt.
- Farmani, R., Walters, G. A., and Savic, D. A., 2005. *Trade-off between total cost and reliability for anytown water distribution network*. Journal of Water Resources Planning and Management, Vol. 131, No. 3, pp. 161–171.
- Farmani, R., Walters, G., and Savic, D., 2006. *Evolutionary multi-objective optimization of the design and operation of water distribution network: total cost vs. reliability vs. water quality*. Journal of Hydroinformatics, pp. 165 – 179.
- Formiga, K., Chaudhry, F. H., Cheung, P.B., and Reis, L., 2003. *Optimal design of water distribution system by multi-objective evolutionary methods*. Springer Verlag Berlin Heidelberg.
- Fu, G., Kapelan, Z., and Reed, P., 2012. *Reducing the complexity of multi-objective water distribution system optimization through global sensitivity analysis*. Journal of Water Resources Planning and Management, Vol. 138, No. 3, pp. 196–207.
- Gaspar-Cunha, A. and Covas, J.A., 2008. *Robustness in multi-objective optimization using*

- evolutionary algorithms*. Comput Optim Appl, Vol. 39, pp. 75–96.
- Geem, Z. W., 2006. *Optimal cost design of water distribution networks using harmony search*. Engineering Optimization, Vol. 38, No. 3, pp. 259–280.
- Geem, Z.W, Kim, J.H., and Jeong, S.H., 2011. *Cost efficient and practical design of water supply network using harmony search*. African Journal of Agricultural Research Vol. 6(13), pp. 3110-3116.
- Gerner, A., 2013. *A novel strategy for estimating groundwater recharge in arid mountain regions and its application to parts of the Jebel Akhdar Mountains (Sultanate of Oman)*. PhD Dissertation, TU Dresden.
- Grundmann, J., Schütze, N., and Lennartz, F., 2013. *Sustainable management of a coupled groundwater–agriculture hydrosystem using multi-criteria simulation based optimization*. Water Science and Technology, Vol. 67, pp. 689-698.
- Grundmann, J., Schütze, N., Schmitz, G.H., and Al-Shaqs, S., 2012. *Towards an integrated arid zone water management using simulation based optimization*. Environ Earth Sciences, Vol. 65, pp. 1381–1394.
- Grundmann, J., 2011. *Integrated water management: the concept of the management system*. 4<sup>th</sup> workshop on the Oman - German IWAS - APPM cooperation project.
- Grundmann, J., Pham, V.T., Müller, R., and Schütze, N., 2014. *A simulation-optimization approach for designing water distribution networks under multiple objectives*. European Geoscience Union General Assembly, Vienna, Austria.
- Gupta, I., Bassin, J. K., Gupta, A., and Khanna, P., 1993. *Optimization of water distribution system*. Environmental Software, Vol. 8, pp. 101 – 113.
- Gupta, I., Gupta, A., and Khanna, P., 1999. *Genetic algorithm for optimization of water distribution systems*. Environmental Modelling and Software, Vol. 14, pp. 437–446.
- Hachicha, W., Ammeri, A., Masmoudi, F. and Chachoub, H., 2010. *A comprehensive literature classification of simulation optimisation methods<sup>1</sup>*.
- Han, S. and Mangasarian, O., 1979. *Exact penalty functions in nonlinear programming*. Mathematical Programming, Vol. 17, pp. 251-269.
- Hansen, N., 2011. The CMA Evolution Strategy: A Tutorial.
- Hansen, N., Mueller, S.D., and Koumoutsakos, P., 2003. *Reducing the time complexity of the derandomized evolution strategy with covariance matrix adaptation (CMA-ES)*. Evolutionary Computation, Vol. 11(1), pp. 1-18.
- Hansen, N. and Ostermeier, A., 2001. *Completely derandomized self-adaptation in evolution strategies*. Evolutionary Computation, Vol. 9(2), pp. 159-195.

---

<sup>1</sup> <http://mpra.ub.uni-muenchen.de/27652/> MPRA Paper No. 27652.

- Hassanli, A. M. and Dandy, G. C., 1996. *Application of genetic algorithms to the optimum design and layout of drip irrigation systems*. Research report No. R. 134.
- Igel, C., Hansen, N. and Roth, S., 2007. *Covariance matrix adaptation for multi-objective optimization*. Evolutionary Computation, Vol. 15(1), pp. 1-28.
- Igel, C., Heidrich-Meisner, V. and Glasmachers, T., 2008. *Shark*. Journal of Machine Learning Research, Vol. 9, pp. 993-996.
- Iman, R.L. and Conover, W.J., 1982. *A distribution free approach to inducing rank correlation among input variables*. Commun. Stat., Vol. 11, pp. 311 – 334.
- Iorio, A.W. and Li, X., 2005. *Solving rotated multi-objective optimization problems using differential evolution*. In G. I. Webb and X. Yu (Eds.), Proceedings of the 17<sup>th</sup> Joint Australian Conference on Artificial Intelligence, Vol. 3339, pp. 861–872.
- Jain, A. K. and Dubes, R., 1998. *Algorithms for clustering data*. Prentice-Hall, Inc.
- Kapelan, Z. S., Savic, D. and Walters, G. A., 2005. *Multi-objective design of water distribution systems under uncertainty*. Water Resource Research, Vol. 41.
- Keedwell, E. and Khu, S.T., 2005. *A hybrid genetic algorithm for the design of water distribution networks*. Engineering Applications of Artificial Intelligence, Vol. 18, pp. 461–472.
- Kessler, A. and Shamir, U., 1991. *Decomposition technique for optimal design of water supply networks*. Eng. Opt. Vol. 17, pp. 1 – 19.
- Kessler, A. and Shamir, U., 1989. *Analysis of the linear programming gradient method for optimal design of water supply networks*. Water resource research, Vol. 25, No. 07, pp. 1469-1480.
- Kulkarni, M. and Patil, K. A., 2011. *Optimization of pipe distribution network for irrigation by genetic algorithm*. International Journal of Earth Sciences and Engineering 231, ISSN 0974-5904, Vol. 04, No 06, pp. 231-234.
- Labye, Y., Olson, M.A., Galand, A., and Tsiourtis, N., 1998. *Design and optimization of irrigation distribution network*. FAO irrigation and drainage paper.
- Lahiouel, Y., Haddad, A. and Chaoui, K., 2005. *Evaluation of head losses in fluid transportation networks*. Sciences and Technologie B – No.23, pp. 89-94.
- Lamaddalena, N. and Sagardoy, J. A., 2000. *Performance analysis of on-demand pressured irrigation system*. FAO.
- Lansey, K. E. and Mays, L. W., 1989. *Optimization model for water distribution system design*. Journal of Hydraulic Engineering, Vol. 115 (10), pp. 1401–1418.
- Lansey, K.E., Duan, N., Mays, L. and Tung, Y., 1989. *Water distribution system design under uncertainties*. Journal of Water Resources Planning and Management, Volume 115.



- Lejano, R., 2006. *Optimizing the layout and design of branched pipeline water distribution systems*. Irrigation and Drainage Systems, Vol. 20, pp. 125–137.
- Liang, T., Yang, K. and Wu, I., 1974. *Dynamic programming optimization: A water distribution system design*. Technical Report No. 83, HAES Journal Series No. 1871.
- Liong, S.Y. and Atiquzzaman, M., 2004. *Optimal design of water distribution network using shuffled complex evolution*. Journal of the Institution of Engineers, Singapore, Vol. 44, pp. 93 – 107.
- López-Ibáñez, M., Prasad, T. D. and Paechter, B., 2008. *Ant Colony Optimization for Optimal Control of Pumps in Water Distribution Networks*. Journal of Water Resources Planning and Management, Vol. 134, No. 4, pp. 337–346.
- Matlab 2008b, 2011b. *The MathWorks, Inc.*
- MacMe, G., Savic, D. A., and Waltess, G. A., 1995. *An application of genetic algorithms to pump scheduling for water supply*. Genetic Algorithms in Engineering Systems: Innovations and Applications, Conference Publication No. 414.
- Maier, H. R., Simpson, A. R., Zecchin, A. C., Foong, W. K., Phang, K. Y., Seah, H.Y., and Tan, C.L., 2003. *Ant colony optimization for design of water distribution systems*. Journal of Water Resources Planning and Management, Vol. 129, No. 3, pp. 200 - 209.
- Mays, L.W., 2000. *Water Distribution System Handbook*. The McGraw-Hill Companies, Inc.
- Miller, G. A., 1956. *The magical number seven, plus or minus two: Some limits on our capacity for processing information*. Psychological Review, Vol. 63, pp. 81-97.
- Ministry of Agriculture and Fisheries of Oman (MAF), 1992. *Study of a new organization of irrigation In Barka-Rumais area*. Report.
- Ministry of Agriculture and Fisheries of Oman (MAF), 1994. *South Batinah integrated study*. Report Volume 1 – 3.
- Ministry of Agriculture and Fisheries of Oman (MAF), 2005. *Agricultural Census*.
- Ministry of Water Resources, 1996. *National Well Inventory*.
- Ministry of Water Resources, 2001. *Water Metering Pilot Project – Data compilation report*.
- Ministry of Regional Municipalities, Environment and Water Resources, 2004. *Integrated Catchments Management Plan*.
- Moneim, M.A., Moawad, Molla, A.A., and Selavy, A.A., 2008. *Model application for reliability - based optimization of water distribution networks*. World engineering and Applied Science Journal, Vol. 1, pp. 01 – 08.
- Montalvo, I., Izquierdo, J., P´erez, R. and Tung, M., 2008. *Particle Swarm Optimization applied to the design of water supply systems*. Computers and Mathematics with

- Applications, Vol. 56, pp. 769–776.
- Moradi-Jalal, M. and Karney, B. W., 2008. *Optimal design and operation of irrigation pumping stations using mathematical programming and Genetic Algorithm (GA)*. Journal of Hydraulic Research Vol. 46, No. 2, pp. 237–246.
- Moradi-Jalal, M., Maríño, M. A., Hon, M. and Afshar, A., 2003. *Optimal design and operation of irrigation pumping stations*. Journal of Irrigation and Drainage Engineering, Vol. 129, No. 3, pp. 149–154.
- Moreno, M.A., Planells, P., Córcoles, J., Tarjuelo, J. and , Carrion, P., 2009. *Development of a new methodology to obtain the characteristic pump curves that minimize the total cost at pumping stations*. Biosystemengineering, Vol. 102, pp. 95-105.
- Müller, R., 2012. *Threaded MO-CMA-ES framework for multi-objective combined simulation-optimization*. TU Dresden, Institute of Hydrology and Meteorology.
- Murphy, L.J, Simpson A. R., and Dandy, G. C., 1993. *Pipe network optimization using an improved Genetic algorithm*. Research report No. R109.
- Noory, H., 2012. *Optimizing irrigation water allocation and multicrop planning using discrete PSO algorithm*. Journal of Irrigation and Drainage Engineering, Vol. 138, No. 5, pp. 437–444.
- Norman, W.R., Shayya, W., Al-Ghafri, A., and McCann, I., 1998. *Aflaj irrigation and on-farm water management in northern Oman*. Kluwer Academic Publishers.
- Nyende-Byakika, S., Ngirane-Katashaya, G., and Ndambuki, J. M., 2011. *Significance of water distribution networks in water supply*. Social science research network.
- Nyende-Byakika, S., Ngirane-Katashaya, G., and Ndambuki, J. M., 2010. *Behaviour of stretched water supply networks*. Nile Water Science and Engineering Journal, Vol. 3(1).
- OECD, 2010. *Food and Agriculture: Current themes and results*. Report
- OECD, 2008. *Guidance on evaluating conflict and peace building activities*. Report.
- OECD, 2010. *Sustainable Management of Water Resources in Agriculture Sustainable Management of Water Resources in Agriculture*. Report.
- Ostfeld, A., 2011. *Ant Colony Optimization - Methods and Applications*. Published by InTech. Janeza Trdine, Vol. 9, 51000 Rijeka, Croatia.
- Ostfeld, A. and Tubaltzev, A., 2008. *Ant Colony Optimization for Least-Cost Design and Operation of Pumping Water Distribution Systems*. Journal of water resources planning and management © ASCE, pp. 107-118.
- Paly, M. and Zell, A., 2009. *Optimal irrigation scheduling with evolutionary algorithms*. Applications of Evolutionary Computing, Vol. 5484, pp. 142-151.
- Pham, V. T., Grundmann, J., Schütze, N., and Schmitz, G., 2012. *Multi-objective design of a*

- water distribution network using simulation-based optimization*. In 14th Water Distribution Systems Analysis Conference, Adelaide, Australia. American Society of Civil Engineers.
- Perelman, L., Krapivka, A., and Ostfeld, A., 2009. *Single and multi-objective optimal design of water distribution systems: application to the case study of the Hanoi system*. Water Science and Technology: Water Supply, pp. 395-404.
- Phocaides, A., 2000. *Technical handbook on pressured irrigation techniques*. Food and agriculture organization of the United Nations.
- Prasad, T.D., 2010. *Design of pumped water distribution networks with storage*. Journal of water resources planning and management, ASCE.
- Prasad, T. D. and Park, N., 2004. *Multi-objective Genetic Algorithms for Design of Water Distribution Networks*. Journal of Water Resources Planning and Management, Vol. 130, pp. 73-82.
- Raad, D., Sinskeb, A. and Vuurena, J. V., 2009. *Robust multi-objective optimization for water distribution system design using a meta-metaheuristic*. International transactions in operational research, pp. 595 – 626.
- Reca, J., Martínez, J., Gil, C. and Baños, R., 2008. *Application of Several Meta-Heuristic Techniques to the Optimization of Real Looped Water Distribution Networks*. Water Resource Manage, Vol. 22, pp.1367–1379.
- Reca, J , Martínez, J., Baños, R. and Gil, C., 2008. *Optimal Design of Gravity-Fed Looped Water Distribution Networks Considering the Resilience Index*. Journal of Water Resources Planning and Management, Vol. 134, No. 3, pp. 234–238.
- Reca, J. and Marti'nez, J., 2006. *Genetic algorithms for the design of looped irrigation water distribution networks*. Water Resources Research, Vol.42.
- Reddy, M. J. and Kumar, D. N., 2007. *Multi-objective particle swarm optimization for generating optimal trade-offs in reservoir operation*. Hydrological Process, Vol.21, p. 2897–2909.
- Rosmaini, E., 2010. *A Multi-stage stochastic optimization model for Water Resources Management*. Proceedings of the 6th IMT-GT Conference on Mathematics, Statistics and its Applications (ICMSA), Universiti Tunku Abdul Rahman, Kuala Lumpur, Malaysia, pp. 951-961.
- Salomons, E., Goryashko, A., Shamir, U., Rao, Z., and Alvisi, S., 2007. *Optimizing the operation of the Haifa-A water-distribution network*. Journal of Hydroinformatics.
- Sana, A., Baawain, M., and Al-Sabti, A., 2013. *Feasibility study of using treated wastewater to mitigate seawater intrusion along northern coast of Oman*. International Journal of Water Resources and Arid Environments, Vol. 3(2), pp. 56-63.
- Sarbu, I., 2011. *Nodal analysis model of looped water distribution networks*. ARPN Journal

- of Engineering and Applied Sciences, Vol. 6, No. 8, pp. 115-125.
- Savic, D. A., 2002. *Single-objective vs. Multi-objective Optimisation for Integrated Decision Support*, In: *Integrated Assessment and Decision*. CiteSeer.
- Savic, D. A., Walters, G. A., and Schwab, M., 1997. *Multi-objective Genetic Algorithms for Pump Scheduling in Water Supply*. Evolutionary computing, Lecture notes in computer science, Vol. 1305, pp. 227-235.
- Savic, D. and Walters, G., 1982. *Genetic algorithms for least cost design of water distribution networks*. Journal of water resource planning and management, Vol. 123, No. 2, pp. 67 – 77.
- Schmitz, G.H., Al Hattaly, S., Grundmann, J., and Schütze, N., 2010. *An integrated assessment, prognosis, planning and management tool (APPM) for sustainable aridzone water management*. The 9th Gulf Water Conference, Water Sustainability in the GCC Countries - The Need for a Socio-Economic and Environmental Definition, Sultanate of Oman.
- Schütze, N., Kloss, S., Lennartz, F., Bakri, A., and , Schmitz, G., 2012. *Optimal planning and operation of irrigation systems under water resource constraints in Oman considering climatic uncertainty*. Environ Earth Sci, Vol. 65, pp.1511–1521.
- Schütze, N., Paly, M., and Shamir, U., 2012. *Novel simulation-based algorithms for optimal open-loop and closed-loop scheduling of deficit irrigation systems*. Journal of hydroinformatics, Vol. 14, pp. 136-151.
- Setämaa-Kärkkäinen, A., Miettinen, K. and Vuori, J., 2006. *Best compromise solution for a new multi-objective scheduling problem*. Computers and Operations Research, Vol. 33, pp. 2353–2368.
- Shamir, U., 1974. *Optimal design and operation of water distribution system*. Water resource research, Vol. 10, No. 01, pp. 27-36.
- Shau, H.M., Lin, B.L., and Huang, W.H., 2005. *Genetic algorithms for design of pipe network systems*. Journal of Marine Science and Technology, Vol. 13, No. 2, pp. 116-124.
- Shibu, A. and Reddy, M. J., 2012. *Least cost design of WDNs under demand uncertainty by fuzzy - cross entropy method*. Journal of Environmental Research and Development, Vol. 6 No. 3A.
- Simpson, A., 2000. *Optimization of design of water distribution systems using genetic algorithms*. Acta hydrotechnica.
- Simpson, A. R., Dandy, G. C., and Murphy, L., 1994. *Genetic algorithms compared to other techniques for pipe optimization*. Journal of Water resource planning and management, Vol. 120, No. 4.
- Srinivas, N. and Deb, K., 1994. *Multi-objective optimization using nondominated sorting in*

- genetic algorithms*. Evolutionary computation, Vol. 2, No. 3, pp. 221 – 248.
- Sun, S., Khu, T., Kapelan, Z., and Djordjevic, S., 2011. *A fast approach for multi-objective design of water distribution networks under demand uncertainty*. Journal of Hydroinformatics, Vol.13, pp.143 – 152.
- Sunantara, J. and Rami'res, J. A., 1997. *Optimal stochastic multicrop seasonal and intraseasonal irrigation control*. Journal of water resources planning and management, Vol. 123, No. 1, pp. 39 - 48.
- Suribabu, C. R., 2010. *Differential evolution algorithm for optimal design of water distribution networks*. Journal of Hydroinformatics, Vol.12, pp. 66-82.
- Suribabu, C. R. and Neelakantan, T. R., 2006. *Particle swarm optimization compared to other heuristic search techniques for pipe sizing*. Journal of Environmental Informatics, Vol. 8, pp. 1-9.
- Sánchez, G., Felici, S., Pelechano, J., Pelegri, J., and PCrez, J., 1999. *Optimal design of irrigation networks using genetic algorithm*. IEEE.
- Sâbru, I. and Klamár, F., 2002. *Optimization of looped water supply networks*. Periodical Polytechnical Ser. Mech. Eng. Vol. 46, No. 1, pp. 75–90.
- Tanyimboh, T. and Setiadi, Y., 2008. *Joint layout, pipe size and hydraulic reliability optimization of water distribution systems*. Engineering Optimization, Vol. 40, No. 8, pp. 729–747.
- Tarquin, A.J. and Dowdy, J., 1989. *Optimal Pump Operation in Water Distribution*. Journal of Hydraulic Engineering, Vol. 115, No. 2, pp. 158-168.
- Theocharis, M., Tzimopoulos, C., Yannopoulos, S., and Sakellariou-Makrantonaki, M., 2005. *Optimal design of irrigation networks using the dynamic method and a simplified nonlinear method*. Proceedings of the 5th WSEAS Int. Conf. on simulation, modeling and optimization, Corfu, Greece, pp. 384-390.
- The U.S. Department of Energy's Industrial Technologies Program and the Hydraulic Institute (ITP and HI), 2006. *Improving Pumping System Performance: A Sourcebook for Industry*. Second Edition.
- Todini, E., 2000. *Looped water distribution networks design using a resilience index based heuristic approach*. Urban Water, Vol. 2, pp. 115 – 122.
- Tolson, B., Maier, H., Simpson, A.R., and Lence, B., 2004. *Genetic algorithms for reliability-based optimization of water distribution systems*. Journal of Water Resources Planning and Management, Vol. 130(1), pp. 63– 72.
- Vamar, K., Narasimhan, S., and Bhallamudi, S.M., 1997. *Optimal design of water distribution network using an NLP method*. Journal of Environmental Engineering. Vol 123, No. 04, pp. 381 – 388.

- Vamvakieridou-Lyroudia, L. S., Savic, D. A., and Walters, G. A., 2007. *Tank Simulation for the Optimization of Water Distribution Networks*. Journal of Hydraulic Engineering, Vol.133, No. 6, pp. 625–636.
- Vasan, A. and Simonovic, S. P., 2010. *Optimization of water distribution network design using differential evolution*. Journal of Water Resources Planning and Management, Vol. 136, No. 2, pp. 279–287.
- Vrugt, J.A. and Robinson, B.A., 2007. *Improved evolutionary optimization from genetically adaptive multimethod search*. PNAS, Vol. 104, No. 3, pp. 708-711.
- Walski et al., 2003. *Advanced water distribution modeling and management*. Bentley Institute press.
- Walters, G.A. and Lohbeck, T., 1993. *Optimal layout of tree networks using genetic algorithms*. Eng. Opt. Vol. 22. pp. 27-48.
- Walters, G. A., Halhal, D., Savic, D., and Ouazar, D., 1999. *Improved design of "Anytown" distribution network using structured messy genetic algorithms*. Urban Water, Vol. 1, pp. 23-38.
- Walther, M., Delfs, J., Grundmann, J., Kolditz, O., and Liedl, R. 2011. *Salt water intrusion modeling: Verification and application to an agricultural coastal arid region in Oman*. Journal of Computational and Applied Mathematics, Vol. 236, pp. 4798–4809.
- Wardlaw, B. and Barnes, J., 1999. *Optimal allocation of irrigation water supplies in real time*. Journal of Irrigation and Drainage Engineering, Vol. 125, No. 6, pp 345–354.
- Weise, T., 2008. Global optimization algorithms: Theory and Application<sup>1</sup>.
- Werisch, S., Grundmann, J., Al-Dhuhli, H., Algharibi, E. and Lennartz, F., 2013. *A multi-objective framework for robust parameter estimation of soil hydraulic properties and its application for a field site in Oman*. TU Dresden, Institute of Hydrology and Meteorology.
- Woldesenbet, Y.G., and Tessema, B.G., and, Yen, G.G, 2007. *Constraint handling in multi-objective evolution optimization*. IEEE, pp. 3070 – 3084.
- Wu, Z. Y. and Simpson, A. R., 2001. *Competent Genetic-Evolutionary Optimization Of Water Distribution Systems*. Journal of Computing in Civil Engineering, ASCE, Vol.15, No.2, pp. 89-101.
- Wöhling, T., Vrugt, J. A. and Barkle, G. F., 2008. *Comparison of three multi-objective optimization algorithms for inverse modeling of vadose zone hydraulic properties*. SSSAJ: Vol. 72, Number 2.

---

<sup>1</sup> <http://www.it-weise.de/>.

- Xu, C. and Goulter, I.C., 1999. *Reliability-Based Optimal Design of Water Distribution Networks*. Journal of Water Resources Planning and Management, Vol. 125, No. 6, pp. 352-362.
- Yeniay, Ö., 2005. *Penalty function methods for constrained optimization with genetic algorithms*. Mathematical and Computational Applications, Vol. 10, No. 1, pp. 45-56.
- Yoshizumi, T. and Okano, H., 2007. *A simulation-based algorithm for supply chain optimization*. IEEE Proceedings of the 2007 winter simulation conference.
- Zecchin, A.C., Maier, H.G., Simpson, A.R., Leonard, M., and Nixon, J.B., 2007. *Ant colony optimization applied to water distribution system design: Comparative study of five algorithms*. Journal of water resource planning and management ASCE, pp. 87-92.





## LIST OF FIGURES

Figure 2.1: A simple branched PWDN including a reservoir, a pump, a tank, 3 nodes, and 3 pipes.....	6
Figure 2.2: A simple looped PWDN including a reservoir, a pump, a tank, 4 nodes, and 5 pipes.....	6
Figure 2.3: A typical pump curve along with system curve (Mays, 2000) .....	10
Figure 2.4: An outline of non-linear impact of various pipe diameter on nodal pressure (m), flow velocity (m/s), and unit head-loss (m/km) .....	10
Figure 2.5: Non-linear impact of various flows on nodal pressure (m), flow velocity (m/s), and head-loss (m/km) in a constant pipe diameter of 1016mm. ....	10
Figure 2.6: Outline of the Epanet capability (Rossman, 2000) .....	10
Figure 3.1: A typical optimization formulation procedure (Walski et al., 2003).....	17
Figure 3.2: Total cost of a PWDN as an objective function of pipe diameter (Lock et al., 2000).....	19
Figure 3.3: Pareto solutions (Walski et al., 2003) .....	20
Figure 3.4: A basic simulation-based optimization method based on Mays (2000) .....	30
Figure 4.1: The outline of the simulation-based CMA-ES optimization approach.....	38
Figure 4.2: The basic flowchart of simulation-based single optimization CMA-ES-EP .....	41
Figure 4.3: The basic flowchart of simulation-based multi-objective optimization (MO-CMA-ES-EP).....	42
Figure 4.4: General CMAES procedure flow chart.....	44
Figure 4.5: Illustration for the measure of determining the best compromise solution from the Pareto optimal front.....	50
Figure 4.6: Procedure for evaluating robustness probability of PWDN optimal design under demand uncertainty.....	53
Figure 5.1: Layout and nodal demands of the two - loop benchmark network.....	56
Figure 5.2: Convergence of norm-decision variables of TLN optimization with popsize 3....	58
Figure 5.3: Nodal pressures (a) and velocities in pipes (b) produced by optimal solution .....	59
Figure 5.4: Hanoi water network layout representing nodes and pipes.....	61
Figure 5.5: The convergence of decision variables of Hanoi with popsize 3.....	62

Figure 5.6: (a) Pattern of demand multiplies for an operation scheduling and (b) time series of nodal pressures corresponding to multi demand loadings of TLN. ....	63
Figure 5.7: (a) Basic layout for Benchmark network No.3 and three optimal layouts representing pipe diameters and nodal pressures obtained by (b) Geem et al., (c) Afshar and Jabbari, and (d) current study. ....	66
Figure 5.8: (a) Pipes and nodes of the predefined maximum layout and (b) the simplest layout achieved by CMA-ES-EP without any additional required layout reliability. ....	65
Figure 5.9: Different optimal layout solutions representing pipe diameters and nodal pressures obtained with required reliability level 1 by using (a) GA and (b) CMA-ES-EP. ....	68
Figure 5.10: Different layout solutions representing pipe diameters and nodal pressures achieved with required layout reliability level 2 by different methods. ....	69
Figure 5.11: Layout representing pipes, pumps, nodes, tank, and reservoirs for Benchmark network No.5. ....	72
Figure 5.12: Time series of tank water levels obtained by (a) Ostfeld and Tubaltzev using AOCA and (b) current study using CMA-ES-EP approach. ....	73
Figure 5.13: Network layout representing pipes, pumps, nodes, tank, and reservoirs for benchmark network No.6 (Ostfeld and Tubaltzev, 2008). ....	74
Figure 5.14: Average silhouette values corresponding to the number of clusters with respect to TLN Pareto data ....	76
Figure 5.15: Three corresponding centroid solutions (yellow cross) and the best compromise solution (red circle) on the TLN optimal front ....	77
Figure 5.16: Comparison of the Pareto solutions obtained by AMALGAM (red crosses) and MO-CMA-ES-EP (blue circles) with respect to the two-loop network optimal design ....	78
Figure 17: Average silhouette values corresponding to five clusters from Hanoi Pareto data	79
Figure 5.18: Five corresponding centroid solutions (yellow cross) and the best compromise solution (red circle) on the Hanoi Pareto optimal front ....	79
Figure 5.19: Comparison of the Pareto solutions obtained by AMALGAM (red crosses) and MO-CMA-ES-EP (blue circles) with respect to the Hanoi network optimal design. ....	80
Figure 5.20: Five corresponding centroid solutions (yellow cross) and the best compromise solution (red circle) derived from the Pareto solutions of Benchmark network No.4 optimization with the required layout reliability level 1 ....	81
Figure 5.21: Different configurations specifying pipe diameters and nodal pressures of the Benchmark No.4 optimization under the required layout reliability level 1 ....	83
Figure 5.22: Six corresponding centroid solutions (yellow cross) and the best compromise solution (red circle) derived from the Pareto solutions. ....	84

Figure 5.23: Different configurations representing pipe diameters and nodal pressures of the Benchmark No.4 under the required layout reliability level 2.....	85
Figure 5.24: Robustness probabilities (RP) corresponding to two assumptions of standard deviations (case 1 and 3) for five representative solutions of (a) TLN and (b) HN network...	87
Figure 5.25: The comparison of robustness probabilities under uncertain uncorrelated and correlated demands (Case 1 and Case 3) for five representative solutions of (a) TLN and (b) HN network. ....	88
Figure 6.1: Study area.....	90
Figure 6.2: Cropping pattern in the study area in 1994 (Volume 1 - MAF, 1994) .....	92
Figure 6.3: Global cropping pattern in the Batinah area in 2004 (Agriculture Census, 2004) .....	92
Figure 6.4: The irrigation method applied in the study area (Agriculture Census, 2004).....	93
Figure 6.5: Proposed scenario cropping pattern in the study area (SA: Sub-area).....	94
Figure 6.6: Demand diagram in the study area.....	95
Figure 6.7: Distribution of irrigation water demand in the study area.....	96
Figure 6.8: The backbone network layout representing nodes, tanks, and wells locations....	101
Figure 6.9: The significant solutions on the Pareto front achieved from backbone design and operation optimization.....	103
Figure 6.10: Hourly pumped volume and demand corresponding to the best compromise solution with respect to the backbone network .....	104
Figure 6.11: The PML representing pipes and pumps .....	105
Figure 6.12: The significant solutions on the Pareto front obtained from the predefined maximum layout network design and operation optimization .....	106
Figure 6.13: Hourly pumped volume and demand corresponding to the best compromise solution with respect to the predefined maximum layout .....	107
Figure 14: Water level in tanks during a 24-hour operating cycle corresponding to the best compromise solution with respect to (a) the backbone network and (b) the predefined maximum network.....	108
Figure 6.15: Robustness probability corresponding to uncertain uncorrelated and correlated demands of (a) backbone Pareto solutions and (b) PML Pareto solutions.....	109



## LIST OF TABLES

Table 4.1: Notable parameters need to be defined for CMA-ES model.....	45
Table 5.1: Optimization results obtained by CMA-ES-EP for TLN network with N = 8 .....	57
Table 5.2: Comparison of optimization results for the two-loop network .....	58
Table 5.3: Selected parameters for the model .....	60
Table 5.4: Population size and optimization results for testing model with Hanoi network....	59
Table 5.5: Comparison of optimization results for the Hanoi network. ....	61
Table 5.6: Solutions obtained with different approaches for benchmark network 4 .....	69
Table 5.7: Comparison of optimal cost solutions obtained by ACOA and CMA-ES-EP .....	72
Table 5.8: Comparison of optimal pump powers .....	73
Table 5.9: Several representative solutions for TLN produced by MO-CMA-ES-EP .....	77
Table 5.10: Representative solutions for Hanoi network produced by MO-CMA-ES-EP.....	79
Table 5.11: Comparison of the minimum cost solutions obtained by AMALGAM and MO-CMA-ES-EP .....	80
Table 5.12: Robustness probability under uncertain uncorrelated demands corresponding to five different cost solutions and different samples (a:1,000 samples; b: 10,000 samples, and c: 100,000 samples) .....	86
Table 6.1: Estimated average monthly temperature (T), rainfall, evapotranspiration (ET), and humidity (H) for South Batinah region (Volume 1 –MAF, 1994) .....	91
Table 6.2: Water requirements for the proposed scenario (Mi.m <sup>3</sup> ) .....	95
Table 6.3: Pipe cost data.....	98
Table 6.4: Demanded multiplier and energy tariff (\$/kWh).....	100



## APPENDIX

Appendix A: Conservation laws of mass and energy for PWDN

Appendix B: Several main CMA-ES-EP matlab codes

Appendix C: Benchmark network

Appendix D: Real world case study (The Southern Batinah region)





## Appendix A: Laws of conservation of mass and energy for PWDN

### (i) Conservation of mass (continuity equation)

The continuity equation at a node ensures that the flows entering are equal to the flows leaving that node. Hence, the continuity equation at each node  $j$ ,  $j = 1, 2, \dots, nn$  ( $nn$ : number of nodes in the PWDN) may be written as:

$$\sum_{\text{connected\_to\_}j} Q_{j\_in} = \sum_{\text{connected\_to\_}j} Q_{j\_out} + q_j^{req} \quad (2.1)$$

where  $Q_{j\_in}$  and  $Q_{j\_out}$  are the flows in and out connected to node  $j$  directly, and  $q_j^{req}$  is the required demand at node  $j$ .

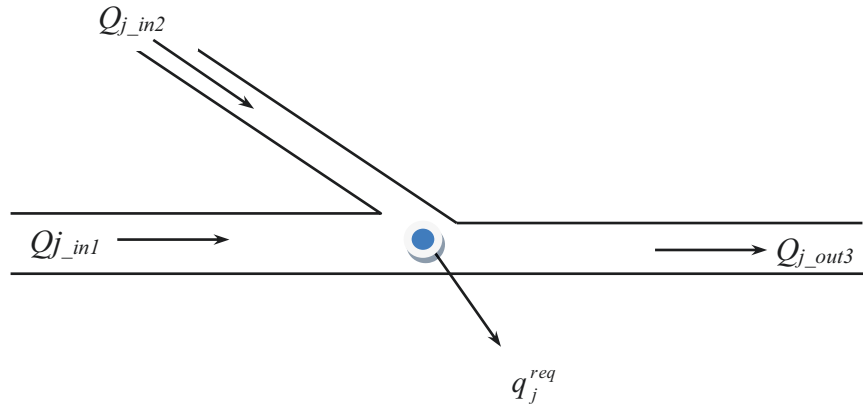


Figure A.1: Illustration of conservation of mass principle at a demand node

### (ii) Conservation of energy

The difference in energy between two points must be equal to the summation of major and minor head losses and the energy added or extracted between these points (Eq. 2.2):

$$E_1 + \sum h_m = E_2 + \sum h_{L_{1-2}} \quad (2.2)$$

where:  $\text{Energy } E = z + \frac{p}{\gamma} + \frac{v^2}{2g}$  (2.3)

$z$ ,  $\frac{p}{\gamma}$ ,  $\frac{v^2}{2g}$  are the elevation head or potential energy, pressure head, and velocity head, respectively

$\sum h_{L_{1-2}}$  is the total head loss in the pipe caused by major and minor losses between two points (1) and (2);

$\sum h_m$  is the head added by pump.

Summation of head losses over any loop must be equal to zero since the loop begins and ends at the same node:

$$\sum_{loop\_c} h_c = 0 \quad (2.4)$$

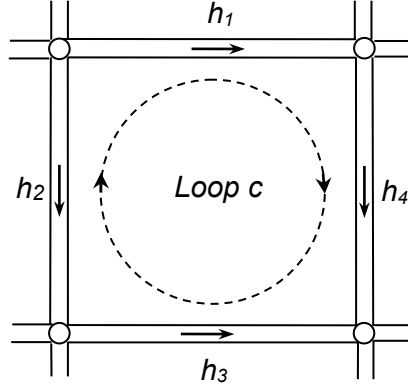


Figure A.2: Illustration for the law of conservation of energy,  $h_1 - h_2 - h_3 + h_4 = 0$ , in which head losses are positive if having the same direction with assumed loop direction, otherwise, negative (Bhave, 1991).

(iii) Major head loss

This type of head loss is caused by friction force regarding flow within a pipe system; hence, it is often called friction head loss. There are several friction head loss relationships with flow and head that have been used in the past. These relationships can be expressed under the general form (Eq. 2.5):

$$h_{ij} = |H_i - H_j| = K_{ij} \cdot Q_{ij}^n \quad (2.5)$$

where

$h_{ij}$  is the friction head loss in pipe  $ij$ , which connects node  $i$  and node  $j$

$H_i, H_j$  are the pressure head at node  $i$  and  $j$

$K_{ij}$  is the resistance coefficient for pipe  $ij$

$Q_{ij}$  is the discharge in pipe  $ij$

$n$  is an exponent

The values of  $K_{ij}$  and  $n$  depend on the nature of the head loss formula used. Three notable forms of head loss relationship, namely, Darcy-Weisbach, Hazen-Williams and Chezy-Manning formula (Bhave, 1991) have been widely used.

\* The Darcy-Weisbach formula expresses the head loss ( $h_{ij}$ ) in a pipe as:

$$h_{ij} = \frac{8 \cdot f_{ij} \cdot L_{ij}}{g \cdot \pi^2 \cdot D_{ij}^5} \cdot Q_{ij}^2 \quad (2.6)$$

where

$f_{ij}$  is the friction coefficient of a pipe, which is function of Reynolds number and relative roughness ( $r_{ij}/D_{ij}$ ) and can be obtained from the Moody's diagram (Bhave, 1991).

$L_{ij}$  is length of the pipe  $ij$

$D_{ij}$  is diameter of the pipe  $ij$

An obstacle with regard to the Darcy-Weisbach formulation is the interdependence of friction roughness  $f_{ij}$  and flow  $Q_{ij}$ . Hence, they need to be calculated simultaneously.

\* The Hazen-William formula:

$$h_{ij} = \frac{10.68 L_{ij}}{C_{HW}^{1.852} D_{ij}^{4.87}} \cdot Q_{ij}^{1.852} \quad (2.7)$$

where  $C_{HW}$  is Hazen-William coefficient of pipe  $ij$ , that is given according to different pipe diameters and materials (Bhave, 1991). Although it is an empirical equation, it is widely applied in the fields of water supply engineering.

\* The Manning head loss formula is likewise an empirical relationship (Eq. 2.8). It works accurately for rough surfaces, and, therefore, is well suited for open channel flow rather than pipe flow.

$$h_{ij} = \frac{10.29 N^2 L_{ij}}{D^{16/3}} \cdot Q_{ij}^2 \quad (2.8)$$

where  $N$  is Manning roughness coefficient for different pipe materials (Bhave, 1991).

(iv) *Minor head loss*

Minor head loss in pipes occurs when the pattern of flow in pipe changes due to a local obstruction, such as valve, bend, and other appurtenances within the pipe, or due to sudden or gradual change in the pipe diameter such as sudden or gradual enlargement, and contraction. The minor head loss  $h_m$  is demonstrated in terms of velocity as follows:

$$h_m = K_m \cdot \frac{v^2}{2g} \quad (2.9)$$

where

$v$  is average flow velocity in the pipe before the element causing head loss (m/s)

$K_m$  is minor head loss coefficient.  $K_m$  value depends on both diameter ratios before and after the minor head loss element and velocity in case of a sudden change. In case of gradual change,  $K_m$  depends on the angle of enlargement or contraction.

**Appendix B: Several main CMA-ES-EP matlab codes***Input:*

- Epanet input data file (\*.INP) provides information about the needed contents mentioned in Figure 2.6

- Pipe data: available commercial diameters (DAVL) and corresponding cost (Cdavl)

- Other inputs such as constraints (required minimum pressure (Hmin), maximum velocity (vmax), etc...), penalty factor ( $\alpha_p$ )

%% Start optimization

load initial\_settings % load options - opts, initial means - xini, and standard deviation - sig

[XMIN FMIN] = cmaes('objective\_function name',xini,sig,opts) % execute CMA-ES

%% denormalize decision variables (PAR) and assign pipe diameter from diameter set

for i=1:length(DAVL)

    dset(i) = i \* 1/length(DAVL);

end

for i = 1:length(PAR(1:(number of pipes)))

    j = 1;

    while (PAR(i) > dset(j))

        j = j + 1;

    end

    PAR(i) = DAVL(j);

end

%% Load and write Epanet network file

ep.netfile = 'filename.inp'; % epanet network description file

ep.tplfile = 'filename.tpl'; % template network description file

asciireplace(ep.netfile, ep.tplfile, PAR) % read & replace description files

epanetloadfile(ep.netfile); % load and simulate the \*.inp file

[net,nodetypes,linktypes] = ep\_getnet(ep.netfile); % analyze network

[ep.d\_N] = getdata('EN\_DEMAND'); % get nodal demands

[ep.P] = getdata('EN\_PRESSURE'); % get nodal pressures

[ep.Q] = getdata('EN\_FLOW'); % get flows

```
[ep.v] = getdata('EN_VELOCITY');          % get velocities
[ep.h] = getdata('EN_HEADLOSS');          % get head loss
[ep.Status] = getdata('EN_STATUS');        % get status of links
[ep.energy] = getdata('EN_ENERGY');        % get network energy

epanetclose();                            % close the simulation

%% Penalty function for head constraint

Cpen = 0;

for i = 1:(number of demand nodes)
    if ep.Hmin(i) > H(i)    % check required nodal pressure constraints
        Cpen = Cpen +  $\alpha_p * ((H(\text{mini}) - H(i)) / (H(\text{mini})))^2$ ; % penalty function
    end
end

end

%% Get objective function (Cost)

CS = 0;

for i = 1:(number of decision variables)
    idx10 = find(DAVL(:) == PAR(i));      % find corresponding PAR index
    CS = CS + (LP(i)*Cdavl(idx10));        % Cost function
end

end
```

## Appendix C: Benchmark network data

### Appendix C.1: Benchmark network No.1 (Two-loop network)

Two-loop network consists of 8 pipes, 6 junction nodes and is supplied by a single elevated reservoir.

#### Appendix C.1.1: Nodal characteristics

Node	Demand (m <sup>3</sup> /h)	Elevation (m)
1	-1200	210
2	100	150
3	100	160
4	120	155
5	270	150
6	330	165
7	200	160

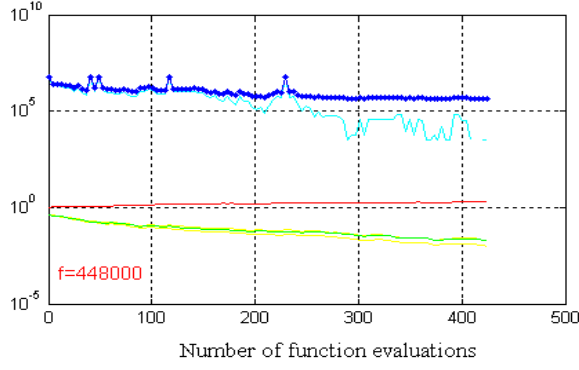
#### Appendix C.1.2. Available commercial cost

Diameter (mm)	25.4	50.8	76.2	101.6	152.4	203.2	254	304.8	355.6	406.4	457.2	508	558.8	609.6
Cost(\$/m)	2	5	8	11	16	23	32	50	60	90	130	170	300	550

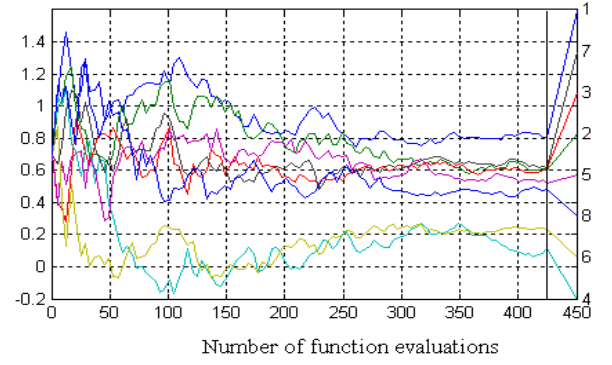
*Appendix C.1.3: The convergence of decision variables of two-loop network with different population sizes.*

(a)  $\text{popsize} = \text{floor}(2 * \log(N))$

Abs(f) Blue, f-min(f) (cyan), Sigma(green), Axis Ratio(red)

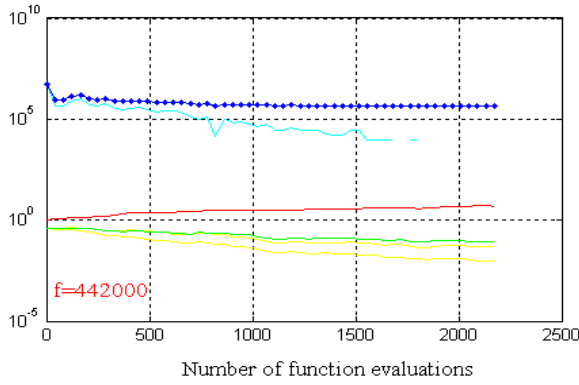


Objective variables (8D)

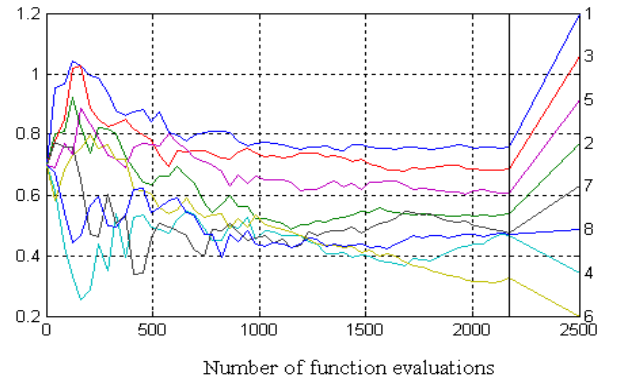


(b)  $\text{popsize} = \text{floor}(20 * \log(N))$

Abs(f) Blue, f-min(f) (cyan), Sigma(green), Axis Ratio(red)

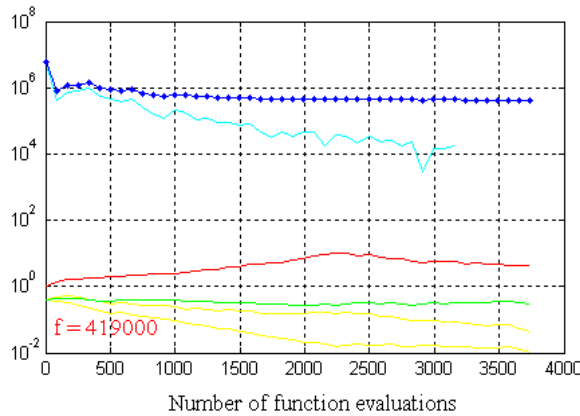


Objective variables (8D)

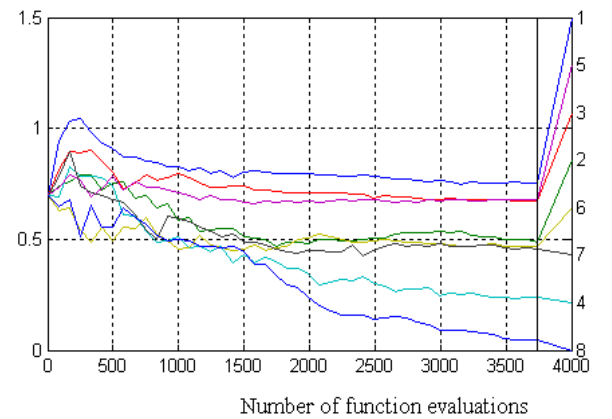


(c)  $\text{popsize} = \text{floor}(40 * \log(N))$

Abs(f) Blue, f-min(f) (cyan), Sigma(green), Axis Ratio(red)

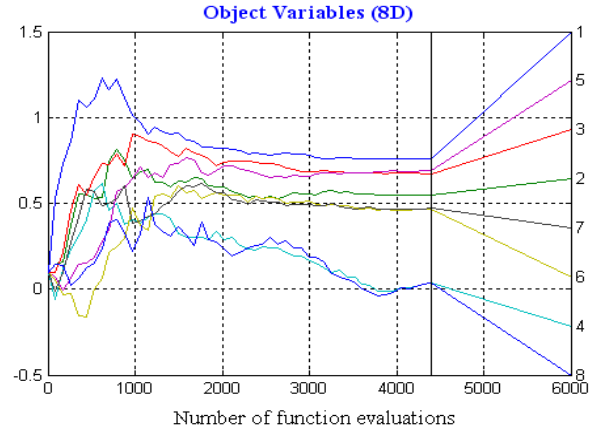
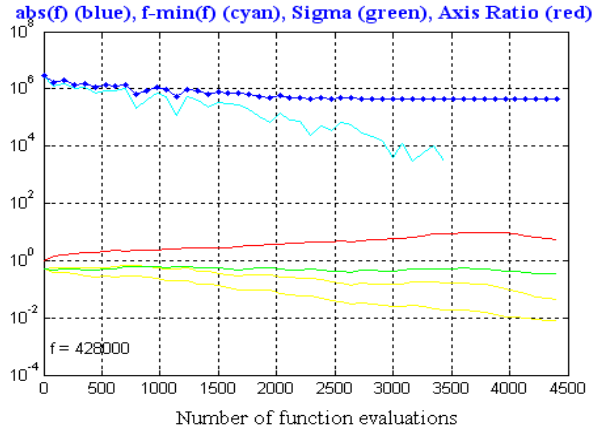


Objective variables (8D)

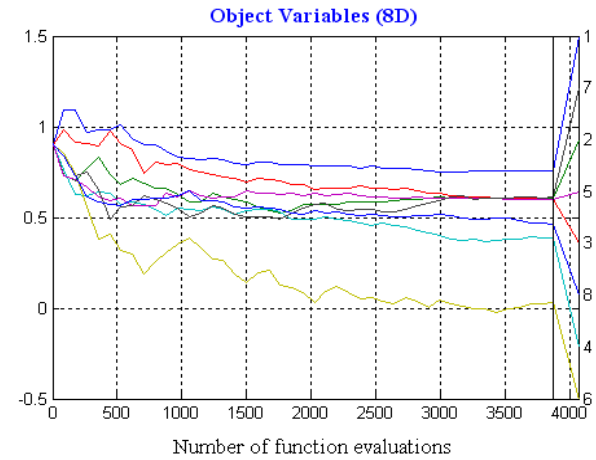
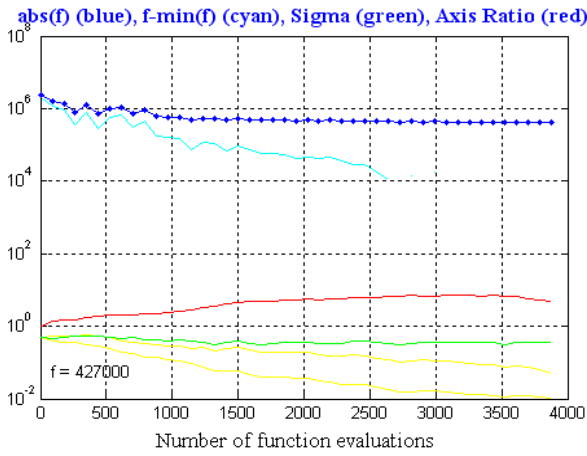


*Appendix C.1.4: Performance of the CMA-ES-EP model with different normalized initial decision variables ( $x_{ini}$ )*

(a)  $x_{ini} = 0.1$



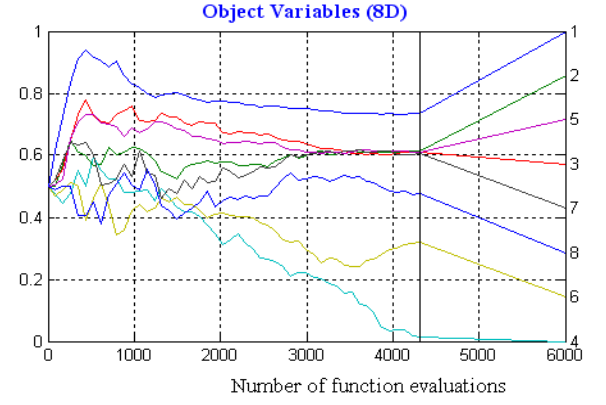
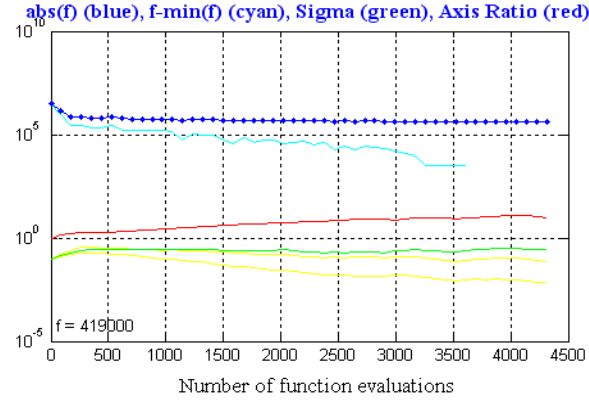
(b)  $x_{ini} = 0.9$



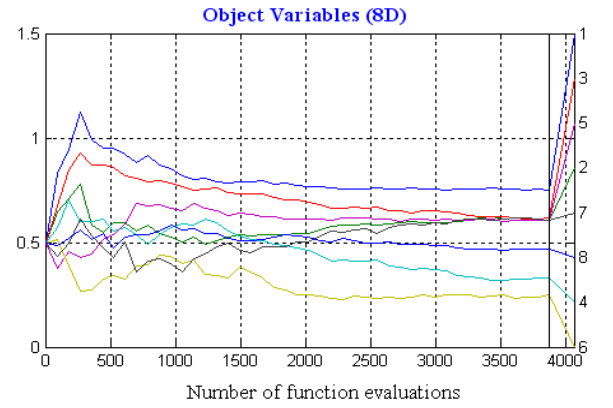
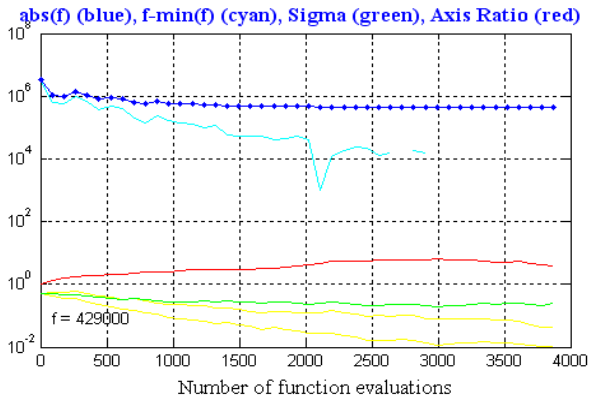


*Appendix C.1.5: Performance of the CMA-ES-EP model with different standard deviation ( $\sigma$ )*

(a)  $\sigma_x = 0.1$



(b)  $\sigma_x = 0.9$



*Appendix C.1.6: Comparison of optimization results for TLN produced by CMA-ES-EP*

Pipe \ Method	(1)		(2)	(3)	(4)	(5)	(6)	(7)	(8)
	LPG		CRS2	GA	ACCOL	GEO	GANEO	ACOA	CMA-ES-EP
	L (m)	D (mm)							
1	256 744	508 457.2	457.2	457.2	558.8	457.2	457.2	457.2	457.2
2	996.38 3.62	203.2 152.4	254	355.6	457.2	254	254	254	254
3	1000	457.2	406.4	355.6	508	406.4	406.4	406.4	406.4
4	319.38 680.62	203.2 152.4	101.6	25.4	76.2	101.6	101.6	101.6	101.6
5	1000	406.4	406.4	355.6	406.4	406.4	406.4	406.4	406.4
6	784.94 215.06	304.8 254	254	25.4	101.6	254	254	254	254
7	1000	152.4	254	355.6	457.2	254	254	254	254
8	990.93 9.07	152.4 101.6	50.8	304.8	406.4	25.4	25.4	25.4	25.4
Cost (\$)	497,525		422,000	424,000	447,000	419,000	419,000	419,000	419,000

*Appendix C.1.7: Maximum solutions with five network reliability definitions for TLN.*

D1 (mm)	D2 (mm)	D3 (mm)	D4 (mm)	D5 (mm)	D6 (mm)	D7 (mm)	D8 (mm)	Cost (\$. $10^6$ )	MSHI	TSHI	RI	NR	PUC
(1) Maximize minimum surplus head index (MSHI)													
609.6	609.6	609.6	25.4	609.6	25.4	609.6	609.6	3.304	12.8559	127.0719	0.9002	0.6223	0.8773
(2) Maximize total surplus head index (TSHI)													
609.6	609.6	609.6	609.6	609.6	203.2	609.6	609.6	3.873	12.7000	127.5184	0.9038	0.8007	0.8786
(3) Maximize resilience index (RI)													
609.6	609.6	609.6	609.6	609.6	609.6	609.6	609.6	4.400	12.7292	127.5159	0.9038	0.9038	0.8786
(4) Maximize network resilience (NR)													
609.6	609.6	609.6	609.6	609.6	609.6	609.6	609.6	4.400	12.7292	127.5159	0.9038	0.9038	0.8786
(5) Maximize pressure uniformity coefficient (PUC)													
609.6	609.6	609.6	609.6	609.6	203.2	609.6	609.6	3.873	12.7000	127.5184	0.9038	0.8007	0.8786

*Appendix C.1.8: Representative solutions of TLN produced by MO-CMA-ES-EP*

<div>Solution Pipe</div>	Minimum cost solution	Centroid of cluster 3	Centroid of cluster 2	Best compromise solution	Centroid of cluster 1
1	457.2	508	508	558.8	558.8
2	254	355.6	406.4	355.6	508
3	406.4	406.4	457.2	508	508
4	101.6	254	355.6	355.6	457.2
5	406.4	355.6	355.6	406.4	457.2
6	254	101.6	355.6	355.6	406.4
7	254	254	355.6	355.6	457.2
8	25.4	254	355.6	355.6	406.4
Cost (\$)	419,000	487,000	690,000	860,000	1,210,000
NR	0.1535	0.4153	0.6418	0.7251	0.7874

*Appendix C.1.9: TLN robustness probabilities in case of uncertain correlated demands*

Solutions	Cost (\$)	Network reliability	Robustness probability with demand uncertainty (%)
Solution 1	419,000	0.1535	47.00
Solution 2	487,000	0.4153	79.66
Solution 3	690,000	0.6417	100
Solution 4	860,000	0.7251	100
Solution 5	1,220,000	0.7925	100

*Appendix C.1.10: Errors between the rank correlation matrix and the desired correlation matrix*

Solutions	Node 2	Node 3	Node 4	Node 5	Node 6	Node 7
Solution 1	0.0013	0.0017	0.0009	0.0017	0.0011	0.0017
Solution 2	0.0013	0.0010	0.0009	0.0008	0.0008	0.0015
Solution 3	0.0010	0.0015	0.0011	0.0018	0.0019	0.0011
Solution 4	0.0005	0.0007	0.0012	0.0017	0.0017	0.0019
Solution 5	0.0008	0.0011	0.0010	0.0018	0.0021	0.0022

**Appendix C.2: Benchmark network No.2 (Hanoi network)**

Hanoi network consisting of 34 pipes, 32 nodes, and 3 loops which is supplied by a single fixed head source at an elevation of 100 m

*Appendix C.2.1: Available commercial cost data*

Pipe options	Diameter		Cost (\$/m)
	(inches)	(mm)	
1	12	304.80	45.73
2	16	406.40	70.4
3	20	508.00	98.39
4	24	609.60	129.33
5	30	762.00	180.75
6	40	1016.00	278.28

*Appendix C.2.2: Nodal characteristics*

Node ID	Elevation (m)	Demand (m <sup>3</sup> /hr)	Minimum Pressure	Node ID	Elevation (m)	Demand (m <sup>3</sup> /hr)	Minimum Pressure
1	100	-19616	---	17	0	865	30
2	0	890	30	18	0	1345	30
3	0	850	30	19	0	60	30
4	0	130	30	20	0	1275	30
5	0	725	30	21	0	930	30
6	0	1005	30	22	0	485	30
7	0	1350	30	23	0	1045	30
8	0	550	30	24	0	820	30
9	0	525	30	25	0	170	30
10	0	525	30	26	0	900	30
11	0	500	30	27	0	370	30
12	0	560	30	28	0	290	30
13	0	940	30	29	0	36	30
14	0	615	30	30	0	360	30
15	0	280	30	31	0	105	30
16	0	310	30	32	0	805	30

*Appendix C.2.3: Pipe characteristics*

Pipe	From node	To node	Length (m)	H-W factor	Pipe	From node	To node	Length (m)	H-W factor
1	1	2	100	130	18	19	18	800	130
2	2	3	1350	130	19	3	19	400	130
3	3	4	900	130	20	3	20	2200	130
4	4	5	1150	130	21	20	21	1500	130
5	5	6	1450	130	22	21	22	500	130
6	6	7	450	130	23	20	23	2650	130
7	7	8	850	130	24	23	24	1230	130
8	8	9	850	130	25	24	25	1300	130
9	9	10	800	130	26	26	25	850	130
10	10	11	950	130	27	27	26	300	130
11	11	12	1200	130	28	16	27	750	130
12	12	13	3500	130	29	23	28	1500	130
13	10	14	800	130	30	28	29	2000	130
14	14	15	500	130	31	29	30	1600	130
15	15	16	550	130	32	30	31	150	130
16	17	16	2730	130	33	32	31	860	130
17	18	17	1750	130	34	25	32	950	130

*App. C.2.4: Comparison among five representative solutions achieved by MO-CMAES-EP*

Solution Pipe	Centroid of cluster 2	Centroid of cluster 1	Best compromise	Centroid of cluster 4	Centroid of cluster 5
1	40	40	40	40	40
2	40	40	40	40	40
3	40	40	40	40	40
4	40	40	40	40	40
5	40	40	40	40	40
6	40	40	40	40	40
7	40	40	40	40	40
8	30	30	30	30	40
9	30	30	30	30	30
10	30	30	30	30	30
11	24	24	24	24	30
12	20	20	24	24	24
13	16	12	24	24	30
14	20	20	24	24	30
15	20	20	24	30	30
16	40	40	40	40	40
17	40	40	40	40	40
18	40	40	40	40	40
19	40	40	40	40	40
20	40	40	40	40	40
21	24	24	24	24	40
22	20	20	24	24	40
23	24	30	30	40	40
24	16	16	24	30	40
25	12	12	16	24	30
26	24	24	24	20	24
27	24	24	24	20	24
28	30	30	30	30	30
29	12	16	16	16	20
30	12	12	12	12	16
31	12	12	12	12	16
32	12	12	12	12	16
33	12	12	16	16	24
34	20	20	24	20	24
Cost (Mi.\$)	6.4504	6.6039	6.9822	7.3438	8.2901
NR	0.279	0.295	0.3163	0.3324	0.3558

*Appendix C.2.5: Robustness probability under uncertain uncorrelated demands corresponding to different cost solutions for Hanoi network (1,000 samples)*

Solutions	Cost (Mi.\$)	Network reliability	Robustness probability with demand uncertainty (%)	
			Case 1: $\sigma = 0.1\mu$	Case 2: $\sigma = 0.3\mu$
Solution 1	6.3697	0.2703	46.3	37.6
Solution 2	6.6538	0.2996	50.7	47.3
Solution 3	7.2271	0.3268	99.9	81.0
Solution 4	7.8922	0.3495	100	87.4
Solution 5	8.6149	0.3601	100	96.2

*Appendix C.2.6: Robustness probabilities in case of uncertain correlated demands (case 3)*

Solutions	Cost (Mi.\$)	Network reliability	Robustness probability with demand uncertainty (%)
Solution 1	6.3697	0.2703	48.4
Solution 2	6.6538	0.2996	50.9
Solution 3	7.2271	0.3268	85.0
Solution 4	7.8922	0.3495	89.8
Solution 5	8.6149	0.3601	96.9

***Appendix C.3: Benchmark network No.3 (Geem et al. s' network)***

This network proposed by Geem et al. (2000) consists of one reservoir at an altitude of 50 m, 8 demand nodes at an altitude of 0 m, and 12 interconnected pipes with the length of 100 m

***Appendix C.3.1: Nodal demand and elevation data***

Node	1	2	3	4	5	6	7	8	9
Demand (l/s)	10	20	10	20	10	20	10	20	-120

***Appendix C.3.2: Cost data***

Diameter (mm)	80	100	120	140	160	180	200	220	240	260	280	300	320
Cost (units/m)	23	32	50	60	90	130	170	300	340	390	430	470	500



***Appendix C.4: Benchmark network No.4 (Part of the Winnipeg network)***

The network is a part of the Winnipeg network consisting of 2 sources, 18 junction nodes, and maximum 37 possible pipelines

***Appendix C.4.1: Available commercial diameters and equivalent monetary unit per length unit for benchmark network 4***

DAVL	125	150	200	250	300	350	400	450	500	550	600	650	700
\$/m	58	62	71.7	88.9	112.3	138.7	169	207	248	297	347	405	470

*Appendix C.4.2: Pipe length, demand and required minimum head for benchmark network 4*

Pipe	Length (m)
1	760
2	520
3	890
4	1120
5	610
6	680
7	680
8	870
9	860
10	980
11	890
12	750
13	620
14	800
15	730
16	680
17	480
18	860
19	800
20	770
21	350
22	620
23	670
24	790
25	1150
26	750
27	550
28	700
29	500
30	450
31	750
32	720
33	540
34	700
35	850
36	750
37	970

Node	Nodal demand(l/s)	Required Min Head (m)
1	165	75
2	220	74
3	145	73
4	165	72
6	140	73
7	175	67
8	180	72
9	140	70
10	160	69
11	170	71
12	160	70
13	190	64
14	200	73
15	150	73
17	165	67
18	140	70
19	185	70
20	165	67
5	----	102
16	----	96

*Appendix C.4.3: Comparison of cost, network resilience and minimum surplus head among six significant solutions from Pareto data under the required layout reliability level 1*

Solutions	Cost (Mi.\$)	Network reliability	Minimum surplus head (m)	At node
(a) Minimum cost solution	2.1249	0.2943	0.67	7
(b) Centroid solution of cluster 1	2.3474	0.4392	6.33	7
(c) Centroid solution of cluster 5	2.7197	0.5804	13.42	7
(d) The best compromise solution	3.0826	0.668	16.40	4
(e) Centroid solution of cluster 2	3.8205	0.7584	20.05	14
(f) Centroid solution of cluster 3	4.7441	0.7988	19.06	1

*Appendix C.4.4: Comparison of cost, network resilience and minimum surplus head among six significant solutions with the required layout reliability level 2*

Solutions	Cost (Mi.\$)	Network reliability	Minimum surplus head (m)	At node
(a) Centroid solution of cluster 5	2.2830	0.4178	3.68	4
(b) Centroid solution of cluster 4	2.6748	0.5793	12.12	7
(c) The best compromise solution	3.2557	0.7066	17.64	7
(d) Centroid solution of cluster 3	4.0469	0.7688	20.04	14
(e) Centroid solution of cluster 2	4.8418	0.8104	20.90	14
(f) Centroid solution of cluster 6	6.2833	0.8404	21.95	14

**Appendix C.5: Benchmark network No.5**

The network consists of 11 pipes, 6 demand nodes, 2 junction nodes, 1 equalizing tank, 2 pumps that supply water for the network from two constant head reservoirs

*Appendix C.5.1: Given unit length cost of candidate pipe diameters*

Diameter	25	51	76	102	152	203	254	305	356	407	457	508	559	610
Cost (\$/m)	2	5	8	11	16	23	32	50	60	90	130	170	300	550

*Appendix C.5.2: Given nodal data for benchmark network 5*

Node	Elevation	Base demands (m <sup>3</sup> /h)	Minimum pressure (m)
1	120	100	30
2	150	100	30
3	150	270	30
4	155	120	30
5	160	200	30
6	165	330	30
7	150	0	NA
8	165	0	NA
9	180	Reservoir	NA
10	200	Tank	NA
11	130	Reservoir	NA
12	120	Reservoir	NA

NA: not applicable

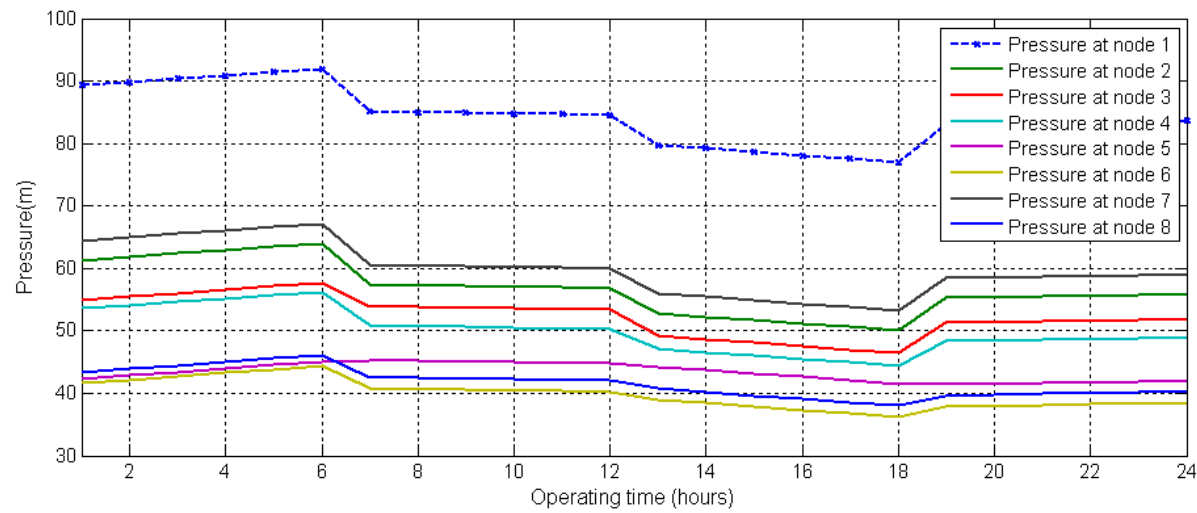
*Appendix C.5.3: Demand multiplier pattern and energy tariffs*

Time of day (hours)	Demand multiplier pattern	Energy tariffs (\$/kWh)
00:00 – 06:00	0.20	0.020
07:00 – 12:00	0.80	0.064
13:00 – 18:00	1.20	0.120
19:00 – 24:00	0.60	0.048

Appendix C.5.4: Optimal pipe diameter solutions obtained by CMA-ES-EP (mm)

Pipe	1	2	3	4	5	6	7	8	9	10	11
Diameter	356	254	305	203	203	254	254	356	406	406	25

Appendix C.5.5: Time series nodal pressures produced by CMA-ES-EP



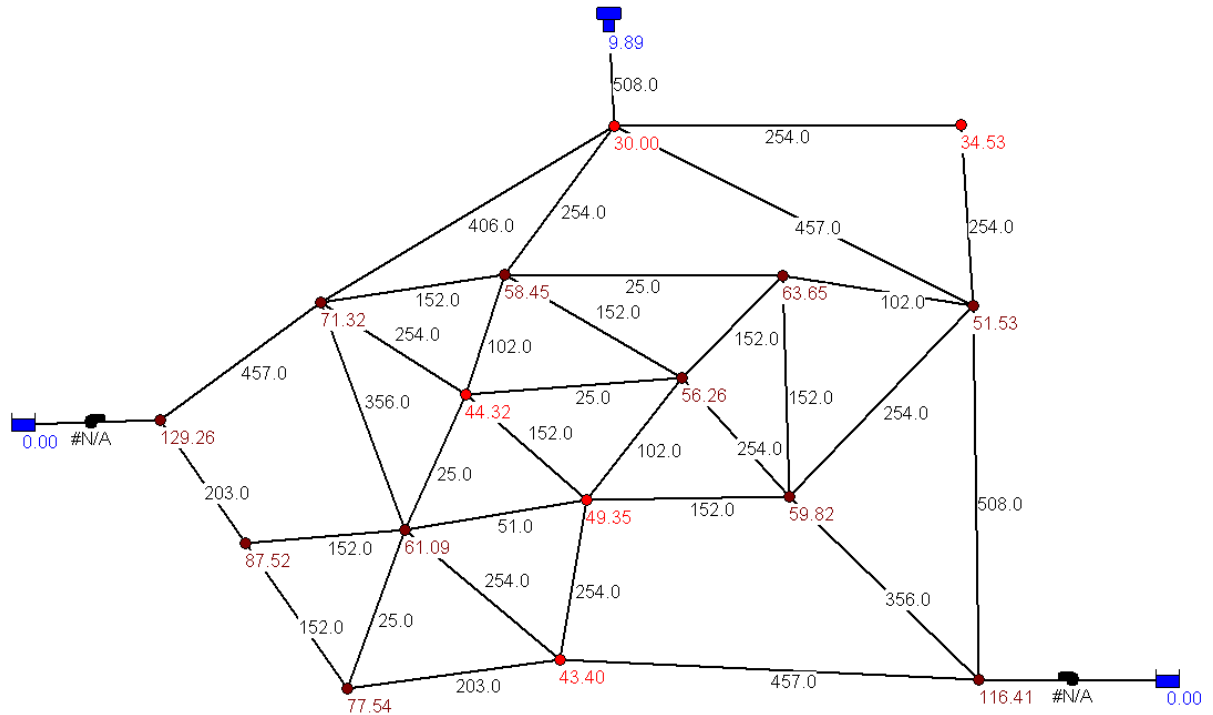
***Appendix C.6: Benchmark network No.6***

This network consists of 34 pipes, 16 demand nodes, and 1 tank is supplied by 2 pumps. The length of pipes 1, 2, 3, 30, and 32 is 3000 m, of pipe 34 is 100 m, and of the rest is 1000 m

***Appendix C.6.1: Given data for benchmark network 6***

Node	Elevation (m)	Base demand (m <sup>3</sup> /h)	Min required pressure (m)
1	140	400	30
2	155	300	30
3	160	200	30
4	120	200	30
5	130	500	30
6	130	200	30
7	130	300	30
8	140	300	30
9	150	400	30
10	110	200	30
11	100	200	30
12	120	200	30
13	145	200	30
14	130	300	30
15	65	-	-
16	85	-	-
17	60	(Pump 18)	-
18	80	(Pump 19)	-
19	180	(Tank)	-

*Appendix C.6.2: Optimal solution representing pipe diameters and nodal pressures of benchmark network 6 achieved by CMA-ES-EP approach*



*Appendix C.6.3: Comparison of optimal cost solutions*

Component costs	Reference study (ACOA)	Current study (CMA-ES-EP)
Pipe cost, PIC	3,575,000	2,029,000
Pump operational cost, PUOC	7,994,000	7,459,700
Pump construction cost, PUCC	7,947,000	4,632,000
Tank construction cost, TCC	840,000	877,786
Total cost, CS	20,356,000	14,998,468

*Appendix C.6.4: Comparison of optimal pump powers*

Pumps	ACOA	CMA-ES-EP			
	Max power (KW)	H <sub>P</sub> (m)	Q <sub>P</sub> (m <sup>3</sup> /h)	Average Power (KW)	Max Power (KW)
Pump 1	670	256	505	394	414
Pump 2	1,117.5	248	1324	953	1019
Total	1,787.5			1,347	1,433

## Appendix D: Real world case study (The Southern Batinah region)

### Appendix D.1: Nodal properties including demand nodes, junction nodes and tanks

Nodes	Easting	Northing	Altitude (m)	Notes
1	574564.1	2622383.67	16.0	Sub-area 1
2	570127.95	2623379.76	16.5	Sub-area 1
3	575208.2	2625270.21	12.0	Sub-area 9
4	571916.12	2625771.18	10.0	Sub-area 7
5	579478.36	2623743.45	13.0	Sub-area 9
6	582590.9	2620976.84	13.0	Sub-area 8
7	583891.66	2622741.51	11.0	Sub-area 8
8	584723.27	2618104.87	19.0	Sub-area 6
9	587671.04	2621789.22	4.0	Sub-area 8
10	586499.56	2620017.7	9.0	Sub-area 8
11	589855.58	2619520.99	8.0	Sub-area 8
12	591352.63	2620654.13	12.0	Sub-area 10
13	594356.79	2620398.2	12.5	Sub-area 10
14	593290.79	2618375.92	16.0	Sub-area 10
15	578657.3	2620676.57	16.0	Sub-area 1
16	589058.71	2617018.32	18.5	Sub-area 6
17	592060.42	2616390.33	19.5	Sub-area 5
18	576271.15	2617720.28	30.5	Sub-area 2
19	581518.07	2615502.55	33.0	Sub-area 4
20	586951.49	2614081.78	44.0	Sub-area 4
21	590763	2614032.83	51.0	Sub-area 3
22	581634.77	2619109.25	17.5	Sub-area 6
23	578263.62	2616760.15	32.5	Junction nodes
24	588839.14	2613929.76	53.0	
25	570648.67	2624111.22	12	
26	574921.93	2623290.19	13.5	
27	579096.67	2621262.46	15	
28	582030.92	2619902.68	16	
29	585275.29	2618757.61	17	
30	589139.91	2617779.53	18	
31	592670.55	2617087.72	19	
44	574039.27	2606805.92	92.0	Tanks
45	587618.47	2605950.72	103.0	



*Appendix D.2: Proposed location of water source nodes:*

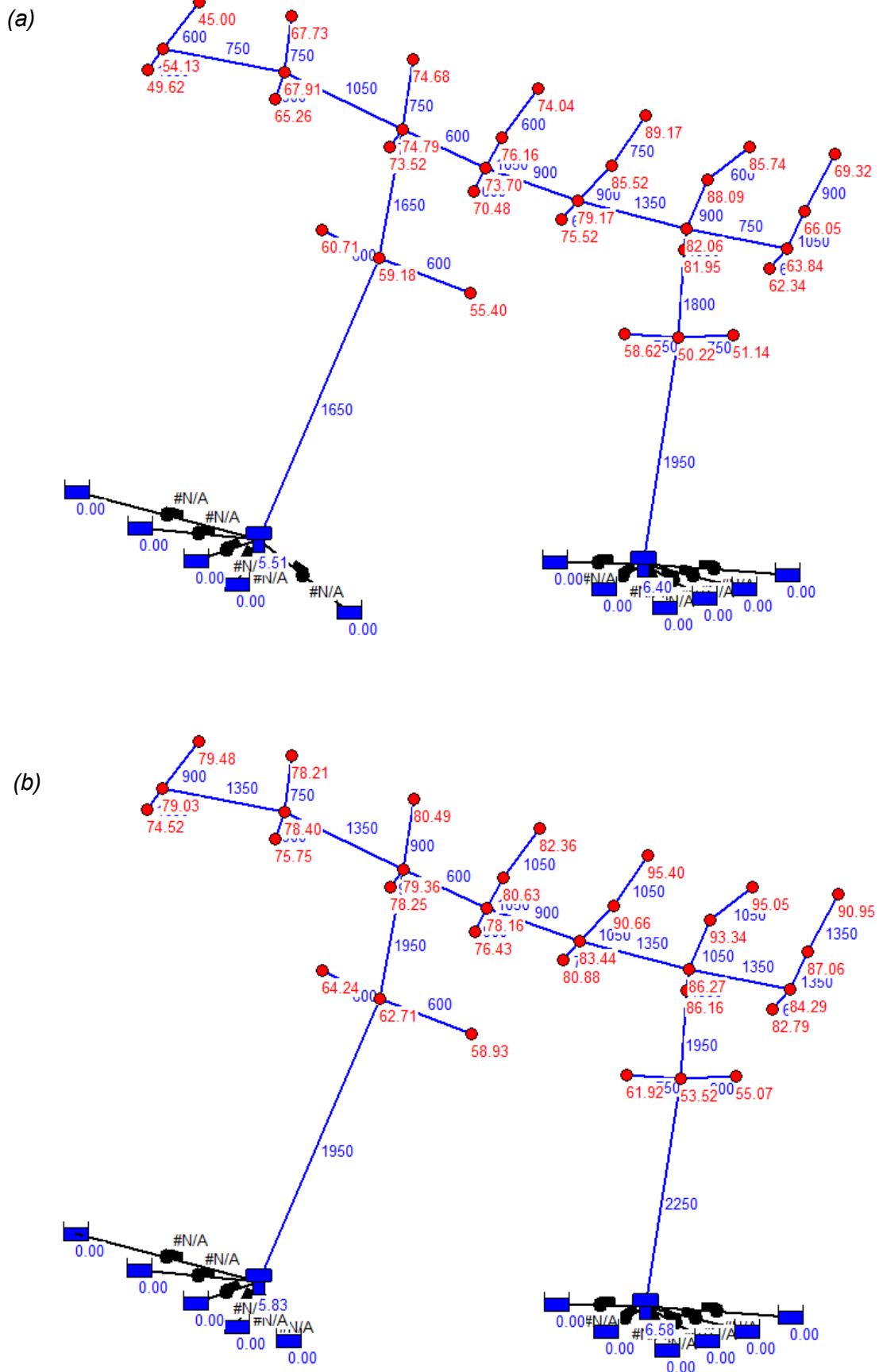
Nodes	Easting	Northing	Altitude (m)	Min water table (m)	Notes
1	592656.36	2605575.01	89.0	46	
2	591147.54	2605072.07	80.0	54	
3	589734.52	2604760.72	81.0	67	
4	588330.11	2604404.86	93.0	75	
5	586201.13	2605075.89	87.0	74	
6	584449.05	2606003.47	57.0	60	
7	577211.47	2604238.19	92.0	54	
8	575078.08	2604738.2	109.0	62	
9	573244.69	2605238.21	102.0	58	
10	571811.32	2606071.57	95.0	57	
11	569811.26	2607204.94	89.0	52	
12	567615.31	2608511.35	110.0	45	

**Backbone network optimization***Appendix D.3: Characteristics of representative solutions achieved by the backbone optimization*

Solutions	Minimum cost solution	Centroid of cluster 2	Best compromise solution	Centroid of cluster 4	Centroid of cluster 3	Centroid of cluster 5	Maximum cost solution
PIC (Mi.\$)	54.5456	59.7527	76.1821	93.9958	117.0283	128.6582	137.2638
PUOC (Mi.\$/month)	0.9985	1.0078	1.0033	1.0041	0.8887	0.8841	0.8879
PUCC (Mi.\$)	16.6039	16.7549	16.6832	16.6248	14.4849	14.4341	14.4711
TCC (Mi.\$)	2.2500	2.2500	2.2500	2.2500	2.2500	2.2500	2.2500
Total cost (Mi.\$)	85.3818	90.8509	107.1546	124.9194	144.4279	155.9514	164.6393
NR	0.6777	0.7579	0.8756	0.9130	0.9466	0.9513	0.9525
Number of working pumps	11	11	11	11	10	10	10
Closed pumps	[7]	[7]	[7]	[1]	[1, 3]	[1, 3]	[1, 3]
Total maximum power (kW)	3,051.7	3,079.5	3,066.3	3,055.6	2,662.3	2,652.9	2,659.7
Total average power (kW)	2,509.8	2,533.2	2,522.1	2,526.6	2,247.3	2,230.8	2,240.4
Maximum velocity(m/s)	2.15	1.83	1.81	1.93	2.22	2.22	2.23
$\varepsilon$ of T 44 (m)	0.0794	0.005	0.1502	0.1976	0.0194	0.0958	0.0890
$\varepsilon$ of T 45 (m)	0.3431	0.1866	0.3622	0.1876	0.1432	0.4451	0.0677
Min surplus head (m)	0.005 node 4	7.14 node 21	10.07 node 21	14.45 node 19	13.60 node 19	13.49 node 19	13.49 node 19

$\varepsilon$ : difference of initial water level in tank after one operating cycle

Appendix D.4: Pipe diameters and nodal pressures at 10:00 produced by (a) the minimum cost solution and (b) the best compromise solution of backbone network optimization



*Appendix D.5: Pump characteristics corresponding to the best compromise solution for the backbone network*

Pump	Pump curve		Average power (kW)	Maximum power (kW)
	Discharge (m <sup>3</sup> /h)	Head (m)		
1	3140.40	55.89	523.20	653.37
2	5.28	359.51	1.97	2.28
3	2727.00	238.08	769.43	925.17
4	567.31	128.04	124.01	153.21
5	1081.38	198.57	253.82	315.47
6	472.66	98.67	131.99	148.85
7	-----	-----	-----	-----
8	214.38	53.27	37.38	42.40
9	1220.61	100.54	281.75	345.93
10	1.33	86.16	0.30	0.36
11	623.16	347.96	187.96	233.65
12	683.05	128.43	210.28	245.60
Total			2,522.1	3,066.3

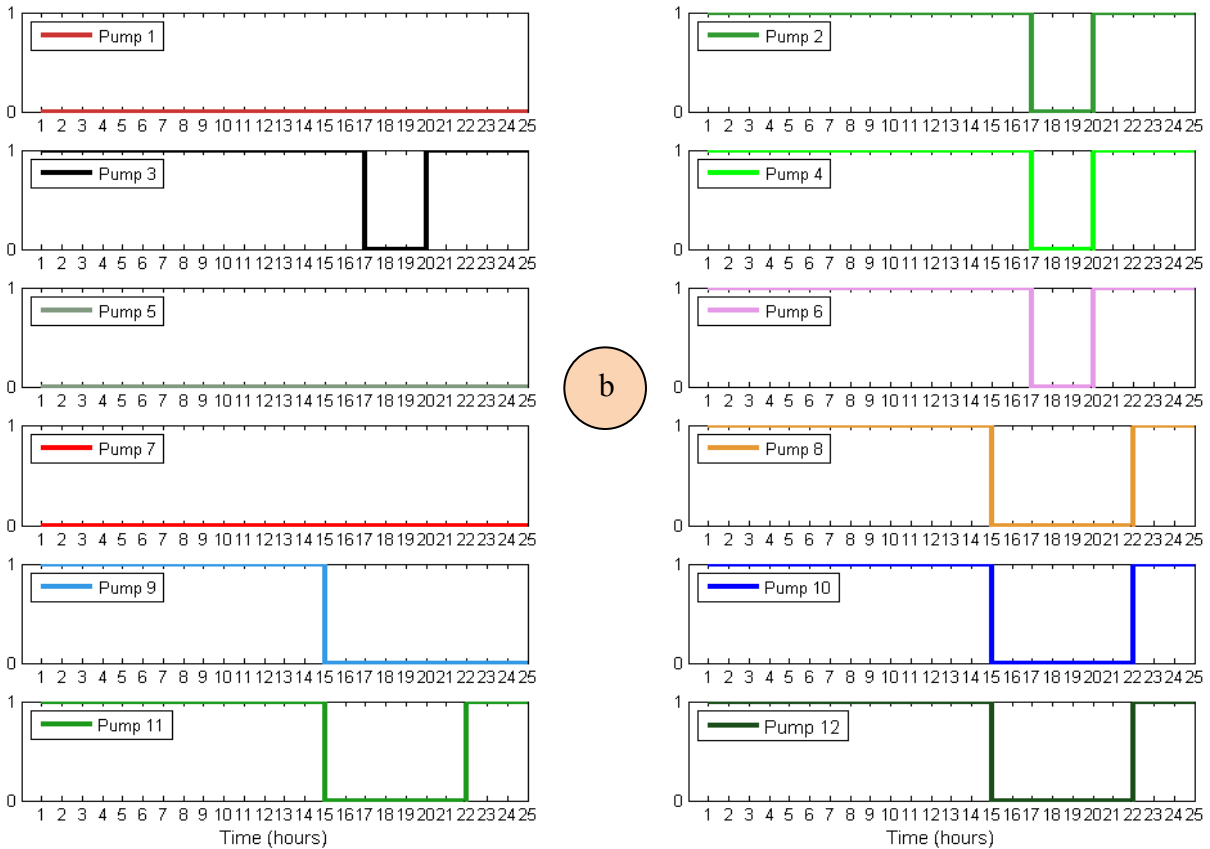
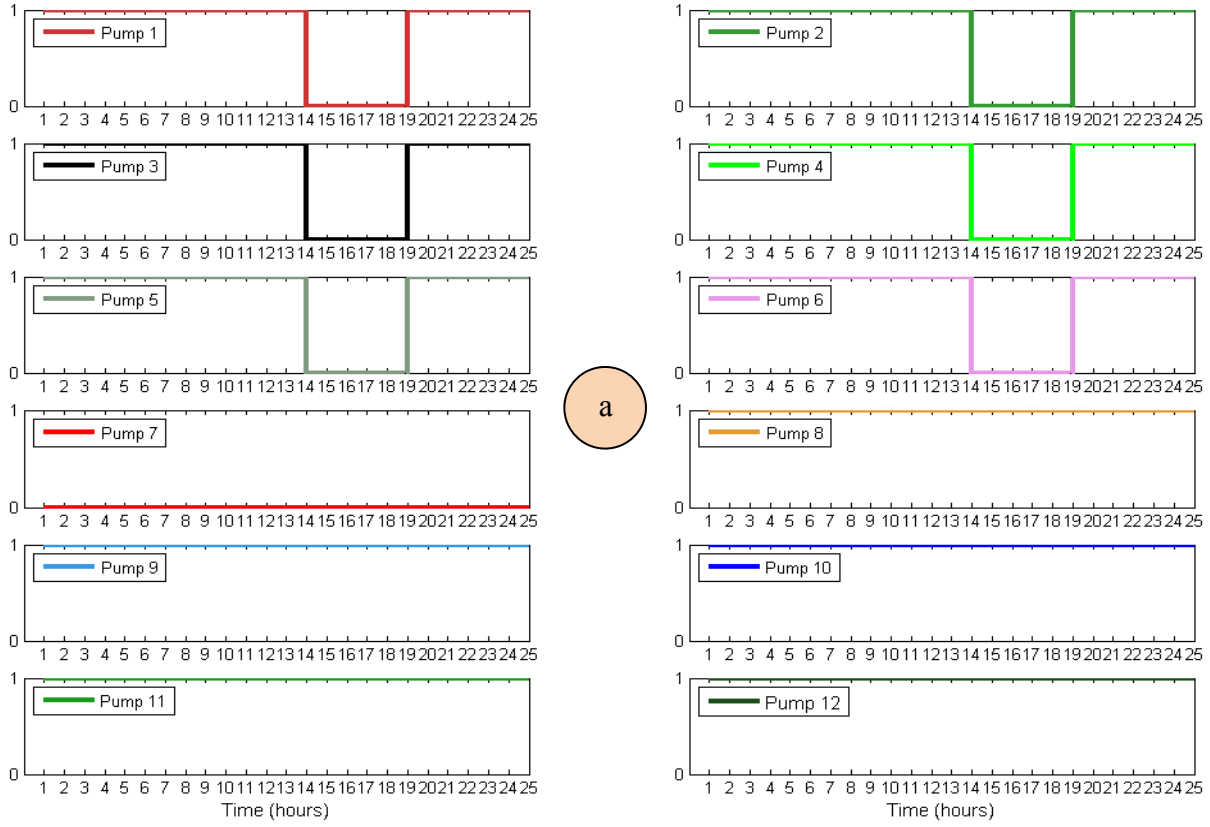
*Appendix D.6: Monthly average discharges (m<sup>3</sup>/hour) corresponding to the best compromise solution of backbone network optimization*

Average discharge	JAN	FEB	MAR	APR	MAY	JUN
Pump (1)	2,962.75	3,002.70	3,051.94	2,959.82	3,217.88	2,959.82
Pump (2)	10.00	10.05	0.00	10.04	10.07	10.04
Pump (3)	5,134.60	5,139.08	5,145.08	5,134.31	5,157.76	5,134.31
Pump (4)	0.00	1,038.64	1,040.99	0.00	1,046.13	0.00
Pump (5)	2,040.49	2,042.61	2,045.45	2,040.35	2,051.49	2,040.35
Pump (6)	774.87	777.01	779.79	774.73	786.11	774.73
Pump (8)	332.74	290.30	342.20	331.21	337.92	331.21
Pump (9)	2,110.23	1,817.16	2,153.37	2,105.13	2,142.30	2,105.13
Pump (10)	2.08	2.16	0.00	2.19	2.21	2.19
Pump (11)	0.00	1,071.49	0.00	0.00	1,072.56	0.00
Pump (12)	1,172.20	1,044.15	0.00	1,170.38	1,178.43	1,170.38
<i>PUOC (Mi.\$)</i>	<i>0.6883</i>	<i>0.7264</i>	<i>0.7568</i>	<i>0.8356</i>	<i>0.9874</i>	<i>0.8356</i>

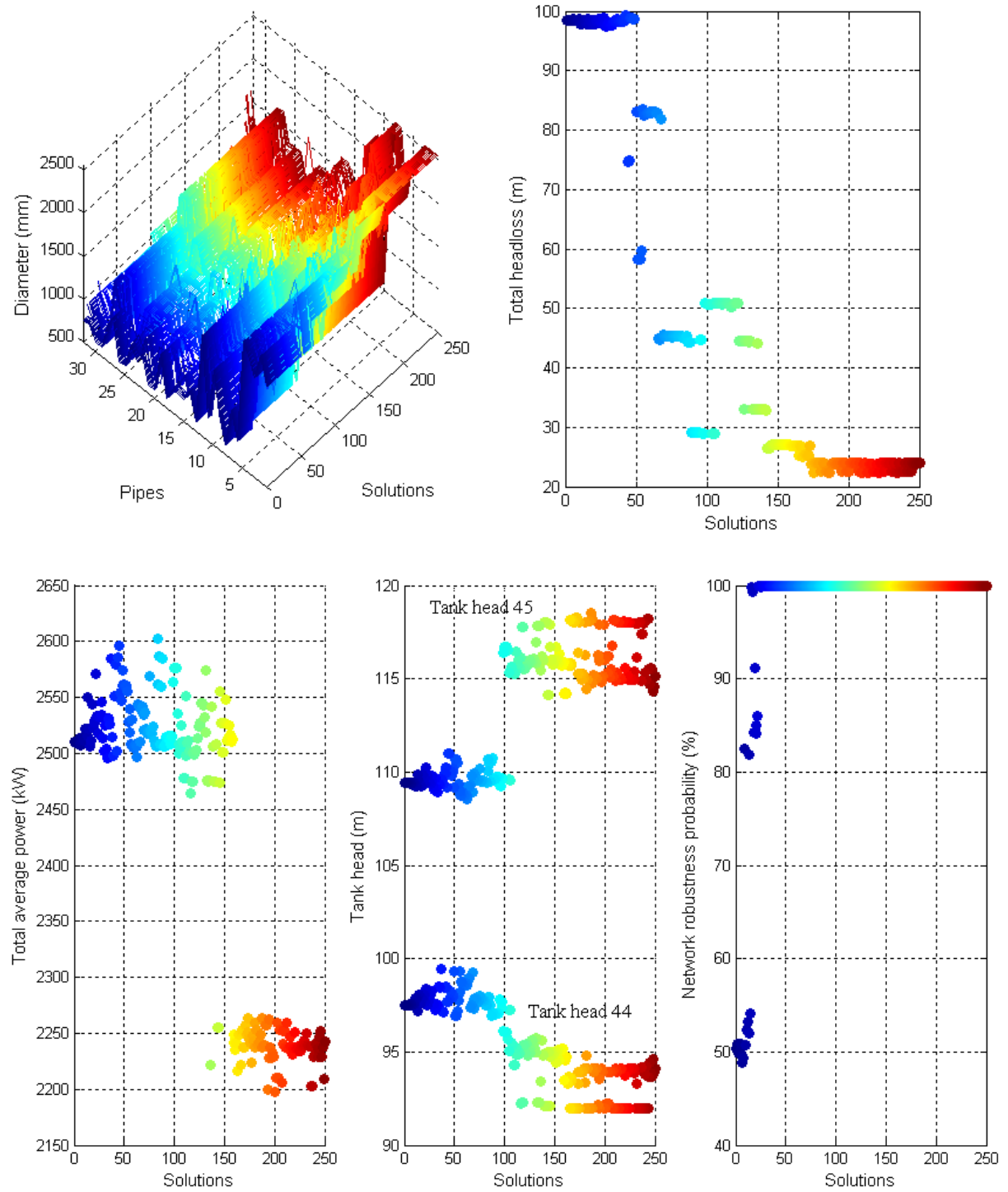
*Appendix D.6: (continued)*

Average discharge	JULY	AUG	SEP	OCT	NOV	DEC
Pump (1)	3,132.45	3,132.45	3,051.94	3,085.41	2,971.89	0.00
Pump (2)	0.00	0.00	0.00	0.00	0.00	10.07
Pump (3)	5,152.89	5,152.89	5,145.08	5,146.67	5,135.62	5,159.73
Pump (4)	1,044.11	1,044.11	1,040.99	1,041.67	0.00	1,046.92
Pump (5)	2,049.16	2,049.16	2,045.45	2,046.22	2,040.97	0.00
Pump (6)	783.56	783.56	779.79	780.68	775.36	787.05
Pump (8)	333.52	333.52	342.20	412.68	331.86	317.83
Pump (9)	2,108.78	2,108.78	2,153.37	1,646.87	2,107.79	2,060.98
Pump (10)	2.20	2.20	2.17	2.17	2.17.00	2.17
Pump (11)	1,194.47	1,194.47	0.00	1,191.75	0.00	1,188.93
Pump (12)	1,173.23	1,173.23	0.00	1,164.14	1171.16	1,154.74
<i>PUOC (Mi.\$)</i>	<i>0.7869</i>	<i>0.7869</i>	<i>0.7568</i>	<i>0.7212</i>	<i>0.6879</i>	<i>0.6252</i>

*Appendix D.7: The status of pumps (1: ON, 0: OFF) during a 24-hour operating cycle in MAY (a) and DECEMBER (b) with respect to the best compromise of the backbone network*



*Appendix D.8: Correlation between backbone network properties and network robustness probability of Pareto solutions in case uncertain correlated demands*



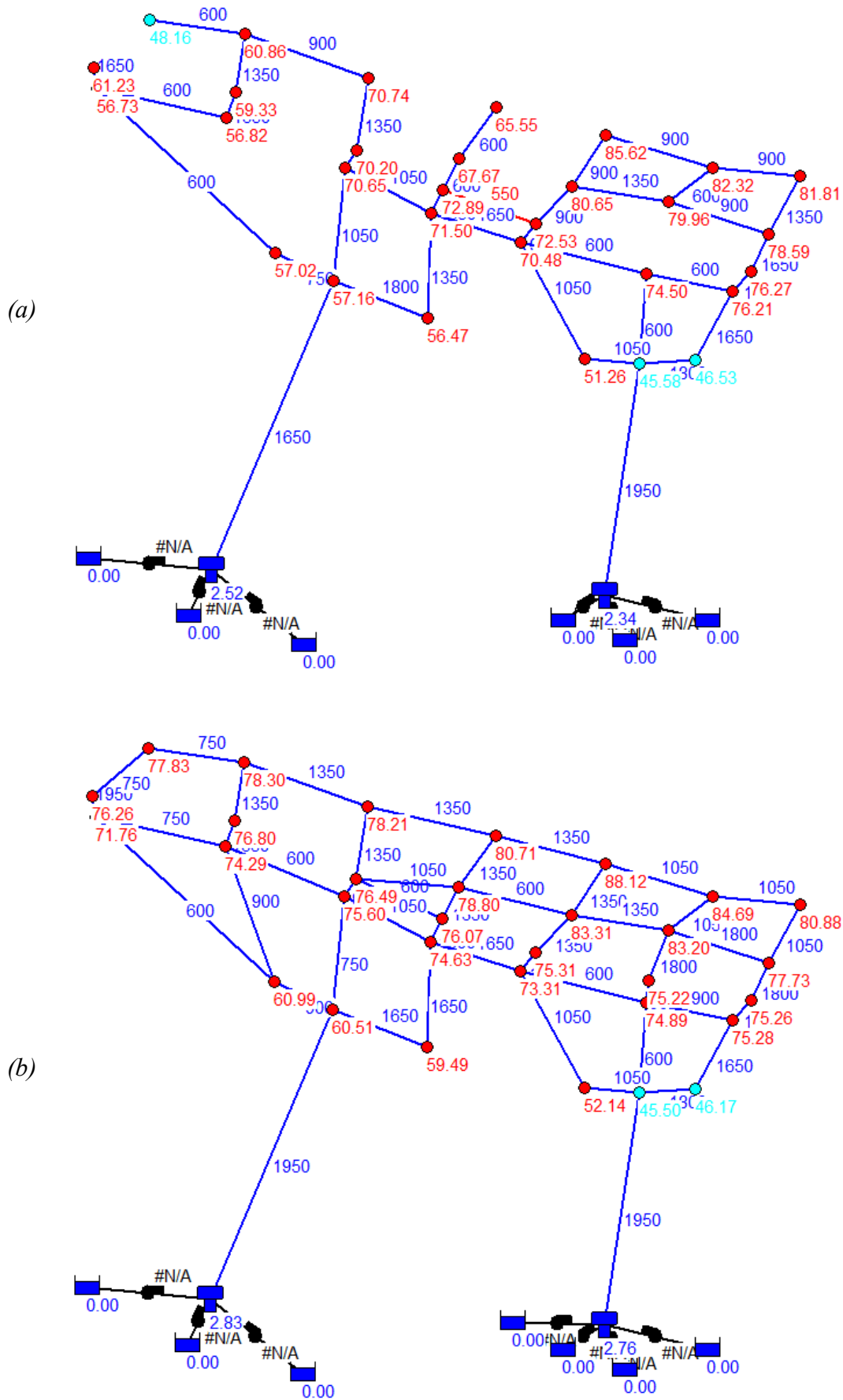
**Predefined maximum network optimization**

*Appendix D.9: Characteristics of representative solutions achieved by the PML optimization.*

Solutions	Minimum cost solution	Centroid of cluster 2	Centroid of cluster 3	Best compromise solution	Centroid of cluster 4	Centroid of cluster 5	Maximum cost solution
PIC (Mi.\$)	73.7437	77.0584	100.1028	105.7163	113.0728	127.8698	156.8032
PUOC (Mi.\$/month)	0.6203	0.6219	0.6452	0.6416	0.7167	0.7183	0.7212
PUCC (Mi.\$)	17.1340	17.1956	18.6771	18.6293	18.5537	20.3027	19.6103
TCC (Mi.\$)	2.2500	2.2500	2.2500	2.2500	2.2500	2.2500	2.2500
Total cost (Mi.\$)	100.5707	103.9668	128.7717	134.2948	142.4772	159.0425	187.3176
NR	0.4873	0.5555	0.6727	0.7287	0.7657	0.8271	0.8826
Number of working pipes	37	43	45	48	48	50	50
Closed pipes	[5,6,7,8,9,10,11,12,13,24,33,36,38,44,45,46,47]	[6,7,8,9,10,11,13,24,33,38,44]	[6,7,9,10,11,33,38,44,45]	[6,7,9,10,11,33]	[6,7,9,10,11,38]	[6,7,10,11]	[6,7,10,11]
Number of working pumps	6	6	7	7	7	7	7
Closed pumps	[1,3,6,8,10,12]	[1,3,6,8,10,12]	[1,3,8,10,12]	[1,3,8,10,12]	[3,7,8,10,12]	[3,7,8,10,12]	[3,7,8,10,12]
Total maximum power (kW)	3,149.1	3,160.5	3,432.8	3,424.0	3,410.1	3,731.6	3,604.3
Total average power (kW)	1,723.2	1,721.8	1,770.0	1,759.1	1,920.7	1,895.7	1,891.3
Maximum velocity (m/s)	2.25	1.79	1.60	1.59	1.64	1.67	1.77
$\varepsilon$ of T 44 (m)	0.2672	0.0284	0.7447	0.5829	0.0568	0.5216	0.6301
$\varepsilon$ of T 45 (m)	0.0267	0.1532	0.5263	0.2709	0.6038	0.2375	0.7200
Min surplus head (m)	1.54 node 21	1.49 node 21	1.43 node 21	1.17 node 21	1.75 node 21	2.72 node 21	2.34 node 21



Appendix D.10: Pipe diameters and nodal pressures at 22:00 produced by (a) the minimum cost solution and (b) the best compromise solution



*Appendix D.11: Pump characteristics corresponding to the best compromise solution for the predefined maximum layout network*

Pump	Pump curve		Average power (kW)	Maximum power (kW)
	Discharge (m <sup>3</sup> /h)	Head (m)		
1	-----	-----	-----	-----
2	1773.59	267.81	429.11	715.17
3	-----	-----	-----	-----
4	3718.52	134.98	492.99	952.16
5	2680.12	101.93	356.19	666.57
6	1224.12	28.38	24.88	88.02
7	1771.64	30.76	19.12	199.46
8	-----	-----	-----	-----
9	4075.66	35.70	357.65	541.98
10	-----	-----	-----	-----
11	751.88	206.80	79.16	260.62
12	-----	-----	-----	-----
Total			1,759.1	3,4240

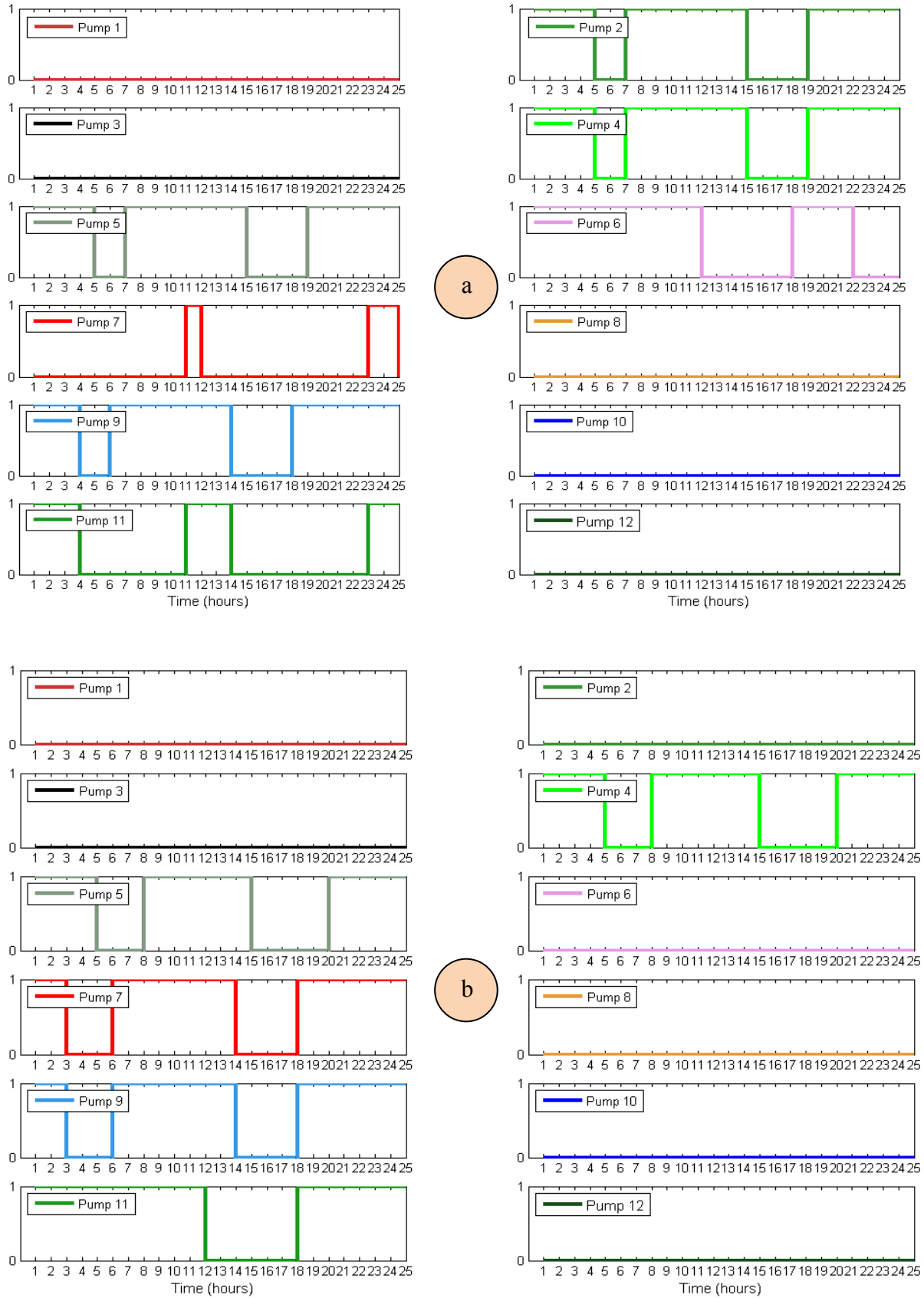
*Appendix D.12: Typical average pump discharges (m<sup>3</sup>/hour) corresponding to the best compromise solution of predefined maximum layout optimization*

Average discharge	<i>JAN</i>	<i>FEB</i>	<i>MAR</i>	<i>APR</i>	<i>MAY</i>	<i>JUN</i>
Pump (2)	0	0	0	3,304.52	3,308.01	3,304.52
Pump (4)	4,834.13	4,794.98	4,838.52	4,874.17	4,888.62	4874.17
Pump (5)	4,753.33	4,714.44	4,757.68	4,792.88	4,807.01	4792.88
Pump (6)	0	217.43	160.58	440.28	440.24	440.28
Pump (7)	1,305.93	1,345.93	1,355.93	1,375.93	1,405.93	1,375.93
Pump (9)	3,119.04	3,177.35	3,470.00	3,949.96	3,967.45	3949.96
Pump (11)	1,358.65	0	1,362.15	1,364.90	1,379.32	1364.90
<i>PUOC</i> (Mi.\$)	<i>0.4862</i>	<i>0.5340</i>	<i>0.5682</i>	<i>0.6316</i>	<i>0.6415</i>	<i>0.6316</i>

*Appendix D.12 (continued)*

Average discharge	<i>JULY</i>	<i>AUG</i>	<i>SEP</i>	<i>OCT</i>	<i>NOV</i>	<i>DEC</i>
Pump (2)	0	0	0	0	0	0
Pump (4)	4,883.58	4,883.58	4,838.52	4,811.83	4,836.17	4,810.03
Pump (5)	4,802.20	4,802.20	4,757.68	4,731.23	4,755.36	4,729.39
Pump (6)	664.07	664.07	160.58	517.64	0	0
Pump (7)	1,873.68	1,163.68	1,153.68	1,106.68	987.68	812.68
Pump (9)	3,614.42	3,614.42	3,470.00	3,338.67	3,261.19	2,861.19
Pump (11)	0	0	1,362.15	0	1,232.50	1,232.50
<i>PUOC</i> (Mi.\$)	<i>0.6021</i>	<i>0.5894</i>	<i>0.5682</i>	<i>0.5621</i>	<i>0.4897</i>	<i>0.4325</i>

*Appendix D.13: The status of pumps (1: ON, 0: OFF) during a 24-hour operating cycle in (a) MAY and (b) DECEMBER (b) with respect to the best compromise of the PML network*



*Appendix D.14: Correlation between PML network properties and network robustness probability of Pareto solutions in case uncertain correlated demands*

